ESL-TR-90-05

D-A242 161

SORPTION EQUILIBRIA OF VAPOR PHASE ORGANIC POLLUTANTS ON UNSATURATED SOILS AND SOIL MINERALS

L.W. LION, S.K. ONG, S.R. LINDER,
J.L. SWANGER, S.J. SCHWAGER, AND
T.B. CULVER

CORNELL UNIVERSITY
DEPT OF CIVIL AND ENV ENGINEERING
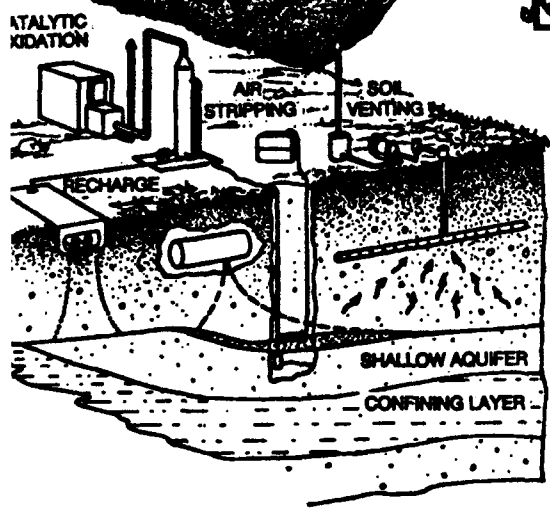ITHACA NY 14853-3501

APRIL 1990

FINAL REPORT

MARCH 1985 — MARCH 1989

CATALYTIC
OXIDATION

AIR
STRIPPING

SOIL
VENTING

RECHARGE

SHALLOW AQUIFER

CONFINING LAYER

91-14394

91 10 29 008

NOTICE

REPORT DOCUMENTATION PAGE

Form Approved
OMB No. 0704 0188

1a REPORT SECURITY CLASSIFICATION	1b RESTRICTIVE MARKINGS
2a SECURITY CLASSIFICATION AUTHORITY	3 DISTRIBUTION/AVAILABILITY OF REPORT
2b. DECLASSIFICATION/DOWNGRADING SCHEDULE	Approved for Public Release Distribution Unlimited

4. PERFORMING ORGANIZATION REPORT NUMBER(S)	5 MONITORING ORGANIZATION REPORT NUMBER(S) ESL-TR-90-05

6a NAME OF PERFORMING ORGANIZATION Cornell University Dept of Civil and Env Engineering	6b OFFICE SYMBOL (If applicable)	7a NAME OF MONITORING ORGANIZATION Air Force Engineering & Services Center

6c ADDRESS (City, State, and ZIP Code) Ithaca NY 14853-3501	7b ADDRESS (City, State, and ZIP Code) HQ AFESC/RDVC Tyndall AFB FL 32403-6001

8a NAME OF FUNDING/SPONSORING ORGANIZATION Engineering & Services Center	8b OFFICE SYMBOL (If applicable) RDVC	9 PROCUREMENT INSTRUMENT IDENTIFICATION NUMBER F-08635-85-C-003 Subtask 3.04

8c ADDRESS (City, State, and ZIP Code) Air Force Engineering & Services Center Tyndall AFB FL 32403-6001	10 SOURCE OF FUNDING NUMBERS			
	PROGRAM ELEMENT NO 62601F	PROJECT NO 1900	TASK NO 20	WORK UNIT ACCESSION NO 76

11 TITLE (Include Security Classification)
(U) Sorption Equilibria of Vapor Phase Organic Pollutants on Unsaturated Soils and Soil Minerals

12 PERSONAL AUTHOR(S) Lion, Leonard W.; Ong, Say Kee; Linder, Sharon R.; Swanger, Jean L.; Schwager, Steven J.; and Culver, Teresa B.

13a TYPE OF REPORT Final	13b TIME COVERED FROM 8503 TO 890331	14 DATE OF REPORT (Year, Month, Day) Apr 90	15 PAGE COUNT 281

16 SUPPLEMENTARY NOTATION
Availability of this report is specified on reverse of the front cover

17	COSATI CODES		18 SUBJECT TERMS (Continue on reverse if necessary and identify by block number)
FIELD	GROUP	SUB-GROUP	Vapor Sorption Pollutants Transport
			Unsaturated Porous Media Organics

19 ABSTRACT (Continue on reverse if necessary and identify by block number)

Most groundwater pollutants are volatile organic compounds; however, there is relatively little understanding of the sorption reactions that control the transport and fate of organic vapors in the vadose zone. This investigation identified the physical/chemical properties of the soil matrix and organic vapors which control vapor-solid phase distribution.

The dominant property which regulates vapor sorption in the unsaturated zone is the moisture content of the soil. Under very dry conditions, soil mineral/vapor interactions are regulated by specific surface area, indicating the dominance of a relatively non-specific physical adsorption process. However, at moisture contents exceeding an average surface coverage of four to eight layers of water, vapor uptake is

20 DISTRIBUTION/AVAILABILITY OF ABSTRACT [X] UNCLASSIFIED/UNLIMITED [ ] SAME AS RPT [ ] DTIC USERS	21 ABSTRACT SECURITY CLASSIFICATION Unclassified
22a NAME OF RESPONSIBLE INDIVIDUAL Thomas B. Stauffer	22b TELEPHONE (Include Area Code) (904) 283-2982	22c OFFICE SYMBOL RDVC

DD Form 1473, JUN 86   Previous editions are obsolete   SECURITY CLASSIFICATION OF THIS PAGE

Block 19 (Continued)

controlled by partitioning reactions into soil moisture and soil organic
matter. Moisture conditions that satisfy this criterion exist in the
unsaturated zone of most soil profiles and vapor fate can be adequately
described by a model which incorporates Henry's law partitioning into the
aqueous phase and a linear partition coefficient proportional to the soil
organic content. This conclusion is supported by experiments with
trichlorethylene (TCE) vapor onto several soil minerals soils, and a cored
profile from the unsaturated zone.

Important exceptions to these general conclusions include:

1. Soils occurring in arid or semiarid regions or at the top of the soil
profile under seasonally dry conditions. In such cases, the sorption of
vapors was significantly greater than predicted by the linear partition
coefficient based on saturated conditions and the Henry's law constant *for*
dissolution into soil moisture. The increase in vapor uptake on drier
sorbents is a complex process which likely involves physical adsorption to the
surfaces of both minerals and organic matter in soils.

2. Soils exposed to high vapor concentrations form a nonaqueous phase
liquid. At very high vapor pressures increased uptake of volatile organics
through vapor condensation occurred and was regulated by the available pore
volume of the sorbent.

3. Soils exposed to vapor mixtures. In unsaturated soils, nonideal behavior
of vapors in mixture was observed relative to the sorption behavior of single
vapors. Comparable behavior of organic solutes is generally not observed
under saturated conditions. The interaction of vapors in their sorptive
uptake is tentatively attributed to activity effects in the thin water films
which exist under unsaturated conditions. However, alternate explanations may
also play a role such as in the expected nonlinearity of isotherms for vapor
uptake that is controlled by weak physical adsorption processes. The extent
to which vapor interaction was observed depended on the moisture content of
the sorbent. Interactions of vapors generally resulted in increased uptake
although suppressed sorption was also observed in solvent mixtures.

The increased sorption of vapors noted in each of the above instances will
retard contaminant movement in the unsaturated zone and reduce volatilization
loss from soils to the atmosphere.

The properties of vapor sorbates which have the greatest influence upon their
relative uptake were shown to be solubility and related parameters such as the
octanol water partition coefficient. Because vapors partition into a sorbent
which includes a condensed aqueous phase, vapor uptake on sorbents with low
organic contents such as aquifer materials, is directly proportional to
aqueous solubility, rather than inversely proportional as is observed with
sorption from saturated solution.

A finite-element model modified to incorporate the sorption behavior of vapors
under dry conditions has been used to illustrate the dependence of volatile
contaminant movement to the atmosphere and the saturated zone upon vapor
properties.

SUMMARY

A. OBJECTIVE

The research described in this report was designed to provide a systematic evaluation of the binding of organic vapors to unsaturated soils and soil minerals. The objective was to identify the physical/chemical properties of both the stationary phase (ie, soil, aquifer media, etc.) and organic vapors which act to control vapor binding.

B. BACKGROUND

The most common groundwater pollutants are the nonionic organic components of fuels and solvents. These pollutants are introduced into the subsurface through a variety of means including spills, and leaking storage tanks. Several U.S. Air Force bases have experienced problems with groundwater contamination by fuels and solvents. The components of fuels and solvents are generally quite volatile. Therefore, in unsaturated regions of the subsurface, volatile pollutants will exist as vapors in the gas phase. Organic pollutant vapors can move in the unsaturated zone by the process of gaseous diffusion. Gas diffusion coefficients are large compared to diffusion coefficients for the same compounds when they are dissolved in water. As a result, vapor diffusion can be a major subsurface transport mechanism for volatile pollutants. Vapors can also bind or "sorb" to the surfaces of the porous medium in which they exist. Sorption reactions of vapors will act to retard their movement. Detailed knowledge of vapor sorption behavior is, therefore, a prerequisite to the prediction of volatile pollutant migration in the unsaturated zone.

Much of knowledge of organic pollutant behavior in soils has developed through research which was directed toward understanding the fate of relatively nonvolatile toxic compounds such as the pesticides employed in agriculture. As a result, the sorption of nonionic organic pollutants in saturated porous media can now be predicted within an order of magnitude based upon the properties of the pollutant (such as its solubility in water), and the soil (ie., its weight fraction of organic carbon). In spite of their common occurrence, a comparable predictive capability is lacking for the sorption reactions which control the transport and fate of organic vapors.

A major difficulty encountered in the prediction of vapor behavior is that sorption is complicated by the variable moisture contents which can exist in the unsaturated zone. Soil moisture content content can range from extremely dry in arid or semiarid regions or at the soil surface in seasonally dry climates to saturation at the capillary fringe of the water table. Soil moisture in the unsaturated zone can act as a "reservoir" into which organic vapors

may dissolve and also can act as a vapor which competes with organic pollutants for sorption to soil mineral surfaces and soil organic matter.

Condensation can occur when vapor pressures are high, and is another feature of vapor behavior that complicates description of vapors relative to the behavior that is observed for dissolved nonionic organic pollutants in saturated soils.

The sources of most organic vapors in the subsurface are complex mixtures such as fuels and solvents. It is generally assumed that the components of such mixtures behave independently, ie., the sorption of one component is not influenced by the presence of another. Independent behavior has been confirmed for nonionic organic pollutants in saturated soils; however, the behavior of vapor mixtures has not been evaluated.

The research described in this report was undertaken to improve the understanding of the sorption behavior of organic pollutant vapors over a range of moisture conditions and vapor pressures representative of those which occur in the field. In addition, the properties of both vapors and the porous media which influence sorptive behavior were evaluated in order to compare vapor behavior to the predictive relationships which exist for nonionic organic pollutants under saturated conditions.

C. SCOPE

The research was approached from two perspectives. A series of controlled experiments were performed using well-defined mineral phases to determine organic vapor sorption at low and high relative vapor pressure, the effect of competition between organic vapors and to quantify organic vapor competition with water vapor. The use of sorbents with reproducible, well-characterized features enhanced the interpretation of the mechanistic role of variables such as specific surface area, pore size distribution, and moisture content as well as the evaluation of sorbate properties such as vapor pressure, solubility and octanol-water partition coefficients. Additional experiments were performed using soils and aquifer materials with a range of physical-chemical characteristics. These results provide direct information on vapor sorption onto natural materials at the expense of complete characterization of the sorbent.

D. METHODOLOGY

Two different methods were adopted for measurement of vapor binding. At low vapor pressures, a headspace method was employed. The method relies on measurement of vapor concentrations of mixtures of solid samples with volatile organic compounds

contained in gas-tight sealed vials. Vapor concentrations were measured by gas chromatography. A variation of this method was also used to measure the sorption of dissolved vapors under saturated conditions. At higher vapor pressures, uptake of vapors onto the solid phase of interest was measured by direct analysis of its change in weight. Weight change was determined by observing the extension of a sensitive quartz spring from which solid samples were suspended while being exposed to a gas stream containing water vapor and/or the organic vapor.

E. TEST DESCRIPTION

All analyses of vapor sorption were carried out in the Cornell University Environmental Engineering Laboratories. Vapor sorption kinetics were evaluated prior to studies of vapor uptake to ensure that equilibrium was attained. All tests were carried out under isothermal conditions in controlled temperature environments. Solid phases for experiments were generally oven dried and then adjusted to the desired moisture content by addition of water or by exposure for several days to a constant humidity. Some field samples were delivered to the Cornell laboratory in sealed containers and analysed at their ambient field moisture content. At low organic vapor pressures, vapor uptake was typically related in a linear manner to the equilibrium vapor concentration (ie, a linear isotherm was attained). The slope of this relationship is referred to as the vapor partition coefficient. Vapor partition coefficients were compared to evaluate the influence of changes in the solid moisture content, changes in the type of solid or its organic content, changes in the nature of the organic vapor and the effect of vapor mixtures. In some cases (eg., on oven dried solids, and at higher organic vapor pressures), a nonlinear relationship between vapor uptake and the equilibrium vapor concentration was observed. In such cases results were interpreted using nonlinear isotherms such as the Langmuir and BET equations.

F. RESULTS

The dominant property which regulates vapor sorption in the unsaturated zone is the moisture content of the soil. Under very dry conditions soil mineral/vapor interactions were found to be regulated by the specific surface area of the solid surface, indicating the dominance of a relatively non-specific physical adsorption process. However, at moisture contents exceeding an average surface coverage of four to eight layers of water, vapor uptake was controlled by linear partitioning reactions into soil moisture and soil organic matter. This behavior was demonstrated in experiments with trichloroethylene (TCE) vapor onto several soil minerals soils, and a cored profile from the unsaturated zone. Moisture conditions sufficient to exceed four to eight layers of water surface coverage exist in the unsaturated zone of most soil profiles. Under these conditions, vapor uptake can be adequately described by the Henry's Law constant for

vapor partitioning into the soil water and the saturated partition coefficient for the dissolved organic compound into soil organic matter.

Important exceptions to this general behavior include:

1. Soils occurring in arid or semiarid regions or at the top of the soil profile under seasonally dry conditions. In such cases, the sorption of vapors was significantly greater that predicted by the linear partition coefficient based on saturated conditions and the Henry's law constant for dissolution into soil moisture. The increase in vapor uptake on drier sorbents is a complex process which likely involves physical adsorption to the surfaces of both minerals and organic matter in soils.

2. Soils exposed to high vapor concentrations from a nonaqueous phase liquid. At very high vapor pressures increased uptake of volatile organics through vapor condensation occurred and was regulated by the available pore volume of the sorbent.

3. Soils exposed to vapor mixtures. In unsaturated soils, nonideal behavior of vapors in mixture was observed relative to the sorption behavior of single vapors. Comparable behavior of organic solutes is generally not observed under saturated conditions. The interaction of vapors in their sorptive uptake is tentatively attributed to activity effects in the thin water films which exist under unsaturated conditions. However, alternate explanations may also play a role, such as the expected nonlinearity of isotherms for vapor uptake that is controlled by weak physical adsorption processes. The extent to which vapor interaction was observed depended on the moisture content of the sorbent. Interactions of vapors generally resulted in increased uptake although suppressed sorption was also observed in solvent mixtures.

The properties of vapor sorbates which have the greatest influence upon their relative uptake were shown to be solubility and related parameters such as the octanol water partition coefficient. Because vapors partition into a sorbent which includes a condensed aqueous phase, vapor uptake on sorbents with low organic contents, such as aquifer materials, is directly proportional to aqueous solubility, rather than inversely proportional as is observed with sorption from saturated solution.

A finite-element model modified to incorporate the sorption behavior of vapors under dry conditions has been used to illustrate the dependence of volatile contaminant loss to the atmosphere upon vapor properties.

G. CONCLUSIONS

Under many conditions the sorptive uptake of individual volatile organic contaminants in unsaturated soils can be adequately described based upon knowledge of sorptive behavior under saturated conditions and the air/water distribution coefficient for the vapor. This information is readily available for a large suite of the organic components of fuels and solvents and can be incorporated into existing models to predict pollutant transport and fate.

At soil moisture contents lower than those necessary to give an average surface coverage of four to eight layers of water, sorption of vapors will be increased above that which can be accounted for by linear partitioning into soil water and organic matter. Vapor sorption under dry conditions will retard contaminant movement in the unsaturated zone, reduce volatilization loss from soils to the atmosphere, and can only be adequately described with a numerical model in which the influence of the variation in soil moisture content on vapor uptake is considered. Linear partitioning of vapors into soil water and soil organic matter will also fail to account for vapor condensation into available pore space which is not occupied by soil moisture. Vapor condensation is most likely to occur close to field sources such as nonaqueous phase organic liquids.

Most fuels and solvents used by the Air Force are mixtures of many nonionic organic compounds. The research results obtained in this study indicate that sorption of organic vapors may display mixture effects under some soil moisture conditions. Mixture effects can include both enhanced and reduced sorption, depending upon the components of the mixture. The conditions under which these effects are exhibited and the direction of the effect, have not been sufficiently characterized to permit their prediction. Mixture effects are typically not observed in the partitioning of dissolved organic compounds. Therefore, vapor mixture effects are expected to be insignificant in soils which are near saturation.

H. RECOMMENDATIONS

Use of saturated linear partition coefficients and Henry's law constants is recommended to predict vapor uptake in unsaturated soils. Mixture effects, dry conditions and high vapor concentrations may result in violations of the assumptions implicit in such predictions. These discrepancies are, however, likely to be no more severe than those which result from assuming homogeneity in the soil medium and uniform fluid flow.

The greatest uncertainty with regard to the transport of organic vapors in the unsaturated zone now lies in prediction of vapor diffusion coefficients as a function of the properties of the porous media. The biological degradation of organic vapors in unsaturated soils is another area in which research is needed if we are to be better able to predict vapor fate.

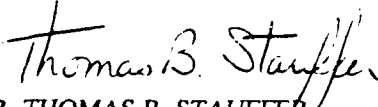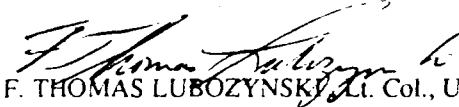| Accesion For		
NTIS CRA&I	☑	
DTIC TAB	☐	
Unannounced	☐	
Justification		
By		
Distribution /		
Availability Codes		
Dist	Avail and / or Special	
A-1		

PREFACE

The research described in this report was carried out at the School of Civil and Environmental Engineering, Cornell University in Ithaca, New York under contract No. F08635-85-C-003 with the U.S. Air Force Engineering Systems Command. The individuals responsible for authorship of sections of this report are indicated at the beginning of each section.

Mention of trademarks and trade names of material and equipment in this report does not constitute endorsement or recommendation for use by the Air Force. This report has been reviewed by the Public Affairs Office (PA) and will be released to the National Technical Information Service (NTIS); through NTIS, it will be available to the general public, including foreign nationals.

This technical report has been reviewed and is approved for publication.

DR. THOMAS B. STAUFFER
Chief, Subsurface Chemical Processes
Research Group

F. THOMAS LUBOZYNSKI, Lt. Col., USAF
Chief, Environics Division

F. THOMAS LUBOZYNSKI, Lt. Col., USAF
Chief, Environmental Engineering Branch

FRANK P. GALLAGHER III, Colonel, USAF
Director, Engineering and
Services Laboratory

(The reverse of this page is blank.)

TABLE OF CONTENTS

SECTION I

INTRODUCTION

A. OBJECTIVES

The objectives of this research were to characterize the sorptive properties of volatile organic compounds (VOCs) in the unsaturated regions of soils and aquifers. Given the frequent occurrence of groundwater contamination by VOCs, it is unfortunate that most research regarding groundwater pollutant fate and transport has focused on more toxic pesticides and herbicides which are often relatively nonvolatile. As a result, considerable attention has been given to pollutant migration under saturated conditions while relatively little is known about the reaction and migration of volatile organics in the vapor phase. This research addresses this deficiency.

B. BACKGROUND

Volatile organics constitute the most commonly encountered pollutants which contaminate groundwaters in the United States (Council on Environmental Quality, 1981; Plumb and Pitchford, 1985). One major class of volatile organics includes the chlorinated components of solvents and degreasers which can be introduced into groundwaters through accidental spills, improper disposal by land application or in landfills, and through commercial uses such as in septic tank cleaning fluids. Another source of volatile organic hydrocarbons is leaky underground storage tanks and fuel lines related to petroleum production and use. As a major user of fuels and solvents, the U.S. Air Force has experienced incidents of groundwater contamination from these materials, as have producers and users of solvents and fuels in the private sector.

An understanding of groundwater pollutant behavior is essential to the rational design of efforts to clean up contaminated sites, and to assess risk to populations using groundwater subject to contaminant inputs. Sorption is a major abiotic process influencing the movement of organic pollutants relative to bulk water movement (Banerjee et al., 1985). Until recently, sorption research has focused on partitioning under saturated conditions. For nonionic organic pollutants, several empirical relationships have been developed for predicting sorptive partition coefficients on the basis of pollutant properties, such as aqueous solubility, and soil properties, notably the weight fraction of organic carbon (Abdul et al., 1987; Karickhoff et al., 1979; Schwarzenbach and Westall, 1981). The behavior of organic pollutants in the unsaturated or vadose zone has received little study, and is not well understood (Pye and Patrick, 1983; Kuhlmeier, 1988).

1

The presence of gas space in the unsaturated zone adds a phase that must be considered in addition to soil and water. If the organic pollutant of concern is volatile, as many are, it will occur in the soil vapor phase as a gas as well as in the soil aqueous phase as a solute. The moisture content in the unsaturated zone varies. This is important because of the anticipated competition between water and organic vapors for sorption sites (Chiou and Shoup, 1985; Chiou et al., 1985).

Sorption under saturated conditions is often characterized by a linear partition coefficient. This is useful in modelling because of its mathematical simplicity (Voice and Weber, 1983). Partition coefficients determined for saturated conditions are often used to model pollutant transport in the unsaturated zone (eg. Jury et al., 1983). However, Peterson et al. (1988) found that partition coefficients for trichloroethylene (TCE) sorption on unsaturated simulated soil (humic coated aluminum oxide) were up to four orders of magnitude greater than the values measured under saturated conditions. Similarly, Chiou and Shoup (1985) showed much greater sorption for four vapors onto soil under dry vs. moist conditions. Under extremely dry conditions soil mineral surfaces are thought to be available for sorption of vapors, and vapor uptake will reflect mineral surface area rather than the organic content of the sorbent as is observed under saturated conditions (Chiou et al. 1985). Sorption of vapors to mineral surfaces will exhibit nonlinear isotherms, vapor competition for surface sites, and vapor condensation may occur. Vapor condensation is governed by the pore size distribution of the sorbent, and is anticipated to occur in unsaturated soils at sufficiently high relative vapor pressures of organic pollutants. As a consequence of these features of vapor behavior, it may not always be appropriate to assume that sorptive partition coefficients measured under saturated conditions apply to vapors in the vadose zone.

C. SCOPE

The research was approached from two perspectives. A series of controlled experiments were performed using well-defined mineral phases to determine organic vapor sorption at low and high relative vapor pressure, the effect of competition between organic vapors and to quantify organic vapor competition with water vapor. The use of sorbents with reproducible, well-characterized features enhanced the interpretation of the mechanistic role of variables such as specific surface area, pore size distribution, and moisture content as well as the evaluation of sorbate properties such as vapor pressure and octanol-water partition coefficients. Additional experiments were performed using soils and aquifer materials with differing physical-chemical characteristics. These results provide direct information on vapor sorption onto natural materials at the expense of complete characterization of the sorbent.

2

The research results are organized in this report as follows:

Section II provides the results and analysis of vapor sorption onto a cored soil profile from an unsaturated aquifer region. To the authors' knowledge, this represents the first and only report of the variation in vapor partition coefficients over depth in the field. Results are given for two vapors: toluene, an aromatic hydrocarbon component of fuels, and trichloroethylene (TCE), a component of cleaning solvents and degreasers. Results are also provided from soil moisture profiles simulated in the laboratory using well characterized solids.

Sections III, and IV detail the vapor sorption results for a single vapor, TCE, in competition with water vapor on a wide array of well characterized mineral surfaces. In Section III, a simple model is suggested which adequately accounts for TCE sorption at high moisture contents and low TCE vapor pressure. In Section IV sorption and condensation of TCE on well-characterized mineral surfaces at high vapor pressures and the effects of competition with water vapor are documented.

Section V provides results of TCE sorption at low vapor pressure onto natural soils and aquifer materials. A wide range of material properties are evaluated to elucidate characteristics which regulate vapor behavior in natural systems.

Sections VI and VII examine the sorption of several selected components of fuels and solvents onto a single, well characterized sorbent. In Section VI, a new statistical approach to fitting linear, Langmuir and B.E.T. isotherms is demonstrated. In Section VII, this method of data reduction is applied to results for several selected vapors to evaluate sorbate properties which govern vapor sorption.

In Section VIII, competition between organic vapors is evaluated at low and high moisture conditions.

Section IX presents results from a numerical model which explicitly incorporates and accounts for vapor sorption. Model calculations are used to illustrate the influence of vapor sorption on volatile pollutant migration in the vadose zone.

Section X presents a comprehensive summary of the conclusions attained in the preceding sections.

The Appendix to the report provides a review of range of moisture conditions that occur in the unsaturated zone and a discussion of models which are frequently used to describe the sorption of nonionic compounds from the vapor phase and from saturated solutions. This discussion is augmented, as appropriate, in various Sections of the report.

3

SECTION II

VAPOR-PHASE SORPTION OF TRICHLOROETHYLENE AND TOLUENE ONTO MINERALS WITH SIMULATED MOISTURE PROFILES AND A CORED DEPTH PROFILE FROM AN UNSATURATED AQUIFER ZONE

By: J.L. Swanger and L.W. Lion

A. INTRODUCTION

One of the salient features of the vadose zone is that it usually contains a profile of moisture contents. Generally, soil moisture may be envisioned as fluctuating at the surface in response to daily and seasonal conditions. These fluctuations are dampened in the subsurface moisture profile which reflects the annual precipitation less evaporation and transpiration and the depth to the groundwater table. A wide range of conditions can therefore exist, ranging from marsh soils, which are typically saturated, to soils in arid and semiarid regions which can have decreasing moisture contents with increasing depth until the water table is approached (Herbel and Gile, 1973; Purtymun et al. 1971). In addition to moisture content variation, soil chemical characteristics, such as organic content, also commonly change with depth. In this section the sorptive behavior from the vapor and aqueous phase of two representative volatile organic compounds (TCE and toluene) is compared for a cored depth profile obtained from an unsaturated soil and for simulated profiles using inorganic solids. The soil and solids profiles are characterized for selected physical-chemical properties that might influence sorption including moisture and organic contents. Sorption, as characterized by partition coefficients, is then correlated to soil properties to examine the dependencies of vapor-phase sorption in the unsaturated zone.

B. METHODS AND MATERIALS

1. Sorbate Choice And Sorbate Properties

Two compounds, trichloroethylene (TCE) and toluene, were chosen as sorbents for this phase of the research. Each represents of a different class of common groundwater pollutant. Both are listed as hazardous substances, hazardous wastes, and priority toxic pollutants by the U.S. Environmental Protection Agency.

4

TCE ($Cl_2C=CHCl$) is one of the most widely produced chlorinated hydrocarbons in the world. It is included among the chlorinated hydrocarbons found universally in the atmosphere (normal concentration of 1 to 10 ng/L), and widely distributed in rain water, rivers, and the sea (μg/kg level or lower) (McConnell et al., 1975). TCE was the most common contaminant in a 1980 study of 2894 wells containing volatile organics (CEQ, 1981). TCE is an animal carcinogen and suspected human carcinogen (Sittig, 1985). The main use of TCE is as a metal degreasing solvent. It is also used in dry cleaning, to clean septic tanks, and in the manufacture of various chemicals. The major sources of groundwater contamination by TCE are improper land disposal, and leaking underground storage tanks.

Toluene ($C_6H_5CH_3$) is an aromatic hydrocarbon, and is a product of petroleum refining, coal tar distillation, and benzene manufacture. It is a component of automobile and aviation fuels (Sittig, 1985). Leaking underground storage tanks and land disposal are likely sources of underground contamination. TCE and toluene were the most frequently identified compounds in a study of 546 abandoned dump sites (Abelson, 1985).

Several properties of TCE and toluene are listed in Table II-1. Note that TCE has a higher vapor pressure, Henry's Constant, and solubility.

TABLE II-1. PROPERTIES OF TCE AND TOLUENE.

Property	TCE	Toluene	Reference
Vapor pressure	60 mm @ 20°C	22 mm @ 20°C	Verschueren (1983)
Solubility	1.10 g/L @ 25°C	470 mg/L @ 20°C	Verschueren (1983)
Henry's Constant (dimensionless)	0.397 @ 25°C	0.261 @ 25°C	Garbarini and Lion (1985)
$\log K_{ow}$	2.29		Verschueren (1983)
		2.69	Leo et al. (1971)

2 .Sorbent Characterization

a. Description of Inorganic Solids and Soils

Inorganic solids were used for initial sorption studies to develop experimental techniques and to allow examination of the functional dependence of sorption without the complexities introduced by the heterogeneous mix of minerals and organic matter found in a natural soil profile. Inorganic solids studied include silica oxide (Min-U-Sil 5, Pennsylvania Glass Sand Corporation, Berkeley Springs, West Virginia), and adsorption alumina (80-200 mesh, Fisher Scientific). The alumina was coated with humic acid (Aldrich Chemical Company, Milwaukee, Wisconsin) to provide a mixed organic/inorganic surface for sorption (Peterson et al., 1988).

Samples of a natural unsaturated zone profile came from a soil core obtained by Dr. Marvin Piwoni of the U.S. Environmental Protection Agency. The core was taken at the U.S. Coast Guard Station, Traverse City, Michigan on August 14, 1986. A hollow stem auger was employed and samples were obtained beginning 15 cm below the surface to the first productive saturated zone. The water table was reached at a depth of 3.33 meters. Extruded material from 25.4 cm increments was immediately placed in a double set of zip-lock polyethylene bags for a total of 13 samples (Dr. Marvin Piwoni, U.S. Environmental Protection Agency, Robert S Kerr Environmental Research Laboratory, Ada, OK, personal communication). All the samples appeared similar (coarse, brown sand), except for the top two samples which were noticeably finer in texture and darker in color. Soil samples were stored at $4^{\circ}C$ upon receipt at Cornell to retard moisture loss and possible microbial alteration. For identification purposes, the samples were labeled 44U1 to 44U13 from top to bottom. A core log is given in Figure II.1.

b. Moisture Content

Moisture content, w, was measured gravimetrically after drying to constant weight at $105^{\circ}C$, and expressed as percentage on a dry weight basis.

c. Surface Area

Surface area was measured by several different procedures to overcome limitations inherent in individual methods. Most methods are relative, involving a quantitative measurement of the amount of a particular compound adsorbed to the surface.

Depth
(m)

0.15 — Chocolate -brown sand

Moist, coarse sand grading from dark orange-
brown to caramel tan
0.56 —

Buff-beige very coarse, moist sand with no
clay content

1.9 —

Same as above with slightly more orange sand
grains and some slight orange staining

2.6 —

Same material as above with noticeably more
orange staining

3.1 —

Coarse, buff-tan sand with noticeably more
3.4 — white chert
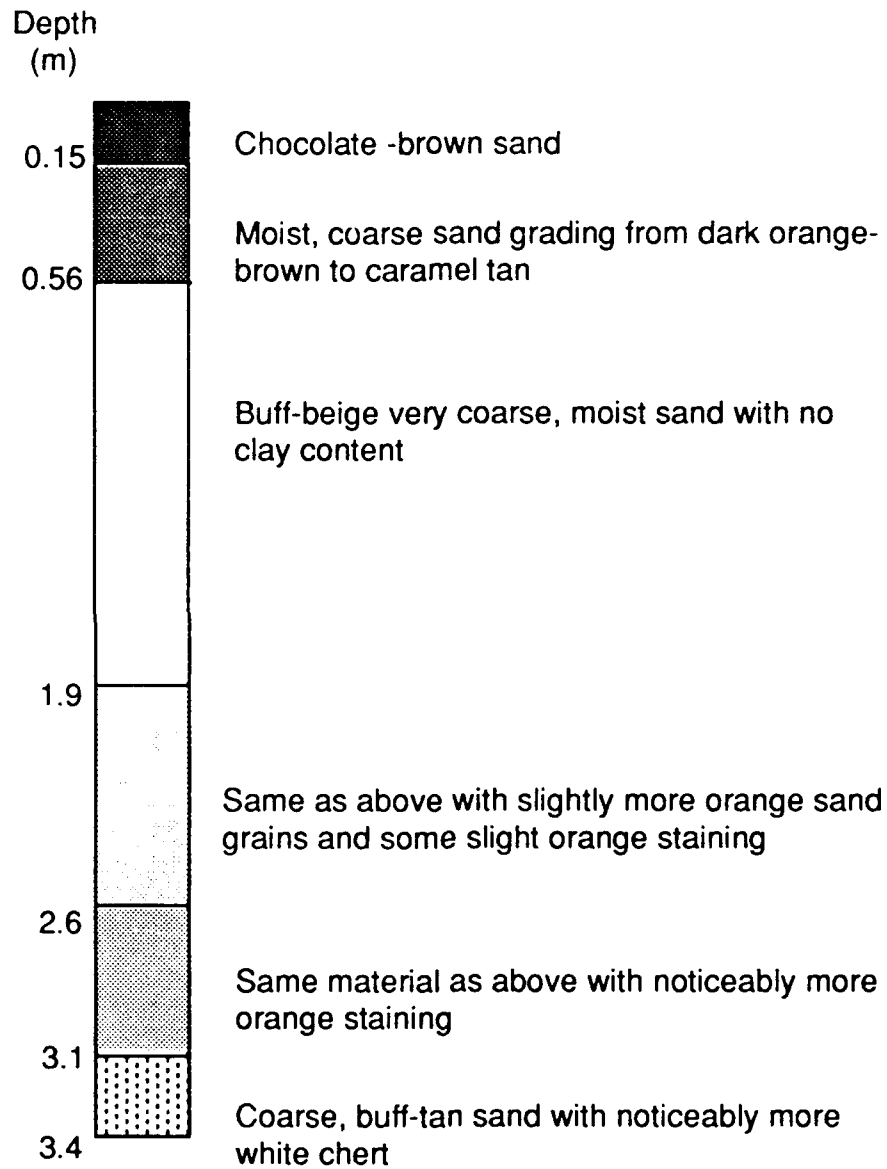
Figure II.1 Core Log for Soil Core 44U

Perhaps the most widely used method of measuring powder surface areas is by N_2 gas adsorption. A Quantasorb Surface Area analyzer was used for this analysis in the Cornell Environmental Laboratory. Nitrogen sorption does not give reliable values for surface areas in expandable clays such as montmorillonite. Because N_2 is only weakly adsorbed, it does not penetrate the interlayer surfaces of clay minerals where most of the total surface area is located (Carter et al. 1986). In addition, interlayer surfaces are not readily available for adsorption when the sample is dried as in the BET analysis.

A common method of measuring soil surface area is to gravimetrically measure sorption of ethylene glycol monoethyl ether (EGME). EGME is highly polar, so it adsorbs on internal clay surfaces. An assumption in the data analysis is that all EGME taken up by the sample exists as a monolayer (Heilman et al., 1965; Cihacek and Bremmer, 1979). This will lead to high estimates of surface area in soils where EGME undergoes multilayer sorption.

Surface area measurements may also be obtained from sample characterization by mercury porosimetry. This determination is discussed in more detail below.

d. Organic Carbon

Methods for determining soil carbon usually involve oxidizing the carbon and measuring a reaction product. A method sensitive to small differences in low carbon levels was needed because of the suspected very low organic carbon of soil core 44U due to its coarse, sandy texture.

Three methods of measuring soil carbon were available through the Analytical Laboratories, Department of Agronomy, Cornell University: CHN analysis, application of the Walkley-Black method (Allison, 1965), and wet combustion (Allison, 1960). Total carbon, inorganic carbon, or organic carbon can be measured depending on the sample pretreatment method. A preliminary comparison of samples analysed by all three methods (Swanger, 1990), indicated the wet combustion method was the most sensitive of the available methods, especially at low carbon levels. An additional reason for using wet combustion was that the method permitted increasing sample size to obtain greater accuracy. Sample size is chosen to obtain 20-40 mg of carbon to ensure an appreciable weight gain in the CO_2 absorbent. Because soil core 44U had very low carbon content, sample size was increased from the usual 2 g to 10 grams.

e. Pore Volume and Pore Size Distribution

Information about the size distribution of pores in soils and inorganic solids was obtained with a mercury porosimeter (PMI Automated Porosimeter, Porous Materials. Inc., Ithaca, NY). Mercury porosimetry is based on the relationship between the exterr. pressure needed to force a nonwetting liquid (mercury) into a pore against the opposing force of the liquid surface tension. For cylindrical pores, this relationship is:

$$P_L - P_G = \frac{-4 \, \sigma \cos \theta}{d_P}$$

II.1

where:

P_L = pressure of intrusion liquid

P_G = pressure of gas inside pore

σ = surface tension of intrusion liquid

θ = contact angle of intrusion liquid with pore wall

d_P = pore diameter

The pressure required to force mercury into a pore is therefore inversely proportional to the pore diameter. The PMI porosimeter measures the volume of mercury intruded into pores as a function of increasing pressures, up to 60,000 psi. This intrusion curve provides cumulative pore volume. A pore volume distribution is derived from pressure increments of the intrusion curve. For each increment in pressure, the change in intrusion volume is equal to the volume of pores whose diameters fall within an interval that corresponds to the interval in pressure.

The assumption of cylindrical pores allows an approximate measure of sample surface area. Substitution of the definition for the surface area, SA, of an open-ended cylinder into the formula for its volume gives:

$$SA = \frac{4V}{d}$$

II.2

where:

V = cylinder volume

d = cylinder diameter

The surface area in a specified pore diameter interval can be calculated by using an average pore diameter, $\overline{d_p}$, and the incremental intrusion volume (ΔV_p) for the specified interval. Total surface area (S_t) is given by summing surface areas over all pore sizes:

9

$$S_t = \sum_{d_p} \left(\frac{4(\Delta V_p)}{\bar{d}_p} \right)$$

f. Cation Exchange Capacity (CEC)

CEC on soil samples was determined by the Analytical Laboratories, Department of Agronomy, Cornell University. Exchangable cations were defined as those removable with 1 N ammonium acetate at pH = 7.0 (Holmgren, et al. 1977). After evaporation of the extract and treatment of the residue to destroy organic matter and to dehydrate silica, the cations Ca^{+2}, Mg^{+2}, K^+, Na^+ were determined by atomic absorption and emission.

g. Particle Size Distribution

Particle size distribution for several 44U sections was determined by sieve analysis. This method is preferable to the hydrometer method when nearly all grains are retained on a No. 200 sieve, as with this soil. The nest of sieves included the following U.S. Sieve sizes: 4, 20, 40, 120, and 200.

After the clean sieves were weighed. 500 grams of air-dried soil were put in the top sieve and shaken by a mechanical shaker. Each sieve with its trapped soil was weighed. The percentage soil retained on each sieve was added cumulatively to plot percentage finer than versus grain diameter. A curve drawn through data points may be used to classify the soil (Lambe, 1951).

3. Induced Moisture Contents In Solids

a. Constant Humidity Environments

Moisture content was adjusted in silica by exposing solids to environments with different humidities. A closed container with circulating water at 25°C or 37°C provided water-saturated environments. Another method used to obtain constant humidity was to use a saturated solution of $CaCl_2 \cdot 6H_2O$ as a desiccant. This maintains a constant relative humidity of 33 percent at 20°C (Bolz and Ture, 1973). Different moisture contents were also obtained by air-drying at ambient laboratory humidity. Oven-dried solids at 105°C were operationally defined as having zero moisture content, although it is recognized that bound water is not entirely removed from the surface under this condition.

b. Simulated Soil Columns

Moisture contents representing those found in unsaturated soil zones were necessary to define the effect of moisture content on sorption. To simulate a soil moisture profile in an arid region, 6.7 meters of clear Nalgene tubing, 1.91 cm I.D., was filled with sorbent, and suspended vertically with the bottom 12 cm submerged in 0.01 N $CaCl_2$ solution (Figure II.2).
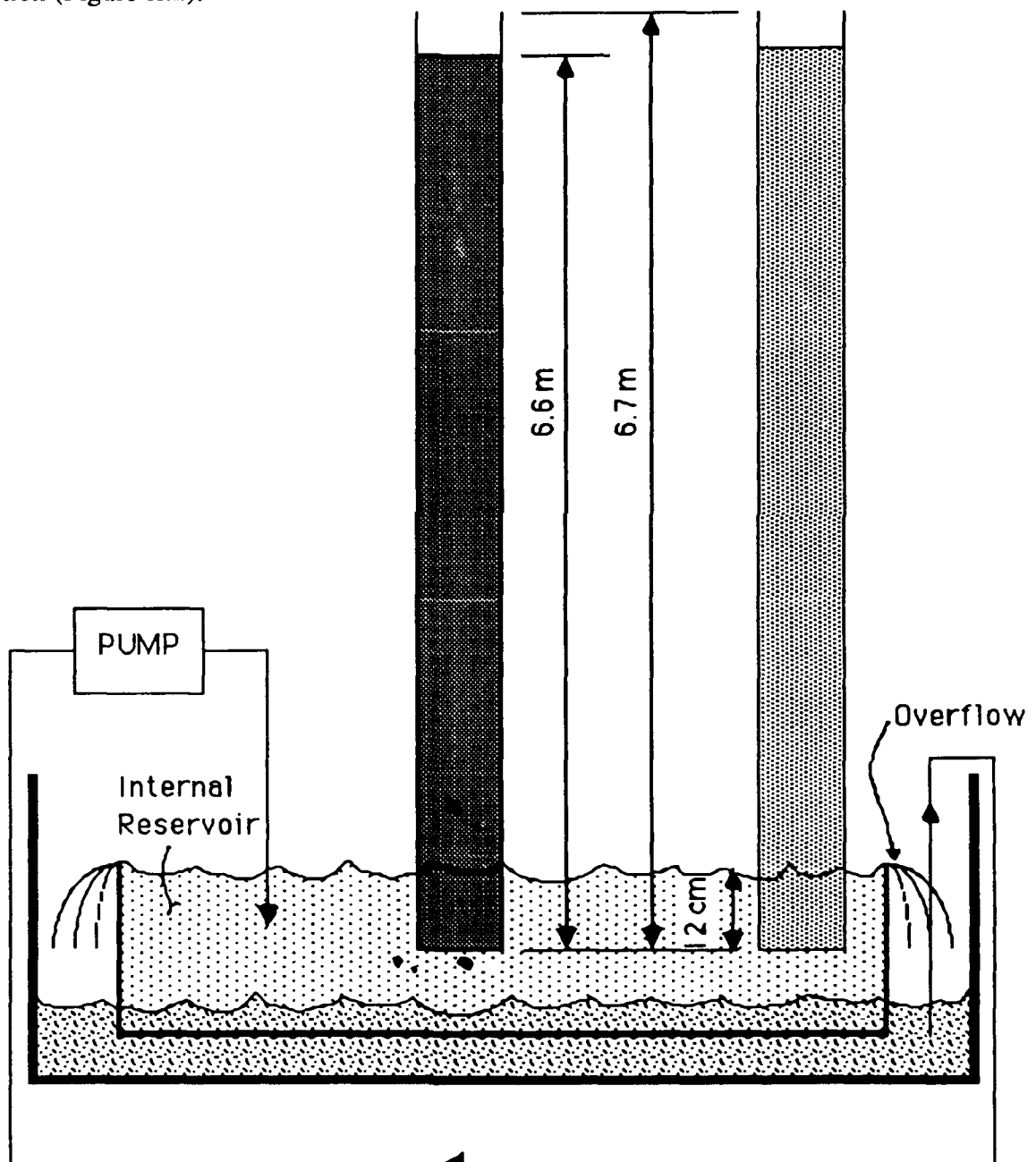
Figure II.2 Apparatus for Equilibration of Simulated Soil Columns with Water

11

The simulated soil solution was kept at constant level and recirculated by pumping. The bottom ends of the columns were covered with fine Teflon® mesh (Spectrum Medical Industries, Inc, Los Angeles, CA) to contain solids and allow free passage of solution. The columns were left open to the atmosphere at the top. No attempt was made to simulate the effects of precipitation on soil moisture.

Coated alumina and silica were each used as sorbents in the columns. The alumina, coated with humic acids to provide a low organic content comparable to that observed in subsurface aquifer materials, has been used in previous studies (Garbarini and Lion 1985; Gustafson, 1986; Peterson et al., 1988). Therefore, previous TCE vapor sorption studies were available to compare partition coefficients generated on moist coated alumina (Gustafson, 1986). Column results for silica were compared to those obtained in the constant humidity environments.

The columns were filled by hand after they were erected. Column contents were packed and air pockets eliminated by running a hand-held vibrating tool along the column length. Within hours after placing the column ends into the simulated soil solution, a capillary wetting front was visible in the coated alumina. The wetting front moved to 21 cm above the water surface, where it remained. The silica did not show an observable wetting front, but the consistency of the silica changed with the addition of moisture. Wetted silica occupied less volume than dry silica, so air pockets formed above the wet solid. Air pockets were removed by tapping the columns.

The columns were taken down after 3 months of exposure. The tubing was sliced into sections which were sealed at both ends with Parafilm and placed into double zip-lock plastic bags to preserve the moisture contents. The size of column sections allowed for sufficient sample to determine moisture contents and to obtain a TCE partition coefficient using the methods described below.

4. Sorption From The Vapor Phase

Vapor phase partition coefficients (K_d') were determined using the headspace analysis technique of Peterson et al. (1988). The procedure is based on a comparison of two systems, each a gas-tight bottle. One system contains sorbent and the other (blank) has no sorbent. By injecting the same mass of sorbate (TCE or toluene vapor) into each system, the mass balances in each can be equated:

$$C_{g1} V_1 = C_{g2} V_2 + X \hspace{4cm} \text{II.4}$$

where:

C_{g1} = gaseous phase equilibrium concentration in blank

C_{g2} = gaseous phase equilibrium concentration in sample

V_1 = blank bottle volume

V_2 = sample bottle volume

X = mass of sorbate sorbed

If the vapor obeys a linear adsorption isotherm (see Appendix, Equation A.17), substitution into Equation II.4 and rearrangement gives:

$$\frac{C_{g1}V_1}{C_{g2}V_2} = K_d' \frac{M}{V_2} + 1 \qquad \text{II.5}$$

Plotting the sample mass over bottle volume versus the ratio of gaseous sorbate mass in the blank and sample bottles gives a slope of K_d' and an intercept of 1.0. No attempt was made to force the intercept through the point (0, 1). The deviation of the actual intercept from the theoretical value was used as a check on model applicability. Partition coefficients were determined by linear regression on the isotherm data points. In comparisons, overlap of 95 percent confidence intervals for isotherm slopes (K_d') indicates that partition coefficients were not significantly different.

Use of Equation II.5 is valid only in the lower, linear portion of the vapor sorption isotherm since a linear partition coefficient definition is assumed in the derivation. For the experimental conditions used in the tests described here, the assumption of isotherm linearity is likely to be obeyed (see below).

Procedures for determining solid-vapor partitioning coefficients were modified by Peterson et al. (1988) from techniques developed by Garbarini and Lion (1985) to examine solid-liquid partitioning. The test procedure employed is briefly described here. Sixty mL serum bottles representing blanks (no sorbent), or containing a range of sorbent masses were injected with sorbate vapor by gas-tight syringe (Precision Sampling Corp., Baton Rouge, LA), and immediately sealed with rubber/Teflon® septa and aluminum tear-away seals (Supelco, Inc., Bellefonte, PA). Sorbate vapor was 1 mL of headspace from sealed source bottles containing liquid sorbate at 25°C. Sample bottles and blanks were then placed in a tumbler to ensure vapor contact with all particles. Approximately 1 1/2 hours before sampling, bottles were removed from the tumbler and put into a 25°C circulating water bath. Bottles were kept at 25°C for both tumbling and quiescent phases of the equilibration period.

13

Bottles were sampled by withdrawing a 1 mL vapor sample with a gas-tight syringe and injecting it into a Hewlett-Packard 5890 Gas Chromatograph with a HP 3392A Integrator. The gas chromatograph, equipped with a column of 0.1 percent Carbowax 1500, 20 percent SP 2100 on 100/180 mesh Supelcoport® (Supelco, Inc.), was operated isothermally at 135°C for TCE, and 150°C for toluene.

Preliminary kinetic tests were conducted to determine the length of time required to reach equilibrium. Bottles with the same sample mass and blanks were injected, and a set of bottles was sampled at different times after injection ranging from 1/2 to 72 hours. Equilibrium in silica/TCE systems was reached after 4 hours (Figure II.3). An 8-hour equilibrium period was chosen for TCE vapor sorption experiments to include a safety factor. Toluene vapor kinetics tests also indicated that an 8-hour equilibrium time was satisfactory).

TCE/Silica Kinetics
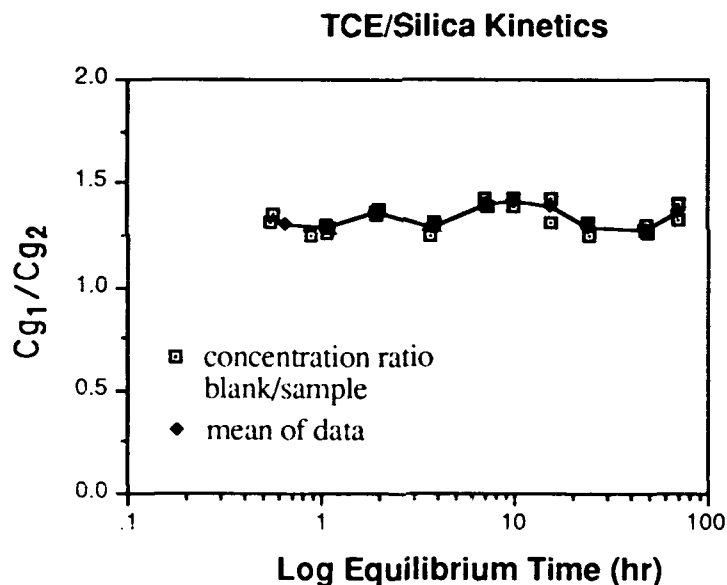
Figure II.3 Sorption Kinetics for TCE Vapor onto Silica

A kinetics experiment was also conducted using a soil sample (44U12) and toluene to verify that this compound was not degraded by soil microorganisms within the time interval required to reach equilibrium. Headspace analysis to determine partition coefficients is valid only if equilibrium has been reached and if sorption is the only mechanism for removing volatile organics from the gaseous phase. The kinetic results confirmed the validity of an 8-hour equilibrium time for toluene vapor experiments (Figure II.4), and indicated that any loss of toluene through microbial metabolism was negligible.
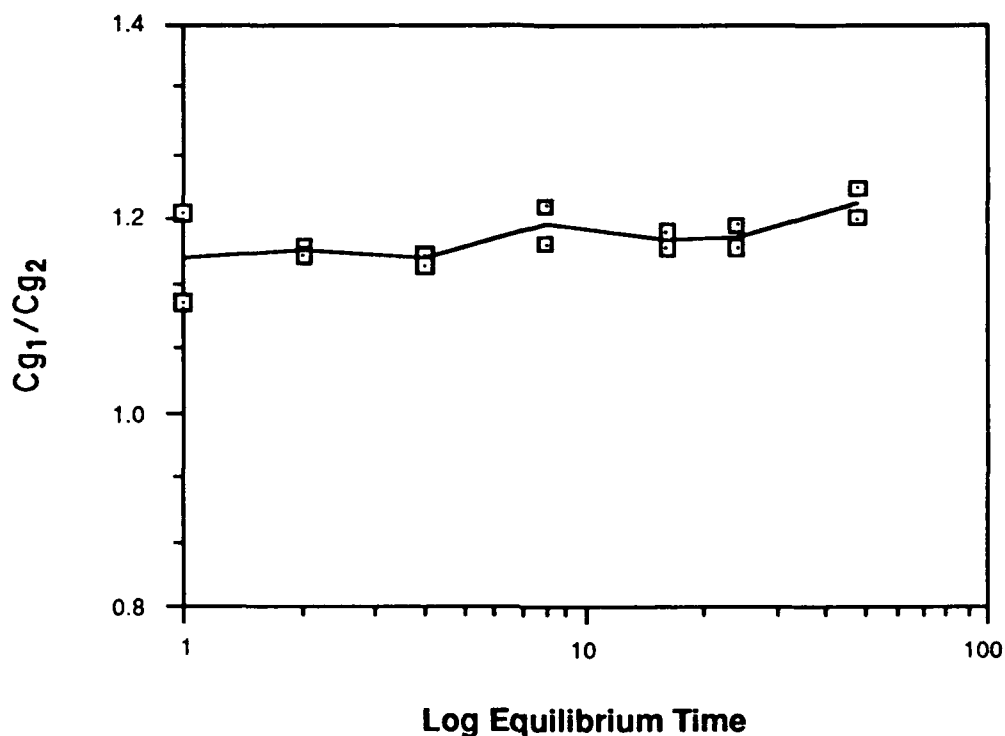
Figure II.4 Sorption Kinetics for Toluene on Soil Sample 44U12

The range of sample masses used for an isotherm varied depending on the sorbent and moisture conditions. More sample mass was required when the sorbent was moist or not porous. The upper limit was determined by the size of the serum bottles. When the sorbents were inorganic solids, replicates were used at each sample mass. Because the amount of sample in soil core 44U was limited and moisture would be lost during weighing before the bottles could be sealed, replicates were not used. In these cases, a range of soil masses was obtained by varying the amount of soil placed into tared bottles. Soil mass was then determined by weighing after sorbate vapor was injected and the bottles sealed.

5. Sorption From The Aqueous Phase

Headspace analysis can also be used to determine partition coefficients in saturated systems (K_d). As in vapor-liquid systems, the basis is a mass balance between two bottles injected with equal sorbate mass, one bottle with sorbent and one blank.

15

The presence of an aqueous phase requires additional terms in the mass balance equations for the two bottles:

$$C_{g1}V_{g1} + C_{L1}V_{L1} = C_{g2}V_{g2} + C_{L2}V_{L2} + X \qquad \text{II.6}$$

where:

C_{g1} = gaseous phase equilibrium concentration in blank

C_{g2} = gaseous phase equilibrium concentration in sample

C_{L1} = liquid phase equilibrium concentration in blank

C_{L2} = liquid phase equilibrium concentration in sample

V_{g1} = volume of gas in blank

V_{g2} = volume of gas in sample

V_{L1} = volume of liquid in blank.

V_{L2} = vclume of liquid in sample

X = mass of sorbate sorbed

If the partition coefficient K_d is defined by a linear adsorption isotherm:

$$\frac{X}{M} = K_d\, C_{L2} \qquad \text{II.7}$$

and the relationship between the concentration of sorbate in the gaseous and liquid phases at equilibrium is given by Henry's Law:

$$C_g = H_c C_L \qquad \text{II.8}$$

then combining equations II.6, II.7, and II.8 gives (see Peterson et al., 1988):

$$\left(\frac{C_{g1}}{C_{g2}}\right)\left(\frac{V_{g1}H_c\,\gamma + V_{L1}}{V_{g2}H_c\,\gamma + V_{L2}}\right) = K_d\left(\frac{M}{V_{g2}H_c\,\gamma + V_{L2}}\right) + 1 \qquad \text{II.9}$$

Plotting the left hand side of Equation II.9 versus the sample mass divided by a combined liquid and modified gas volume gives a slope equal to the saturated partition coefficient (K_d) and an intercept of 1.0.

Using the above computational procedure, headspace analysis for determining partition coefficients is limited to the linear portion of the adsorption isotherm. It is also valid only if the sorbent does not significantly contribute to the ionic strength of the

aqueous solution. To prevent this, a 0.1 M NaCl solution was used for the aqueous phase as a swamping electrolyte. Garbarini and Lion (1985) have shown that this electrolyte has no significant effect on sorption partition coefficients of TCE. Headspace analysis is most accurate for sorbates with low Henry's Constants (<3.0) and sorbents with high sorptive capacity (Garbarini and Lion, 1985). Partition coefficients for sorbents with low capacity (K_d < 0.5 mL/g) can be determined by increasing the mass of sorbent. The dimensionless Henry's Constants for TCE (0.397) and toluene (0.261), and aqueous ionic activity coefficients for TCE in 0.1 M NaCl (1.055) and toluene in 0.1 M NaCl (1.054) reported by Garbarini and Lion (1985) were assumed in this study.

Experiments to determine saturated partition coefficients were conducted in 60 mL serum bottles. Twenty mL of 0.1 M NaCl solution were pipetted into blank bottles and sample bottles containing a range of sorbent masses. TCE or toluene was added in solution as 100 μL aliquots of aqueous solution using an Eppendorf pipette. The TCE solution was TCE-saturated distilled water. The toluene stock solution was prepared by dissolving 500 μL of toluene in 2 L of distilled water. Sample bottles were immediately capped with Teflon®/rubber septa and aluminum tear-away seals (Supelco, Inc.). Bottles were placed in a tumbler, then removed to a water bath for 1 1/2 hours before sampling, both maintained at 25°C. Equilibrium times were 8 hours for toluene and 24 hours for TCE (Garbarini, 1985). Bottles were sampled by withdrawing 1 mL of headspace by Pressure-Lok syringe, and GC analysis as described above.

The partition coefficient measured in saturated conditions must be modified by Henry's Constant and the activity coefficient before direct comparison can be made to vapor-phase partition coefficients. Recall the linear isotherm definitions of both K_d and K_d':

$$\frac{X}{M} = K_d C_{L2} \qquad\qquad \text{II.10}$$

$$\frac{X}{M} = K_d' C_{g2} \qquad\qquad \text{II.11}$$

Using Henry's Law, and rearranging gives:

$$K_d' = K_d \left(\frac{C_L}{C_L H_c \gamma} \right) = \frac{K_d}{H_c \gamma} \qquad\qquad \text{II.12}$$

The saturated partition coefficients can therefore be compared to vapor partition coefficients by dividing them by the appropriate Henry's Constant and activity coefficient.

17

C. RESULTS AND DISCUSSION

1. Sorbent Characterization

a. Well-Defined Solids

Results of the physical/chemical characterizations of silica and coated alumina are summarized in Table II.2. Organic carbon, was low for the silica, as expected. The alumina coated with humic acids to provide organic carbon, had an organic carbon content of 0.48 percent. This is within the typical range of 0.3 to 3.0 percent organic carbon for surface mineral soils (Bohn et al., 1979).

Mercury porosimetry provided measurements of total pore volume, porosity, and pore size distributions as well as an estimate of specific surface area. Total porosity (pore volume/total sample volume) was higher for the alumina, which is expected because of the porous nature of adsorption alumina and the humic acid coating it. The modal pore diameter given in Table II.2 was used to characterize pore size distribution for silica and coated alumina.

Mean moisture contents induced in silica by placing solids in different relative humidity environments are listed in Table II.3. Each moisture content represents a separate isotherm measurement. Variations in moisture content within each experiment were occasionally large as shown by the coefficients of variation. The silica in the simulated soil column (Table II.4) reached much higher moisture contents than those achieved in environments of fixed relative humidity. The silica in the column was essentially air-dry (ambient laboratory humidity) until approximately 100 cm above the water level. Moisture levels increased to 40 percent approaching the water level. The highest moisture content of 46 percent was obtained in silica below the water level. Moisture contents within the coated alumina simulated soil column are also given in Table II.4. Most of the coated alumina was "air-dry". Moisture content started to rise at the wetting front, located at 21 cm above the water level. The moisture content reached a maximum of 69 percent below the water level.

TABLE II.2. CHARACTERISTICS OF SILICA AND COATED ALUMINA.

Parameter	Silica	Coated Alumina[†]
Surface Area (g/m^2)		
BET-N$_2$ adsorption	4.83[*]	206[**]
EGME $\pm$ S.D. (C.V.)	8.70 $\pm$ 1.1 (13%)	250 $\pm$ 1.90 (0.76%)
Hg porosimetry	8.44	37.4
Porosimeter Data		
Pore volume (mL/g)	1.20	0.708
Porosity (percent)	69.8	78.0
Modal pore diameter (μ)	65.2	37.6
Organic Carbon (percent)	0.012*	0.48**

† see Section III for data on the aluminum oxide prior to coating
* S. Lindner, unpublished results
** Gustafson (1986)

TABLE II.3. INDUCED MOISTURE CONTENTS FOR SILICA.

% Mean Moisture Content $\pm$ S.D. (C.V.)	Range (%)	Method
0	-	oven-dry
0.066 $\pm$ 0.0028 (4.2%)	0.064-0.068	sat. CaCl$_2$ solution
0.095 $\pm$ 0.031 (33%)	0.052-0.14	sat. CaCl$_2$ solution
0.48 $\pm$ 0.061 (13%)	0.41-0.53	air-dry
0.58 $\pm$ 0.21 (36‘)	0.24-0.73	air-dry
0.62 $\pm$ 0.14 (23%)	0.45-0.80	37°C over water
0.72 $\pm$ 0.15 (21%)	0.55-0.88	37° C over water
1.6 $\pm$ 0.48 (30%)	1.0-2.2	37° C over water
3.1 $\pm$ 0.39 (13%)	2.8-3.7	37° C over water
5.2 $\pm$ 0.76 (14%)	4.7-5.8	37° C over water

TABLE II.4. MOISTURE CONTENTS AT DIFFERENT HEIGHTS FROM THE
BOTTOM IN SIMULATED SOIL COLUMNS CONTAINING
SILICA AND COATED ALUMINA

SILICA		COATED ALUMINA	
Height (m)	Moisture Content (%)	Height (m)	Moisture Content (%)
6.10	0.14	5.97	5.4
5.49	0.17	4.75	6.0
4.88	0.17	3.53	6.2
4.20	0.15	2.92	6.2
3.66	0.16	2.31	6.1
3.05	0.15	1.70	6.3
2.44	0.21	1.09	6.3
2.13	0.23	0.785	6.7
1.83	0.16	0.632	6.5
1.22	3	0.480	9.8
0.914	41	0.328	12
0.610	39	0.277	30
0.457	40	0.226	48
0.07 2	46	0.175	58
		0.0509	69

b. Soil Core 44U

Soil core samples were sandy, with low organic carbon and cation exchange capacities (Table II.5). The samples were almost pure sand of varying ratios between medium and fine sand, with traces of coarse sand and of silt and clay. The sample closest to the surface (sample 44U1) was the only sample to fall within the range of organic carbon typical of surface mineral soils. Organic carbon dropped sharply in deeper samples, then declined gradually with depth. Cation exchange capacity (CEC) is associated with clays and organic matter in soils. The CEC of these samples was low, as expected from the small amount of organic carbon and clay they contain. The depth profile of CEC is qualitatively similar to that of organic carbon.

TABLE II.5. SELECTED CHARACTERISTICS OF SOIL CORE 44U vs DEPTH.

Sample Number	Depth (m)	Organic Carbon (%)	CEC (meq/100 g)	Particle Size (%)			
				Coarse Sand	Medium Sand	Fine Sand	Silt and Clay
44U1	0.15-0.38	0.33	4.5	0.59	36	62	0.64
44U2	0.38-0.64	0.058	3.0				
44U3	0.66-0.89	0.029	1.5	0.65	28	71	0.26
44U4	0.91-1.14	0.020	1.0				
44U5	1.17-1.40	0.022	1.0				
44U6	1.42-1.65	0.021	1.5	0.46	19	80	0.11
44U7	1.68-1.90	0.020	1.0				
44U8	1.93-2.16	0.015	1.5	0.35	29	71	0.15
44U9	2.18-2.41	0.018	1.0				
44U10	2.44-2.64	0.017	1.0				
44U11	2.67-2.90	0.014	1.5				
44U12	2.92-3.18	0.008	1.0				
44U13	3.18-3.40	0.008	1.0	0.74	25	74	0.20

Specific surface areas are given in Table II.6. Nitrogen adsorption and mercury porosimetry were performed on single samples; the EGME surface area is an average of up to four samples. The lowest surface area values were given by the weakly sorbed nitrogen. The largest values were obtained by the EGME method. This was expected as this method requires material to be sieved through a No. 60 sieve (0.25 mm) which removes large solid particles with a low specific surface area. The EGME method also measures the interlamellar surface of any expanding clay minerals, unlike nitrogen adsorption or mercury porosimetry. The surface sample (44U1) had the largest specific surface area in all three methods. Student's t tests comparing pairs of methods showed that surface areas measured by different methods were statistically different at the 99.9 percent level.

TABLE II.6. SPECIFIC SURFACE AREAS (m^2/g) OF SOIL CORE 44U BY THREE DIFFERENT METHODS.

Sample Number	N_2 Adsorption	Hg Porosimeter	EGME + S.D. (% C.V.)
44U1	1.98	2.56	16.6 ± 3.21 (19)
44U2	0.866	1.11	7.96 ± 0.261 (3.3)
44U3	0.298	1.28	3.82 ± 0.832 (22)
44U4	0.201	1.29	3.23 ± 0.177 (5.5)
44U5	0.193	1.16	2.65 ± 0.401 (15)
44U6	0.283	1.01	2.69 ± 0.425 (16)
44U7	0.228	0.881	4.72 ± 1.18 (25)
44U8	0.247	1.56	5.17 ± 1.39 (27)
44U9	0.341	1.48	2.17 ± 0.743 (34)
44U10	0.359	1.68	1.47 ± 0.455 (31)
44U11	0 217	1.05	2.65
44U12	0.177	1.65	2.79 ± 0.921 (33)
44U13	0.172	1.18	3.78 ±0.446 (12)

The sandy nature of these soils is reflected in their low surface area measurements. Surface areas are greatly enlarged by the presence of clays and organic matter, both of which were found only in trace amounts in this soil. Organic matter, for example, has a surface area of 800-900 m^2/g (Bohn et al., 1979), and the addition of 0.48 percent organic matter to adsorption alumina increased the surface area by 30 percent (see Section III).

Pairwise linear regressions of soil parameters (Table II.7) showed that organic carbon content, CEC, and surface area were all closely related in the core samples. With respect to specific surface area, the best correlation was between the N_2 adsorption method and the EGME method. As discussed in Section II.B., surface area as measured by porosimetry is an approximation based on the assumption of cylindrical pores, which may explain its low correlation with the other measurements of this property.

TABLE II.7. COEFFICIENTS OF DETERMINATION , r^2, FOR SELECTED
PARAMETERS OF SOIL CORE 44U.

| Soil Parameter | CEC | Surface Area | | |
		BET	Porosimetry	EGME
Organic carbon	0.82	0.94	0.61	0.89
CEC		0.92	0.37	0.89
BET			0.55	0.90
Porosimetry				0.49

Mercury porosimeter data showed no striking differences between samples in soil core 44U (Table II.8). Pore volume was quite consistent over depth, but modal pore diameters varied considerably. Pore size distributions were characterized by modal pore diameter. Porosity values were in the 40 to 50 percent range typical of sandy soils (Lambe, 1951).

TABLE II.8. PORE VOLUME, MODAL PORE DIAMETER, AND POROSITY DATA
FROM MERCURY POROSIMETRY FOR SOIL CORE 44U SECTIONS.

Sample Number	Pore Volume (mL/g)	Modal Pore Diameter (μ)	Porosity (percent)
44U1	0.254	163	38.8
44U2	0.287	149	46.6
44U3	0.274	114	45.8
44U4	0.273	93.5	45.5
44U5	0.274	94.7	45.8
44U6	0.280	93.5	46.9
44U7	0.262	93.5	43.8
44U8	0.257	143	42.9
44U9	0.237	85.9	39.8
44U10	0.279	69.3	46.6
44U11	0.269	94.5	45.1
44U12	0.270	129	45.2
44U13	0.274	115	45.8

Ambient moisture of soils was measured shortly after arrival at Cornell by averaging the moisture content of three samples from each depth. Table II.9 lists the results plus standard deviation and coefficient of variation. The ambient moisture profile was concave vs depth with more moist soils near the surface and the water table. The deepest sample contained the capillary fringe and extended into the water table. These moisture contents cover the range typically found in sandy soils. Moisture contents were checked at later dates as soils were oven dried for bottle experiments. Sample moisture contents stayed relatively constant over time, proving the effectiveness of storage in double polyethylene bags at 4°C.

TABLE II.9.   AMBIENT MOISTURE CONTENTS FOR SOIL CORE 44U
MEASURED ON SEVERAL DIFFERENT DATES.

Sample No.	9/22/86 % Mean Moisture Content ± S.D. (C.V.)	12/13/86 Moisture Content (%)	1/8/87 Moisture Content (%)
44U1	5.37 ± 0.30 (5.4)	6.06	6.01
44U2	3.98 ± 0.095 (2.4)	4.00	3.97
44U3	2.58 ± 0.015 (0.59)	2.62	2.54
44U4	2.99 ± 0.053 (1.8)	7.00	2.82
44U5	4.24 ± 0.20 (4.7)	4.17	4.07
44U6	3.85 ± 0.18 (4.5)	3.72	3.68
44U7	4.13 ± 0.10 (2.5)	4.16	4.19
44U8	3.68 ± 0.12 (3.4)	4.06	3.93
44U9	3.76 ± 0.26 (6.8)	3.94	4.00
44U10	5.10 ± 0.48 (9.5)	4.59	4.50
44U11	5.16 ± 0.11 (2.1)	5.77	5.02
44U12	11.6 ± 1.3 (11)	11.8	12.0
44U13	18.6 ± 0.66 (3.5)	17.6	18.2

2. Partition Coefficients

Sorption of TCE or toluene vapor onto silica, coated alumina, and soil core 44U was characterized by the vapor partition coefficient, K_d', obtained from the slope of the best fit line through isotherm data points fit to Equation II.5. The basis for selection of this form of the linear isotherm equation is discussed in detail in Section VI. An example of an isotherm (Figure II.5a) for TCE sorption onto silica with 0.066 percent moisture content shows the linear regression line, and demonstrates the applicability of a linear sorption model.

Different ranges of sample masses were used in bottle experiments depending on the sorptive capacity of the sorbent. The practical lower limit was the sample mass at which detectable sorption could be observed compared to blank bottles. The upper limit was determined most often by the physical bottle size or by the need to keep all soil particles below the liquid level in saturated experiments. It was also considered desirable to minimize alterations in GC range settings, which limited the range of sample masses employed with the more porous sorbents. Table II.10 lists the ranges of sample masses used for the different sorbate/sorbent combinations.

The number of data points per isotherm varied according to sorbent. Usually six to eight different sample masses spread over the ranges listed below were used to construct an isotherm. Three replicates at each sample mass were used in experiments with silica exposed to different humidities. This produced an isotherm as in Figure II.5a. Replicates were not the exact same mass because prolonged weighing meant exposure to ambient humidity, which might have changed the moisture content. When the amount of sorbent was limited, as in the simulated soil columns, replicates were not used. Slices of simulated soil columns were made as thin as possible to minimize moisture content change within each slice. Isotherms from the silica soil column contained only two or three data points; the isotherms from the coated alumina column each had four data points (Figure II.5b). Sample quantities were also limited for soil core 44U; therefore isotherms typically contained six to eight data points without replicates as illustrated in Figure II.6. Raw data used for construction of all isotherms have been tabulated by Swanger (1990).

Silica at 0.066% Moisture Content

a)

Slope = 4.71
Intercept = 1.03
r^2 = 1.00

$(C_{g1} V_1)/(C_{g2} V_2)$

Sample Mass/Bottle Volume

Coated Alumina at 6.2% Moisture Content

b)

Slope = 287
Intercept = 1.03
r^2 = 1.00

$(C_{g1} V_1)/(C_{g2} V_2)$

Sample Mass/Bottle Volume
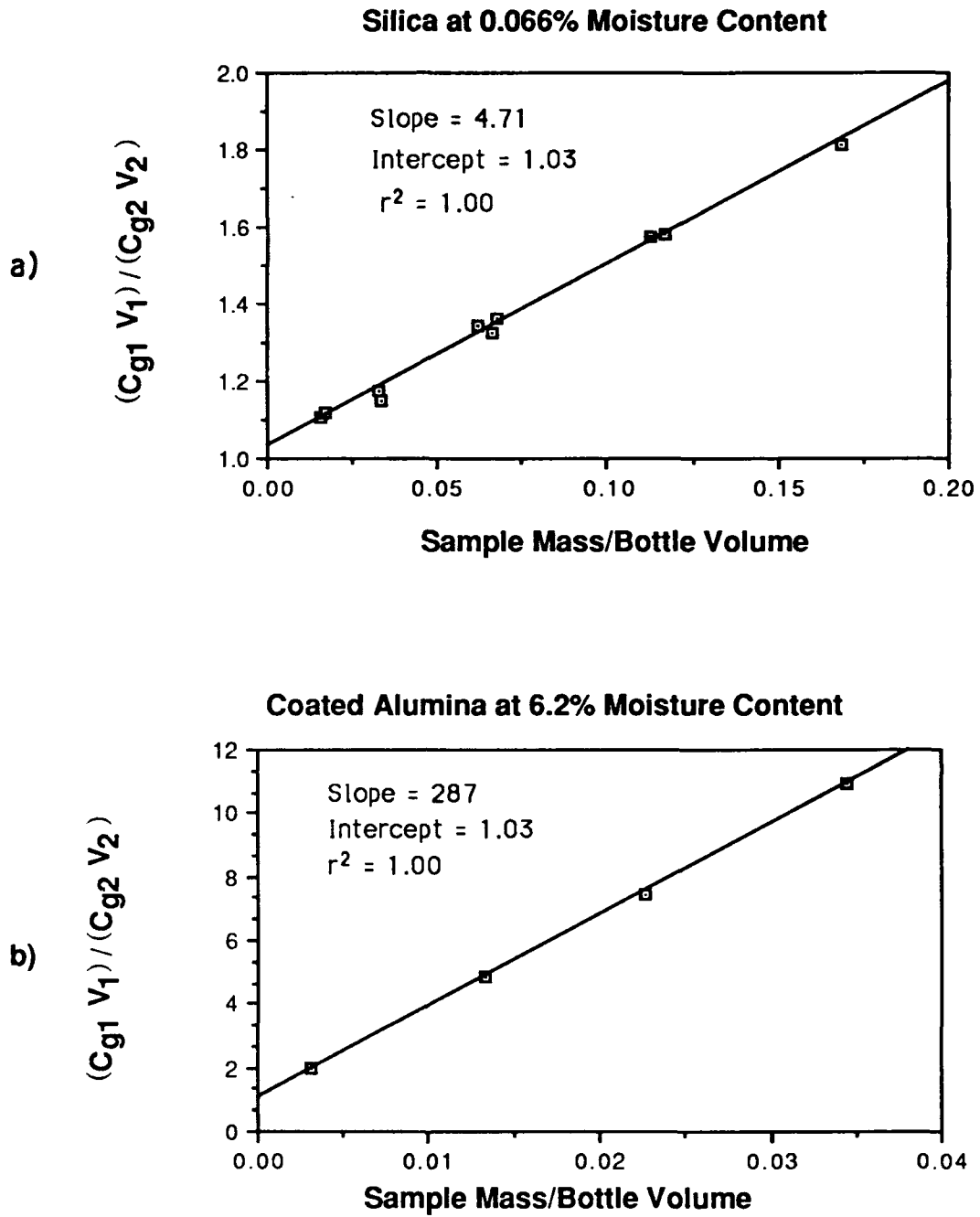
Figure II.5. Sample Isotherms for TCE Sorption onto: (a) Silica at 0.066 Percent Moisture Content, and (b) Humic-Coated Alumina at 6.2 Percent Moisture Content

26

a)

Section 44U1
5.37% moisture

Sample mass/bottle volume

b)

Section 44U3
Oven-dry

Sample mass/bottle volume

c)

Section 44U12
Saturated

Sample mass/volume
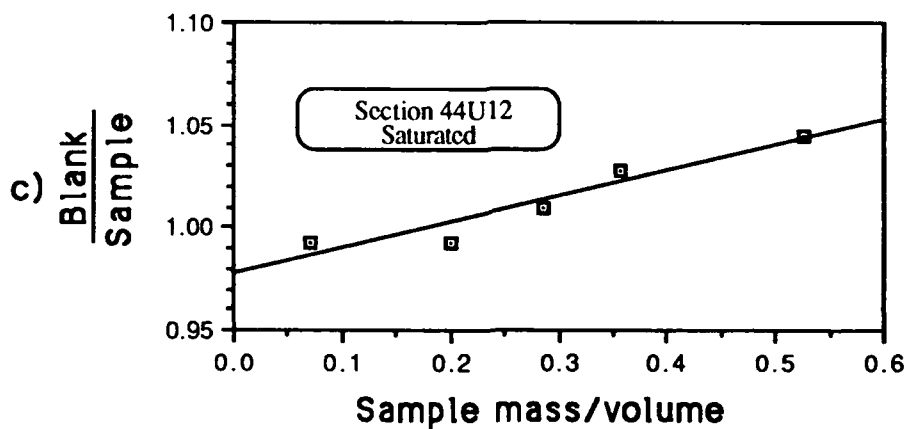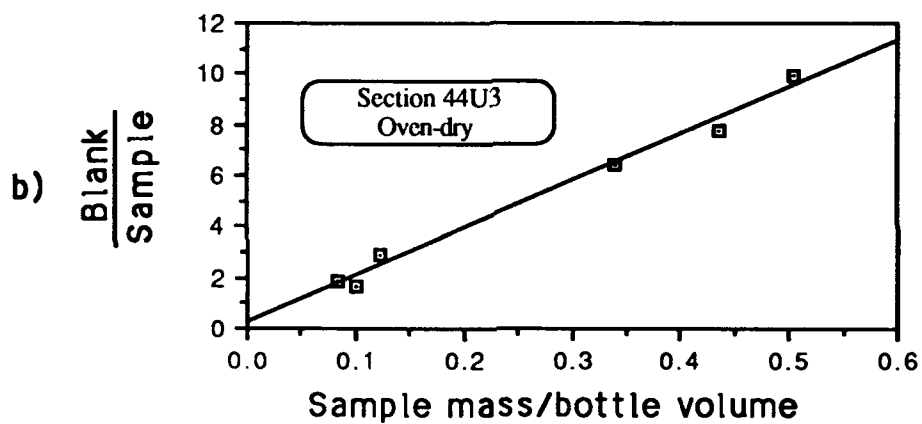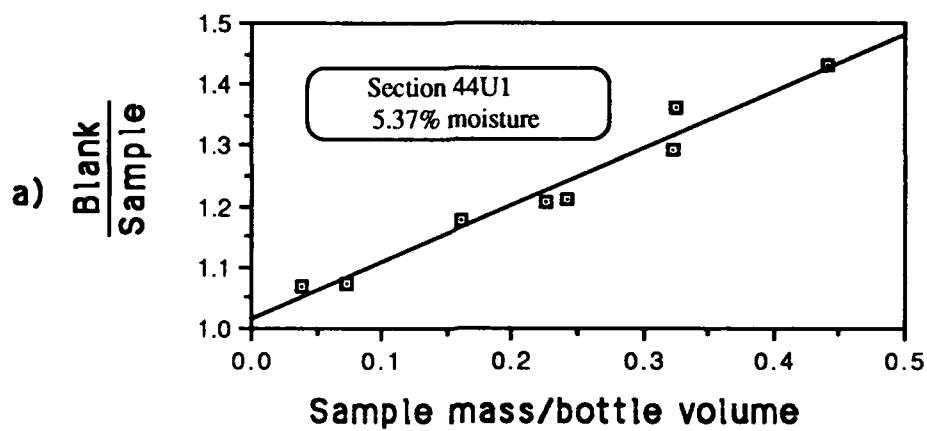
Figure II.6.   Example Isotherms for TCE Sorption onto Soil Core 44U at Three
                 Different Moisture Conditions

27

TABLE II.10. SAMPLE MASS USED IN ISOTHERM BOTTLE EXPERIMENTS.

Sorbent	Range of Sample Mass (grams)	
	TCE	Toluene
Silica		
controlled humidity	0.5-15	0.5-15
column	2-18	
Coated alumina	0.1-6.0	
Soil core 44U		
dry	1-35	1-35
ambient moisture	2-50	2-50
saturated	2-20	2-20

a. Well-Characterized Solids

Results of TCE sorption onto silica and coated alumina are listed in Tables II.11 and II.12. Confidence intervals at the 95 percent level are given for partition coefficients and intercepts. Partition coefficients for saturated experiments are presented both as saturated partition coefficients (K_d) and the equivalent partition coefficient on a gas concentration basis (K_d') to allow comparison with vapor partition coefficients. Adsorption isotherms for water vapor sorption onto silica and coated alumina (see Section IV) were used to convert moisture contents to relative humidities. Silica from different environments of controlled relative humidity was also used as a sorbent for toluene (Table II.13).

The effect of moisture on sorption of the organic vapors of interest is easily examined in silica and coated alumina because of their physical/chemical homogeneity and since a wide range of different moisture contents are available. A plot of partition coefficients versus moisture content for TCE sorption onto silica (Figure II.7a) shows a rapid decline in sorptive partition coefficient with increasing moisture. This decrease is much more gradual at moisture contents greater than 0.5 percent. Figure II.7b is a log-log plot of moisture content versus partition coefficient. This plot is linear ($r^2 = 0.99$) and may be fitted by the following empirical relationship:

$$\log K_d' = -0.62 \times \log \text{Moisture Content} - 0.094 \qquad \text{II.13}$$

28

TABLE II.11. PARTITION COEFFICIENTS AND INTERCEPTS WITH 95% CONFIDENCE INTERVALS, AND COEFFICIENTS OF DETERMINATION FOR TCE SORPTION ONTO SILICA AT DIFFERENT MOISTURE CONTENTS.

Moisture Content (percent)	$K_d' \pm$ C.I.	Intercept $\pm$ C.I.	r^2	Relative Humidity (percent)
Different Humidity Environments				
oven-dry	17.9 $\pm$ 1.1	0.75 $\pm$ 0.14	0.98	0
0.066	4.71 $\pm$ 0.26	1.0 $\pm$ 0.023	1.0	1.2
0.095	3.12 $\pm$ 0.13	1.0 $\pm$ 0.017	0.99	1.8
0.48	1.20 $\pm$ 0.16	0.99 $\pm$ 0.019	0.93	37
0.62	1.18 $\pm$ 0.15	1.0 $\pm$ 0.015	0.95	57
3.1	0.40 $\pm$ 0.16	1.0 $\pm$ 0.017	0.61	94
saturated	0.088 $\pm$ 0.11	1.0 $\pm$ 0.012	0.12	--
Simulated Soil Column*				
0.14	5.88	0.97	0.99	3.2
0.15	4.93	1.1	0.94	3.2
0.15	5.20	0.97	1.0	3.2
0.16	5.22	0.98	1.0	3.3
0.16	3.50	1.1	0.98	3.3
0.17	5.14	1.0	0.94	3.3
0.17	4.04	1.1	1.0	3.3
0.21	4.39	1.0	1.0	5.7
0.23	5.05	1.0	1.0	5.9
35	8.01	0.84	0.89	--
39	4.52	0.87	1.0	--
40	2.76	1.0	1.0	--
41	4.55	0.99	1.0	--
46	3.72	0.94	1.0	--

*Confidence intervals are not calculated because isotherms are based on as few as two data points in some cases.

TABLE II.12. PARTITION COEFFICIENTS AND INTERCEPTS WITH 95 PERCENT
CONFIDENCE INTERVALS, AND COEFFICIENTS OF
DETERMINATION FOR TCE SORPTION ONTO COATED ALUMINA
AT DIFFERENT MOISTURE CONTENTS.

Moisture Content (percent)	$K_d' \pm$ C.I.	Intercept $\pm$ C.I.	r^2	Relative Humidity (percent)
5.4	308 ± 10	1.0 ± 0.38	1.0	29
6.0	291 ± 15	0.93 ± 0.38	1.0	34
6.1	287 ± 8.4	1.0 ± 0.019	1.0	35
6.2	298 ± 1.0	1.1 ± 0.019	1.0	36
6.2	298 ± 0.63	1.1 ± 0.010	1.0	36
6.2	290 ± 11	0.94 ± 0.22	1.0	36
6.3	321 ± 24	0.84 ± 0.64	1.0	36
6.4	286 ± 6.0	0.98 ± 0.11	1.0	37
6.6	277 ± 3.6	0.99 ± 0.060	1.0	37
9.7	59.0 ± 4.8	1.0 ± 0.15	1.0	51
12	7.82 ± 4.4	1.1 ± 0.11	0.94	79
38	0.84 ± 2.1	1.0 ± 0.12	0.45	--
48	1.23 ± 1.2	0.98 ± 0.078	0.85	--
57	1.15 ± 0.24	0.98 ± 0.019	0.99	--
69	1.13 ± 0.81	0.99 ± 0.054	0.91	--

from Peterson et al. (1988)

0	11,900			0
8.2	207			42
11.6	53.9			72
saturated	0.29			--

Figure II.7.   Moisture Content vs Partition Coefficients for TCE Sorption on Silica on
(a) Linear Scale and (b) Log-log Scale

31

TABLE II.13. PARTITION COEFFICIENTS AND INTERCEPTS WITH 95 PERCENT
CONFIDENCE INTERVALS, AND COEFFICIENTS OF
DETERMINATION FOR TOLUENE SORPTION ONTO SILICA AT
DIFFERENT MOISTURE CONTENTS.

Moisture Content (percent)	$K_d' \pm$ C.I.	Intercept $\pm$ C.I.	r^2	Relative Humidity (percent)
oven-dry	226 ± 40	-3.4 ± 5.2	0.89	0
0.095	29.4 ± 2.0	0.85 ± 0.36	0.98	1.8
0.58	4.30 ± 0.15	0.96 ± 0.019	1.0	48
0.72	4.38 ± 0.32	1.0 ± 0.040	0.98	72
1.6	3.23 ± 0.45	1.0 ± 0.056	0.92	93
5.2	2.40 ± 0.40	1.0 ± 0.057	0.91	>100
saturated	-0.348 ± 0.49	1.0 ± 0.037	0.27	>100

TCE sorption onto low-moisture-content silica from the simulated soil columns was similar to that observed at low moistures obtained by different humidities. The decrease in TCE sorption with increasing moisture is consistent with other studies showing that water out-competes neutral or weakly polar organic vapors for available mineral sorption sites (Call, 1957; Yaron and Saltzman, 1972; Hance, 1977; and Chiou and Shoup, 1985). Based on the low moisture results, very low sorption ($K_d' < 0.5$ mL/g) was expected on the high moisture silica from the bottom section of the simulated soil column. However, instead of low K_d' values, partition coefficients for the wet silica were similar to partition coefficients for air-dry silica. This surprising result may reflect the uncertainty inherent in partition coefficients calculated from isotherms constructed with only two data points. At high moisture contents, the mass of TCE in solution will increase in proportion to the moisture content; this effect may help to explain the results at high silica moisture contents. The magnitude of this effect is discussed in Section III.

The same pattern of rapid decrease in partition coefficients and leveling off was shown by TCE sorption on coated alumina (Figure II.8) and toluene sorption on silica (Figure II.9a). Figure II.9b gives the same information on a log-log plot, represented by the empirical relationship:

$$\log K_d' = -0.62 \text{ X log Moisture Content} - 0.67 \qquad (r^2 = 0.87) \qquad II.14$$

32
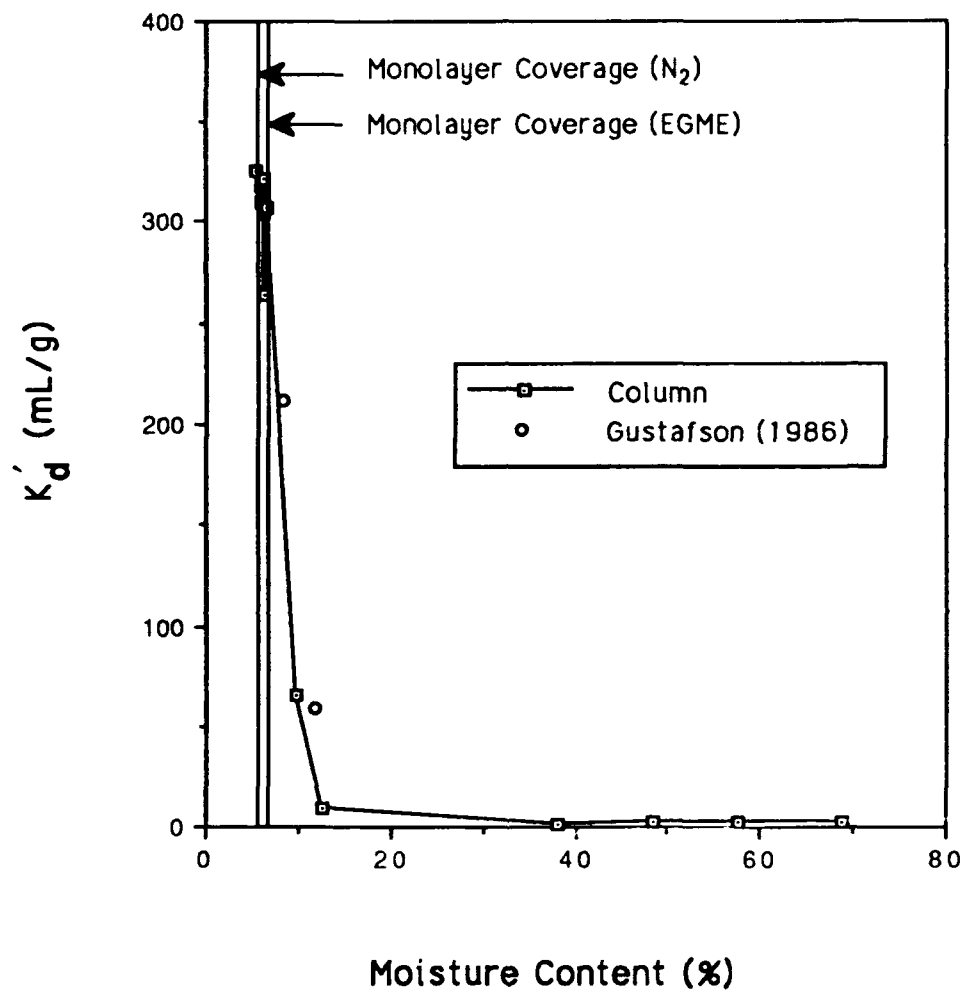
Figure II.8. Moisture Content vs Partition Coefficients for TCE Sorption on Coated Alumina.
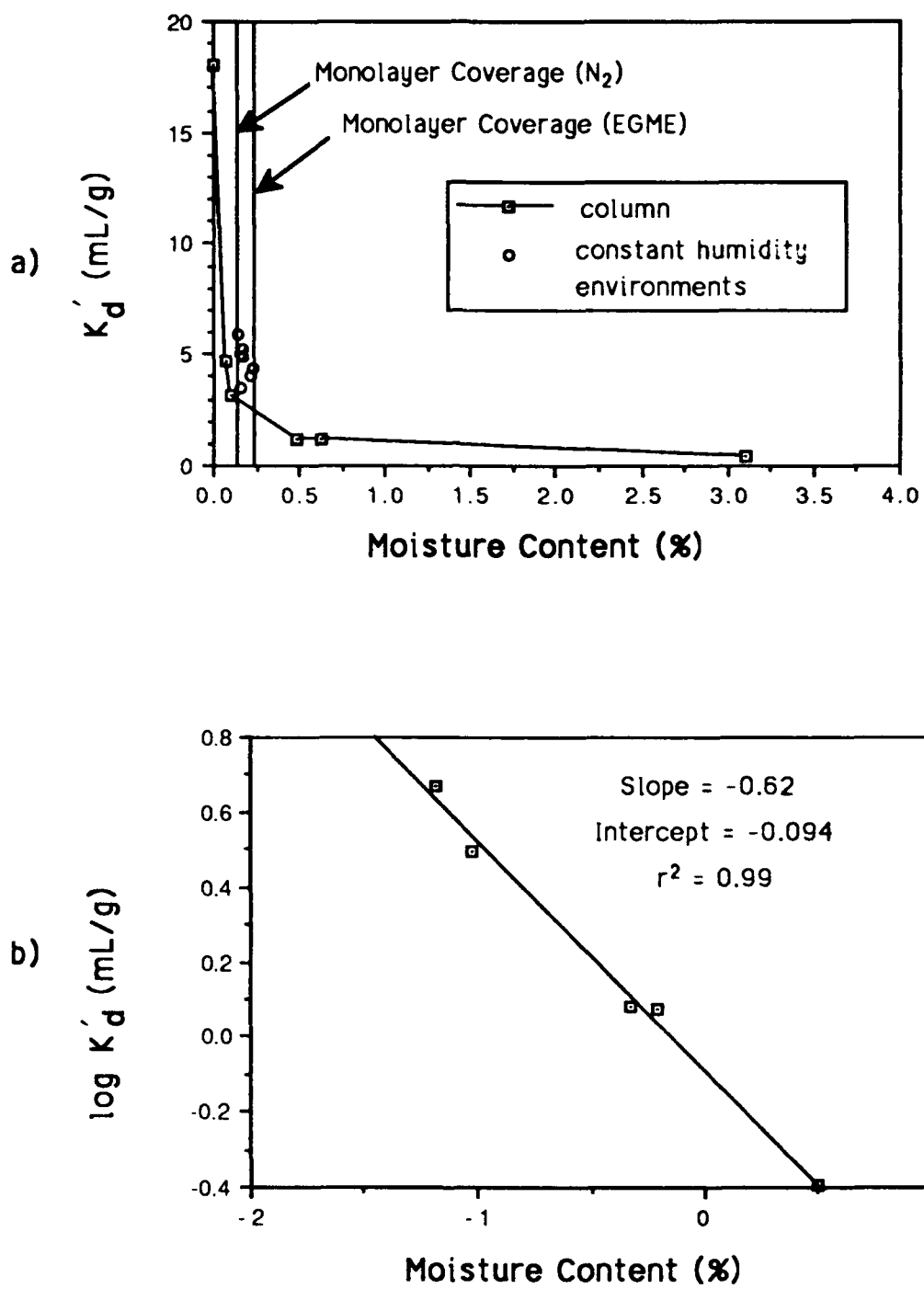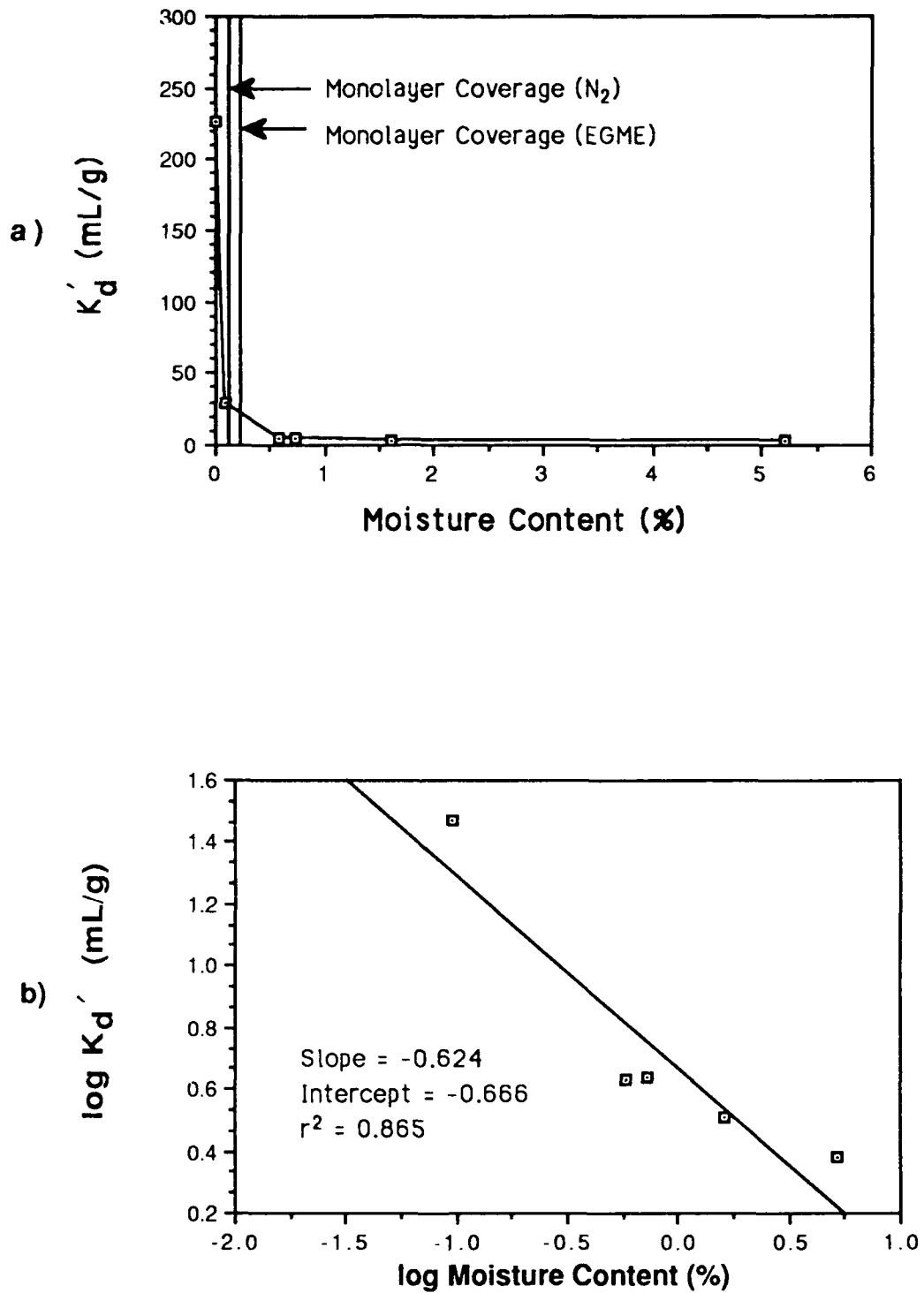
Figure II.9. Moisture Content vs Partition Coefficients for Toluene Sorption on Silica on (a) Linear Scale and (b) Log-log Scale

34

Hance (1977) related the flattening of his Freundlich K versus moisture content curve (see Appendix, Figure A.7) to monolayer coverage by water molecules. It is useful to look at the relationship between monolayer coverage of sorbent to sorption because in the unsaturated zone, the soil particle surfaces always have a layer of hygroscopic water. Using the BET and EGME surface areas for silica and coated alumina and a cross-sectional area of water molecules of 10.8 $\mathring{A}^2$ (Lowell and Shields, 1984), the moisture contents corresponding to monolayer coverage were calculated (Table II.14).

TABLE II.14. MOISTURE CONTENTS AND RELATIVE HUMIDITIES CORRESPONDING TO MONOLAYER COVERAGE BY WATER

Solid	Moisture Content (percent)		Relative Humidity (percent)	
	N_2	EGME	N_2	EGME
Silica	0.13	0.24	3.1	6.0
Coated alumina	5.7	6.9	26	30

Monolayer coverage by water molecules is indicated on Figures II.7a, II.8, and II.9a. Monolayer coverage does occur relatively near the horizontal asymptote of the plot of K_d' vs moisture content in silica, but not in coated alumina. The partition coefficient for TCE vapor sorption onto dry coated alumina (Peterson et al. 1988) was not included in Figure II.8 for scaling purposes. From dry coated alumina to monolayer coverage, the partition coefficients declined by a factor of 40, so a significant reduction in sorption preceded the formation of a water monolayer. From monolayer coverage to the flattening of the curve (moisture content $\approx$ 12 percent), partition coefficients again declined by an additional factor of 40.

Graphs of partition coefficients versus relative humidity show the same decrease and flattening with increasing humidity for silica (Figure II.10a). For coated alumina, the decline with relative humidity is more gradual (Figure II.10b). A gradual decline of sorption on soils with increasing humidity was found in several other studies (Call, 1957; Yaron and Saltzman, 1972; and Chiou and Shoup, 1985). Chiou and Shoup (1985) found that the sorption capacity of their silt loam soil at 90 percent relative humidity was equivalent to that of a saturated aqueous system. The relative humidities corresponding to monolayer coverage of silica and coated alumina (Table II.14) are marked on Figure II.10.
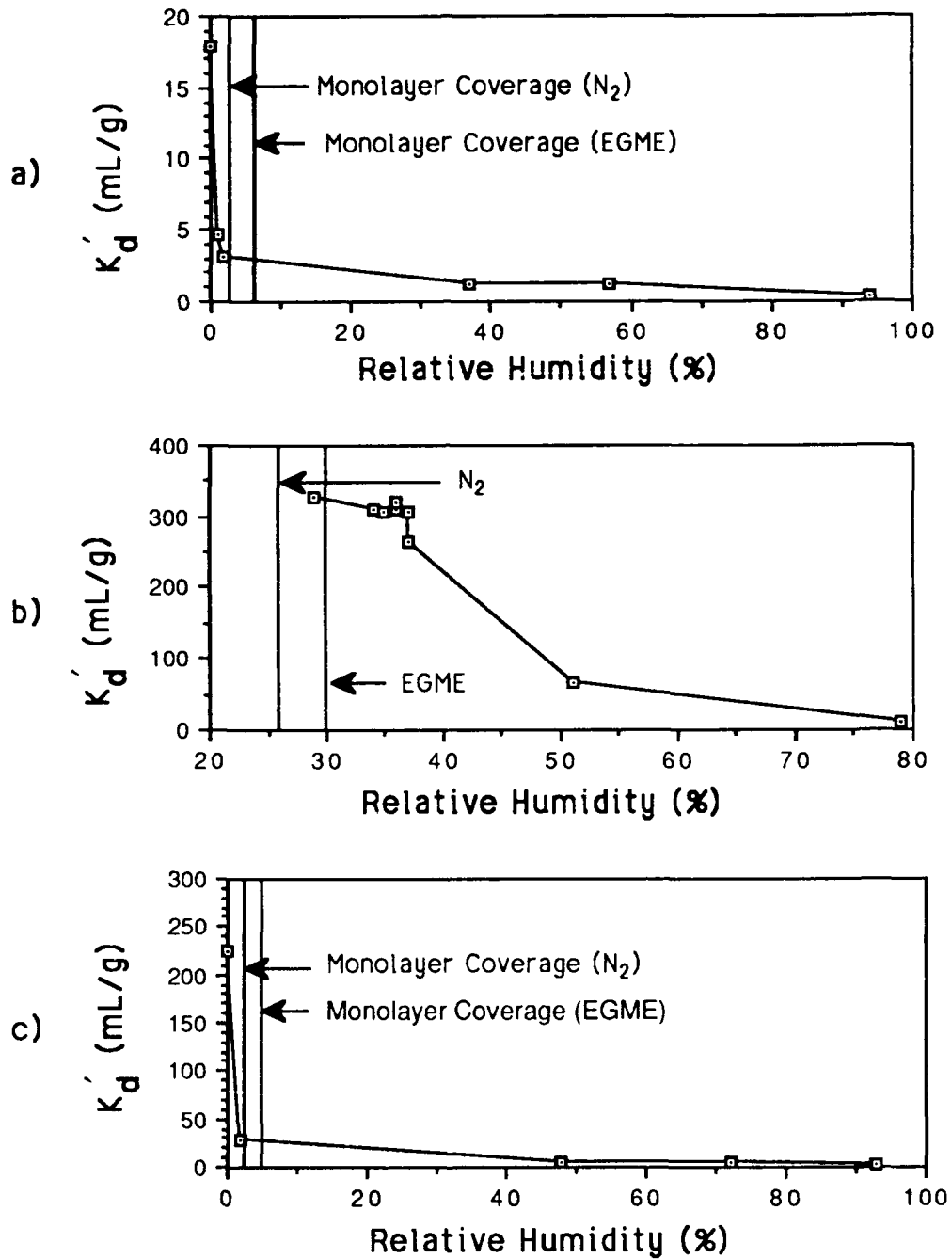
Figure II.10.   Relative Humidity vs Partition Coefficients for Sorption of (a) TCE on
Silica (b) TCE on Coated Alumina and (c) Toluene on Silica

36

Relative humidities at monolayer coverage (18 percent) for silt loam (Chiou and Shoup, 1985) and 10 percent for four other different soils (Call, 1957) fall with. the range observed in this study. Chiou and Shoup (1985) found sorption at monolayer coverage was greater than sorption under saturated conditions. This result agrees with that obtained for coated alumina. Call (1957) found sorption at monolayer coverage was approximately twice to three times that at 50 percent relative humidity. These studies and the results obtained here indicate that monolayer coverage by water molecules is not the moisture condition at which sorption is comparable in magnitude to that in saturated systems.

b. Traverse City, Michigan Soil Core

Unfortunately detailed analysis revealed the Traverse City soil core to have a limited range of physical/chemical properties. Lack of variability in carbon content, CEC, specific surface area, and moisture content over the depth of the cored profile restricted the ability to make statistical inferences regarding the importance of these properties relative to the sorption of TCE and toluene vapors. Nevertheless the Traverse City core is, to the authors' knowledge, the first unsaturated soil profile which has been examined for variability of vapor phase partition coefficients. The discussion which follows summarizes the profile data and trends which could be extracted from it.

Sorption onto soil core 44U was studied at three different moisture conditions: oven-dry, ambient moisture, and saturation. Isotherm data for TCE and toluene sorption onto soil core 44U for the three moisture conditions are listed in Tables II.15 through II.20. Ambient moisture and saturated experiments reproduce conditions found in the environment. Although oven-dry conditions are very unlikely to occur in nature, determining sorption on oven-dry soils serves as an end member (with saturated experiments as the other) to the spectrum of possible moisture conditions. Figure II.6 shows sample isotherms for all three 44U moisture conditions, typical of TCE or toluene sorption. Use of a linear sorption isotherm model was again deemed appropriate based on the close fit of the data to the linear model. Intercepts for the ambient and saturated conditions were at or close to 1.0. The intercepts for dry soils were often lower than the theoretical intercept, although 1.0 was typically within the 95 percent confidence interval.

The relationship between moisture content and sorption was more difficult to determine in soil core 44U samples because the moisture contents considered for each sample were limited to dry, ambient, and saturated. A narrow range of moisture contents was available within the ambient moisture samples, however the effect of variation in the ambient moisture content on partition coefficients for TCE and toluene was not significant.

TABLE II.15. PARTITION COEFFICIENTS FOR TCE SORPTION ONTO SOIL CORE 44U AT AMBIENT MOISTURE.

Sample No.	$K_d' \pm$ C.I.	Intercept $\pm$ C.I.	r^2
44U1	0.940 $\pm$ 0.15	1.0 $\pm$ 0.045	0.97
44U2	0.492 $\pm$ 0.097	1.0 $\pm$ 0.042	0.96
44U3	0.206 $\pm$ 0.11	1.0 $\pm$ 0.038	0.52
44U4	0.132 $\pm$ 0.037	1.0 $\pm$ 0.037	0.82
44U5	0.305 $\pm$ 0.090	1.0 $\pm$ 0.055	0.90
44U6	0.299 $\pm$ 0.11	0.98 $\pm$ 0.027	0.53
44U7	0.285 $\pm$ 0.12	1.0 $\pm$ 0.079	0.80
44U8	0.312 $\pm$ 0.13	0.94 $\pm$ 0.095	0.84
44U9	0.312 $\pm$ 0.21	0.95 $\pm$ 0.13	0.70
44U10	0.451 $\pm$ 0.28	0.97 $\pm$ 0.18	0.67
44U11	0.285 $\pm$ 0.080	1.0 $\pm$ 0.047	0.92
44U12	0.236 $\pm$ 0.047	1.0 $\pm$ 0.028	0.96
44U13	0.427 $\pm$ 0.11	1.0 $\pm$ 0.037	0.42

TABLE II.16. PARTITION COEFFICIENTS FOR TCE SORPTION ONTO DRY SOIL CORE 44U.

Sample No.	$K_d' \pm$ C.I.	Intercept $\pm$ C.I.	r^2
44U1	305 $\pm$ 188	1.4 $\pm$ 59	0.87
44U2	54.0 $\pm$ 17	1.9 $\pm$ 5.2	0.94
44U3	18.2 $\pm$ 2.3	0.20 $\pm$ 0.86	0.99
44U4	5.37 $\pm$ 4.6	1.5 $\pm$ 1.8	0.69
44U5	2.53 $\pm$ 3.0	1.3 $\pm$ 1.1	0.54
44U6	2.36 $\pm$ 0.50	0.94 $\pm$ 0.19	0.97
44U7	2.49 $\pm$ 0.60	1.1 $\pm$ 0.23	0.97
44U8	3.17 $\pm$ 0.66	1.0 $\pm$ 0.26	0.98
44U9	11.5 $\pm$ 7.0	0.097 $\pm$ 2.0	0 86
44U10	7.89 $\pm$ 6.0	1.1 $\pm$ 2.3	0.74
44U11	3.40 $\pm$ 0.90	1.0 $\pm$ 0.32	0.99
44U12	2.76 $\pm$ 1.2	1.0 $\pm$ 0.34	0.89
44U13	2.33 $\pm$ 0.74	1.0 $\pm$ 0.28	0.94

TABLE II.17. SATURATED PARTITION COEFFICIENTS, AND EQUIVALENT VAPOR PHASE PARTITION COEFFICIENTS FOR TCE ONTO SOIL CORE 44U.

Sample No.	$K_d \pm$ C.I.	$K_d' \pm$ C.I.	Intercept $\pm$ C.I.	r^2
44U1	0.569 ± 0.22	1.36 ± 0.53	0.97 ± 0.090	0.92
44U2	0.2479 ± 0.095	0.594 ± 0.23	1.0 ± 0.041	0.92
44U3	0.0730 ± 0.14	0.174 ± 0.33	1.0 ± 0.052	0.32
44U4	-0.0249 ± 0.15	-0.0048 ± 0.36	1.0 ± 0.061	0.001
44U5	0.0613 ± 0.16	0.146 ± 0.38	1.0 ± 0.067	0.19
44U6	0.0698 ± 0.10	0.167 ± 0.24	1.0 ± 0.041	0.44
44U7	-0.0448 ± 0.22	-0.107 ± 0.53	1.0 ± 0.083	0.065
44U8	0.188 ± 0.29	0.449 ± 0.69	0.98 ± 0.089	0.52
44U9	0.0709 ± 0.076	0.170 ± 0.18	0.99 ± 0.033	0.45
44U10	0.0629 ± 0.079	0.150 ± 0.19	0.99 ± 0.028	0.52
44U11	0.175 ± 0.18	0.420 ± 0.43	0.95 ± 0.072	0.42
44U12	0.126 ± 0.058	0.301 ± 0.14	0.98 ± 0.019	0.92
44U13	0.208 ± 0.15	0.497 ± 0.36	0.99 ± 0.051	0.51

TABLE II.18. PARTITION COEFFICIENTS TOLUENE SORPTION ONTO SOIL CORE 44U AT AMBIENT MOISTURE.

Sample No.	$K_d' \pm$ C.I.	Intercept $\pm$ C.I.	r^2
44U1	1.83 ± 0.22	0.92 ± 0.12	0.99
44U2	0.579 ± 0.061	1.1 ± 0.033	1.0
44U3	0.309 ± 0.098	0.99 ± 0.075	0.94
44U4	0.245 ± 0.058	1.0 ± 0.031	0.98
44U5	0.228 ± 0.062	1.0 ± 0.044	0.96
44U6	0.263 ± 0.085	1.0 ± 0.052	0.94
44U7	0.320 ± 0.12	1.0 ± 0.087	0.82
44U8	0.407 ± 0.048	1.0 ± 0.033	0.97
44U9	0.384 ± 0.067	1.0 ± 0.044	0.98
44U10	0.370 ± 0.064	1.0 ± 0.031	0.99-
44U11	0.393 ± 0.075	1.0 ± 0.046	0.98
44U12	0.573 ± 0.098	1.0 ± 0.054	0.968
44U13	0.704 ± 0.067	1.0 ± 0.039	0.99

TABLE II.19. PARTITION COEFFICIENTS FOR TOLUENE SORPTION ONTO DRY
SOIL CORE 44U.

Sample No.	$K_d' \pm$ C.I.	Intercept $\pm$ C.I.	r^2
44U1	245 $\pm$ 38	2.9 $\pm$ 3.6	0.95
44U2	84.7 $\pm$ 25	1.4 $\pm$ 4.0	0.97
44U3	23.6 $\pm$ 3.9	1.2 $\pm$ 0.55	0.98
44U4	43.1 $\pm$ 4.2	0.25 $\pm$ 0.99	0.98
44U5	36.7 $\pm$ 7.5	0.28 $\pm$ 1.7	0.93
44U6	18.6 $\pm$ 3.5	1.4 $\pm$ 1.1	0.93
44U7	29.3 $\pm$ 3.9	-0.17 $\pm$ 1.0	0.97
44U8	47.4 $\pm$ 0.52	-1.2 $\pm$ 5.0	0.77
44U9	41.6 $\pm$ 13	0.73 $\pm$ 3.5	0.85
44U10	19.5 $\pm$ 8.9	3.0 $\pm$ 2.4	0.78
44U11	45.8 $\pm$ 6.6	-0.42 $\pm$ 1.6	0.97
44U12	52.5 $\pm$ 12	0.49 $\pm$ 3.0	0.92
44U13	29.0 $\pm$ 6.6	1.1 $\pm$ 1.5	0.90

TABLE II.20. SATURATED PARTITION COEFFICIENTS AND EQUIVALENT
VAPOR PHASE PARTITION COEFFICIENTS FOR TOLUENE
ONTO SOIL CORE 44U.

Sample No.	$K_d \pm$ C.I.	$K_d' \pm$ C.I.	Intercept $\pm$ C.I.	r^2
44U1	0.664 $\pm$ 0.066	2.41 $\pm$ 0.24	0.99 $\pm$ 0.024	0.99
44U2	0.198 $\pm$ 0.067	0.719 $\pm$ 0.24	0.98 $\pm$ 0.026	0.924
44U3	0.0454 $\pm$ 0.11	0.163 $\pm$ 0.40	1.0 $\pm$ 0.047	0.14
44U4	0.122 $\pm$ 0.11	0.443 $\pm$ 0.40	0.98 $\pm$ 0.044	0.640
44U5	0.119 $\pm$ 0.12	0.432 $\pm$ 0.44	0.96 $\pm$ 0.057	0.46
44U6	0.0847 $\pm$ 0.054	0.309 $\pm$ 0.20	1.0 $\pm$ 0.019	0.70
44U7	0.0602 $\pm$ 0.11	0.218 $\pm$ 0.40	1.0 $\pm$ 0.044	0.25
44U8	0.139 $\pm$ 0.16	0.505 $\pm$ 0.58	0.98 $\pm$ 0.064	0.42
44U9	0.0125 $\pm$ 0.064	0.044 $\pm$ 0.23	1.0 $\pm$ 0.026	0.035
44U10	0.0787 $\pm$ 0.069	0.287 $\pm$ 0.25	1.0 $\pm$ 0.024	0.56
44U11	0.108 $\pm$ 0.069	0.392 $\pm$ 0.25	1.0 $\pm$ 0.031	0.70
44U12	0.131 $\pm$ 0.057	0.476 $\pm$ 0.21	1.0 $\pm$ 0.021	0.84
44U13	0.219 $\pm$ 0.11	0.795 $\pm$ 0.40	1.0 $\pm$ 0.056	0.83

The 95 percent confidence intervals of partition coefficients (all expressed as K_d') at ambient moisture and saturated conditions overlap at almost all depths for both TCE and toluene (Figure II.11). Student's t tests and the nonparametric sign test show that they are statistically indistinguishable at the 99 percent level. This information plus the low correlation between ambient moisture content and partition coefficients leads to the conclusion that for this particular sandy soil, sorption at ambient moisture is the same as that at saturation for TCE and toluene. Partition coefficients for the dry soil samples were significantly different from ambient and saturated partition coefficients for both TCE ($\alpha = 0.1$) and toluene ($\alpha = 0.01$) sorption, using Student's t tests.

Examination of the partition coefficients within the soil core (Tables II.15 through II.20) showed some variation in sorption between samples in the soil profile. Regression analysis of partition coefficients and soil parameters was used to examine which parameters influenced sorption and to what extent.

Because organic carbon is the predominant predictor of sorption in saturated systems, a partition coefficient normalized to organic carbon, K_{oc}, is often used instead of the partition coefficient K_d. Previous studies have indicated that organic carbon is important to vapor phase sorption also, so a logical step is the calculation of partition coefficients normalized with respect to organic carbon, K_{oc}' and K_{oc}, for vapors and saturated conditions respectively. Tables II.21 and II.22 list the K_{oc}' and K_{oc} values calculated by dividing the partition coefficients by f_{oc}, the fraction of organic carbon. In saturated systems studied previously (Karickhoff, 1984), partition coefficients for different organic carbon samples tend to reduce to a uniform K_{oc} value, which can in turn be predicted according to sorbate properties. In Tables II.21 and II.22 the carbon normalized partition coefficients over the soil profile (within any moisture condition) do not converge to a single value for either sorbate. In fact all the K_{oc}'s, except those for TCE sorption onto dry soil, show a trend of increase with increasing depth. The explanation for this behavior may lie in changes in other properties within the soil profile and is evaluated below.
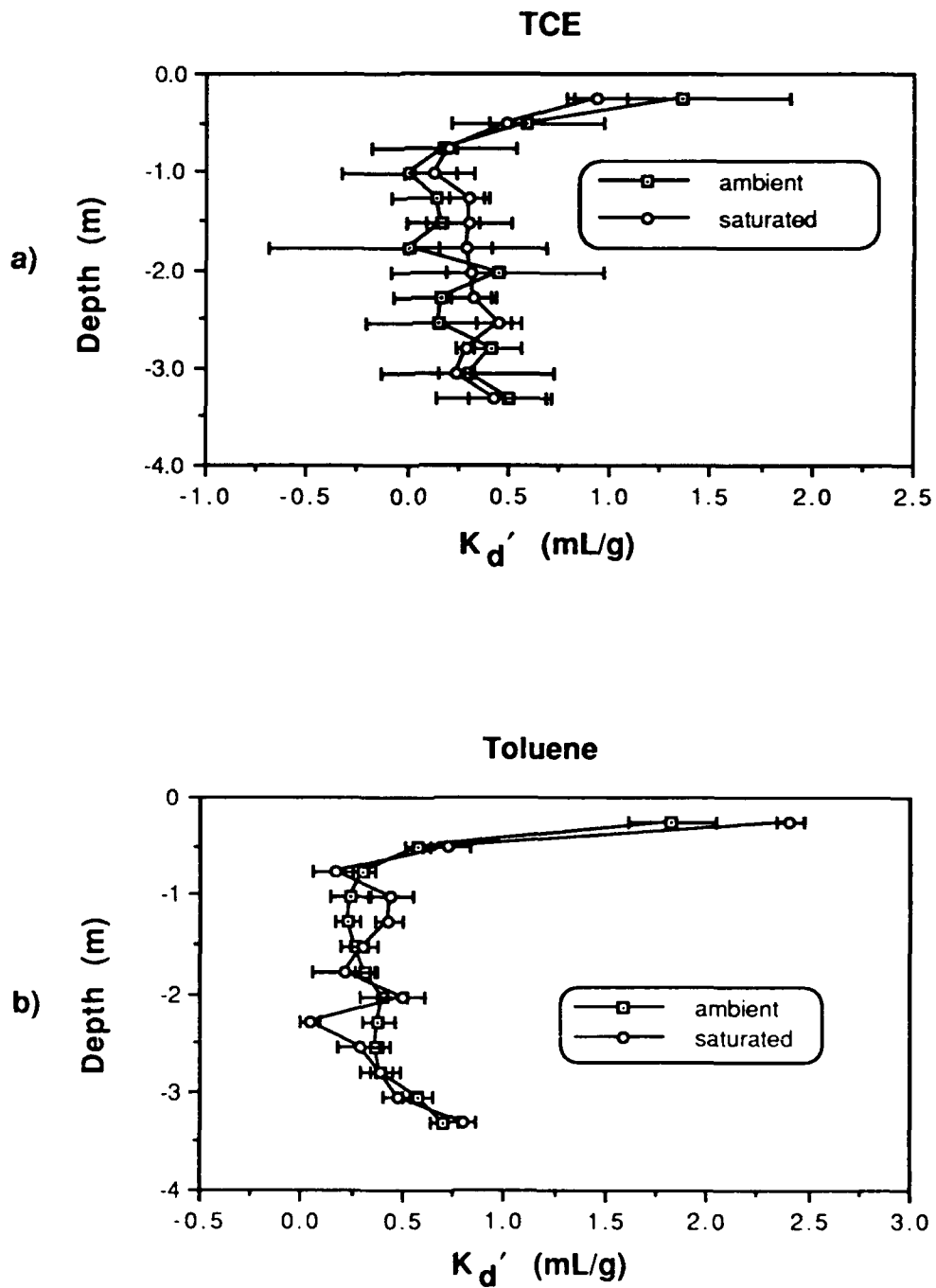
Figure II.11. Sorptive Partition Coefficients with 95 Percent Confidence Intervals at Ambient and Saturated Conditions on Soil Core 44U (a) TCE and (b) Toluene

TABLE II.21. PARTITION COEFFICIENTS NORMALIZED TO ORGANIC
CARBON CONTENT FOR TCE SORPTION ON SOIL CORE 44U.

	K_{oc}'		K_{oc}
Sample No.	Ambient	Oven-Dry	Saturated
44U1	285	92,400	172
44U2	848	93,100	429
44U3	710	62,800	252
44U4	660	26,800	-10.0
44U5	1370	11,500	277
44U6	1420	11,200	333
44U7	1430	12,500	-475
44U8	2080	21,100	1250
44U9	1840	63,900	394
44U10	2650	46,400	371
44U11	2040	24,300	1260
44U12	2950	34,500	1580
44U13	5340	29,100	2600

TABLE II.22. PARTITION COEFFICIENTS NORMALIZED TO ORGANIC CARBON
CONTENT FOR TOLUENE SORPTION ON SOIL CORE 44U.

	K_{oc}'		K_{oc}
Sample No.	Ambient	Oven-dry	Saturated
44U1	554	74,200	201
44U2	998	146,000	341
44U3	1070	81,400	155
44U4	1220	216,000	610
44U5	1040	167,000	541
44U6	1250	88,600	405
44U7	1600	146,000	300
44U8	2710	316,000	927
44U9	2130	231,000	67
44U10	2180	115,000	465
44U11	2810	327,000	771
44U12	7160	656,000	1640
44U13	8800	363,000	2740

The initial statistical analysis performed was simple linear regression between partition coefficients and soil characteristics. Coefficients of determination for regressions of all the partition coefficients (K_d and K_d') versus soil parameters are listed in Table II.23. The parameters that explain most of the variation in partition coefficients are organic carbon, CEC and specific surface area, as measured by either N_2 or EGME adsorption.

TABLE II.23. COEFFICIENTS OF DETERMINATION, r^2, FOR REGRESSION OF PARTITION COEFFICIENTS VS SOIL CORE PARAMETERS.

Samples	TCE ambient	dry	saturated	Toluene ambient	dry	saturated
Moisture content	0.017			0.064		
Specific surface area						
BET	0.84	0.96	0.75	0.83	0.92	0.81
Hg porosimetry	0.52	0.63	0.52	0.65	0.62	0.56
EGME	0.73	0.90	0.75	0.82	0.91	0.86
Organic carbon	0.78	1.0	0.72	0.87	0.94	0.88
CEC	0.72	0.84	0.78	0.71	0.84	0.75
Pore volume	0.034	0.073	0.034	0.077	0.085	0.019
Modal pore dia.	0.29	0.38	0.62	0.46	0.50	0.49
Porosity	0.28	0.40	0.28	0.38	0.43	0.26

Figure II.12 shows organic carbon versus partition coefficients for TCE sorption onto soil core 44U at ambient moisture. Although the r^2 value was relatively high ($r^2 = 0.78$), the coefficient of determination was actually the result of the data point for the higher organic carbon content and a data cluster at low organic carbon content values. This same pattern is shown by the surface area measurements and cation exchange capacity. Because of the uneven distribution of values within the range, the strength of the correlation between these parameters and partition coefficients is not as high as indicated by the r^2 values.

The correlation between sorption and organic carbon content was expected in saturated soils. Virtually the same correlation existed at ambient moisture, again indicating that at ambient moistures this soil was, in effect, "saturated". A correlation between organic carbon and sorption on dry soils was not unexpected, however the r^2 value was surprisingly high (as noted above this is due, in part, to the high carbon content of the surface samples and the resultant clustering of the data at low carbon contents). Because soil mineral surfaces are available for VOC sorption in dry soils, soil surface area rather than organic carbon content has generally been considered the most important parameter for sorption under dry conditions (Jurinak, 1957; Chiou and Shoup, 1985).
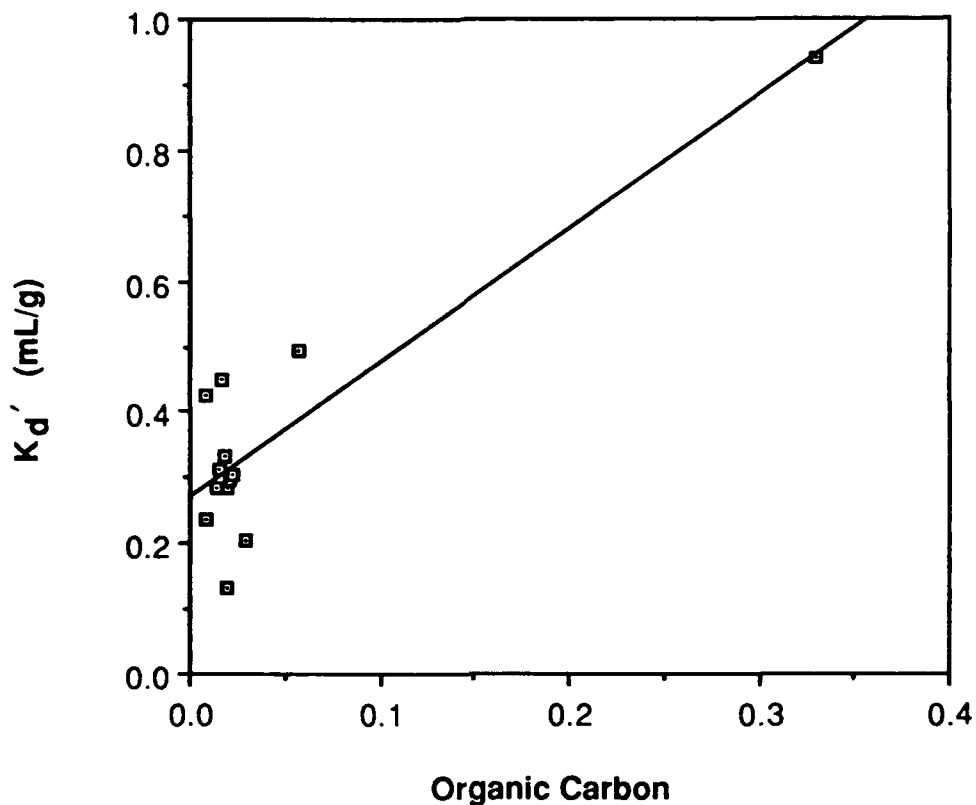
Figure II.12.   Organic Carbon vs Partition Coefficients for TCE Sorption on Soil Core
44U at Ambient Moisture Content.

The correlations between partition coefficients and specific surface area were also very high in dry soils, as expected. The large organic carbon r^2 values may in fact be due to the relation between organic carbon and surface area in these soil samples ($r^2 = 0.94$ for surface area from N_2 sorption). However, this correlation coefficient is also biased by the structure of the data as noted above. Parathion sorption on three dry Israeli soils was directly related to organic matter content (Yaron and Saltzman, 1972), but in these soils, organic matter and surface areas were also highly correlated ($r^2 = 0.99$). Jurinak (157) studied 1,2-dibromo-3-chloropropane vapor sorption on seven dry soils, and reported relatively low sorption on a peaty muck (35 percent organic matter) as compared to the other soils containing less organic matter and higher clay contents. The low sorption was attributed by Jurinak to the low surface area of the peaty muck compared to the clayey soils, and to the presence of microcapillary pores in organic matter that prevented entrance of vapor molecules.

One way to separate the organic carbon and surface area dependencies is to estimate the respective contribution of organic carbon and minerals to the specific surface area. Multiplying organic carbon by the Van Bemmelen factor of 1.724 converts it to organic matter, which has a surface area of 850 m^2/g (Bohn et al., 1979). Mineral surface areas were obtained by subtracting organic matter surface area from EGME surface area. Coefficients of determination, r^2, for partition coefficients versus mineral surface area (Table II.24) indicate a reasonably good correlation (they are comparable in magnitude to r^2 values for partition coefficients versus EGME specific surface area) and suggest a role for mineral surfaces in the sorption process. Given the uncertain nature of the correction for the contribution of soil organic matter to the EGME surface areas, this suggestion must be considered as highly speculative.

TABLE II.24. COEFFICIENTS OF DETERMINATION FOR MINERAL SURFACE AREA, EGME SURFACE AREA, AND ORGANIC CARBON VERSUS PARTITION COEFFICIENTS.

Parameter	TCE ambient	dry	saturated	Toluene ambient	dry	saturated
Mineral surface area	0.66	0.81	0.72	0.72	0.83	0.79
Organic carbon	0.72	1.00	0.72	0.83	0.94 0	0.88
EGME surface area	0.71	0.90	0.76	0.79	0.90	0.86

Another factor to consider when examining sorption is the low organic carbon fraction in these samples. The breakdown in correlation between organic carbon and partition coefficients at low carbon contents (<0.1 percent) has been noted in saturated systems (Schwarzenbach and Westall, 1981; Banerjee et al., 1985; Mackay et al., 1986; Mehran et al., 1987 and Stauffer et al. 1989). All 44U sections except the section closest the surface (44U1) had organic carbon contents less than 0.1 percent. Linear regression of soil parameters versus partition coefficients excluding sample 44U1 (Table II.25) gives much lower r^2 values than linear regression using all sections. This calculation removes the bias in the coefficients of determination which is introduced when the high carbon content and specific surface areas of the top sample in the profile are included in the regression. Coefficients of determination for organic carbon and surface areas decreased least for dry soils, especially for TCE sorption, indicating that these parameters are still useful for predicting sorption in dry soil. However, in ambient moisture and saturated conditions, the variation in partition coefficients can no longer be explained by the soil parameters measured in this study.

TABLE II.25. COEFFICIENTS OF DETERMINATION WITH AND WITHOUT
SAMPLE 44U1 FOR SOIL PARAMETERS VS PARTITION
COEFFICIENTS.

	TCE			Toluene		
	ambient	dry	saturated	ambient	dry	saturated
Organic carbon						
without 44U1	0.12	0.87	0.054	0.00	0.32	0.025
with 44U1	0.78	1.00	0.72	0.87	0.94	0.88
BET surface area						
without 44U1	0.36	0.92	0.18	0.069	0.41	0.51
with 44U1	0.84	0.96	0.75	0.83	0.92	0.81
EGME surface area						
without 44U1	0.094	0.52	0.21	0.13	0.47	0.26
with 44U1	0.73	0.90	0.75	0.82	0.91	0.86
Moisture content						
without 44U1	0.083			0.63		
with 44U1	0.017			0.064		

The results from this study support prior results showing that correlation between organic carbon and sorption breaks down for low carbon content soils. Banerjee et al. (1985) found that, in saturated systems, sorption on low carbon soils was greater than expected (based on calculated K_{oc}) for dimethylphalate but lower than expected for 1,2,4,-trichlorobenzene and o-chlorotoluene. Schwarzenbach and Westall (1981) Mehran et al., (1987) and Stauffer et al. (1989) found that sorption was greater than expected based on organic carbon contents, as was found in this study.

The correlation between toluene partition coefficients and moisture improves when section 44U1 is excluded from the linear regression. The slope of the moisture content-partition coefficient plot for toluene sorption is positive (Figure II.13) instead of negative as would be expected from the preceding discussion of moisture content and sorption. A possible explanation is dissolution of organic vapors into the soil moisture. The headspace technique used in this study assigns all sorbate not in the vapor phase to "sorption" and does not specifically account for sorbate dissolution. The results presented in Section III show that TCE dissolution into soil moisture can significantly contribute to TCE "binding" by moist mineral surfaces.

The correlation between specific surface area and partition coefficients is noted above for the oven-dry soil samples. The correlation at ambient moisture content and for

saturated samples was also high, in some times exceeding the correlation with organic carbon. Particle size was recognized as a parameter of secondary importance in sorption in saturated systems (Karickhoff et al., 1979; Mingelgrin and Gerstl, 1983). In the core samples, the importance of surface area to sorption may result from the high correlation of organic carbon and surface area discussed above. However, the previously noted grouping of the data limits the utility of inferences based on regression analyses for the core profile.

Toluene Sorption on Soil Core 44U
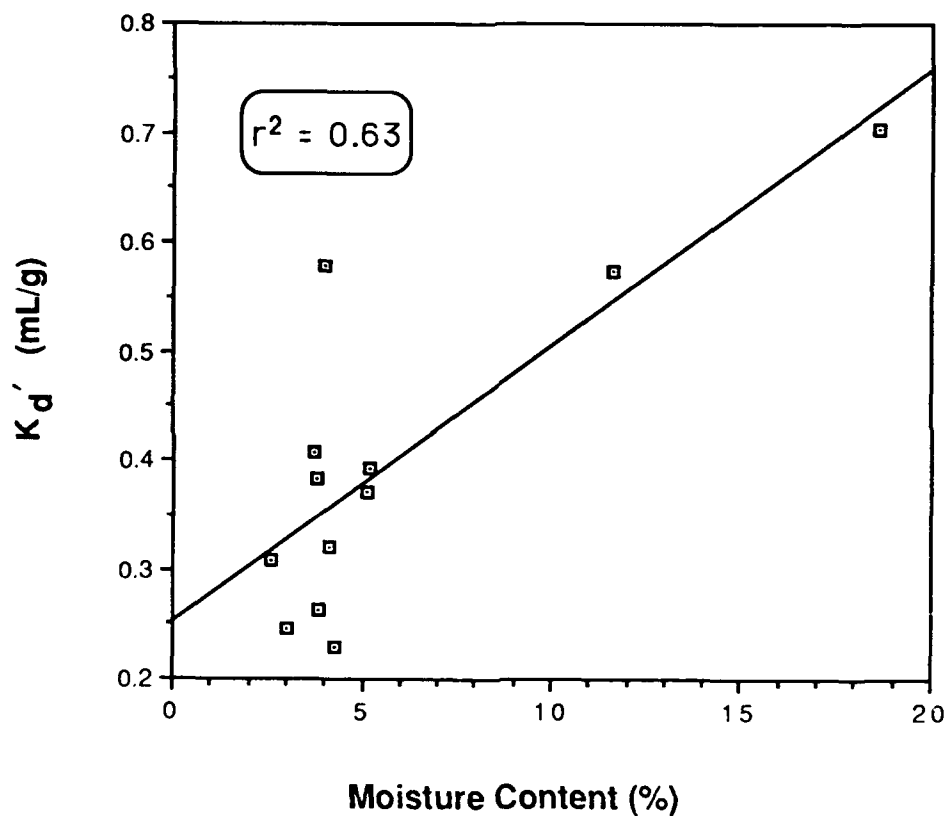
Figure II.13. Moisture Content vs Partition Coefficients for Toluene Sorption on Soil Core 44U Excluding Section 44U1

3. Comparison of TCE and Toluene as Sorbates

A comparison of the partition coefficients for TCE and toluene sorption onto silica at a given moisture content shows that toluene sorbs more strongly than TCE. This is expected because toluene has a lower Henry's Constant and vapor pressure and higher K_{ow} than TCE (Table II.1). A compound with a higher vapor pressure will have a larger mass fraction in the vapor phase at equilibrium (other factors being equal).

Figures II.14, II.15, and II.16 compare TCE and toluene sorption on soil core 44U at the three different moisture conditions. A paired sample Student's t test and nonparametric sign test were used to evaluate the null hypothesis that there was no difference between TCE and toluene partition coefficients at the 95 percent significance level (Table II.26). Both statistical tests showed that the null hypothesis could be rejected for dry conditions respectively, but at not at saturation. Using the sign test, differences between TCE and toluene are also significant at ambient moisture contents.

TABLE II.26. STATISTICAL TESTS COMPARING TCE AND TOLUENE
SORPTION ON SOIL CORE 44U

Decision on Null Hypothesis (95 Percent Significance Level)

Moisture Condition	Paired sample t test	Sign test
Ambient	Reject	Accept
Oven-dry	Reject	Reject
Saturated	Accept	Accept
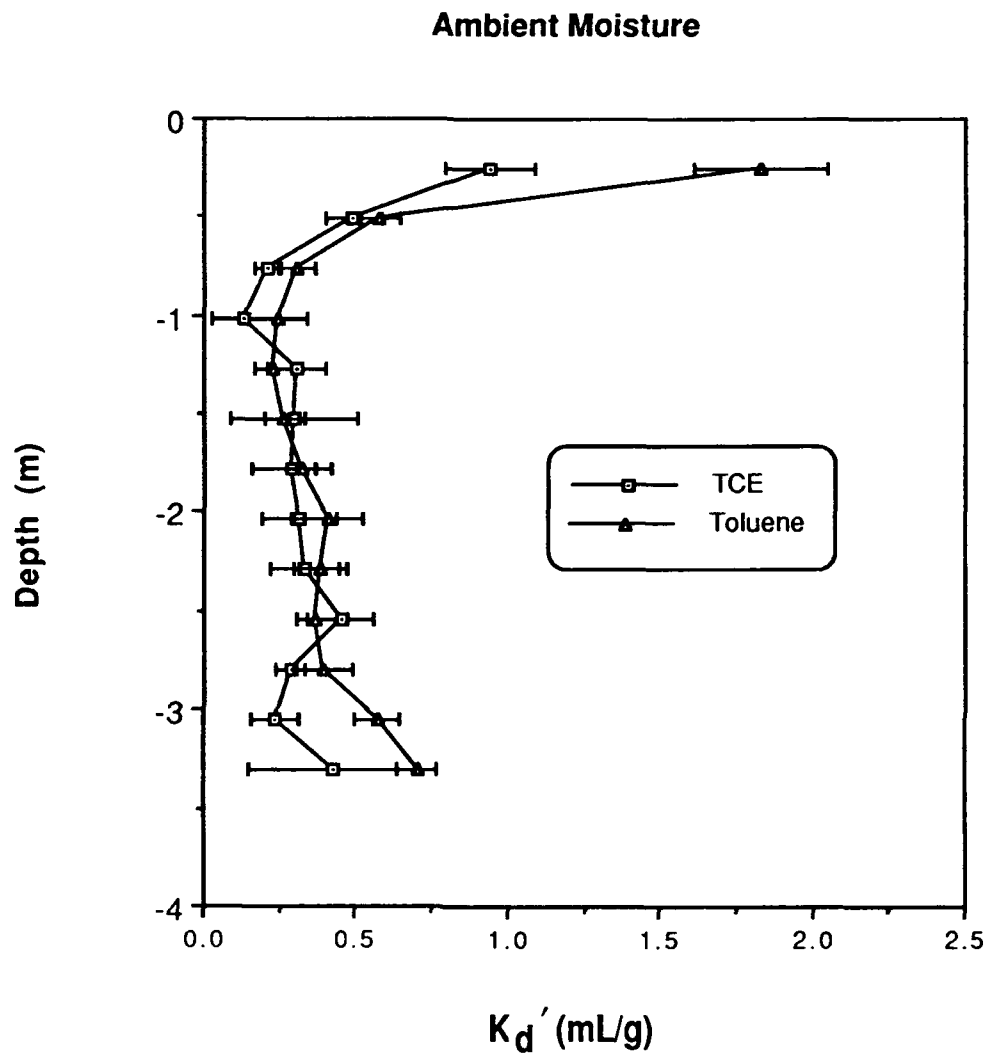
Ambient Moisture

Figure II.14.   Partition Coefficients with 95 Percent Confidence Intervals for TCE and Toluene Sorption onto Soil Core 44U at Ambient Moisture
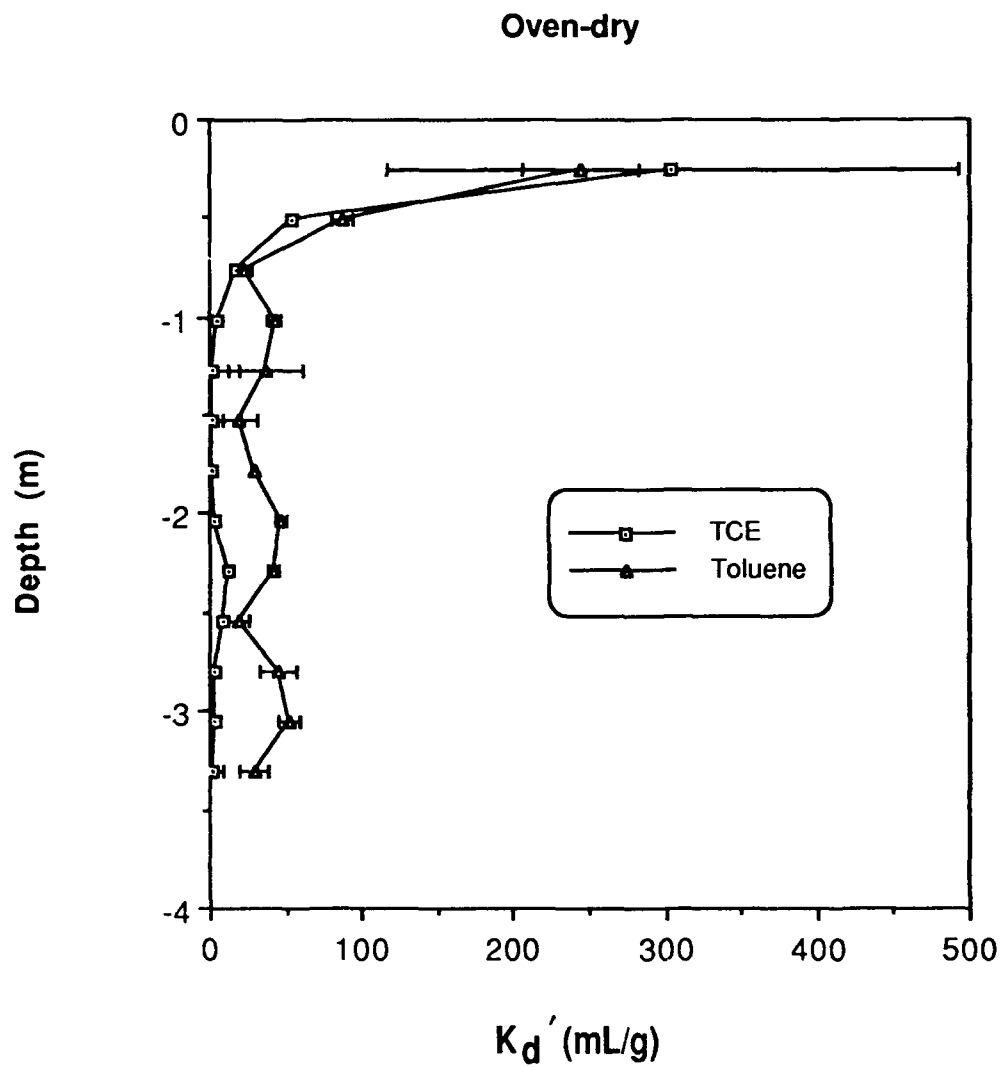
Oven-dry

Figure II.15.   Partition Coefficients with 95 Percent Confidence Intervals for TCE and
Toluene Sorption onto Oven-dry Soil Core 44U
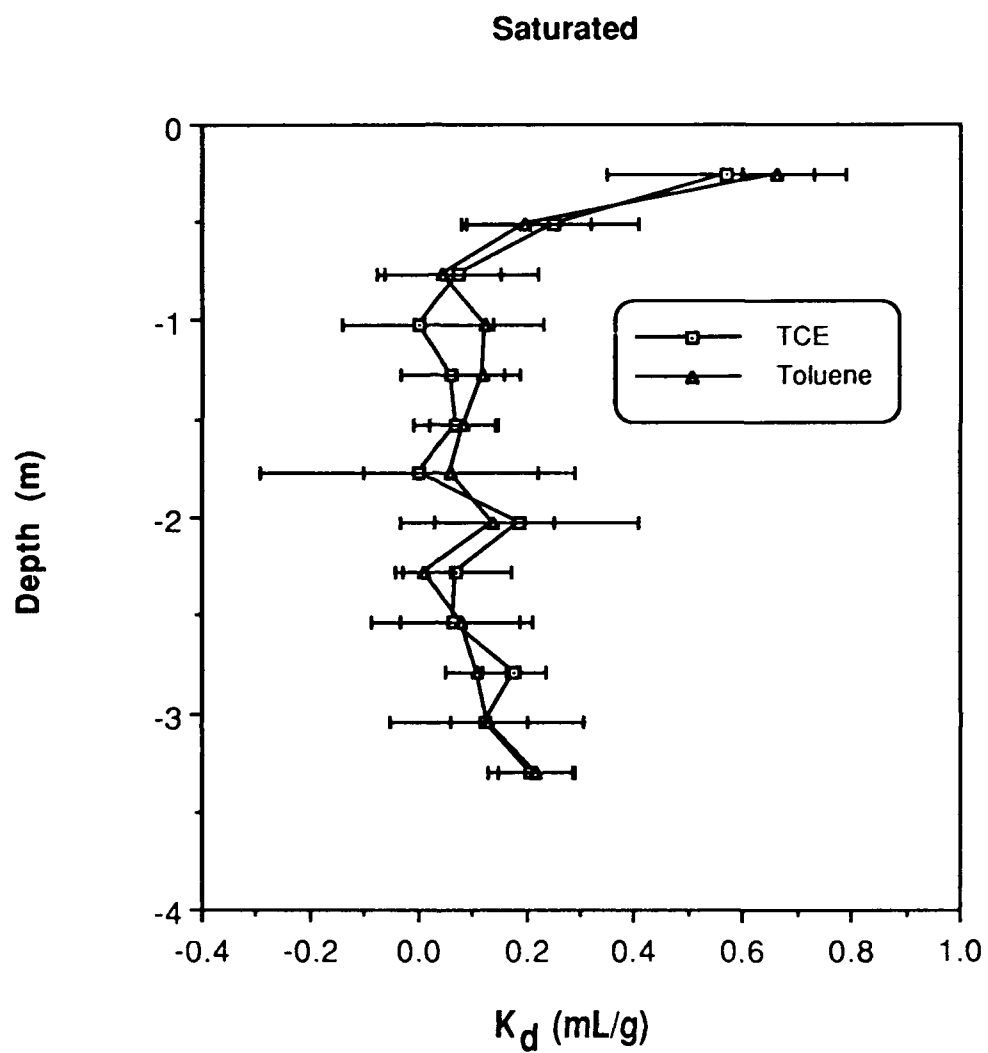
Saturated

Figure II.16. Saturated Partition Coefficients with 95 Percent Confidence Intervals for TCE and Toluene Sorption onto Soil Core 44U.

52

D. SUMMARY AND CONCLUSIONS

The objective of this study was to determine the effect of moisture content variations comparable to those occurring in an unsaturated soil profile on the sorption of volatile organic compounds from the vapor phase. Moisture profiles were established using laboratory columns packed with well-characterized sorbents consisting of oxide mineral phases with and without a coating of humic-type organic material. The sorbents studied were silica, and alumina coated with humic acid. The moisture contents achieved in the laboratory columns were complimented by additional samples placed in constant relative humidity environments. The sorptive partition coefficients of two organic vapors, toluene and TCE, were measured on samples. In addition, an unsaturated soil core profile was obtained in the field and similarly characterized with respect to its sorptive characteristics.

The sorbents employed were also characterized to define selected physical/chemical properties that may have affected sorption of TCE and toluene vapor. Sorbent properties measured included moisture content, organic carbon, cation exchange capacity, pore volume, porosity, modal pore diameter, surface area, and particle size distribution.

The range of moisture contents achieved in silica by placing solids in environments with varying temperatures and relative humidities was 0 to 5.2 percent; silica moisture contents from 0.14 to 46 percent (saturated) were obtained in the laboratory columns. For coated alumina moisture contents ranging from 5.4 to 69 percent (saturated) were obtained in the laboratory columns. The soil core was studied at ambient moisture (2.58 to 18.6 percent mean moisture content), ᵥ.en-dry, and saturated moisture conditions. The soil core was of sandy texture, and was characterized by low organic carbon content, surface area, CEC, and pore volume.

Sorption was measured by generating partition coefficients for vapors and for saturated systems using previously developed headspace analysis techniques. Partition coefficients were then statistically compared with the sorbent properties.

Variation in the partition coefficients for TCE and toluene sorption on silica and coated alumina vs moisture content showed the same pattern. Partition coefficients decreased sharply with increasing moisture, then leveled off approaching the value attained at saturation. Vapor sorption in relation to the onset of monolayer coverage by water molecules is of particular interest, since soils have at least a monolayer of hygroscopic water under natural conditions. With silica, the decline in sorption coincided with monolayer coverage by water molecules. For coated alumina, moisture contents below monolayer coverage were not obtained, but the pattern of sharply declining partition

coefficients with increasing moisture was the same as with silica. On the coated alumina, partition coefficients decreased with increasing moisture content as moisture contents greater than monolayer coverage. For this synthetic soil, a constant partition coefficient could not be assumed at low moisture levels. The major differences between the coated alumina and the silica are the much higher specific surface area of the alumina and, of course, the presence of the humic organic coating. We may speculate therefore that natural soils which contain mineral phases with high specific surface areas (such as iron oxides or expanding clays) and/or organic matter will be more likely to display significant variations in vapor sorption under dry conditions.

There was little correlation between partition coefficients and ambient moisture contents in individual samples from the soil core. This was not surprising because of the sandy nature of the core (low carbon content, and low specific surface area) and because it was obt~~ned from a moist geographical region where unsaturated soils are likely to be near field capacity. Samples from the core profile showed variability in parameters other than moisture content and this obscured dependencies of partition coefficients on moisture levels. Removal of the surface sample in the profile from the statistical analyses increased correlation coefficients between the partition coefficients and moisture content. Comparison of partition coefficients among the three moisture conditions (oven-dry, ambient, and saturated), showed that sorption was essentially the same for this soil core at ambient moisture and at saturation. As expected, oven-dry samples from the core sorbed much more TCE and toluene vapor than samples at ambient moisture.

Of the soil core parameters measured, the highest correlations were obtained between partition coefficients and organic carbon content, and partition coefficients and specific surface area. Correlations were biased by clustering of the values for subsurface samples which had low carbon content and surface areas relative to the topmost sample form the core. Organic carbon and surface area were also highly correlated by virtue of this stratification in soil properties. Deletion of the surface sample from the regression calculations showed surface area and organic carbon explained much of the variance in partition coefficients for oven dry conditions but not for ambient or saturated conditions. The limited range or soil parameters and partition coefficients in the soil core (below the surface sample) restricted the inferences regarding the influence of specific soil properties on vapor sorption. The dependencies of TCE sorptive partition coefficients on mineral surface areas and moisture contents are explored in further detail in section III in which a broader range of well characterized sorbents is considered.

The correlation between partition coefficients and organic carbon content is well-documented in saturated systems, as shown by the development of the organic carbon

normalized partition coefficient. For soils with an organic carbon content over 0.1 percent, K_d when normalized for organic carbon content tends towards a single value (K_{oc}) that can be predicted from empirical formulas using sorbate properties. K_{oc} and K_{oc}' values calculated for saturated and ambient moisture conditions in this study did not converge on a single value, but generally increased for deeper, lower carbon content samples. This variation in K_{oc} and K_{oc}' values and the decrease in coefficients of determination for partition coefficients and organic carbon when organic carbon was less than 0.1 percent are similar to results shown in other studies.

In comparisons of the two vapors used in this study, toluene generally sorbed more to solids and soil than did TCE. The differences between partition coefficients for TCE and toluene sorption increased as the moisture conditions changed from saturated to ambient to oven-dry conditions. Further comparisons between different vapors are provided in Section VII.

SECTION III

SORPTION EQUILIBRIA AND MECHANISMS OF SORPTION FOR TCE VAPOR ONTO SOIL MINERALS

By: S.K. Ong and L.W. Lion

A. INTRODUCTION

Many of the enduring concepts related to adsorption processes, such as the development of the Langmuir and BET isotherms, have emerged from studies of vapor adsorption onto solids. Substantial information exists which permits the characterization of vapor adsorption onto uniform solid surfaces. Unfortunately, competitive sorption of vapors from mixtures and vapor sorption onto complex surfaces such as soils is still not well understood. It can be anticipated that volatile organics and water vapor will compete, in unsaturated soils, to sorb onto a mixture of surface types. This section evaluates, the sorption of an organic vapor from a binary mixture with water over a wide range of moisture conditions for a variety of common soil minerals. In addition, selected studies with an organically coated mineral phase permit an initial evaluation of surface interactions in soil-like mixtures.

Some of the earliest environmentally related studies of sorption of vapors onto soils involved pesticides, herbicides, and fumigants. In these studies the research objective was to define the effects of adsorption on the performance of pesticides in soils. Bailey and White (1964) review this data and indicate that the physical-chemical nature of the adsorbates, soil organic matter content, nature of saturating cation, moisture content, and temperature directly influence adsorption. Call (Call 1957a, Call 1957b, Call 1957c) examined the diffusion and sorption of the fumigant, ethylene dibromide (EDB) vapor in the soil matrix. Moisture content was found to greatly affect the sorption of EDB and, for soils at field capacity, it was possible to predict the sorption coefficient by moisture content alone (Call, 1957b). Spencer and co-workers (Spencer et. al., 1982, Ehlers et al., 1969a; 1969b) confirmed that moisture content affects both volatilization and diffusion of vapors. These investigators evaluated the impact of moisture content, soil bulk density and temperature on the behavior of pesticides such as Dieldrin and Lindane. The effect of variable moisture was removed by Jurinak (1957) who investigated the sorption of 1,2-dibromo-3-chloropropane vapor on oven dry soils. The adsorptive capacity of the dry soils was determined to be a function of their external surface areas.

Even though research related to the fate and behavior of pesticides in the subsurface continues into this decade, it is now complimented by an increased concern over the

presence of carcinogenic volatile organic compounds (VOCs) resulting from poor management of waste disposal sites and leaking underground storage tanks. Although considerable research has focused on the fate of VOCs under saturated conditions, surprisingly little research has been performed to characterize the fate and behavior of VOCs in the vapor phase.

Calvet (1984) noted the lack of studies of the behavior on organic chemicals in the unsaturated zone and the need to understand the effects of water content of the medium on sorption. Chiou and Shoup (1985) evaluated the effects of water on the sorption of a series of volatile chlorobenzene compounds onto a natural soil. Soil moisture was shown to be a strong competitor for hydrophilic mineral adsorption sites relative to nonionic organic compounds. The high sorption of organic compounds at low moisture content was attributed to available surface "sites" on the soil minerals. It is therefore established that soil mineral surfaces "prefer" polar water molecules over nonpolar organic compounds. Recently, Rhue et al. (1988) studied the vapor-phase sorption of three alkylbenzenes (toluene, p-xylene, and ethylbenzene) on oven-dry soils. The conclusion of these investigators was the same as that of Jurinak et al. (1957), in that the amount adsorbed divided by the monolayer capacity of the soil was found to be similar for several of the sorbents used.

With regard to the mechanisms of vapor-phase sorption, Call (1957a) investigated the solubility of EDB in distilled water and also determined the amount sorbed on the surface of pure water but was unable to relate these data to his vapor-phase sorption data for wet soils. Chiou and Shoup (1985) concluded that at a relative humidity of 90 percent, the vapor sorption isotherm was similar to that of a saturated system. Spencer and Cliath (1970) concluded that Henry's Law applies in the vapor-phase desorption of Lindane from unsaturated soils at moisture contents of 3.94 percent and 10 percent. In this study, the binding of vapor (on a relative pressure basis) was directly comparable to sorption behavior in saturated soil (on a relative concentration basis). Applicability of Henry's Law to vapor-liquid-phase partitioning of volatile pollutants is incorporated in several groundwater transport models (ex. Baehr, 1987 and Jury et al. 1983). However, Peterson et al. (1988) observed that the vapor-phase partition coefficients of trichloroethylene (TCE) onto humic acid coated alumina were several orders of magnitude higher than the saturated sorption coefficient. This implied that independent vapor partitioning to the surface may be occurring. Prediction of the transport of TCE based on vapor-phase partition coefficients (Peterson et al., 1988; Shoemaker et al., 1990) showed significant differences from models based on saturated partition coefficients (Jury et al., 1983).

Examination of the data of Chiou and Shoup (1985) reveals that for 1,2,4-trichlorobenzene, the amount sorbed from the vapor phase at 90 percent relative humidity

was in fact more than for aqueous phase sorption. Also, Chiou and Shoup (1985) state that "the benzene isotherm at 90 percent RH shows much greater deviation from the aqueous phase sorption (by more than a factor of 5) in capacity". Yet, these investigators concluded that at this relative humidity (90 percent), aqueous (solid-liquid) phase sorption applies for vapor-phase partitioning. Data showing higher sorption for vapors would seem to indicate that sorption processes other than those at the solid-liquid interface occur, eg. direct sorption of vapors.

Spencer and Cliath (1970), noted above, estimated roughly 1 1/2 monolayers surface coverage by water for Gila Silt Loam at 3.94 percent moisture content. Conceptually, it is difficult to visualize how Lindane can "dissolve" into the soil moisture in such a case. In the studies of Peterson et al. (1988) for the sorption of TCE onto synthetic soil at 8.2 percent moisture content (1.6 monolayers of water) the magnitude of sorption which was observed was large enough to exclude simple dissolution of TCE into the soil moisture. There is also evidence from the vapor sorption of oxygen that the solubility of oxygen in soil water was affected by the type of soil. Nakayama and Scott (1962) showed that the amount of oxygen adsorbed onto the soil water of the mineral bentonite was lower than the solubility of oxygen in pure water. In summary, there are many contradictions in available data reflecting an insufficient understanding of vapor-phase partitioning processes onto soils under varying moisture contents.

The objectives of this study are to extend the understanding of vapor-phase partitioning processes, examine the mechanisms of vapor sorption, and clarify the applicability of Henry's Law to describe VOC partitioning in moist soils. In this section these objectives are approached through the observation of the change of vapor-phase partition coefficients and evaluation of thermodynamic data over a range of moisture contents and through the use of a simple relationship based on aqueous partition coefficient and Henry's constant. This study focuses on one of the most common volatile organic compounds found in groundwater, trichloroethylene (TCE) and its sorption characteristics on to well-characterized hydrous oxides and clay minerals in the presence of varying amounts of moisture.

B METHODS AND MATERIALS

1. Sorbents

Soil components were selected based upon their ubiquitous occurrence in soil. Two types of oxides and two types of clays were employed. The oxides used were aluminum oxide and iron oxide while the clays were Ca^{2+}-montmorillonite and kaolinite. To study the effects of organic matter, a commercial humic acid was used both as a surface coating on the aluminum oxide, and as a sorbent in the absence of a mineral phase.

The Ca^{2+}-montmorillonite (Cheto, # SAZ - 1) originated from Apache county, Arizona and was purchased from the Source Clay Mineral Repository of the Clay Mineral Society. Kaolinite (hydrite flat D type) was obtained from Georgia Kaolin Co. The iron oxide used was hydrated ferric oxide ($Fe_2O_3 \cdot H_2O$ - Batch # YO-5087) provided by Pfizer Inc. The aluminum oxide was chromatographic adsorption alumina, 80-200 mesh size (Fisher Scientific). The activated alumina was deactivated by soaking in distilled water for several hours (pH $\approx$10). Small quantities of concentrated nitric acid were added while mixing until the pH remained constant at about 4.0. Stirring at this pH continued for about 24 to 36 hours before allowing the suspension to settle. The supernatant was decanted and the solids rinsed several times with distilled water adjusted to pH 4. This treatment procedure was followed because a similar procedure was applied in the coating of the alumina with humic acid. Humic Acid from Aldrich Chemical Company was used as the organic coating. The coating procedure followed that of Garbarini and Lion (1985). Nine grams of humic acid were dissolved in 1 liter of distilled water which had been raised to pH 10 with NaOH. About 450 grams of alumina was added and the mixture was stirred continuously with the pH of the mixture gradually lowered to 4.0 with nitric acid. The suspension was allowed to settle for 48 hours after which the supernatant was decanted and the solid rinsed several times with distilled water adjusted to pH 4.0. The solids were air-dried and stored.

2.Characterization of Sorbents

The specific surface areas of the solids were determined using the BET nitrogen adsorption method and the Ethylene Glycol Monoethyl Ether (EGME) method. The EGME method was as described by Carter et al. (1986) except that no pretreatment of the samples was performed (Cihacek and Bremner, 1979). Organic carbon was analysed by the wet combustion method (Allison, 1960). Soil pH was measured in a 1:1 (by volume) soil:water suspension. The ammonium acetate method (Thomas, 1982) was used to determine the cation exchange capacity of the solid. The moisture contents of the samples (weight/weight) were determined by weighing the sample before and after equilibrating for 24 hours in an oven at 105° C. Density of the solids was determined by the pycnometer method (ASTM, 1958) or obtained from manufacturers' literature.

3.Experimental Methods

Linear vapor-phase sorption partition coefficients were determined by the headspace method of Peterson et al. (1988). This method can be described as a mass balance technique which involves the measurement of the headspace vapor concentration in serum type reaction vials by gas chromatography (G.C.). A gas-tight hypodermic syringe (Precision Sampling Inc.) was used to introduce 1 mL of saturated TCE vapor into a vial

(nominal volume of 60 or 120 mL) containing a measured amount of sorbent (see Figure III.1). The vial was immediately sealed with a Teflon®-lined rubber disc and an aluminum crimp cap. Correspondingly, a control vial was set up without sorbent. Saturated TCE vapor was obtained from the head space of a source bottle (approx. 120 mL) containing 10 to 20 mL of pure liquid TCE. The source bottle was kept at a constant temperature of 25°C to maintain a constant vapor concentration. Between twelve to fifteen vials were used to define a sorption isotherm. Typically, between 4 to 6 control vials were used for each isotherm. All vials were tumbled in a constant temperature chamber. The air space above the circulating water in the closed environment was found to fluctuate within ± 2°C at 25°C. After equilibration, the vials were removed from the tumbler and immersed in the circulating water with their necks above the water for about half to one hour to ensure that the vials were at 25°C. One mL of the headspace was then withdrawn from the vials and analysed using a HP 5890A Gas Chromatograph with a Flame Ionization Detector (FID). The G.C. column was 20 percent SP2100, 0.1 percent Carbowax 1500, on 100/180 mesh Supelcoport® (Supelco, Inc.) and was operated at 140°C.

One mL of saturated TCE vapor introduced into a 60 mL control vial would produce a headspace concentration of 8.8 mg/L in the control vial. This value approximates the concentration detected in the vapor phase at some waste sites such as Los Alamos, New Mexico where about 5 mg/L was reported (Springer, 1986).
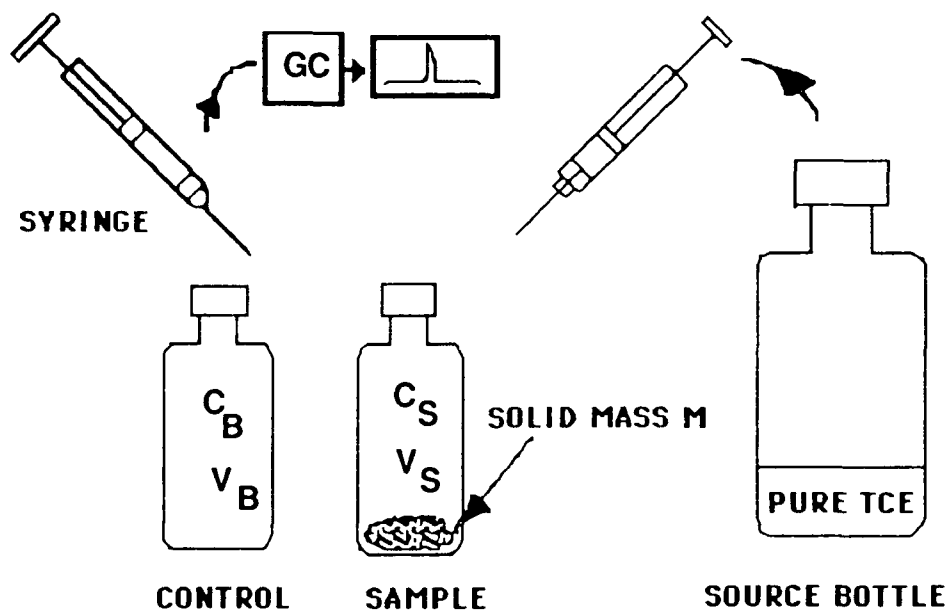
Figure III.1   Headspace Analysis Technique

Using mass balances between the vial with sorbent and the control vial (assuming that the same amount of TCE is introduced into each vial), and assuming a linear sorption isotherm, the following relationship may be obtained (see Section II):

$$V_B C_B = V_S C_S + K_d' M C_S \qquad \text{III.1}$$

where K_d' is the vapor partitioning coefficient (mL/g)

M is the oven-dry mass of the solids (g)

C_B is the G.C. peak area for a control vial

C_S is the G.C. peak area for a sample vial

V_B is the volume of the blank vial (mL)

V_S is the available gas volume of a sample vial (mL) and is computed from the actual volume of sample vial minus the volume occupied by dry mass minus the volume occupied by water associated with the solids:

$$V_S = V_S' - M/\rho - (\text{Wet Mass} - \text{Dry Mass} \{M\})/\rho_w$$

where ρ and ρ_w are the density of the solids and water respectively, and V_S' is the empty bottle volume.

Equation III.1 may be arranged to yield a linear relationship:

$$\frac{V_B C_B}{V_S C_S} - 1 = K_d' \frac{M}{V_S} \qquad \text{III.2}$$

In Equation III.2, the vapor-phase partitioning coefficient K_d' is given by the slope of the plot of $(V_B C_B / V_S C_S - 1)$ versus M/V_S.

Another way of arranging Equation III.1 is the traditional way of expressing the sorption isotherm, ie. mass adsorbed/mass adsorbent, Γ, versus equilibrium concentration:

$$\frac{C_B V_B - C_S V_S}{M} = \Gamma = K_d' C_S \qquad \text{III.3}$$

Linear isotherms were fitted to Equation III.2. Use of this form of the linear equation (versus Equation III.3) is justified on statistical grounds in Section VI.

If the isotherm was curvilinear, the Langmuir isotherm was used:

$$\frac{C_B V_B - C_S V_S}{M} = \Gamma = \frac{\Gamma_m \, k \, C_S}{1 + k \, C_S}$$ III.4

where Γ_m is the monolayer capacity and k is a constant related to the binding energy.

Inverting: $\quad 1/\Gamma \quad = \quad (1/\Gamma_m \, k)(1/C_S) \quad + \quad 1/\Gamma_m$ III.5

From the plot of $1/\Gamma$ versus $1/C_S$, the partition coefficient may be computed from the inverse of the slope ie. $\Gamma_m \, k = K_d'$.

For saturated experiments, the experimental procedure followed that of Garbarini and Lion (1985). Sorbents were mixed with 20 mL of 0.1 M NaCl solution in a reaction vial to maintain a constant ionic strength. A fixed volume of saturated TCE solution was added and after equilibrating, the headspace concentration of the vial was measured. In a manner comparable to the vapor data analysis, the liquid-phase partition coefficient, K_d, can be determined from mass balances (Peterson et al., 1988), ie. :

$$\frac{C_{GB} \, (\gamma \, K_H \, V_{GB} + V_{LB})}{C_{GS} \, (\gamma \, K_H \, V_{GS} + V_{LS})} = K_d \, \frac{M}{(V_{LS} + K_H \, \gamma \, V_{GS})} + 1$$ III.6

where K_H is the Henry's constant and γ is the TCE activity coefficient in the aqueous solution, subscripts G, L, B and S denote gas phase, liquid phase, control (blank) and sample vials, respectively.

The isosteric heat (enthalpy) of adsorption can be found through van't Hoff's equation (Atkins,1986):

$$\ln (K_d)_\Gamma = - \Delta H_{ads}/RT + constant$$ III.7

where K_d is the equilibrium constant (partition coefficient)
  T is temperature (^{o} K)
  ΔH_{ads} is the heat (enthalpy) of adsorption (kcal/mole)
  Γ is surface coverage
and R is the universal gas constant (kcal/mole ^{o}K)

By conducting experiments at different temperatures with a solid at a given moisture content, the slope of the plot of natural logarithm of the partition coefficient versus 1/RT

will yield the heat of adsorption. The total heat of adsorption is obtained by using the partition coefficient as expressed in Equation III.2. In contrast, partition coefficients obtained with relative concentration or pressure [ie. expressing the X-axis in Equation III.3 as C_s/C_0 instead of C_s or as M/V_sC_0 in Equation III.2 instead of M/V_s (where C_0 is the saturated vapor concentration at that temperature)] will yield the net heat of adsorption ie., $\Delta H_{ads} - \Delta H_{condensation}$.

With the use of the headspace analysis technique, the laboratory procedure is greatly simplified since only the headspace gas is sampled and extraction procedures are not required to determine the amount adsorbed. Also since the headspace concentration can be sampled without opening the vials, losses of the volatile sorbates can be minimized. Inspection of Equations III.2, III.3 and III.6 indicates that, if the G.C. peak area response is linearly related to headspace concentration of TCE, then only the G.C. peak area is required since any calibration constant will cancel. Use of Equation III.2, however, is limited to the linear region of the vapor-phase sorption isotherm.

C. RESULTS AND DISCUSSION

1. Characteristics of Sorbents

The properties of the experimental solids are given in Table III.1. The four minerals, as expected, have very low organic carbon contents. Coating of the alumina with humic acid resulted in an organic carbon weight fraction of 0.45 percent. Even though the organic carbon content is not large, the BET surface area increased by 32 percent after coating. However, the cation exchange capacity for coated alumina showed no change compared to the base material, alumina. Coated alumina had the largest surface area measured by the BET nitrogen adsorption method. For montmorillonite, the large discrepancy in surface area between the two methods for determining surface area shows that the EGME method measures the external and interlamellar surface area while the BET nitrogen method measures only the external surface area. This is attributed to the polar nature of EGME which is able to penetrate the interlamellar pores.

TABLE III.1 PHYSICAL-CHEMICAL CHARACTERISTICS OF THE SORBENTS

	Alumina	Coated Alumina	Iron Oxide	Kaolinite	Montmo-rillonite	Humic Acid
Particle Density (g/cm^3)	2.98	2.57	4.03	2.51	1.8	--
pH (H$_2$O extract)	4.5	7.18	6.5	4.2-5.2	8.3	9.96
Org. Carbon (%)	0.02	0.45	0.06	0.01	0.02	35.5
Surface Area (m^2/g)						
BET Nitrogen	143.2	189.3	10.98	8.47	97.42 [†]	--
EGME Method	183.0	250.0	24.9	21.3	733.0	123.8
CEC (meq/100g)	15.5	15.5	18.5	7.5	113.5	--

[†] - from van Olphen and Fripiat (1979)

2. Sorption Kinetics and Typical Sorption Isotherms

Ten to 15 sample vials containing equal sorbent mass were used to determine sorption equilibration time. For each sample vial, a corresponding control vial was also analysed. At fixed time intervals TCE headspace concentrations of a sample and a control vial were measured. With this approach, equilibration could be inferred when the headspace concentration remained reasonably constant. The first series of experiments employed air dried solids while the second series of kinetic experiments were carried out using damp solids with moisture contents ranging from 30 percent to 65 percent. These moisture contents generally reflect the range used in the equilibrium experiments discussed below. Results for all air dried solids except for humic acid and montmorillonite suggest that equilibrium is achieved within 24 hours. For both montmorillonite and humic acid about 30 hours were sufficient. Similarly, for solids with higher moisture content, about 24 to 35 hours was required to achieve equilibrium. An appropriate equilibration time, never less than 24 hours, was used in all sorption experiments.

A set of typical results with iron oxide as the sorbent is plotted using Equation III.2 in Figure III.2 to illustrate the isotherms obtained with the headspace analysis method. When some moisture was adsorbed onto the surface of the sorbents, the sorption of TCE was greatly reduced. This reduction in TCE sorption is in agreement with the observationsof other researchers (Chiou and Shoup, 1985, Peterson et al., 1988, Rhue et al., 1988) who concluded that the mineral surfaces of soils bind polar water molecules more strongly than nonpolar organic chemical compounds.
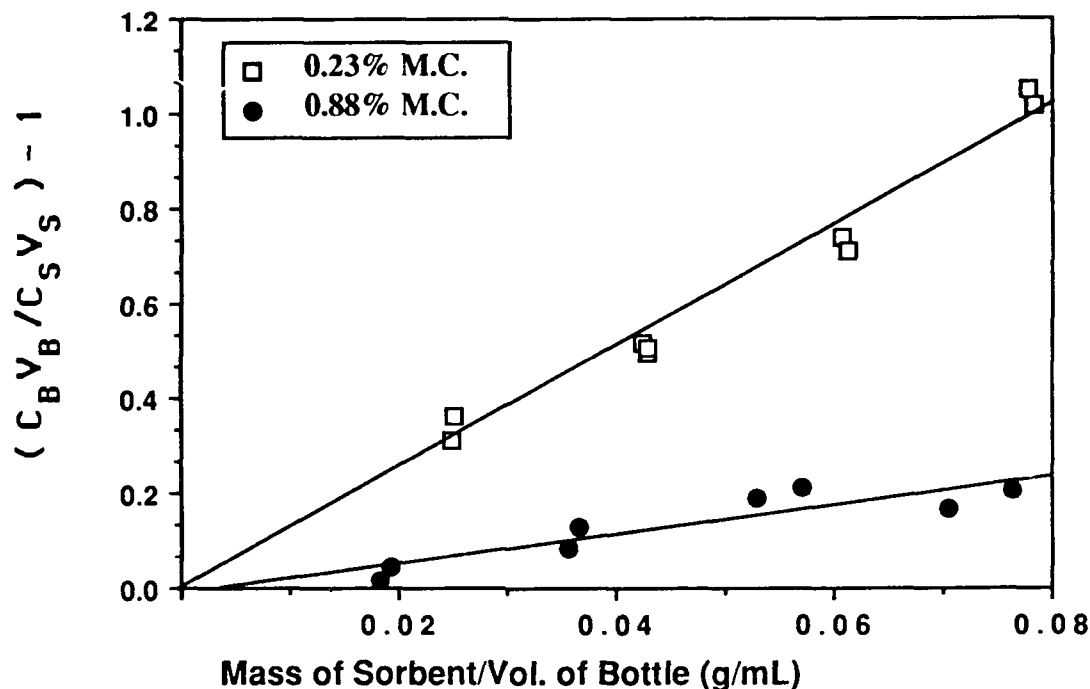
Figure III.2   Typical Iron Oxide Isotherms Obtained Using the Headspace Analysis
Technique with Equation III.2

3.   Sorption Results

a. Effect of Surface Area on Oven Dry Sorbents

Surface area has been found to be important in quantifying the total amount of
sorbate sorbed on oven dried soils (Jurinak, 1957, Rhue et. al., 1988). Figure III.3 gives
the TCE sorption isotherms for all five experimental solids under oven-dried conditions.
Solids with large specific surface areas, such as humic coated alumina and montmorillonite,
were observed to require a small mass to achieve the same amount of TCE sorbed relative
to low specific surface area solids, such as kaolinite and iron oxide. To illustrate the role of
surface area, the mass of sorbent was multiplied by the individual sorbent's BET specific
surface area (Figure III.4) to express the X-axis in terms of surface area. Normalizing for
surface area brought the partition coefficients within the same order of magnitude but
substantial scatter is still evident. One possible reason for this scatter is that there were
sorbent-specific interactions with TCE. Regression of the oven dried partition coefficients
(Table III.2) against selected properties of the solids reveals the expected high correlation
(r^2) with surface area. These results confirm that, for oven-dried solids, surface area acts
as a good indicator of the magnitude of sorbent's partition coefficient.

65
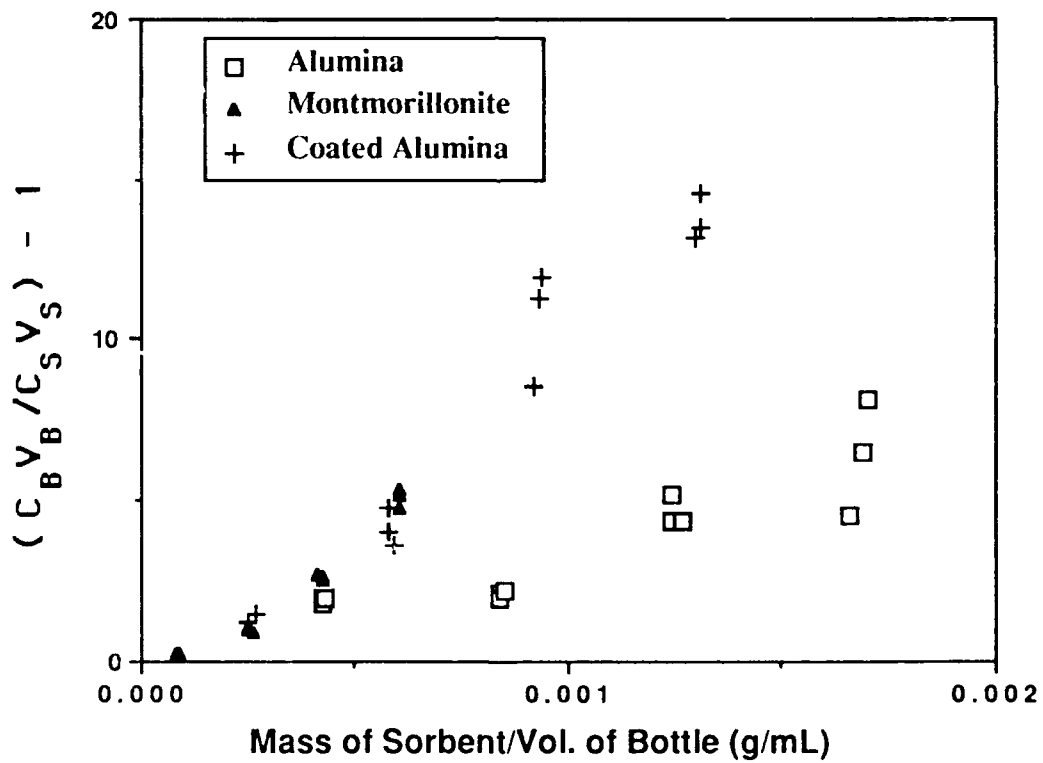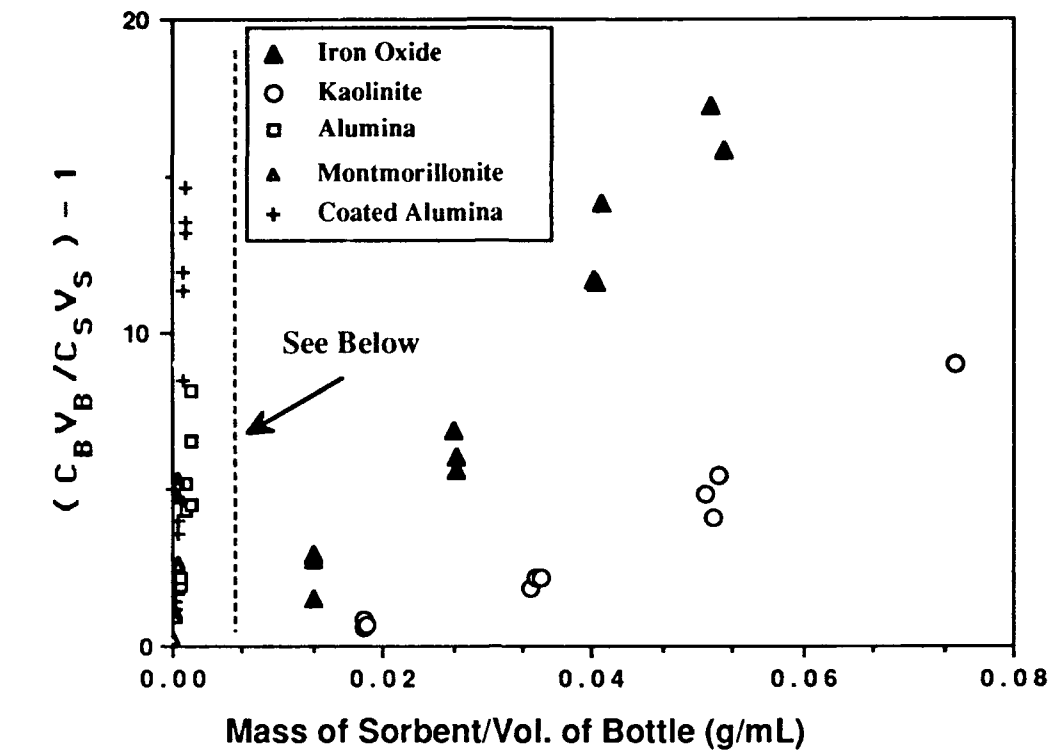
Figure III.3 Sorption of TCE onto Oven Dry Solids
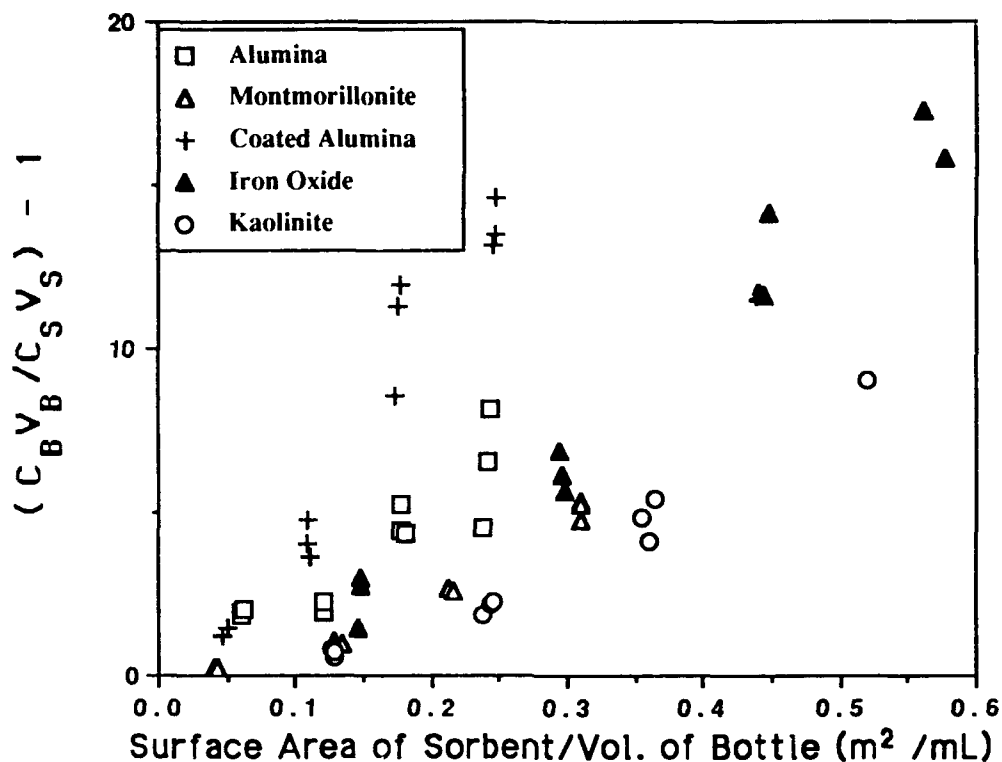
Figure III.4 Sorption of TCE Normalized with Respect to Surface Area Available

---

TABLE III.2   CORRELATION MATRIX FOR OVEN DRIED SOLIDS

	BET N_2 Surface Area	CEC	Organic Carbon
K_d'	0.92	0.82	0.39
BET Surface Area		0.97	0.0
CEC			- 0.15

---

b. Effect of Moisture on Sorption

With increasing moisture content, the TCE vapor partition coefficient decreased rapidly, reached a minimum, and then slowly increased. This trend was observed for all five solids (Figures III.5, III.6 and III.7). Also, the heat of sorption data (Figures III.8, III.9 and III.10) showed a trend similar to that of the TCE partition coefficient data in that the heats of sorption were high for all solids at oven-dry conditions, decreased rapidly as the solid became moist, and then increased with further increase in moisture contents. To generalize these plots, the change in partition coefficients over the full moisture range can be perceived as consisting of three regions (Figure III.11). In each region, different sorption processes are proposed below and evaluated in relation to the experimental data.
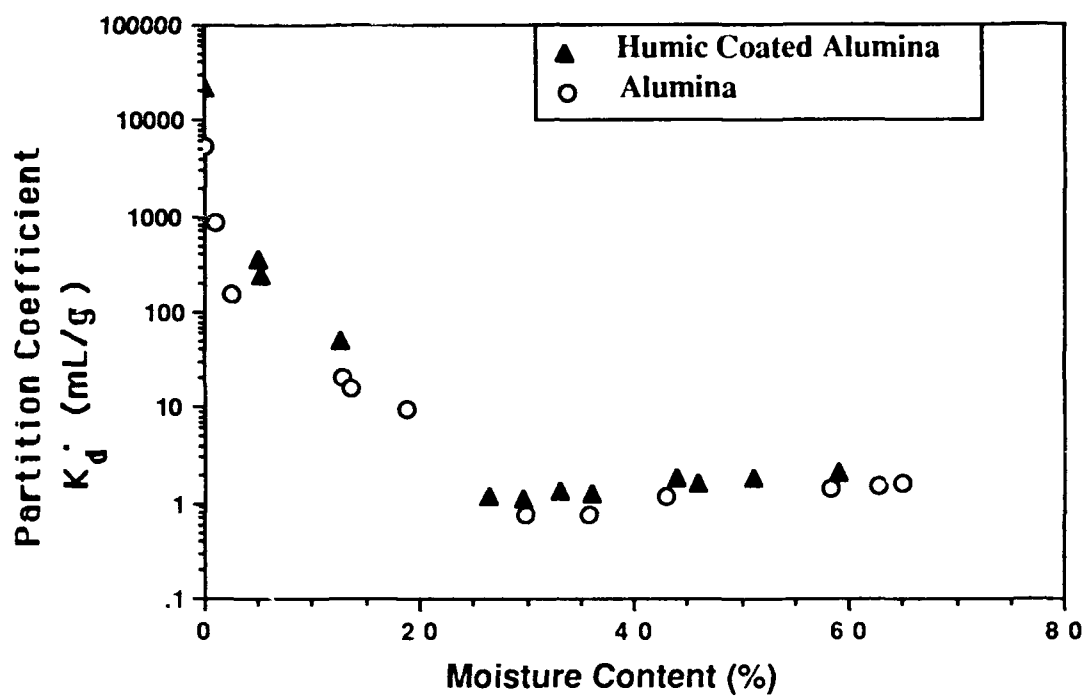
Figure III.5   Effect of Moisture on the Sorption of TCE Vapor onto Alumina and Coated Alumina
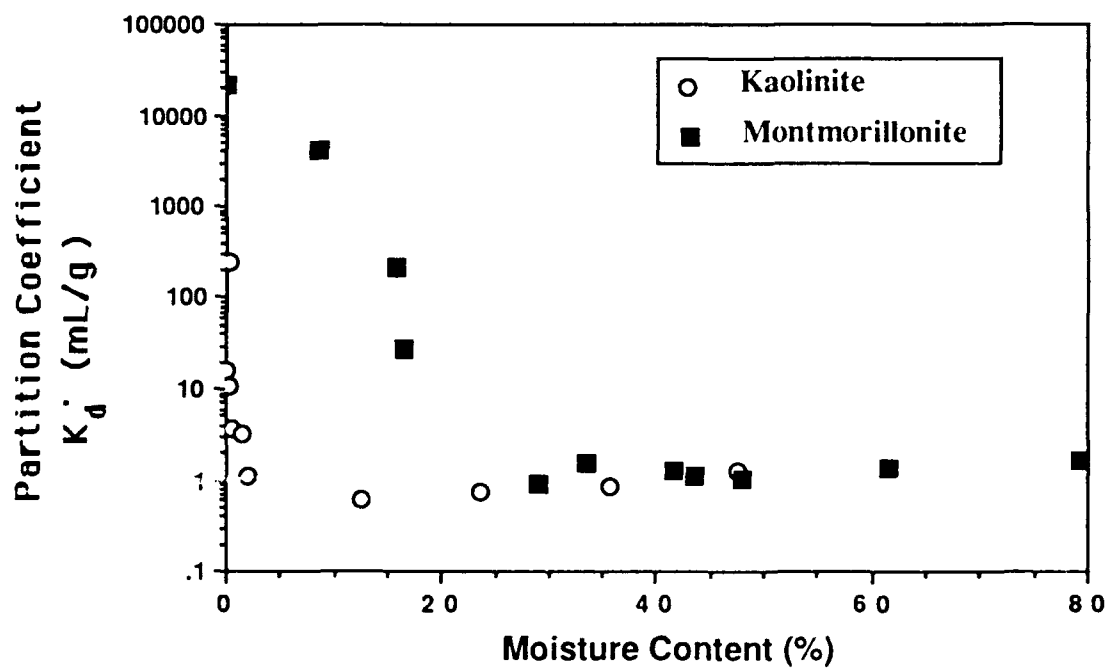
Figure III.6   Effect of Moisture on the Sorption of TCE Vapor onto Montmorillonite and Kaolinite
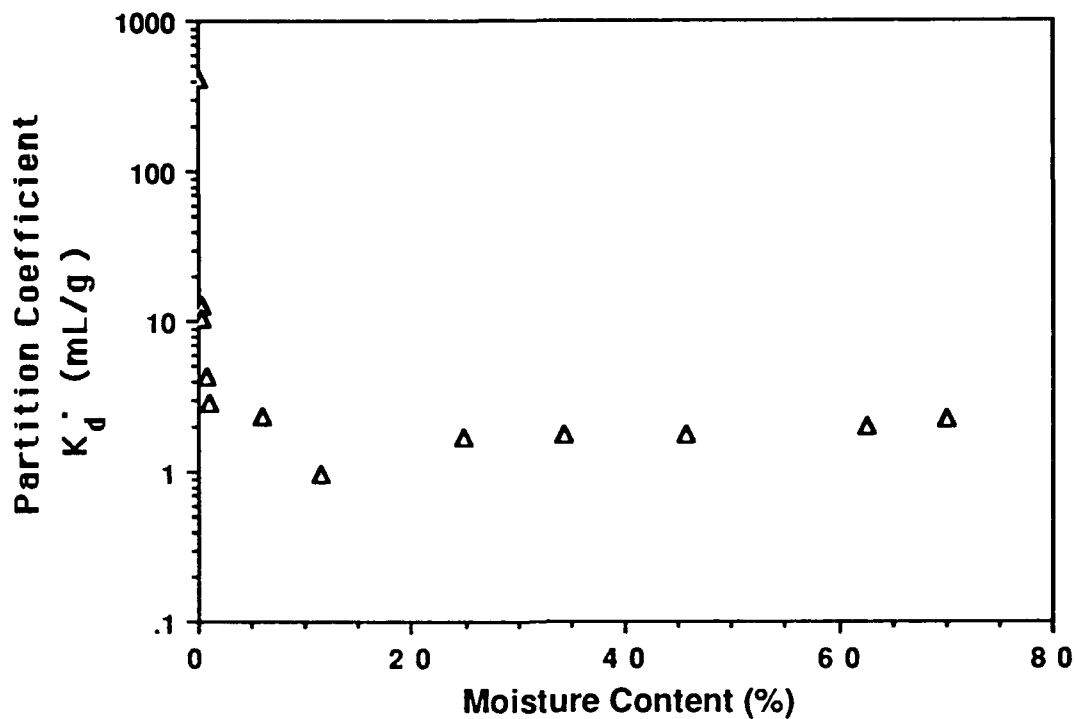
Figure III.7   Effect of Moisture on Sorption of TCE Vapor onto Iron Oxide
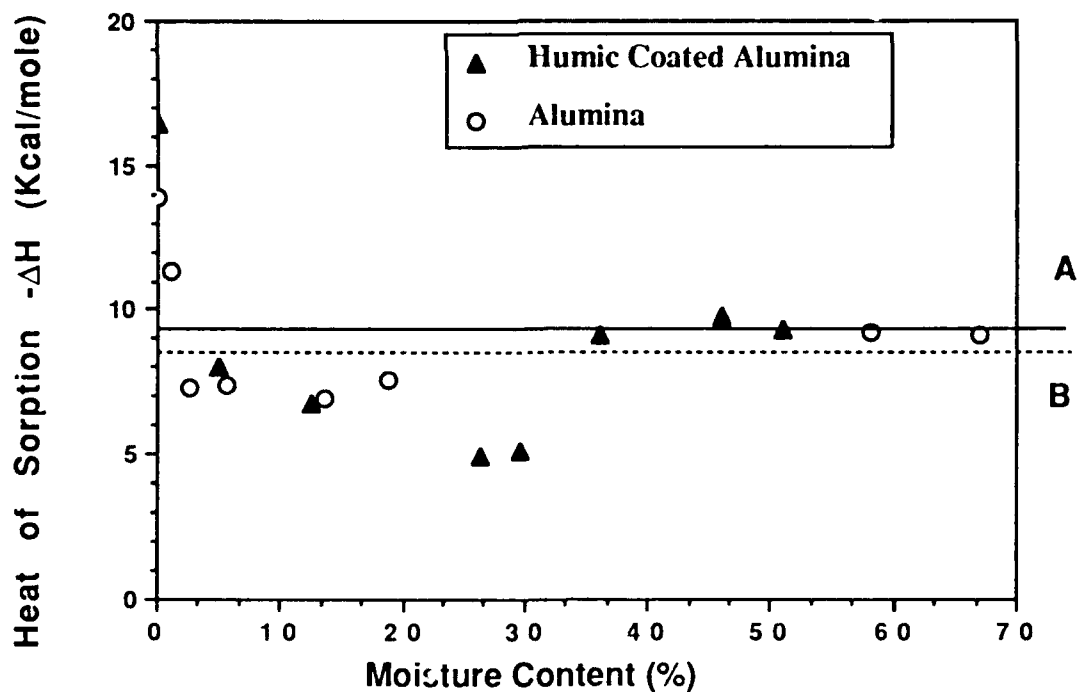
Figure III.8   Change of Heat of Sorption with Moisture Content for Alumina and Coated
Alumina (A= Heat of TCE Dissolution (-9.35 kcal/mol), B = Heat of TCE
Condensation (-8.63 kcal/mole))
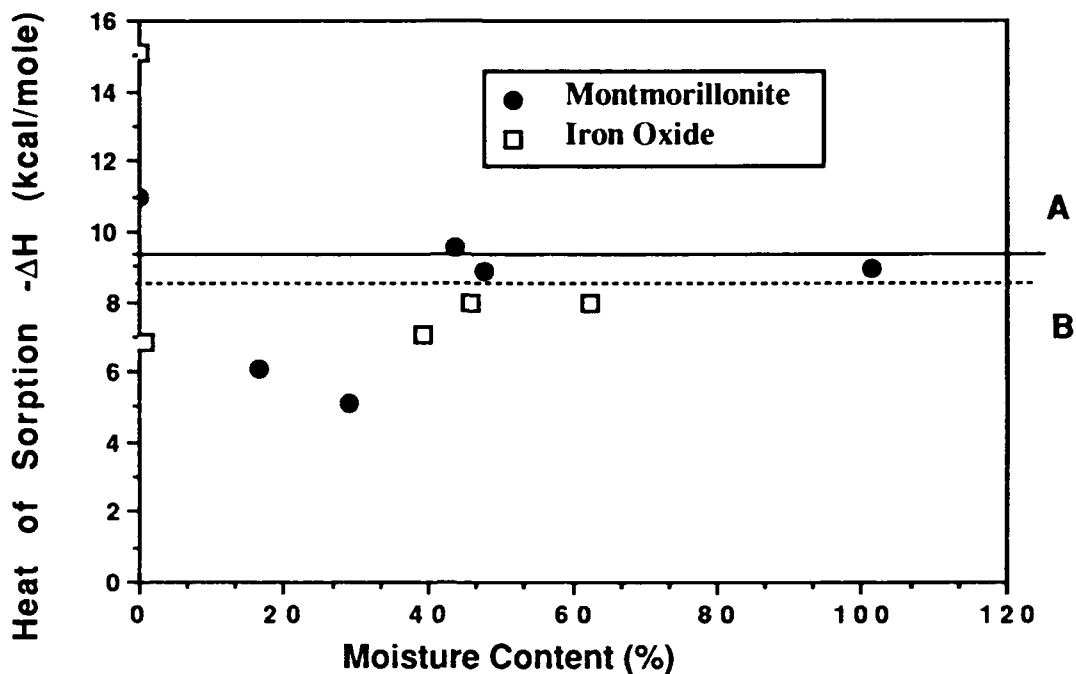
Figure III.9   Change of Heat of Sorption with Moisture Content for Montmorillonite and Iron Oxide [A=ΔH of TCE Dissolution (-9.35 kcal/mol), B=ΔH of TCE Condensation (-8.63 kcal/mole)]
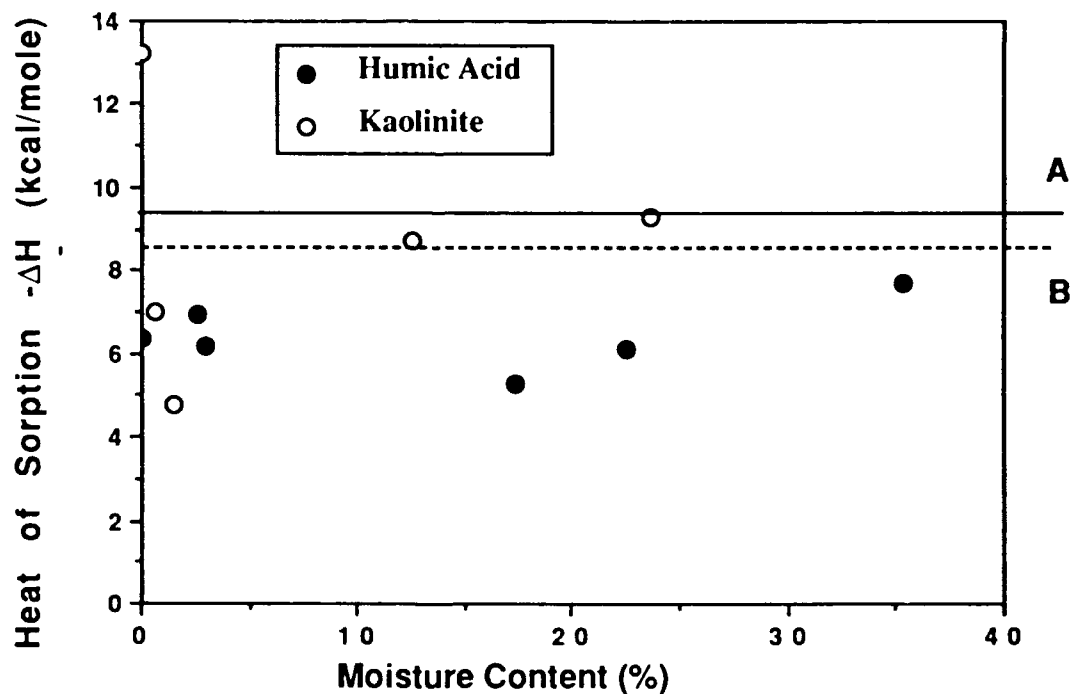
Figure III.10   Change of Heat of Sorption for Kaolinite and Humic Acid [A=ΔH of TCE Dissolution(-9.35 kcal/mol), B=ΔH of TCE Condensation(-8.63 kcal/mol)]

70
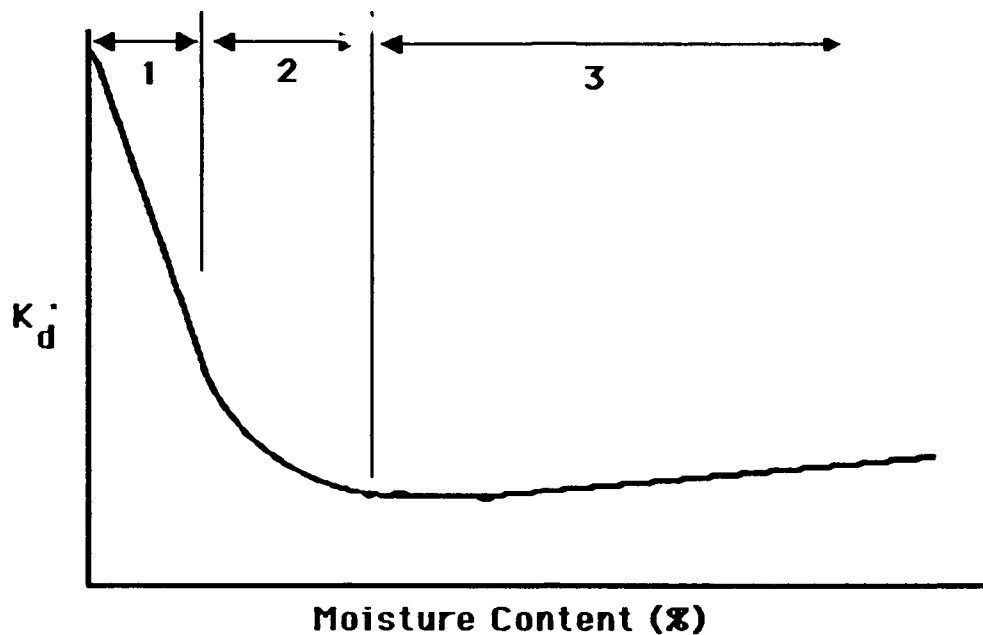
Figure III.11 Designated Regions and Proposed Sorption Mechanisms for Vapor-Phase
Sorption Phenomena as a Function of Moisture Content of the Surface

1. Oven-dry surface to single monolayer coverage by water:
   Direct soil surface sorption along with sorption onto the surface of bound water.
2. Single monolayer coverage to multilayer (4 to 8 monolayers) coverage:
   Sorption onto the surface of bound water with dissolution into liquid water
   becoming important.
3. Greater than 4 to 8 monolayers coverage to field capacity:
   Dissolution of TCE into soil water dominates plus "saturated" sorption behavior.

Region 1 is designated as extending from an oven dry surface to moisture
content corresponding to one monolayer of water. In this region direct sorption of TCE
onto the solid surface is indicated by the strong dependence of sorption on surface area as
discussed above. Competition with water molecules for surface adsorption sites results in
a decrease in the sorption of TCE molecules with increasing moisture. This was observed
for all solids (Figures III.5, III.6 and III.7).

Heats of sorption for all oven dried solids were 10 to 20 kcal/mole with the
humic coated alumina having the highest heat of sorption of the five solids at -16.5
kcal/mole. These values indicate that sorption of TCE on oven dry solids is a physical
sorption process (Hill, 1977). As moisture on the sorbent increased, the heat of sorption
decreased rapidly. The drop in the heat of sorption is typical of most sorption phenomena

71

in which the more reactive, high-energy, sites are occupied first. Given the highly polar nature of water versus that of TCE and the charged nature of the mineral surfaces, it is not surprising that water vapor will out compete TCE for "sites" on the surface. The decrease in the heat of TCE sorption with increasing moisture content supports the concept that water competes with TCE molecules for sorption sites with water being the preferred sorbate. As noted above, this conclusion is also supported by numerous prior observations (Chiou and Shoup, 1985, Rhue et al., 1988).

As the surface of the solid is gradually covered with bound water molecules, it is possible that bound water molecules may, in turn, act as sorption sites for the TCE molecule. The reduction in the reaction enthalpy and partition coefficients may therefore also reflect adsorption of TCE to bound surface water. However, since surface coverage by water is less than one monolayer in Region 1 (by virtue of the definition of the region), it is reasonable to assume that the mineral surfaces were available to both sorbates.

The partition coefficients for TCE on kaolinite (Figure III.6) and iron oxide (Figure III.7) were observed to decrease more rapidly with a small change in moisture content in comparison to those for montmorillonite and alumina. The kaolinite and iron oxide used in this study have low specific surface areas (8.47 and 10.98 m^2/g respectively) and a small quantity of water would be sufficient to occupy most of the surface sites, thus reducing the amount of TCE sorbed. This is further illustrated by the very rapid decrease of the heat of sorption of the two low specific surface area solids, iron oxide and kaolinite (Figures III.9 and III.10), in comparison to the other high specific surface area solids. This is taken as additional evidence that direct vapor-solid sorption occurs in competition with water in Region 1.

The sustained high sorption of TCE by montmorillonite (Figure III.6) even at high moisture levels beyond Region 1 ($\approx$ 15 percent) is likely to be due to the availability of interlamellar surfaces as the clay expands with increased moisture. In the case of humic coated alumina, the amount of TCE sorbed with increasing moisture is slightly higher (more than a factor of two) in comparison to the uncoated alumina. For example, the partition coefficients for humic coated alumina and alumina at about 12.5 percent moisture content were 48.3 and 19.9 mL/g respectively while at about 36 percent moisture content, the partition coefficients were 1.88 and 0.78 mL/g respectively. However, the higher sorption capacity of humic coated alumina over uncoated alumina does not correspond in magnitude to the increase ($\approx$ 32 percent) in specific surface area of humic coated alumina (189 m^2/g) over alumina (143 m^2/g). Given the complex structure of humic acid which contains hydrophobic regions, it is likely that this higher sorption capacity of humic-coated alumina is a result of an increase of sorption sites that are hydrophobic or the presence of a hydrophobic partition medium which continues to be available at higher moisture contents.

72

Region 2 is designated as a transition state ranging from monolayer coverage of the surface by water molecules to multilayer (4- to 8-monolayer) coverage. TCE partition coefficients for all sorbents declined to a minimum value in Region 2. For pure minerals and clays, evidence of TCE sorption in this region could indicate that TCE is being sorbed onto the water molecules on the solid surface or on bare mineral sites exposed at cleavage steps or kinks (Gregg and Sing, 1982). Given their relative affinities for charged mineral surfaces, the possibility of TCE molecules replacing sorbed water at the solid surface is deemed to be quite low. Although TCE dissolution may also conceivably occur in Region 2, water bound to a mineral surface is structurally different from bulk water as it is strongly influenced by the electrostatic forces on the surface (Grim, 1953, Sposito and Prost, 1982). It is therefore anticipated that the highly structured water in the initial monolayers which coat a mineral surface will act differently from water in bulk solution relative to the activity coefficients for nonionic compounds. The reduction in oxygen solubility in water bound to bentonite (Nakayama and Scott, 1962) is consistent with this expectation.

In Region 2, the minimum heat of sorption was found to be around - 5 kcal/mole for humic coated alumina and slightly less than -7 kcal/mole for kaolinite, iron oxide and alumina. These values, however, are lower than the heat of condensation for TCE , -8.63 kcal/mole at 25°C (Flick, 1985). Since, for each solid the only variable is increasing moisture content, it is evident that reduction in the heat of TCE sorption as well as the reduction in partition coefficients is by virtue of TCE interaction with increasing amounts of bound water. Since surface coverage by bound polar water molecules in Region 2 is likely to be nearly complete, TCE is far more likely to be sorbed to the bound water molecules rather than directly to the mineral surface. The interaction energy between a nonionic TCE molecule and a ionic water molecule is expected to be lower than the sorption of TCE onto another TCE molecule as in condensation (Gammage and Gregg, 1972; Iwaki and Jellinek; 1979). This is confirmed by the Region 2 thermodynamic data. Early condensation of TCE in pores is not likely in any of these experiments since the TCE vapor concentration used was low and early condensation, if it occurred, would evolve heat equal to the heat of condensation. The minimum heat of sorption of TCE was also observed to be below the heat of dissolution of TCE into water.

The highly structured nature of the initial hydrating water layers on minerals (Sposito and Prost, 1982, Newman, 1987) represent an effect comparable to electrostriction of bulk water by salt addition. It is deemed likely that "salting out " of TCE from the first two to three layers of bound water molecules occurs and this is reflected in the reduced enthalpy change for TCE sorption in Region 2. It should be noted that, in the normal sense of the term, "dissolution" of TCE into water one monolayer thick is impossible. Therefore TCE dissolution can only be invoked as a mechanism for Region 2 in the case where early condensation of water has occurred (in solids such as alumina with

73

small radius pores) or at the high moisture content end of the region where four or more monolayers of water exist and a "dissolved" TCE molecule can be surrounded by water.

Region 3 extends from 4 to eight monolayers of water to the moisture retention capacity of the sorbent. In Region 3, the slight increase in sorption of TCE can be postulated as resulting from the dissolution of TCE into the water and/or sorption of TCE at the liquid-vapor interface. In addition, TCE dissolved in the solid moisture can accumulate at the solid-liquid interface.

At higher moisture contents (Region 3), heats of sorption for all the solids except for iron oxide increased to the same magnitude as the heat of dissolution (-9.35 kcal/mole). The thermodynamics data, therefore, indicate that dissolution of TCE may play a role for soils at higher moisture contents. With iron oxide, the heats of sorption slowly increased but were still below the heat of dissolution or condensation. In this case, it is possible that TCE sorption onto the liquid-air interface may be important.

The relative contribution of processes such as dissolution and sorption at the liquid-air interface can be assessed through the use of a mass balance. In Region 3, the total mass of vapor sorbed onto the soil, under equilibrium conditions, can be viewed as being distributed between TCE adsorbed at the liquid-air interface, TCE dissolved in the liquid phase and the TCE sorbed at the solid-liquid interface. Figure III.13 illustrates the different possible distribution states for TCE for solids at high moisture content.
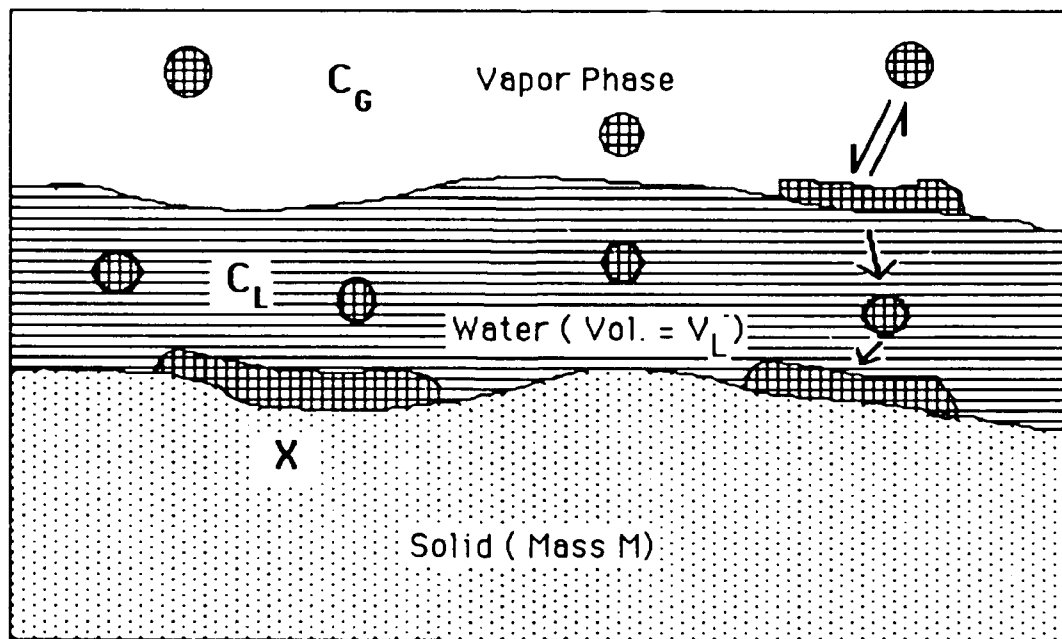
Figure III.12   Diagram of the Possible Distribution of TCE on a Moist Mineral Surface

For vapor-phase partitioning with a moist solid, we have:

Mass sorbed at the solid-liquid interface (X)
     + Mass dissolved in the liquid phase ($C_L V_L$)
       + Mass sorbed at the liquid-air interface
         + condensation (if any)   = $K_d' \, M \, C_G$

where C_G = vapor concentration (mg/L).

This will give:

$$X + C_L V_L + \text{Water-surface Sorption} + \text{Condensation} = K_d' \, M \, C_G \qquad \text{III.8}$$

but, for liquid-phase partitioning:

$$X = K_d \, M \, (\gamma \, C_L) \qquad\qquad\qquad \text{III.9}$$

where X = mass adsorbed on the soil-liquid interface (g)

         K_d = liquid-phase partition coefficient (mL/mg)

         C_L = TCE concentration in the liquid phase (mg/L)

         M = mass of sorbent (g)

         γ = aqueous activity coefficient

Substituting Equation III.9 into III.8 gives: $K_d C_L \gamma + C_L V_L / M + \omega / M = K_d' \, C_G$

where ω is a lumped parameter which includes the effects of water surface sorption and condensation. Therefore,

$$K_d' = K_d C_L \gamma / C_G + C_L V_L / (C_G M) + \omega / (C_G M)$$

If Henry's Law ($C_G = K_H \gamma C_L$) is applicable then:

$$K_d' = K_d / K_H + V_L / (M K_H \gamma) + \omega / (C_G M)$$

Substituting the density of water on the soil surface ($\rho = M_{water} / V_L$), the term V_L / M becomes (M_{water} / M)($1/\rho$) = (moisture content %)/(100 ρ). This results in:

$$K_d' = K_d / K_H + (\text{Moisture Content \%}) / (100 \, K_H \, \gamma \, \rho) + \omega / (C_G M) \qquad \text{III.10}$$

Graphically this equation can be represented as shown in Figure III.13. If Equation III.10 is applied, assuming soil water behaves as pure water ($\gamma = 1.0$, $\rho = 1.0$) and, if water surface sorption and condensation are negligible ($\omega \approx 0$), then for high moisture content a plot of Equation III.10 will be represented as a straight line (AB) on Figure III.13, with the ordinate intercept equal to the contribution of aqueous-phase sorption to vapor-phase partitioning (K_d/K_H). If the activity coefficient of TCE in the soil water is different from one ($\gamma > 1$) or the density of water is different from bulk water, then the tendency is to reduce the amount of TCE in solution. This is represented by line AC. This effect is commonly called the "salting out" effect. If experimental values fall above line AB, then other contributions to sorption such as sorption on the surface of soil water should be considered ($\omega \neq 0$).
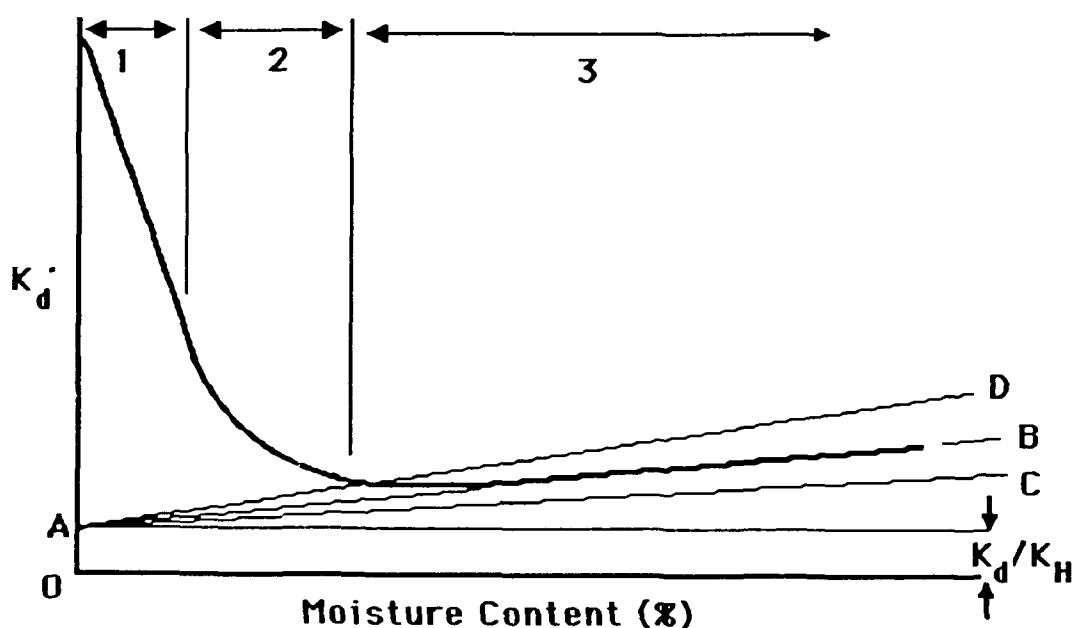
Figure III.13   Interpretation of Experimental Data with Calculated Values from the Proposed Mechanisms in Region 3 (High Moisture Contents)

AB -   Solid-liquid phase sorption along with solution into soil water with minimum salting out effects

AC -   Salting out effects important

AD -   Other sorption processes occurring such as sorption at the water-air interface

OA -   Solid-liquid phase sorption component

76

To compare the data with Equation III.10, the saturated partition coefficient for each solid must be found along with the Henry's constant for TCE. Results for saturated sorption studies are summarized in Table III.3. At the 5 percent level of significance, the partition coefficients of alumina, montmorillonite and kaolinite were not significantly different from zero. Negligible sorption of TCE on these solids is, therefore, assumed. The remaining two solids, iron oxide and humic-coated alumina exhibited significant sorption of TCE. These results are similar to those of Stauffer et al. (1986) who found that iron oxide sorbed more TCE than aluminum oxide.

TABLE III.3 PARTITION COEFFICIENTS OF SOLIDS UNDER SATURATED CONDITIONS

	K_d	std. error	deg. of freedom	t-statistic	prob. > t
Alumina	0.011	0.017	11	0.66	52.5%*
Iron Oxide	0.244	0.069	10	3.56	0.5%*
Mont.	0.049	0.075	14	0.66	51.9%**
Kaolinite	0.270	0.134	11	2.03	7.0%**
C.Alumina	0.308	0.009	14	29.14	0.0*

* K_d is significantly different from 0 at 5 percent level of significance.

** K_d is not significantly different from 0 at 5 percent level of significance.

A modification to the headspace analysis technique developed by Gossett et al. (1985) allowed the determination of the Henry's constant for TCE. Volumes of distilled water ranging from 2 to 30 mL were added to 60 mL vials. As in the experiments with solids, TCE was added to the vials as the saturated vapor. The vials were equilibrated for 24 hours and the headspace concentration tested. By mass balance and using Henry's Law $(C_G = K_H C_L$ with $\gamma = 1)$:

$$V_B C_B = V_L C_L + V_G C_G$$

or:

$$V_B C_B = V_L C_G / K_H + V_G C_G$$

ie.

$$V_B C_B / V_G C_G = V_L / V_G (1/K_H) + 1 \qquad \text{III.11}$$

with V_G being the volume of headspace [vol. of vial - vol. of water added (V_L)]

C_G being the headspace concentration

C_L being the liquid concentration

The reciprocal of the slope of a plot of $\{(V_B C_B / V_G C_G) - 1\}$ against V_L/V_G, gives the Henry's Constant. The dimensionless Henry's constant at 25^{0}C determined by this method (see Figure III.14) was 0.42 which is comparable to that determined by Garbarini and Lion (1985). The heat of dissolution calculated from van't Hoff's equation was -9.35 kcal/mole. This value is slightly lower than the values found by Gossett et al. (1985) using the EPICS method (-9.79 kcal/mole).
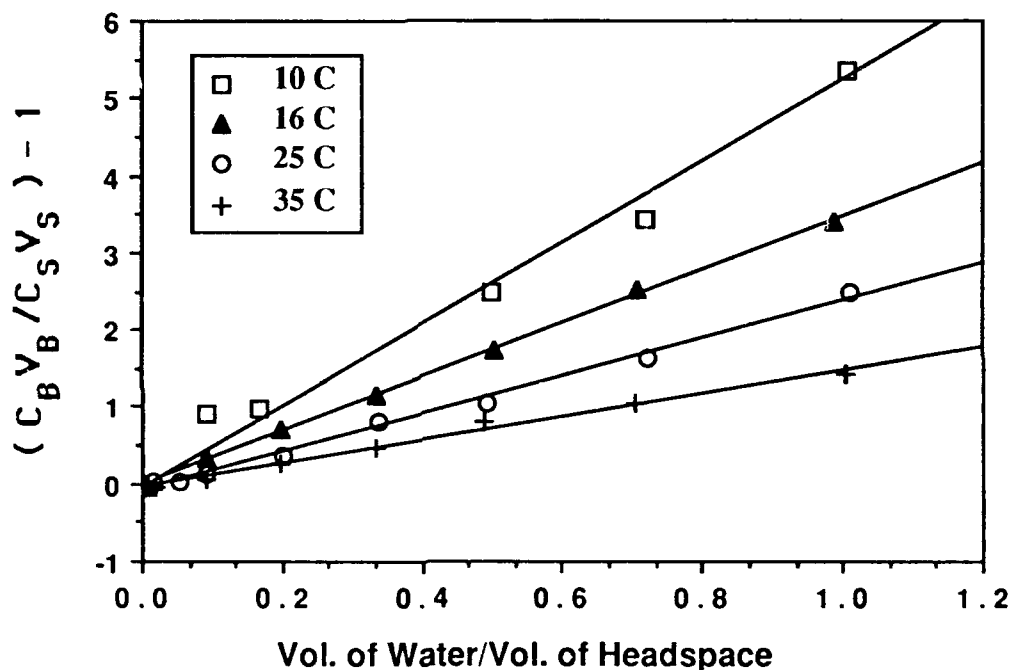
Figure III.14   Determination of Henry's Constant at Various Temperatures

With this information (assuming that the activity of TCE in water, γ, is equal to 1, the density of water is equal to 1 g/mL, and sorption at the water-air interface negligible) the vapor-phase partitioning coefficient with respect to moisture content was computed for each solid. Results are shown in figures III.15 through III.19. Since Equation III.10 is intended to explain vapor sorption in Region 3 (see Figure III.13), most data for low moisture contents have been excluded from these figures.

The experimental data for alumina (Figure III.15, shown with 95 percent CI) matches the calculated vapor-phase partition coefficients based on the Henry's Law constant for TCE with the assumption of a negligible liquid-phase partition coefficient. This result is consistent with the hypothesis that dissolution of TCE into water is occurring.
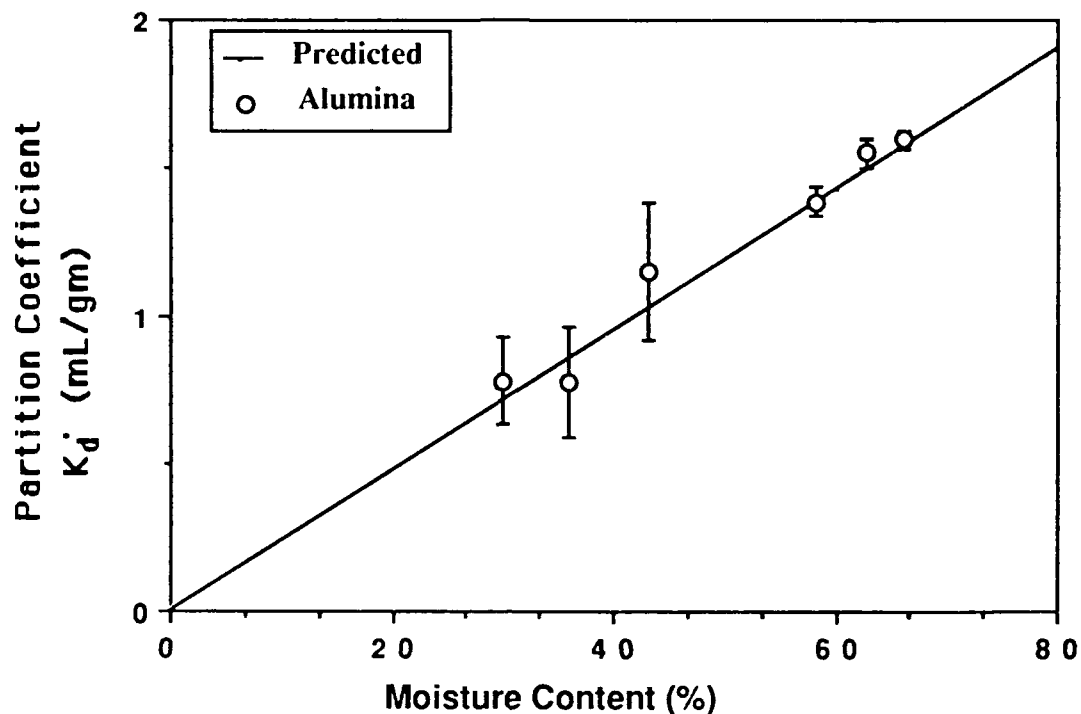
Figure III.15.   Comparison of Experimental Data to Calculated Values for Alumina

With the coating of humic acid on the surface of alumina, sorption of TCE vapor can be accounted for by two components, dissolution of TCE into soil water and sorption at the solid-liquid interface. This is illustrated by the good prediction of the experimental data with Equation III.10 (see Figure III.16). Modifying hydrophilic surfaces such as those of clays by coating with organic molecules to enhance sorption of nonpolar organic pollutants is a common practice among researchers who have sought for alternative sorbents in applications such as wastewater treatment or as for lining materials for waste sites (Wolfe et al., 1986, Boyd et al., 1988) ..In the case of the coated vs uncoated alumina. enhanced sorption of TCE by the coated oxide is accounted for by the addition of a significant contribution from the saturated partition coefficient (ie, $K_d/K_H \neq 0$ in Equation III.10).
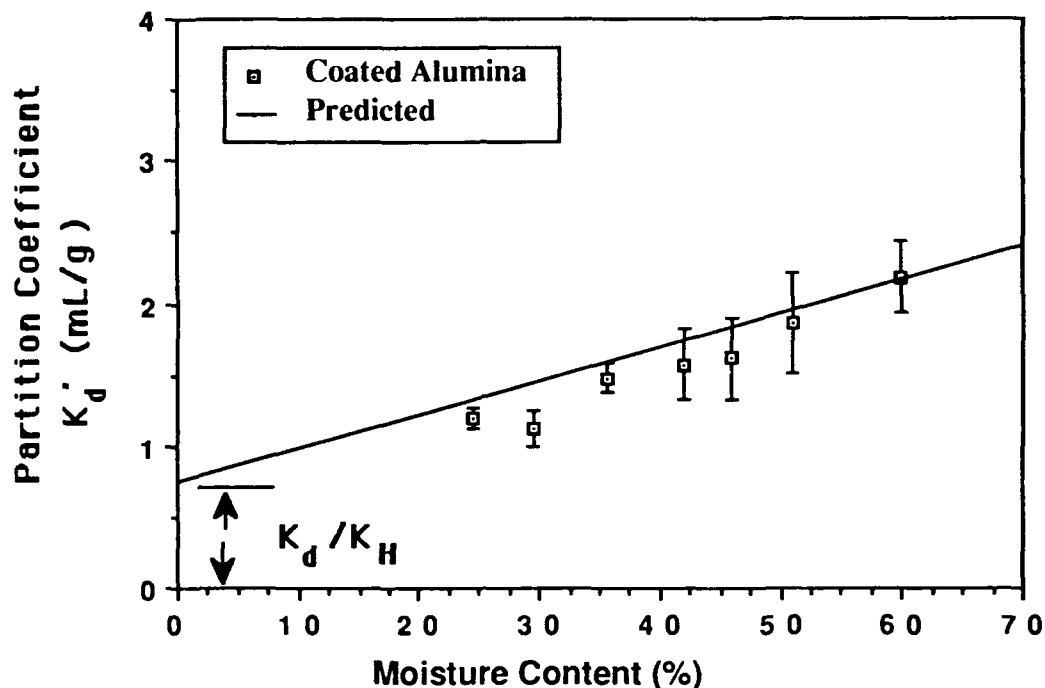
Figure III.16 Comparison of Experimental Data with Calculated Values for Coated Alumina

For iron oxide (Figure III.17), the Region 3 experimental data were also observed to be generally close to the calculated line based on K_H and the observed K_d. An interesting observation is that at a moisture content of 25 percent (about 78 monolayers of water molecules), the partition coefficient was higher than the calculated line. This could indicate that some sorption at the air-water interface is occurring. Most of the experimental data for kaolinite (Figure III.18) lies on or above the calculated line, indicating that dissolution is occurring with a potential small contribution of sorption at the air-water interface. For montmorillonite, the calculated line is slightly above the experimental data (Figure III.19). Prior work on the sorption of water on clays suggests that, for Na^+-montmorillonite, the strong association of the water molecules to the surface oxygen atoms does not extend past the initial monolayer and for Ca^{2+}-montmorillonite it is not more than three layers (Sposito and Prost, 1982). TCE excluded from these layers may account for a slight difference between the experimental data and predictions since the predicted values assumed the activity of these layers to be one.

Given the ability of TCE dissolution and saturated partitioning to explain the observed results in all of the above cases, the magnitude of the contribution of sorption at water-air interface must be relegated to a minor role in the total uptake of TCE in Region 3.
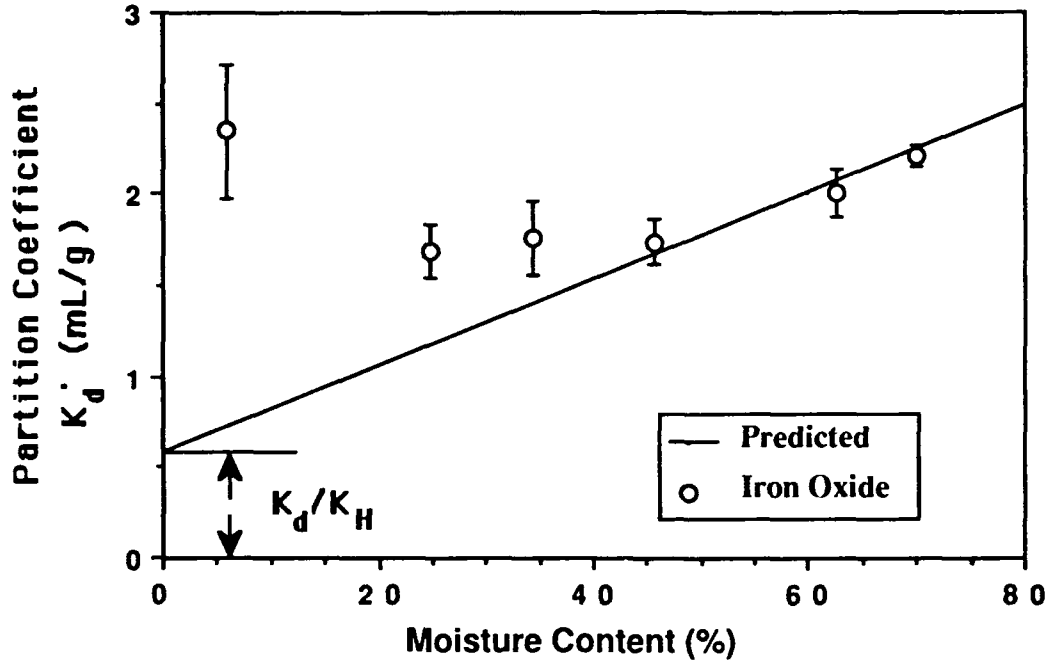
Figure III.17 Comparison of Experimental Data with Calculated Values for Iron Oxide
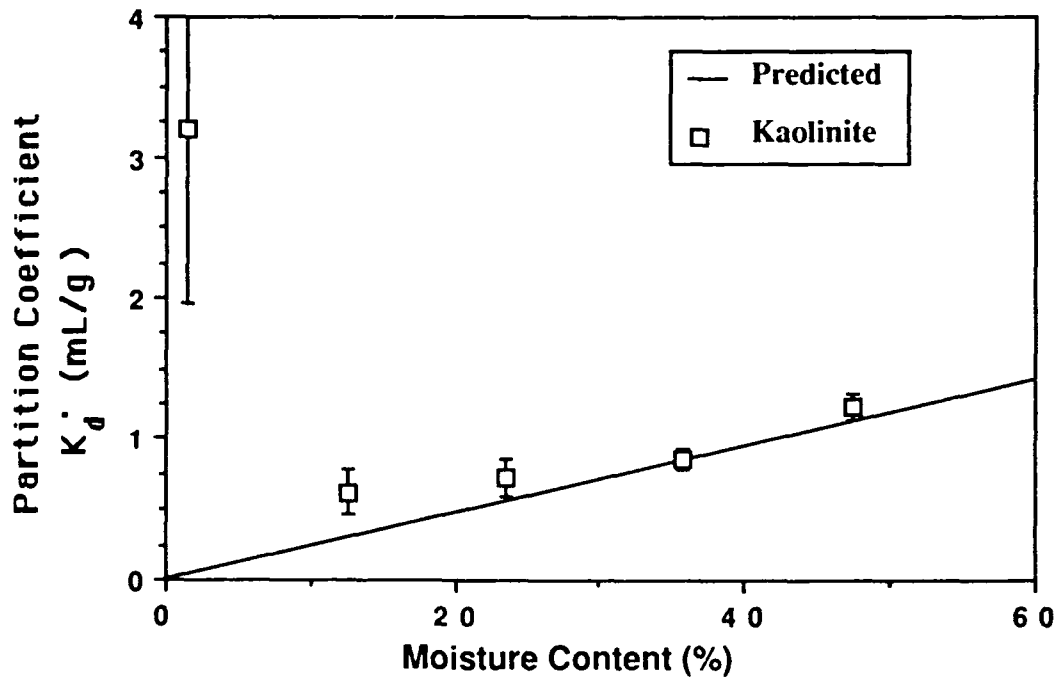
Figure III.18   Comparison of Experimental Data with Calculated Values for Kaolinite
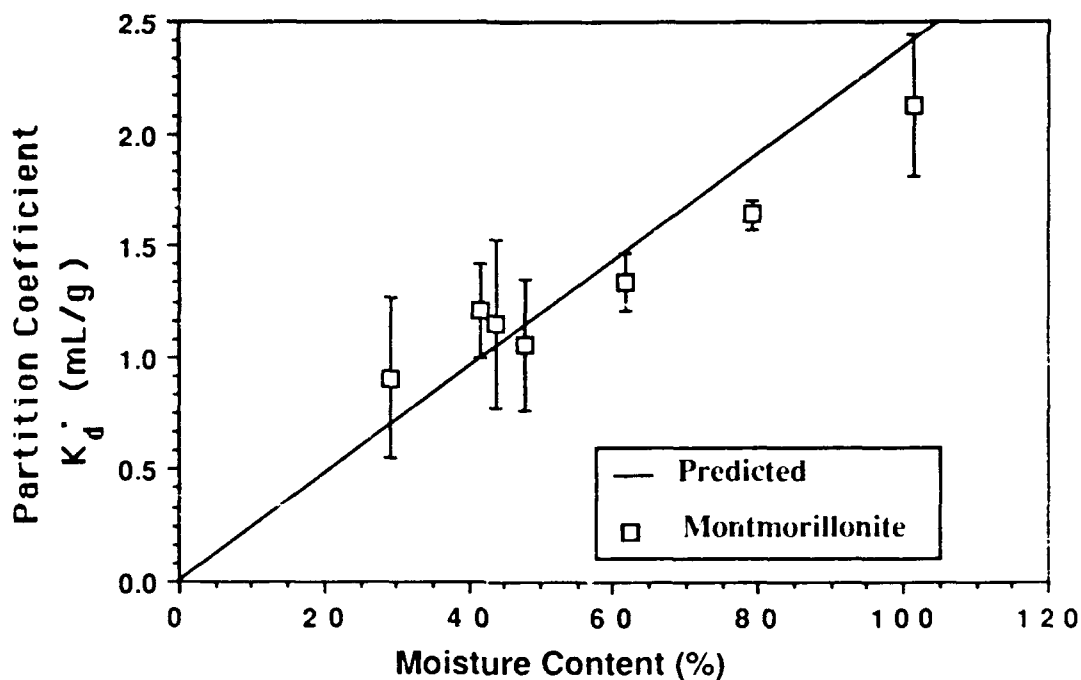
Figure III.19   Experimental Data versus Calculated Values for Montmorillonite

The sorption of TCE vapor by humic acid behaved differently than with the mineral surfaces (Figure III.20). The initial decrease in the partition coefficient was similar to that of the minerals and can be attributed to competition with water. Instead of a slow rise in the partition coefficient as for the minerals in Region 3, a rapid rise was observed with the partition coefficient eventually attaining values higher than the oven dry humic acid. A possible explanation is that under dry conditions, water molecules were driven out from within the structure of the humic acid resulting in greater contact and interaction between polar groups of the humic acid and a reduction in available surface area or pore space. Addition of water causes the humic acid to swell as a result of repulsion between the negative charges of the conjugate bases of the dissociated functional groups (Hayes and Himes, 1986) thereby exposing more sorption sites than when the humic material was dry.

The heat of sorption of TCE onto humic acid (Figure III.10) was different from that observed with the mineral solids in that the heat of sorption for oven-dried humic acid was about -6.3 kcal/mole and continued to remain around -6 to -7 kcal/mole even with increasing moisture. This magnitude of the heat of sorption indicates the interaction of weak intermolecular forces. The slow increase in the heat of sorption with increased moisture content of humic acid implies that dissolving of TCE into condensed water becomes important at higher moisture content.

82
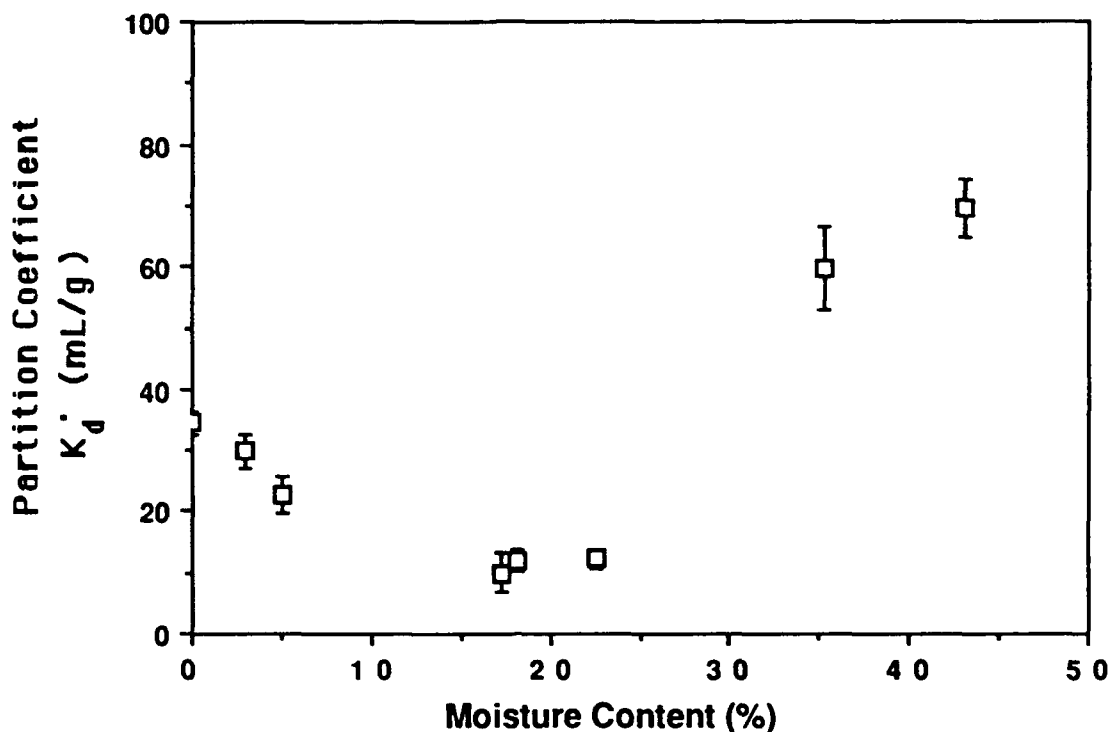
Figure III.20 Effect of Moisture on the Sorption of TCE Vapor onto Humic Acid

c. Applicability of Henry's Constant

To assess when the dissolution of TCE into soil water begins to dominate in the prediction of vapor-phase partitioning or the start of the applicability of Henry's Constant, the vapor-phase data were converted to a transformed variable, $\ln(K_d'-K_d/K_H)$. The transformed variable removes the contribution of liquid-phase partitioning (K_d/K_H) from the overall partition coefficient K_d'. At high moisture content, the transformed variable will reflect only the amount of TCE dissolved in the soil water plus the effects, if any, of TCE sorption on the surface of bound water and condensation of TCE. Examination of Equation III.10 shows that the transformed variable $(K_d'-K_d/K_H)$ should plot as a linear function of moisture content if TCE sorption on the surface of bound water and condensation of TCE are negligible. In addition, if these effects are truly negligible this line should be the same for all surfaces. Since K_d' values under dry conditions can vary considerably depending on the sorbent surface area, the natural logarithm of $(K_d'-K_d/K_H)$ was used to avoid scaling problems. This variable is plotted versus the moisture content (in terms of monolayers of water molecules) in Figure III.21. The number of water monolayers was calculated based on the nitrogen BET specific surface areas of the sorbents assuming that a water molecule would occupy a surface area of 10.8×10^{-10} m^2 (Livingston, 1949).

83
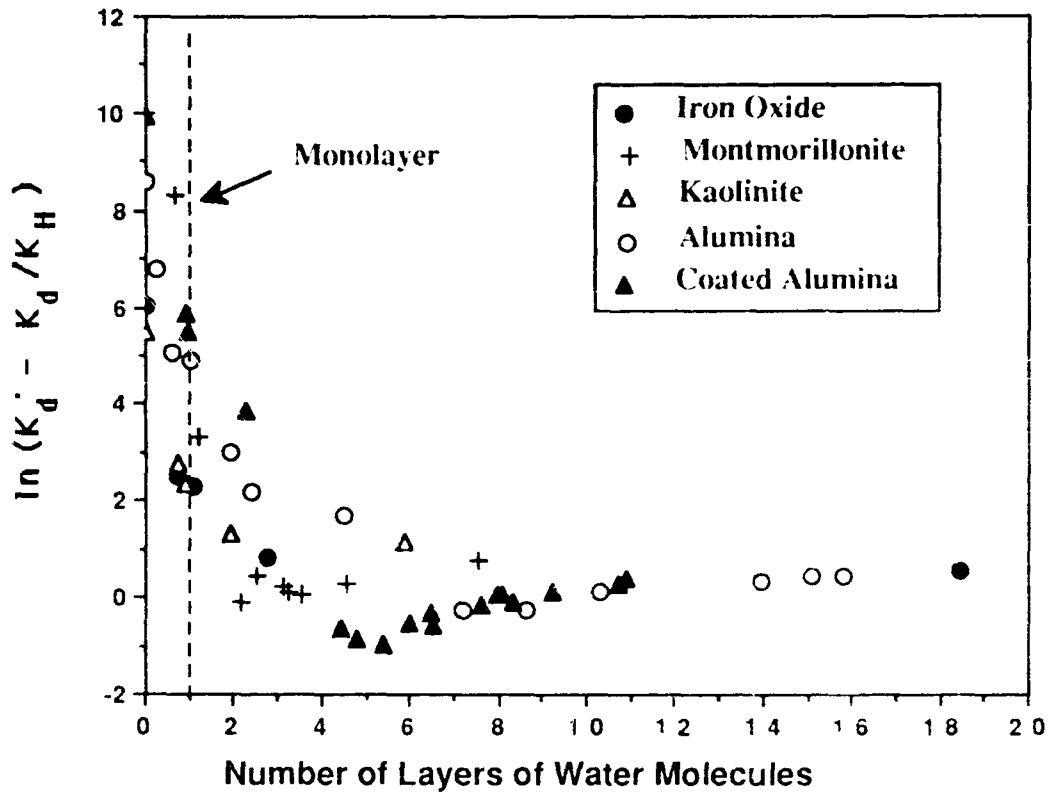
Figure III.21 Plot of Transformed Partition Coefficients vs Water Surface Coverage

Above a minimum of about 4 to 8 monolayers of water, the reduced partition coefficients converge and gently increase, signifying the validity of the assumption that soil moisture dissolves TCE according to Henry's Law. The fact that the transformed variable values for all sorbents are superimposed at high moisture content suggests that a common mechanism (dissolving of TCE into soil moisture) is acting to account for uptake of TCE. On the other hand, below the boundary of 4 to 8 monolayers of water, divergence of the curves for the various solids indicate that direct vapor sorption onto soil minerals and sorption on bound water become important. This is reflected by the rapid rise in partition coefficient as moisture content is decreased. For all the data, at a coverage of one monolayer of water, the amount of TCE sorbed is high (about one to two orders of magnitude above that of solids with > 4 or 5 monolayers of water). Hance (1977) proposed that, after monolayer coverage of the surface by water, an additional change in moisture content would have little influence on partition coefficients. The data obtained here show that the validity of the Henry's Law assumption occurs substantially beyond the arbitrary limit of monolayer coverage; in fact up to eight monolayers of water may be needed in some cases before this assumption can be safely made.

The observations obtained in this study have some implications in the modelling of vapor-phase transport of organic pollutants in the air spaces of the unsaturated zone of the subsurface. For most unsaturated soils in the temperate and humid regions, moisture contents are usually at about field capacity or higher. An estimate of the thickness of the water film at field capacity on the surface of the soil is about 15 to 20 molecular layers (Foth, 1978). This would imply that the incorporation of Henry's Law in vapor-phase transport models is a safe and fair assumption for these regions. However, because of evaporation of moisture at the top layer of surface soil and exposure to fluctuating temperatures and relative humidities, moisture contents that are less than the limiting moisture content (ie. less than 8 monolayers of water required for Henry's Law to be applied) can still occur. In semi-arid and arid regions, soils with very low moisture contents are invariably present throughout the year. For example, Purtymun and Kennedy (1971) found that the soil around Los Alamos National Laboratory, New Mexico to have very low moisture contents for the first half meter of top soil followed by increasing moisture to about field capacity at about 2 meters deep and then decreasing rapidly to moisture contents as low as 2 percent by volume over approximately 100 meters. For these cases, the moisture content may fall below 8 monolayers and the assumption of Henry's Law behavior in transport models will not be valid. The higher sorption affinity of soils with low moisture contents will allow the soils to act as a reservoir for organic pollutant vapors and can retard the volatilization of organic vapors (Peterson et al., 1988; Shoemaker et al. 1990).

D. CONCLUSIONS

The partition coefficients of TCE vapor sorption onto several minerals were found to change greatly with moisture content. Partition coefficients of oven-dried solids were usually several orders of magnitude higher than when the solid was moist. With oven-dried solids, surface area was found to be an important indicator of the sorptive capacity of TCE vapor. Observations of the change of partition coefficients and thermodynamic data with increasing moisture contents resulted in the identification of three distinct regions. Sorption mechanisms have been hypothesized for each region, based upon known surface coverage by water, the observed enthalpy change for TCE partitioning relative to that for TCE condensation or dissolution, and the ability of saturated partition coefficients and TCE dissolution into water to explain the observed data.

Region 1 extends from oven dry conditions to a monolayer coverage by water on the solid surface. In this region, direct TCE vapor sorption on the solid surface is postulated to occur in competition with water for adsorption sites on the sorbents. This hypothesis is supported by (1) the ability of sorbent surface area to remove most of the variance in oven dry partition coefficients, and (2) the observation that water was the preferred sorbate

resulting in a rapid decline in the partition coefficients of TCE vapor onto the minerals. This is consistent with the expected behavior based on the relative polarities of water and TCE sorbates and the hydrophilic nature of charged mineral surfaces. It is possible that weak sorption of TCE on the surface of adsorbed water occurs in Region 1, however, by definition of the region, dry mineral surface sites were also available for TCE.

Region 2 was defined as a transition state extending from between a monolayer water coverage to 4 to 8 monolayers of water molecules. In this region, it is proposed that TCE sorbs onto bound water on the surface of the soil. This is supported by enthalpy data for TCE sorption which are below values for TCE condensation or dissolution into bulk water. TCE condensation into intraparticle pores is also considered unlikely, based on the low experimental vapor pressure employed. Since the water on the surface of minerals is reported to be highly structured within the moisture regime covered by this region, dissolution of TCE is either prohibited (TCE dissolution at one monolayer coverage by water is not possible by definition of the process) or impaired by salting out effects. At the lower end of Region 2 (close to a monolayer coverage) direct sorption on the surface at "dry" cleavage steps and kinks may occur.

Region 3 was defined to extend from 4 to 8 monolayers of water molecules coverage to the water retention capacity of the sorbent. The dissolution of TCE into condensed water along with water-solid interface sorption is postulated to dominate TCE uptake in this region. TCE sorption at the water-air interface sorption was not detectable for most solids used in this study and TCE dissolution plus the saturated partition coefficient could account for all the observed partitioning within the uncertainty (95 percent C.I.) of the data. Enthalpy data were comparable in magnitude to the values expected for TCE dissolution. Depending on the nature of the sorbents, salting out or surface exclusion effects may be important.

Application of Henry's Law to model TCE interaction with water condensed on the solid surface is possible only after 4 to 8 monolayers of water have formed. This assumption may not be valid for soils in arid or semiarid regions or for the top surface soil layer in temperate regions on a seasonal basis.

SECTION IV

TCE VAPOR SORPTION ONTO SOIL MINERALS
AT HIGH VAPOR PRESSURE

By: S.K. Ong and L.W. Lion

A. INTRODUCTION

Isotherms obtained from sorption studies at low vapor concentrations are generally linear and are easily incorporated into transport models to predict the fate of vapor-phase pollutants. Low concentrations can be anticipated to occur in the "far field" at large distances from the pollutant source. However, close to the source or in the presence of nonaqueous-phase liquids (NAPLs), the concentration is usually higher and the relative vapor pressure of the pollutant can approach or is at saturation. Adsorption/desorption information at high vapor pressures is generally not available despite the fact that every fuel or solvent spill and many waste dumps will have vapor concentrations at these levels. Application of the linear partition isotherm at high relative vapor pressures is not likely to be correct since phenomena such as vapor condensation, which is governed by the pore size distribution of a soil, may play a dominant role. The occurrence of multilayer vapor sorption will also invalidate the assumption of linear sorption isotherms. In addition, the presence of water as a vapor phase in competition for sorption sites and in "competition" for pore volume as a condensate complicates the understanding of the vapor sorption/desorption at high vapor pressures.

Relatively few vapor sorption studies have been carried out at high vapor pressure, using soil as the sorbent. Isotherms for oven dry soils are generally found to be curvilinear in shape indicating multilayer sorption and/or condensation (Jurinak and Volman, 1957; Call, 1957a; Chiou and Shoup, 1985; Rhue et al., 1988). Jurinak and Volman (1957) concluded that the number of molecular layers of ethylene dibromide (EDB) vapor sorbed onto some oven-dried soils was restricted. For montmorillonitic soils an average of roughly four monolayers could be formed, while on a peaty muck soil, the number of molecular layers was restricted to six. These results suggest that the formation of EDB monolayers was constrained by the available pore volume of the soils.

In a study on oven-dried soil humic acid, Chiou et al. (1988) found that the limiting vapor sorption capacities of several nonpolar organic compounds were similar when expressed in terms of the volume sorbed per unit weight of soil humic acid. They attributed this finding to the fact that the solubility of a component in a macromolecular medium (ie. humic acid) is best accounted for by its volume faction. Given the similarity between the volume of vapors sorbed, vapor condensation in a finite pore volume could serve as an alternative explanation of the results of Chiou et al. (1988).

Recently, Boyd et al. (1988) hypothesized that, for vapor sorption by dry soil, the soil can be considered as consisting of two fractions in which the mineral fraction behaves as a conventional solid adsorbent while the organic matter acts as a partition medium. However, the external surface area of soils (vs. organic contents) have commonly been found to be a dominant property of oven dry soils in the prediction of their sorptive capacities (Jurinak, 1957; Jurinak and Volman,1957; Rhue et al., 1988).

Sorbent specific differences in vapor uptake can be revealed by the use of the relative isotherm (normalized by the monolayer capacity). The normalized sorptive capacities of soils have been found to be similar for soils with the same dominant mineral components but different for soils with a different dominant mineral component (Jurinak, 1957; Jurinak and Volman, 1957). This indicates that mineral surface area is not necessarily a generic parameter, and that sorbent-specific interactions may need to be taken into account.

In the presence of water vapor, sorption of nonpolar organic compounds at high vapor pressures is greatly reduced relative to that which occurs on oven-dry surfaces (Call, 1957a; Chiou and Shoup, 1985). Competition for sorption surfaces has been cited as a reason for this decrease (Call, 1957a; Chiou and Shoup, 1985). At a relative humidity (RH) of 90 percent, Chiou and Shoup (1985) concluded that the vapor-phase sorption was similar to the saturated liquid phase sorption. Wade (1955) observed that sorption isotherms for EDB continued to be non linear at 90 percent RH.

The objective of this study is to extend the understanding of the vapor-phase sorption phenomenon by considering the influence of soil properties, in particular pore volume, on sorption of an organic vapor in the presence and absence of moisture. Trichloroethylene (TCE), a common volatile organic pollutant found at many waste sites, is used as the sorbate. Sorption of TCE and water vapor onto several common soil minerals, as well as on a commercial humic acid, is evaluated over the full vapor pressure range. Binary vapor sorption experiments are also described for RH up to 80 percent and at variable TCE relative vapor pressures up to 90 percent. The moisture conditions for the binary experiments are typical of semi arid/arid regions or of seasonally dry surface soils.

B. METHODS AND MATERIALS

1.Sorbents Employed and Methods of Characterization

The sorbents employed included the soil mineral components (aluminum oxide and iron oxide, Ca^{2+}-Montmorillonite and Kaolinite) used in the low TCE vapor pressure study of Section III. Silica (Min-U-Sil 5) was also used as an additional mineral phase and was obtained from Pennsylvania Glass Sand Corp. Aldrich humic acid was also used both as a sorbent and as a coating on alumina (Garbarini and Lion, 1985).

88

All the solids were characterized for their specific surface areas, organic carbon content, cation exchange capacity and pH (see Section III). In addition to these properties, the pore volume and pore size distribution of the solids were evaluated by (1) nitrogen adsorption (Quantasorb® Surface Area Analyzer, Quantachrome Co.; Syosset, NY) and (2) mercury porosimetry (Porous Materials Inc.; Ithaca, NY). Adsorption of nitrogen has excellent sensitivity for the lower range of mesopores between 10 Å to 150 Å (Gregg and Sing, 1982). Mercury porosimetry measures the intrusion of mercury into the pores of the samples under high pressure and is applicable to pore sizes as small as 50 Å, given the 60,000 psia intrusion pressure of the instrument in Cornell Environmental Laboratory.

2.Experimental Methods

Vapor sorption was analyzed using a gravimetric technique. Several methods have previously been employed to measure the gain in weight resulting from adsorption; a common method is to use a sensitive spring. The adsorption apparatus employed is illustrated in Figure IV.1 and was adapted from that described by Noll et al. (1985). A small vessel containing 0.1 to 0.25 grams of the sorbent was suspended from a quartz spring (Rocky Mountain Quartz, Colorado). The spring had an extension response of 9.941 milligrams per cm (25.2495 milligrams per inch). Extension of the spring created by sorption of TCE and/or water vapor was measured with a Gaertner cathetometer having a precision of ± 0.00005 cm (ie. ± 5 x 10^{-3} milligrams weight change). Samples were kept at a constant temperature (± 0.5°C) by the use of a water jacket.

Nitrogen gas was dried with Drierite® and then divided into three flow streams. The flow rates through each line were precisely controlled with a Matheson automatic control valve/flow sensor model 8242 in conjunction with a flow rate controller model 8141. Each gas stream had a maximum flow rate of 100 mL/min. The total flow rate through the column was found to have negligible drag force effect on the sample vessel and spring extension could therefore be measured while the gas flow was on. One of the gas streams was saturated with TCE vapor by bubbling through liquid TCE and another was saturated with water vapor. By mixing different ratios of dry nitrogen, TCE and water saturated flows, different RHs and TCE relative vapor pressures (P/Po) in the adsorption column were obtained. For some experiments, the water bath containing the TCE gas washing bottles was heated to assist in the vaporization of the TCE. By heating the TCE gas washing bottles, a high TCE relative vapor pressure could be achieved even at high RH. A maximum of 80 percent RH could be achieved while still varying TCE P/Po from 0 to 90 percent. In experiments with TCE at constant RH, the sorbent was equilibrated with water vapor at the desired humidity prior to introduction of TCE vapor.
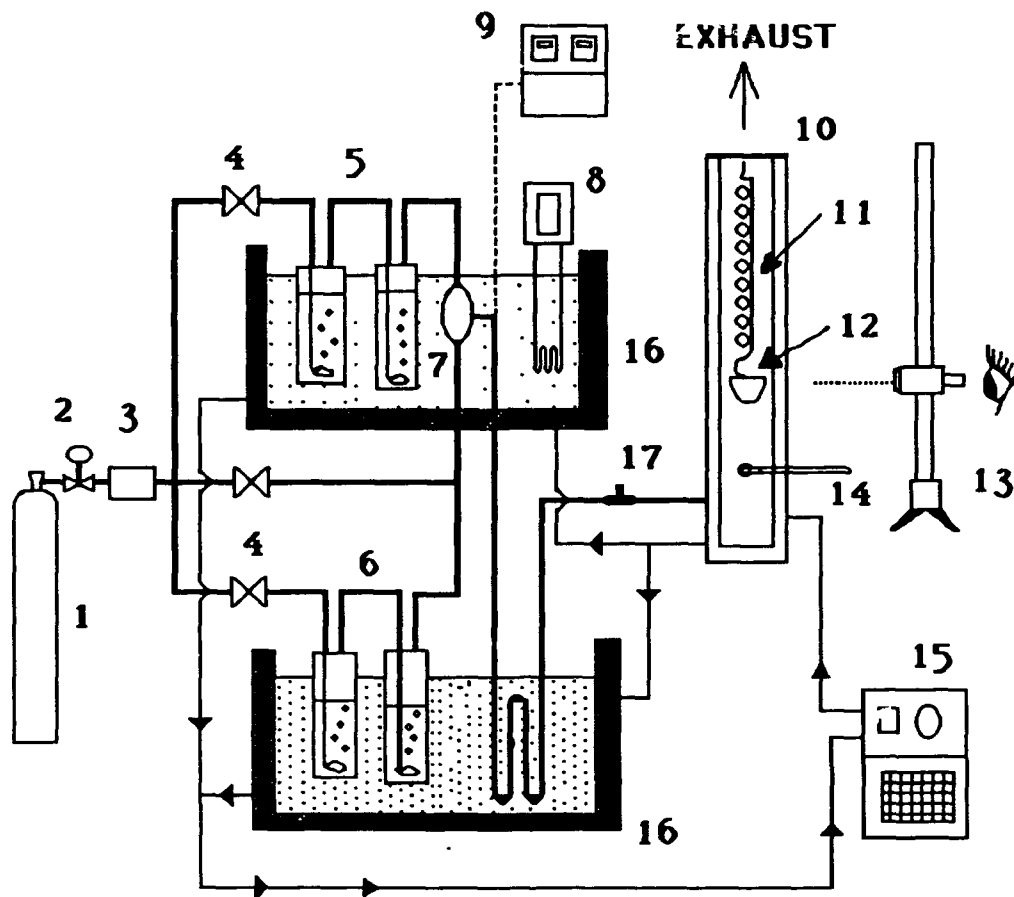
1. Nitrogen Gas Tank
2. Gas Regulator
3. Dessicator
4. Flow Controllers
5. Gas-Washing Bottles (TCE)
6. Gas-Washing Bottles (Water)
7. Mixing Chamber
8. Heater
9. Relative Humidity Monitor
10. Const. Temp. Water Jacket
11. Quartz Spring
12. Soil Sample
13. Cathetometer
14. Thermometer
15. Water Circulator
16. Const. Temp. Water Bath
17. G.C. Sampling Point

Figure IV.1   Gravimetric Adsorption Apparatus

Relative humidity was measured with a hygrometer using an optical dew point sensor (General Eastern Hygrometer Model 1500, Watertown, MA). The vapor pressure of the TCE was computed from the ratio of flow rates. The vapor pressure of TCE was checked by withdrawing a 1 mL sample from the gas line just before it entered the adsorption column (at point 17, Figure IV.1). TCE vapor was subsequently analyzed on a Hewlett Packard Model 5890 Gas Chromatograph (GC) using a flame ionization detector (FID). Since direct injection of the sample overwhelmed the response of the GC FID, the sample was diluted by injecting it into a 60 mL vial. The diluted vapor was within the linear range of the FID. The diluted sample was placed in a water bath (25°C) for 15 to 30 minutes to equilibrate prior to GC analysis. At the same time, a control vial containing 1 mL of saturated TCE vapor was prepared. The saturated TCE vapor was withdrawn from the headspace of a source bottle containing liquid TCE. The ratio of the headspace GC peak area of the sample to that of the control vial gave the relative pressure of TCE in the gravimetric adsorption apparatus. A comparison of this result with the computed vapor pressure from the ratio of the flow rates showed excellent agreement.

All sorbents were prepared by drying in an oven at 105°C for at least 48 hours. Sorbents were immediately transferred from the oven to the sample vessel, weighed and placed in the oven again for 2 to 3 hours. The vessel was then quickly transferred onto the spring of the dynamic flow apparatus. The sample was exposed to dry nitrogen gas for about 12 to 24 hours before the appropriate RH and/or TCE vapor pressure were established. In comparison to the headspace analysis technique discussed in Section III, the spring apparatus can achieve the full range of vapor pressures for TCE.

C. RESULTS AND DISCUSSION

1.Characterization of Sorbents

The properties of the experimental solids are summarized in Table IV.1. As described in Section III, all the sorbent minerals had very low organic carbon contents while the humic coated alumina had an organic carbon content of 0.45 percent. BET surface areas varied from as high as 189.3 m^2/g for coated alumina to as low as 4.88 m^2/g for silica. The BET surface area of the sorbents were computed using an average molecular cross-sectional area (a_m) of 16.2 $Å^2$ for a nitrogen molecule (Livingston, 1949). Montmorillonite had the highest cation exchange capacity while silica had negligible exchange capacity within precision of the analytical method. Despite the presence of humic acid, the cation exchange capacity for coated alumina showed no change when compared to uncoated alumina.

91

TABLE IV.1 PHYSICAL-CHEMICAL CHARACTERISTICS OF THE SORBENTS

	Alumina	Coated Alumina	Iron Oxide	Kaolinite	Montmo-rillonite	Silica	Humic Acid
Particle Density (g/cm^3)	2.98	2.57	4.03	2.51	1.8	2.64	-
pH (H$_2$O extract)	4.5	7.18	6.5	4.2-5.2	8.3	7	9.96
Org. Carbon (percent)	0.02	0.45	0.06	0.01	0.02	<0.01	35.5
Surface Area (m^2/g)							
BET Nitrogen	143.2	189.3	10.98	8.47	97.42 [1]	4.88	0.34 [3]
EGME Method	183.0	250.0	24.9	21.3	733.0	8.7	123.8
CEC (meq/100g)	15.5	15.5	18.5	7.5	113.5	-	
Mean Pore diameter							
- BET Nitrogen (Å)	40	40	*	*	*[2]	*	**
- Mercury							
- Based on Surface Area (Å)	50	50	**	**	**	-	**
- Based on Vol. (microns)	40.3	36.4	**	**	**	0.795	**
Cum. pore vol. (cm^3/gm)							
BET Nitrogen	0.065	0.102	*	*	*	*	**
Mercury	0.833	0.78	**	**	**	**	**
Median Particle size (microns)	150	150	0.9	5.0	**	1.9	**

1 - from van Olphen and Fripiat (1979)

2 - Interlamellar pores cannot be measured by the BET Method

3 - from La Poe (1985)

* - no evidence of pores, nonporous solids

** not measured

The nitrogen adsorption/desorption isotherms for iron oxide, kaolinite and silica showed no hysteresis, confirming the manufacturers' specification that these sorbents are nonporous. For alumina and humic coated alumina, pores of a mean diameter of 40 Å were found. Pores of roughly this size were confirmed with the mercury porosimeter in which mean pore diameters for both solids (calculated on a surface area basis) were 50 Å. The mean pore diameter calculated from porosimeter analysis on a volume basis was much larger at 40.3 and 36.4 microns for alumina and coated alumina, respectively. The larger (volume based) pore diameter is interpreted as indicating the interparticle pores (external) while the smaller (area based) pore diameter indicates the intraparticle pores (internal). Using a similar argument, the pore volumes measured with the BET nitrogen method and mercury porosimeter are expected to differ. The interparticle pore diameter of silica was found to be 0.795 microns while, as anticipated, there were no intraparticle pores.

2.Sorption and Desorption Kinetics of TCE and Water

Direct measurement of the extension of the spring as the sample was exposed to TCE or water vapor provided an excellent and accurate method of determining the sorption and desorption kinetics of the sorbates. Equilibrium was assumed to be attained when the spring extension ceased.

Figure IV.2 shows the sorption kinetics for water on alumina for a change in RH from 38 to 45 percent and 87 to 91 percent. The Y-axis indicates the increase in the amount sorbed over these changes in RH. The sorption of water at both RH was gradual over the first 150 minutes with equilibrium achieved around 200 minutes. However, in desorption studies (Figure IV.3), a much longer time was required to reach equilibrium. In the case of a change in RH from 21 percent to 10 percent about 250 minutes was sufficient to reach equilibrium while at least 400 minutes was required for desorption to reach equilibrium at 88 percent RH.

The sorption kinetics of TCE onto oven-dried solids (ex., coated alumina in Figure IV.4) showed that sorption was rapid for the first 50 minutes followed by a slow approach to equilibrium by 150 minutes. Sorption for a change of TCE vapor pressure from 0 to 3 percent P/P_0 took longer than for a surface that already had TCE molecules on it (ex., for a change of vapor pressure from 14 to 20 percent P/P_0). In the case of uncoated alumina (Figure IV.5), sorption for a change of vapor pressure from 0 to 20 percent was more rapid (< 50 mins) than for a change from 0 to 2.5 percent P/P_0. Comparing the two solids (humic coated and uncoated alumina), about 200 minutes was deemed sufficient for the sorption of TCE to reach equilibrium. Based on the above results, sorption readings were taken after 4 hours while more than 6 hours was allowed for the desorption part of the isotherm.
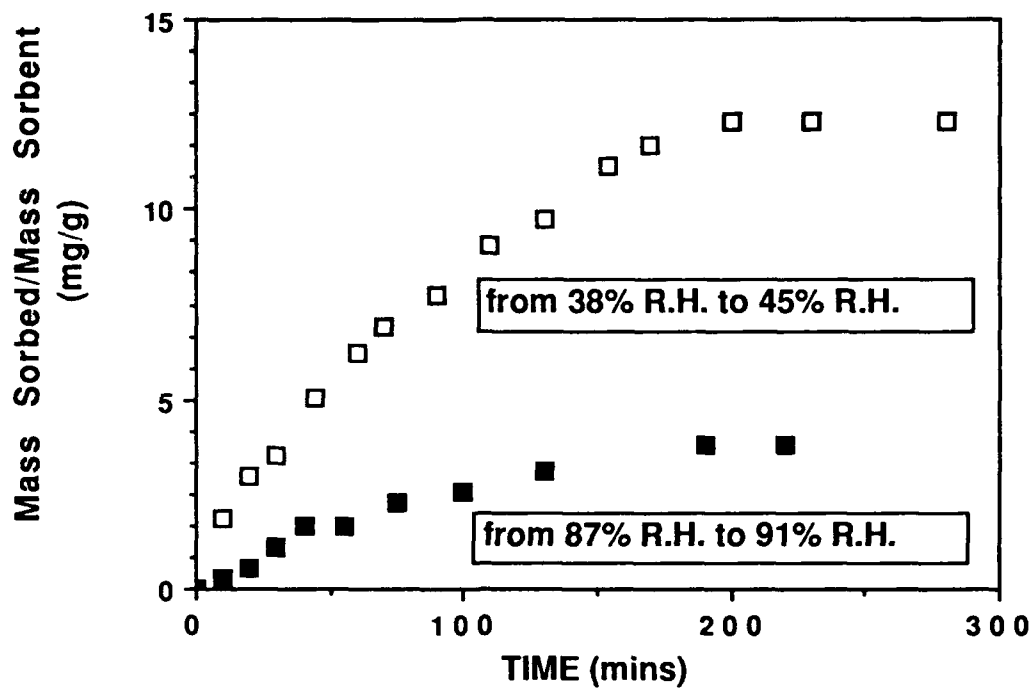
Figure IV.2. Sorption Kinetics of Water onto Alumina

from 38% R.H. to 45% R.H.

from 87% R.H. to 91% R.H.

▲ Desorption from 21% R.H. to 10% R.H.

□ Desorption from 92% R.H. to 88% R.H.
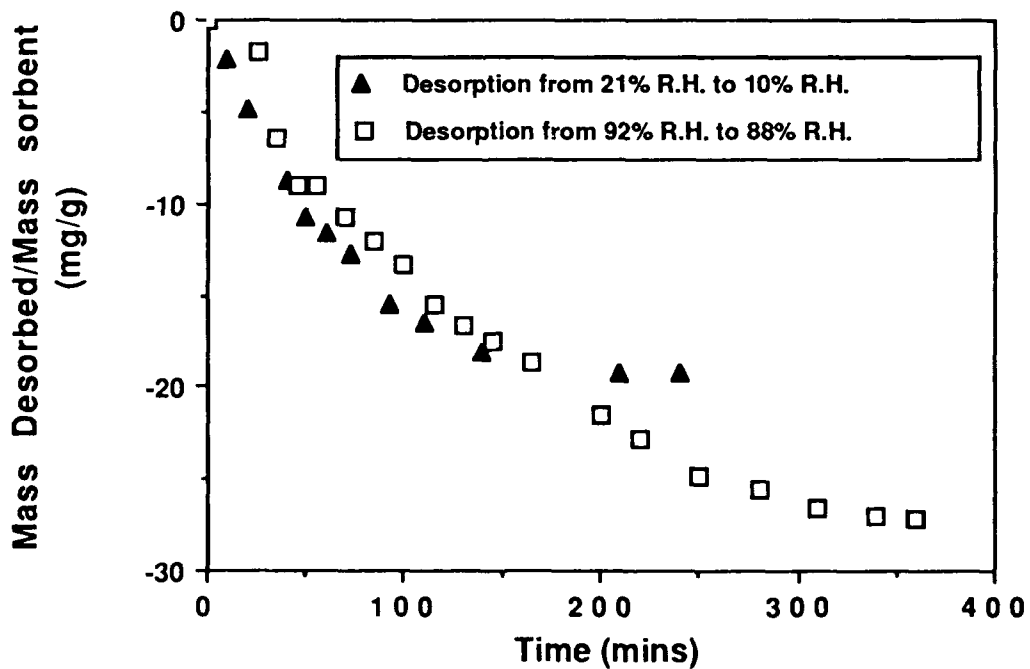
Figure IV.3. Desorption Kinetics of Water from Alumina

94
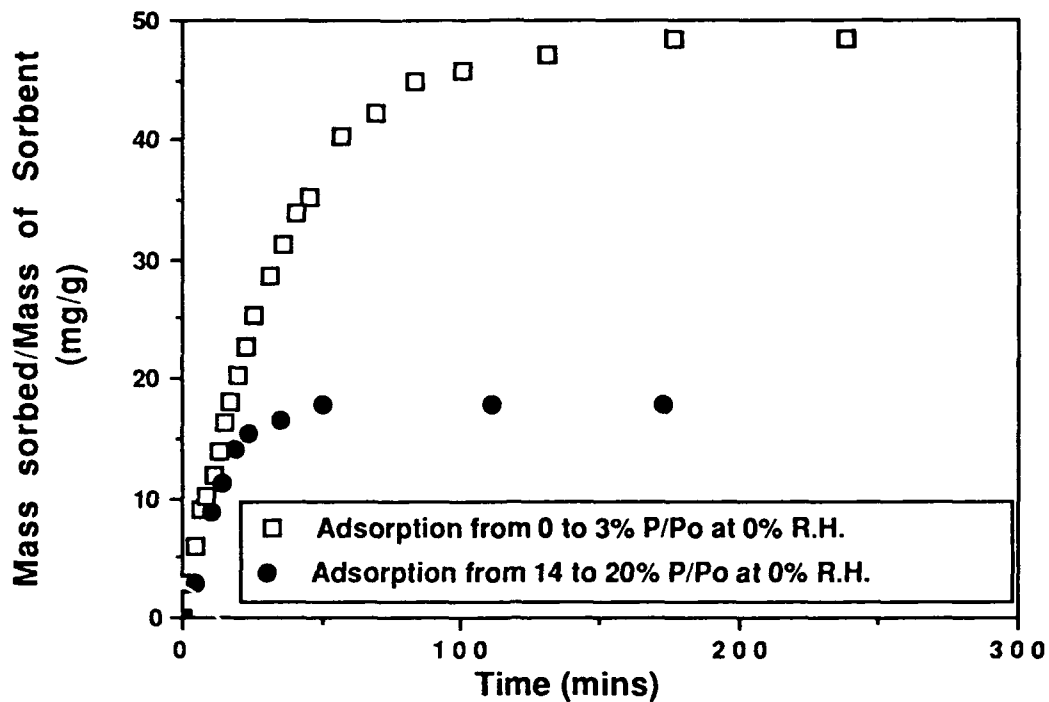
Figure IV.4 Sorption Kinetics of TCE onto Coated Alumina
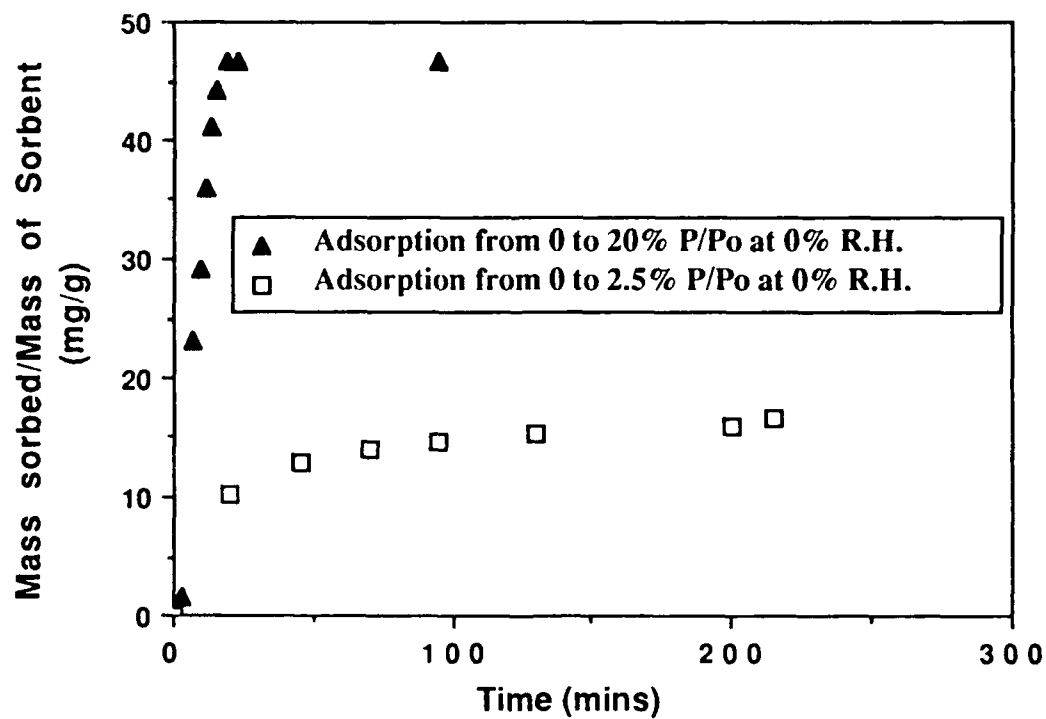
Figure IV.5. Sorption Kinetics of TCE onto Alumina

3.Water Sorption/Desorption on Oven Dry Materials

Adsorption and desorption isotherms of water on all seven materials listed in Table IV.1 are shown in Figures IV.6 to IV.11. Iron oxide, kaolinite and silica (Figures IV.9, IV.10 and IV.11) exhibited a distinctive BET type II isotherm shape. The "knee" of these isotherms was prominent, and the isotherms were without hysteresis. The water adsorption isotherms for both iron oxide and silica increased very slowly after the knee was reached; but at about 90 percent RH, there was a large increase in the amount adsorbed resulting from condensation of water on these surfaces. The water desorption isotherms in Figures IV.9 to IV.11 lie almost exactly on the adsorption isotherm indicating the non-porous nature of the solids. Alumina and coated alumina (Figures IV.6 and IV.7) have BET type IV isotherms. Both solids exhibit some hysteresis with the desorption part of the isotherm merging with the adsorption portion at about 15 percent relative humidity. In spite of its greater (by 30 percent) surface area, the humic acid coated alumina adsorbed the same amount of water as uncoated alumina for RH less than 25 percent (Figure IV.12). However, at higher RH, the coated alumina showed less affinity for water than uncoated alumina. It is possible that the presence of organic matter on the coated alumina increased the density of hydrophobic sites with a decrease or masking of hydrophilic sites. Addition of organic matter could also have rendered the coated alumina less porous. The mercury porosimetry data confirmed a slight (7 percent) decrease in pore volume of the alumina after coating.
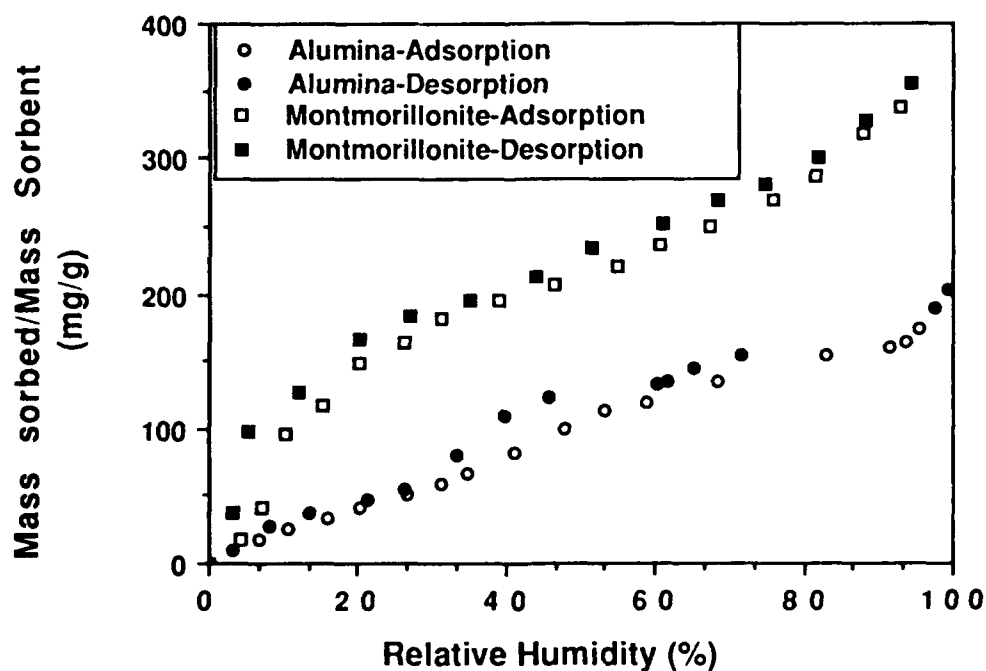
Figure IV.6 Sorption of Water Vapor onto Alumina and Montmorillonite
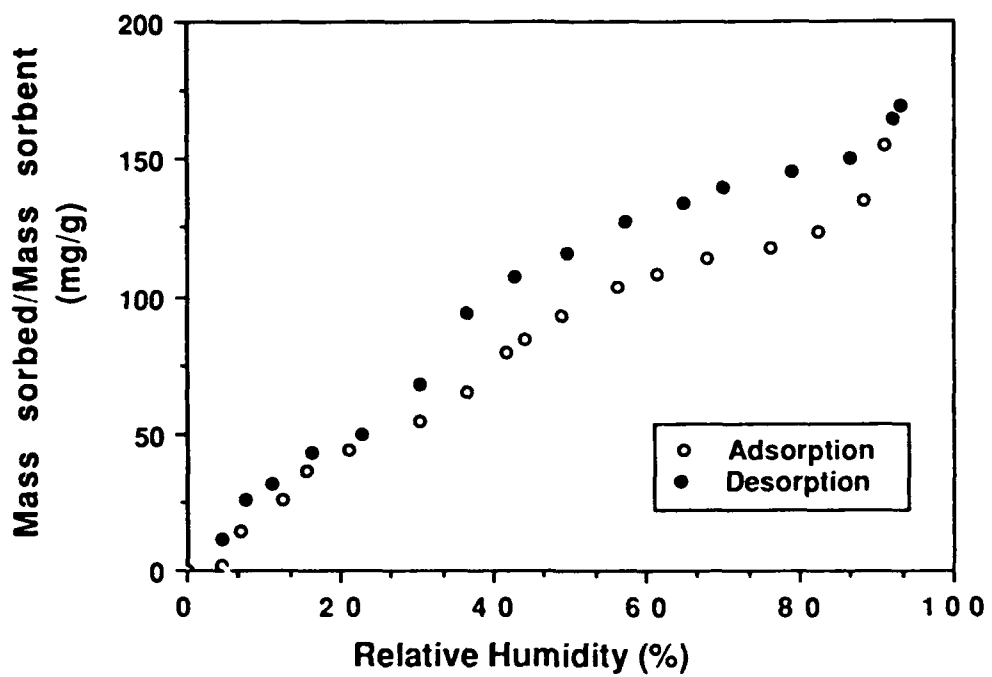
Figure IV.7. Sorption of Water Vapor onto Coated Alumina
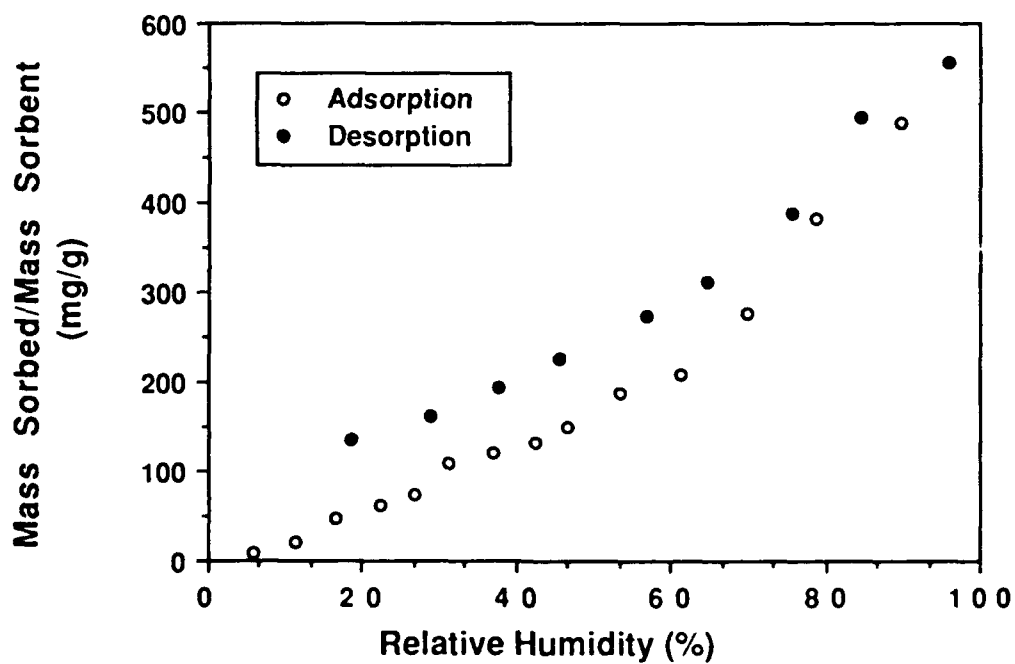
Figure IV.8. Sorption of Water Vapor onto Humic Acid
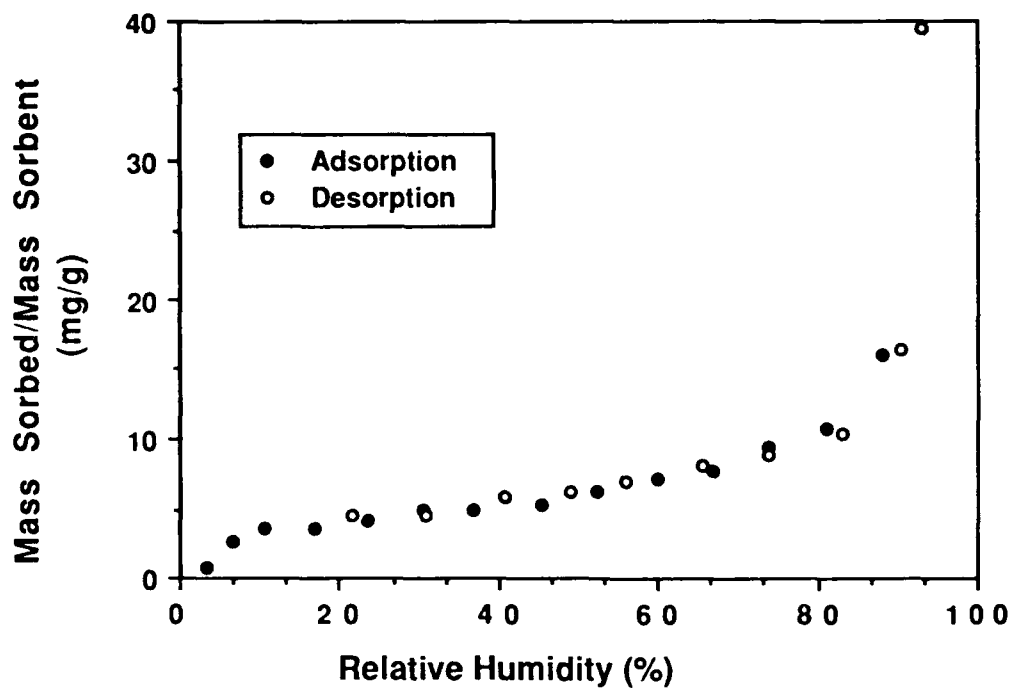
Figure IV.9. Sorption of Water Vapor onto Iron Oxide
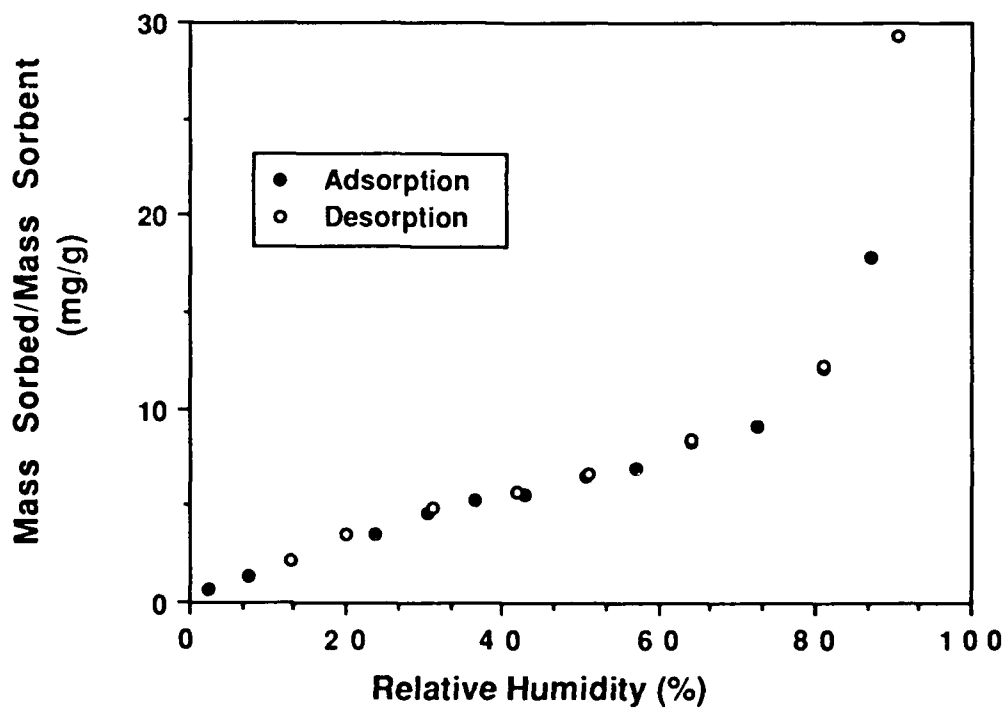
Figure IV.10. Sorption of Water Vapor onto Kaolinite

98
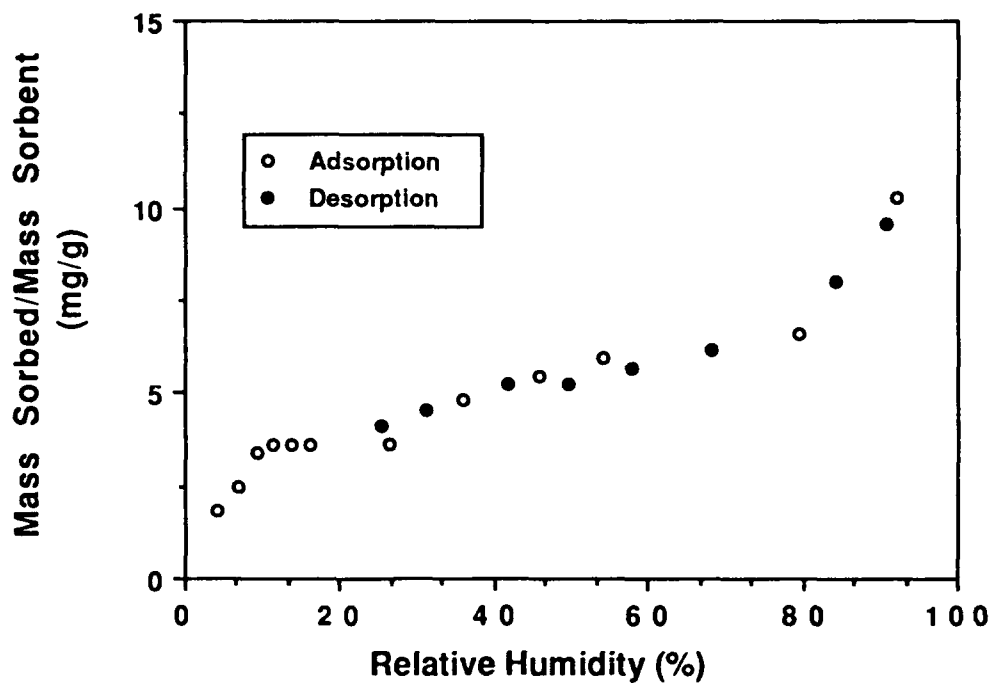
Figure IV.11. Sorption of Water Vapor onto Silica
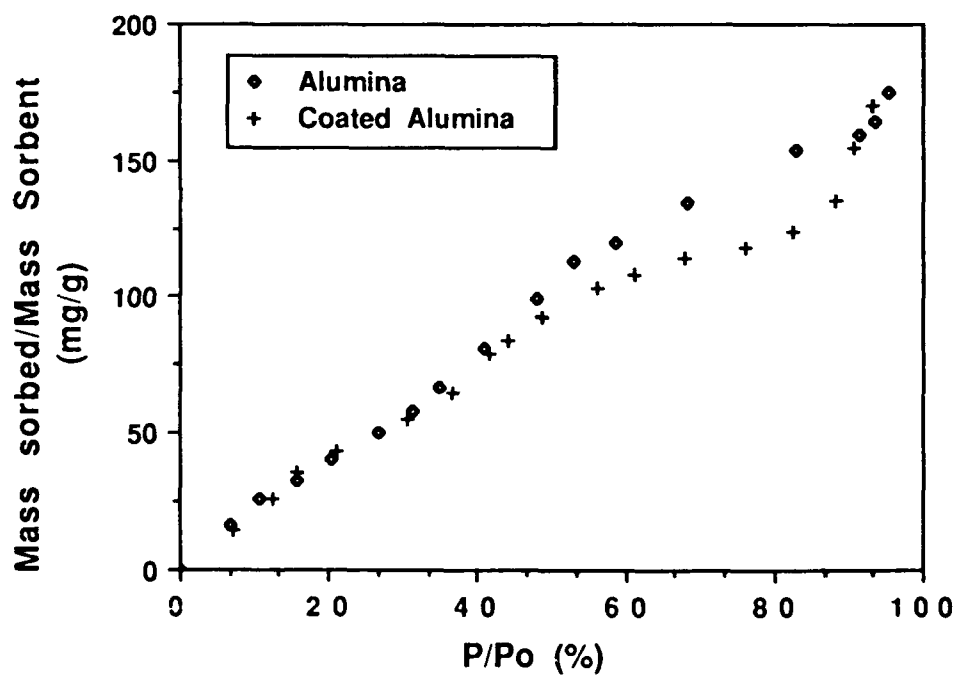
Figure IV.12. Comparison of the Water Vapor Adsorption Isotherms for Coated and Uncoated Alumina

99

The initial branch of the water desorption isotherm (<10 percent RH) for montmorillonite (Figure IV.6) was slightly convex in shape but subsequently became concave. Except for the initial convex shape, which is attributed to the interlayer expansion of the clay platelets (Mooney et al., 1952), this isotherm has a BET Type IV shape. Hysteresis for water sorption on montmorillonite continued to as low as 5 percent RH. This behavior can again be attributed to the sorption of water in the interlamellar pores.

Sorption of water onto humic acid (Figure IV.8) followed a Type III isotherm, having a convex shape but with a gradual slope over 15 to 60 percent RH. This unusual behavior may result from the penetration of water molecules into the matrix of the humic acid which causes the humic acid macromolecules to swell increasing the availability of internal sorption sites (Hayes and Himes, 1986; Degens and Mopper, 1976). The presence of hysteresis in the water adsorption/desorption isotherm for humic acid at low relative humidity supports this hypothesis.

Despite its many simplifying assumptions, the BET model is widely used in analysing vapor adsorption isotherms. The model (with the assumption of a infinite layer capacity of sorbate molecules at saturation vapor pressure) is given by:

$$\frac{\Gamma}{\Gamma_m} = \frac{c\,(P/P_0)}{\left(1 - \dfrac{P}{P_0}\right)\left(1 + \dfrac{P}{P_0}(c-1)\right)}$$

IV.1

where

Γ - amount sorbed per unit mass of sorbent (mg/g)

Γ_m - monolayer coverage (mg/g)

c - parameter related to heat of sorption

P - vapor pressure of sorbate (atm)

P_0 - saturation vapor pressure of sorbate (atm)

Equation IV.1 may be linearized as:

$$\frac{1}{\Gamma\left(\dfrac{P_0}{P} - 1\right)} = \frac{1}{c\,\Gamma_m} + \frac{(c-1)\,(P/P_0)}{c\,\Gamma_m}$$

IV.2

A plot of $1/[\Gamma\,(P_0/P-1)]$ versus P/P_0 should give a straight line with slope, $S = (c-1)/\Gamma_m c$ and intercept, $I = 1/\Gamma_m c$. Solution of these two equations gives:

$$\Gamma_m = 1/(S+I)$$

IV.3

Estimates of Γ_m and c for the experimental solids are shown in Table IV.2 along with estimated specific surface areas. The specific surface areas of the sorbents were computed using an average molecular cross-sectional area (a_m) of 10.8 Å^2 for a water molecule (Livingston, 1949).

The relative heat of sorption ($\Delta H = E_1 - E_L$) was computed from: $\Delta H = RT \ln c$

where: E_1 = Heat of sorption of the first layer (kcal/mole)

E_L = Heat of liquefication (kcal/mole)

TABLE IV.2   ESTIMATED BET PARAMETERS FROM WATER AND TCE
ADSORPTION ISOTHERMS ON OVEN DRY SORBENTS

Sorbent	Sorbate	Γ_m (mg/g)	c	ΔH $E_1 - E_L$ (kcal/mol)	Sp. Surface** Area (m^2/g)	N$_2$ BET Sp. Surface Area (m^2/g)	Area per molecule[†] (Å^2)
Alumina	Water	58.14	5.06	0.96	199.88	143.2	7.36
	TCE	45.35	23.2	1.86	63.68		68.91
Coated	Water	59.17	4.69	0.916	203.4	189.3	9.57
Alumina	TCE	123.31	19.79	1.767	173.16		33.49
Kaolinite	Water	4.46	5.62	1.022	19.32	8.47	5.68
	TCE	3.74	37.82	2.084	5.25		49.43
Mont-	Water	134.97	38.44	2.161	463.3	97.4	2.158
morillonite	TCE	33.6	788.3	3.95	47.18	755*	63.28
Silica	Water	4.02	22.04	1.83	13.81	4.88	3.63
	TCE	2.61	29.54	2.01	3.67		40.77
Iron Oxide	Water	3.22	100.23	2.73	11.07	10.98	10.2
	TCE	6.53	33.28	2.08	9.17		36.68
Humic Acid	Water	-	-		-	-	
	TCE	5.70	15.27	1.61	8.0		

* - surface area measured with the EGME method.

† molecular cross-sectional area computed from Γ_m by assuming the BET nitrogen specific surface area

** computed assuming a_m = 10.8 Å^2 for H_2O and a_m = 30.65 Å^2 for TCE

The theoretical molecular cross-sectional area of a sorbate can be computed from the following equation by assuming hexagonal close packing (Gregg and Sing, 1982) with 12 nearest neighbors as in bulk liquid.

$$a_m = 1.091 \times 10^{-4} \ (M/\rho_L L)^{2/3} \hspace{3cm} IV.5$$

where : M is the molecular weight (g) of the sorbate, ρ_L is the bulk liquid density (g/cm^3) and L is the Avogadro constant. Units of a_m are in m^2.

Except for iron oxide, all the computed surface areas using water as the sorbate were higher than the BET N$_2$ surface area. Many researchers have ascribed such differences to the sensitivity of the polar water molecule to the degree of polarity of the adsorbent surface (Kiselev and Kovalena, 1959; Gregg and Sing, 1982). Assuming the BET nitrogen surface area is valid, the cross-sectional surface areas of water and TCE may be estimated (Table IV.2, last column). For all sorbents the computed molecular cross-sectional areas of water using the BET nitrogen surface areas were less than 10.8 Å^2 (Livingston, 1949) and the estimated value (Equation IV.5) of 10.51 Å^2. This difference may be interpreted to indicate that the sorbed water on the surface of these minerals was highly structured or "ice-like" (Grim, 1953) by virtue of its polar attraction to the mineral surface and is different from bulk water. The specific surface area of montmorillonite using water as a sorbate was calculated to be approximately half of the specific surface area found with the EGME method. The reason for this difference is because at the relative pressure for a monolayer of water to be completed, the interlayer of the clay would contain a single sheet of water while for the sorption of EGME, two layers of the organic compound are formed reflecting the true surface area available (Mooney et al., 1952).

The surface area computation for humic acid using Equation IV.2 was unsuccessful. Figure IV.13 reveals the interesting behavior of humic acid and the breakdown of Equation IV.2. The data, instead of falling on a straight line as in a "normal" linearized BET plot, show substantial scatter. As described earlier, this scatter could indicate that the surface area which was available was changing due to the swelling of the humic acid as more moisture was added.

The relative heat of water sorption (estimated from the value c) ranged from 0.96 kcal/mole for alumina to 2.73 kcal/mole for iron oxide. At 25°C, the heat of vaporization of water is 10.7 kcal/mole. Therefore, the estimated heat of adsorption would range from 11.7 to 13.4 kcal/mole. These values are indicative of the low sorbent-sorbate interaction energies associated with physical adsorption processes (Hill, 1977).
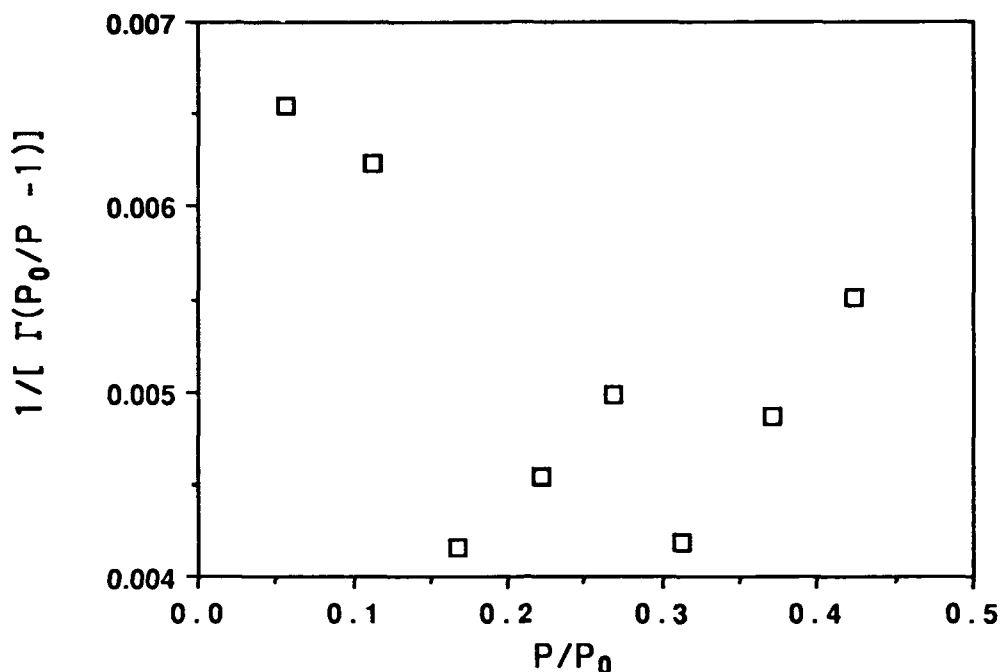
Figure IV.13. Linearized Plot of the BET Equation for Water Sorption on Humic Acid.

The relative or normalized sorption (Γ/Γ_m) of water on all solids as a function of relative humidity is shown in Figure IV.14. Relative adsorption has been used by other researchers (Jurinak, 1957, Rhue et al., 1988) to compare the adsorptive capacity of various sorbents in terms of the number of monolayers coverage of the sorbate. It is commonly assumed that the coincidence of the relative sorption curves for several sorbents can be taken as evidence that sorbate-sorbent interactions are similar in each case. The relative sorption plot for the five sorbents shows some scatter but overall the sorption data were transformed to values that were of the same order of magnitude. Differences in the sorbate-sorbent interaction between predominantly montmorillonitic soils and kaolinitic soils with ethylene dibromide vapor were observed by Jurinak and Volman (1957). The relative sorption of iron oxide was the largest for all sorbents followed closely by silica and montmorillonite. The curves for alumina, coated alumina and kaolinite coincided at RH less than 40 percent but then diverged with coated alumina exhibiting higher values. As observed by Rhue et al. (1988), the magnitude of relative sorption was reflected by the magnitude of the c value, for example, iron oxide (c=100.2), montmorillonite (c=38.2) and alumina (c = 5.06).
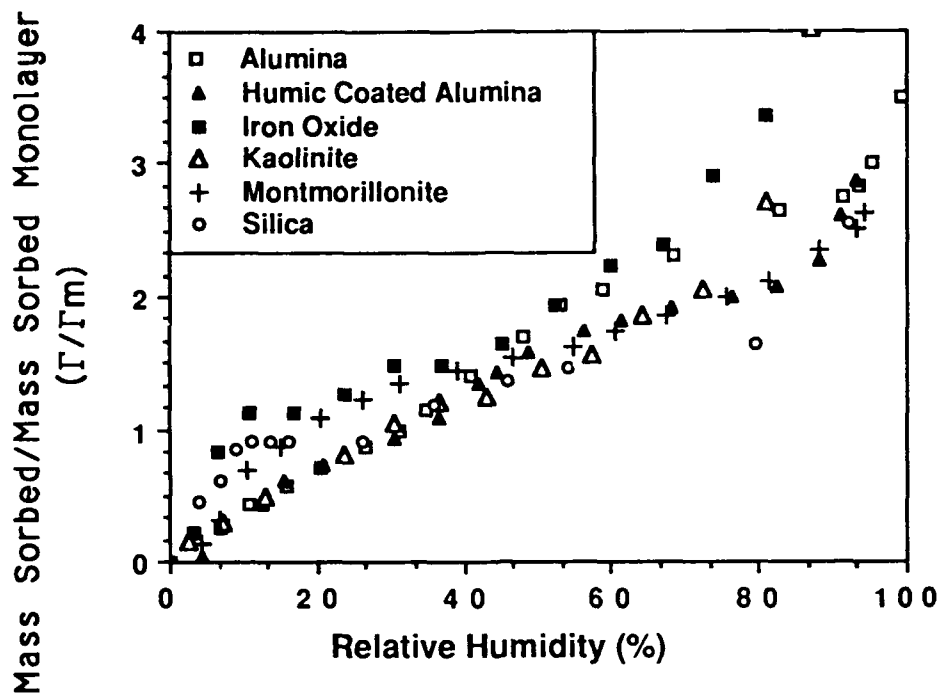
Figure IV.14. Relative Adsorption of Water Vapor on all Solids

4 .Sorption of TCE on Oven Dry Materials

Figures IV.15 to IV.20 show the isotherms for the sorption of TCE onto the oven dry materials listed in Table 1. As a comparison, water sorption data are also shown on the same figures on a volume-sorbed basis. Comparison on a mass basis is avoided since the density of TCE is about 1.5 times that of water. For alumina (Figure IV.15), the amount of TCE sorbed was similar to that of water at $P/P_0 < 30$ percent but showed slightly more sorption at higher relative pressures of TCE. The similarity in sorption of a nonionic compound and a highly ionic compound on this solid indicates that sorption was sorbate independcut. The isotherms for TCE and water on alumina have a BET type IV shape. Hysteresis was observed with the TCE desorption curve merging with the adsorption isotherm at $P/P_0 \approx 35$ percent.

The isotherm for TCE sorption onto coated alumina has a distinctive BET type IV shape (Figure IV.16). When the surface of alumina was altered by coating with organic matter the amount of TCE sorbed was greatly enhanced. Since sorption of water onto coated and uncoated alumina was similar despite the higher surface area of the coated solid (Figure IV.12), the difference in the TCE isotherm for the two sorbents indicates that the addition of humic acid resulted in an increase in the density of hydrophobic sites. Unlike

the sorption of water onto the surfaces of alumina and coated alumina where hysteresis persisted to as low as 15 percent RH, TCE sorption on both surfaces ceased to show any hysteresis at $P/P_0 < 30$ percent. This indicates that TCE can be easily desorbed.

Iron oxide showed a higher capacity for TCE than water (Figure IV.17). The TCE desorption isotherm followed the same curve as the adsorption isotherm indicating the nonporous nature of the iron solid.

Both montmorillonite and humic acid at 0 percent RH (Figures IV.18 and IV.19) exhibited much lower sorption capacity for TCE than water. A common characteristic of these two sorbents is that they expand/swell when sufficient moisture is adsorbed. Therefore, only the external surfaces of these solids (when dry) are available to TCE resulting in lower sorption. No hysteresis was observed for humic acid while some hysteresis was observed for montmorillonite. The lack of hysteresis for the isotherm of humic acid would imply sorption onto the external surfaces and a sorbate-sorbent interaction that is completely reversible.

The sorption isotherms of TCE onto silica and kaolinite (Figures IV.20 and IV.21) were similar to that of water at low vapor pressures but showed a decreased amount sorbed for TCE at higher vapor pressures.
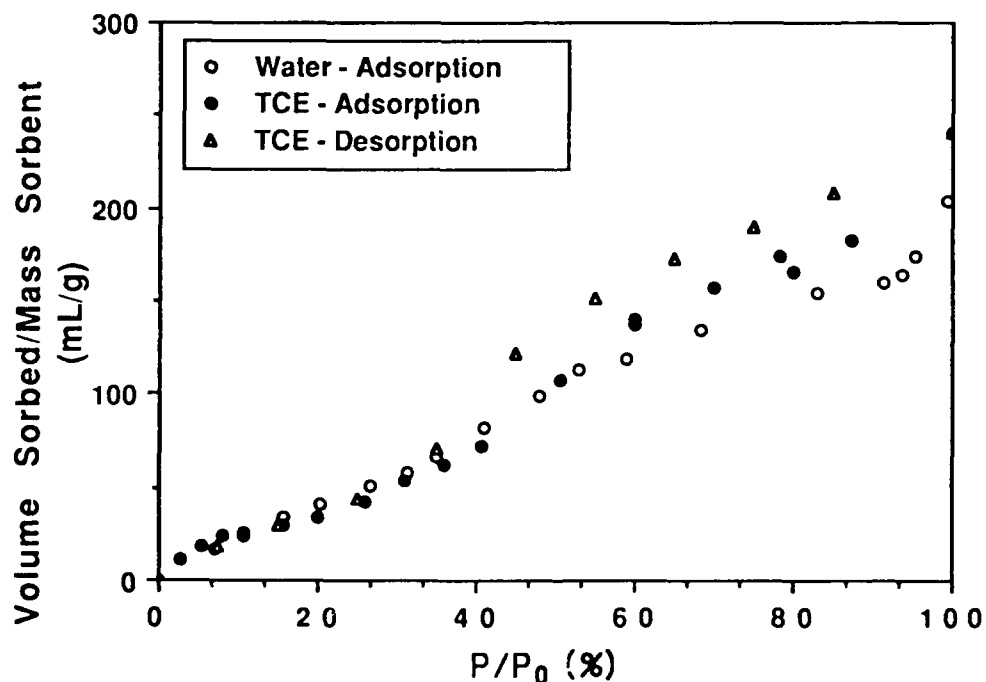
Figure IV.15. Sorption of TCE onto Alumina at Zero Percent Relative Humidity
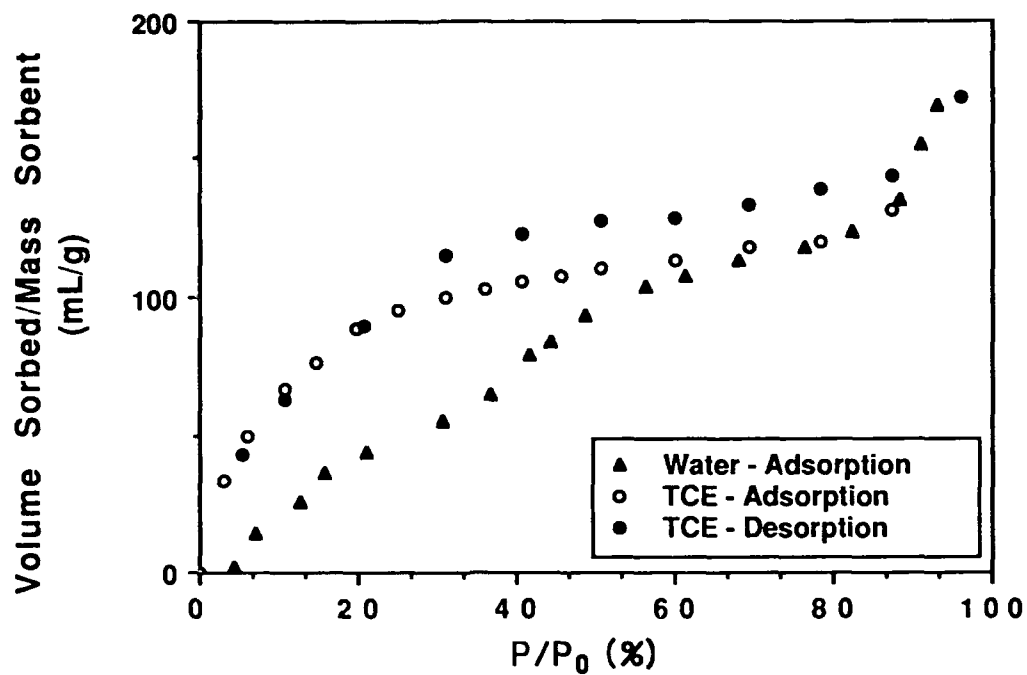
Figure IV.16. Sorption of TCE onto Coated Alumina at Zero Percent Relative Humidity
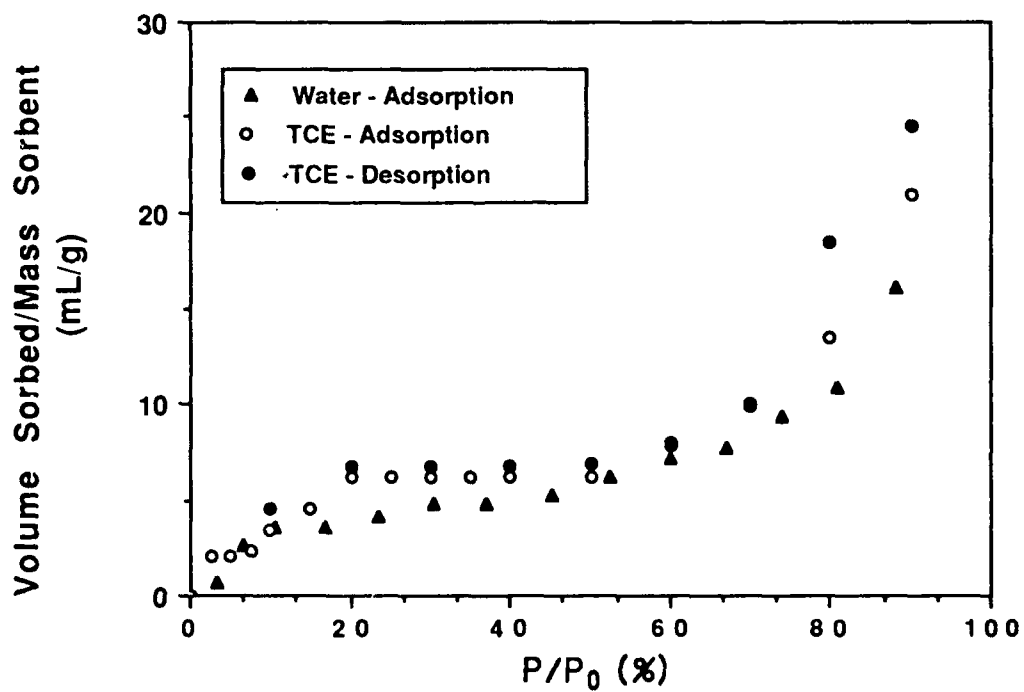
Figure IV.17. Sorption of TCE onto Iron Oxide at Zero Percent Relative Humidity
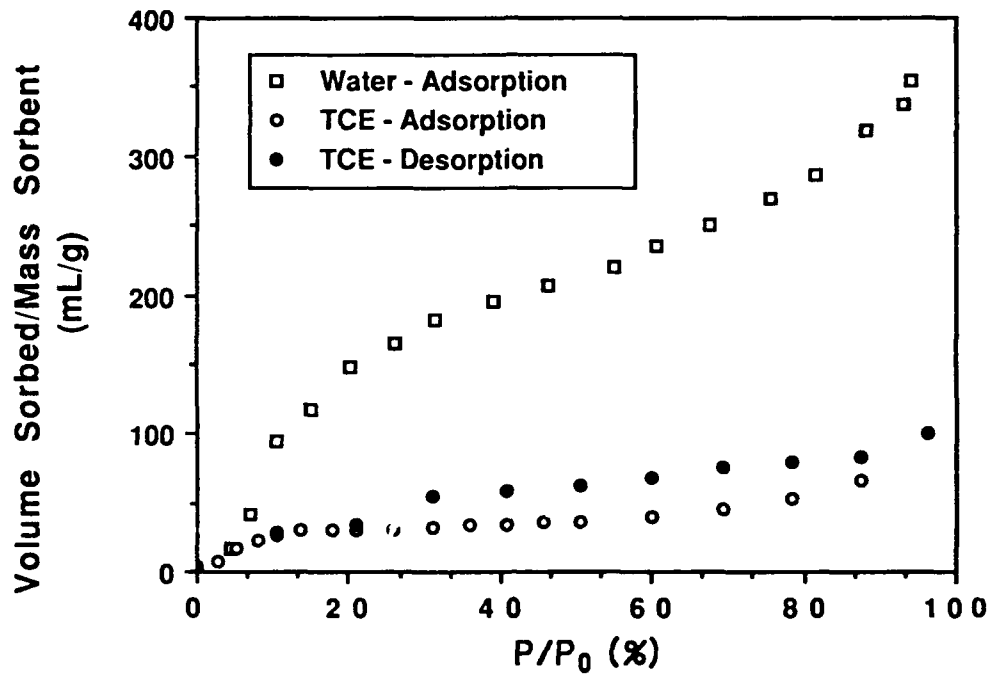
Figure IV.18. Sorption of TCE onto Montmorillonite at Zero Percent Relative Humidity
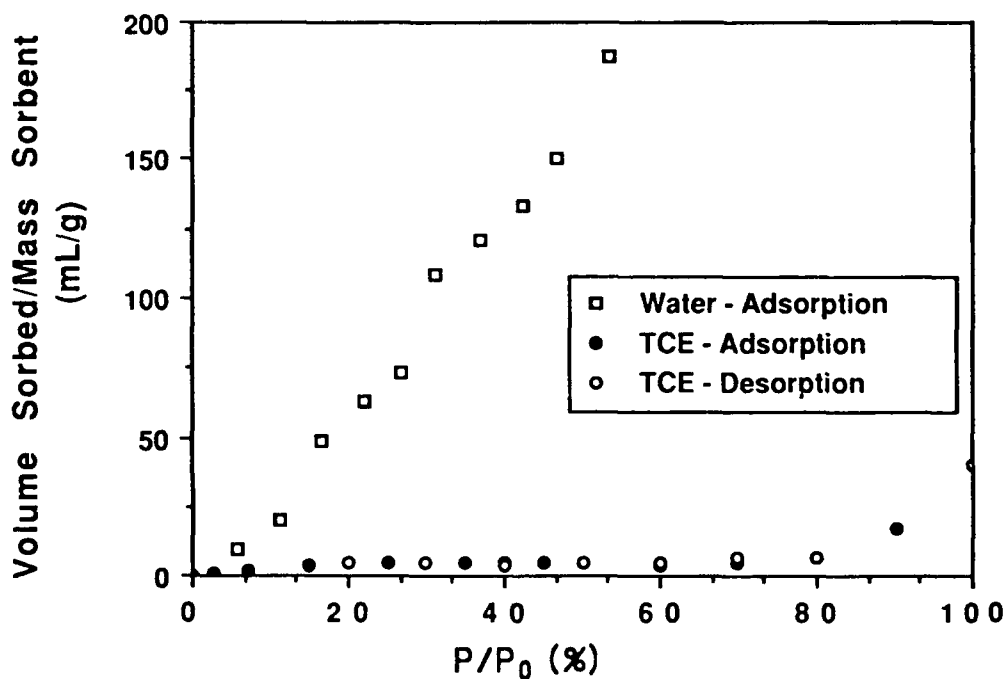
Figure IV.19. Sorption of TCE onto Humic Acid at Zero Percent Relative Humidity

107
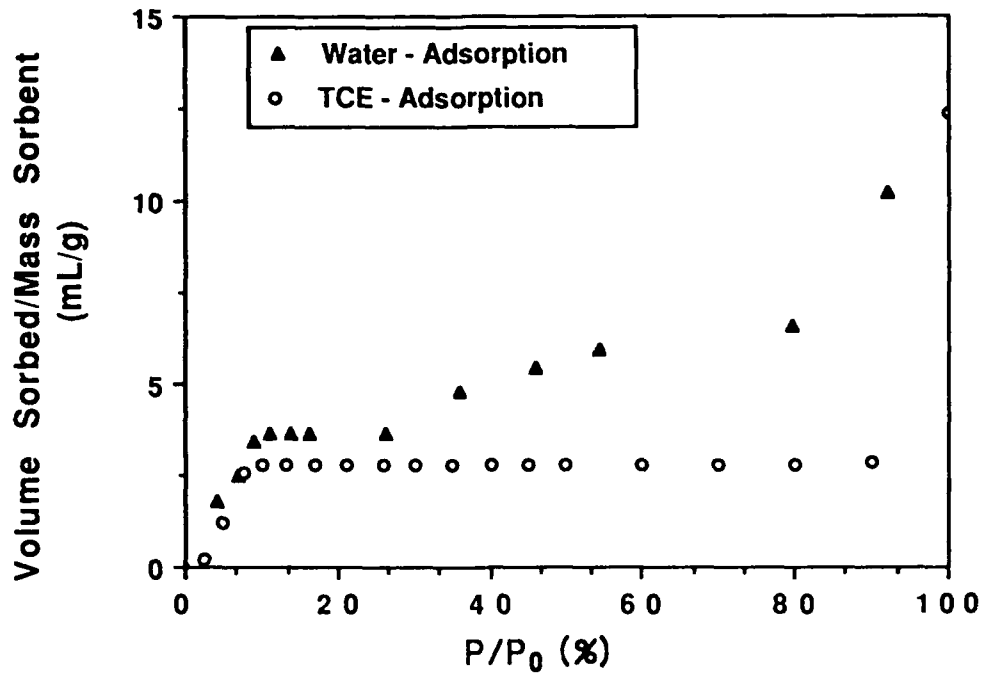
Figure IV.20. Sorption of TCE onto Silica at Zero Percent Relative Humidity
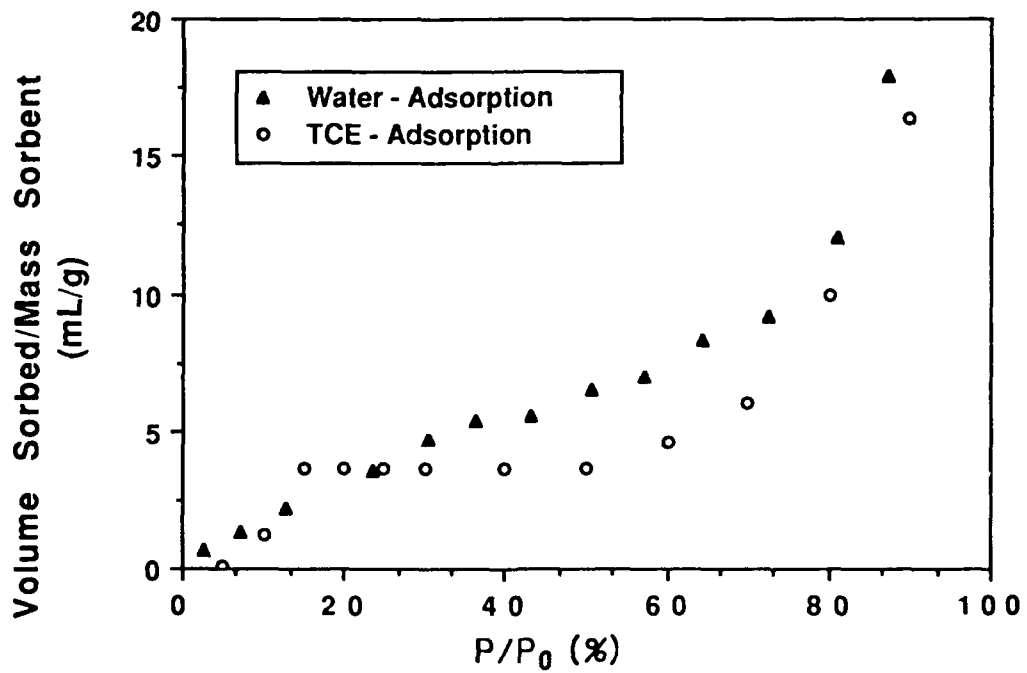
Figure IV.21. Sorption of TCE onto Kaolinite at Zero Percent Relative Humidity

Using Equation IV.2 and an estimated molecular cross-sectional of 30.65 $Å^2$ for a TCE molecule (from Equation IV.5), the surface area of the sorbents was computed (see Table IV.2). For all the solids the surface areas computed using TCE as a sorbate were less than that estimated with BET nitrogen method. Two solids that came close to the BET nitrogen surface areas were those of coated alumina and iron oxide while the value for alumina was half of the BET nitrogen surface area. To evaluate these results, the molecular cross-sectional area for TCE (last column of Table IV.2) was computed for each solid using the BET nitrogen surface area, assuming that these surface areas were accurate. As expected, the TCE cross-sectional areas for coated alumina (33.49 $Å^2$) and iron oxide (36.68 $Å^2$) were approximately equal to the theoretical cross-sectional area of 30.65 $Å^2$ assuming close hexagonal packing. These two solids also gave computed cross sectional areas for water that were similar to the estimated value of 10.51 $Å^2$ using equation IV.5. In the case of alumina and montmorillonite, the TCE computed cross-sectional areas were 68.91 $Å^2$ and 63.28 $Å^2$, about twice the theoretical value. One possibility for this result is that multilayer adsorption occurred well before the surface was fully covered. By way of comparison, Jurinak and Volman (1957) concluded that multilayer adsorption of ethylene dibromide occurred on Ca^{2+}-montmorillonite and Ca^{2+}-kaolin at fractional surface coverages of 0.65 and 0.35 respectively.

The hydrophobic/hydrophilic nature of the experimental test surfaces can be further evaluated through the following comparison. It was observed that all the surface areas computed with the water sorption data were higher than the BET nitrogen surface areas while those for the TCE sorption were lower. Surface areas computed from TCE and water data for both coated alumina and iron oxide were close to the BET nitrogen method in coated alumina (with TCE : 173.16 m^2/g, water : 203.4 m^2/g, N_2 : 189.3 m^2/g) and iron oxide (with TCE : 9.17 m^2/g, water : 11.07 m^2/g, N_2 : 10.98 m^2/g). It appears that the deviation of the computed surface areas relative to the BET nitrogen surface area can indicate surface hydrophobicity. By inference, the closer the computed surface area for TCE is to the BET nitrogen surface area, the more hydrophobic the surface. Therefore, we would conclude the humic coated alumina is relatively more hydrophobic than uncoated alumina. Liquid phase sorption results support this hypothesis as iron oxide and coated alumina (see Section III) were the better sorbents for TCE under saturated conditions while uncoated alumina exhibited negative sorption.

Given the simplifying assumptions in the BET model, the relative heat of sorption estimated from the c value serves only as an 'indicator" of the magnitude of the sorption processes. The relative heats of sorption (which range from 1.77 kcal/mole for coated alumina to 3.8 kcal/mole for montmorillonite) are low energy values that are typical of physical adsorption. In comparison with the heats of sorption obtained from the headspace

analysis (Section III), the heats of sorption measured here are lower. For example, for coated alumina, the heat of sorption is -10.4 kcal/mole [(-8.63) + (-1.77)] versus -16.5 kcal/mole with the headspace analysis method. The heat of liquefaction E_L for TCE at 25°C is -8.63 kcal/mole.

Fig. IV.22 summarizes the TCE sorption data for all solids by dividing the amount sorbed with the monolayer capacity (Γ_m). Except for alumina and coated alumina, the reduced data show substantial scatter, indicating that the sorbate-sorbent interactions are different for each solid. The isotherms of alumina and coated alumina coincide from $P/P_0 = 0$ to 15 percent but then diverge with alumina exhibiting higher sorption. This plot illustrates that the surface of all the sorbents interact with the TCE differently and that differences in TCE binding to dry surfaces cannot be solely attributed to their differences in surface area.
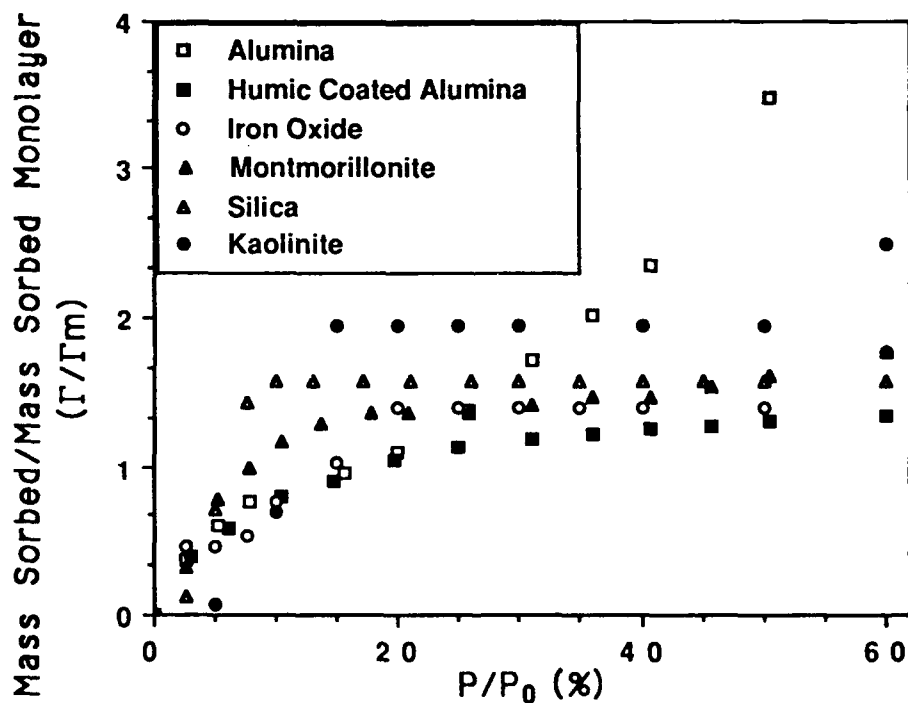
Figure IV.22. Relative Adsorption Isotherms for TCE on all Solids at Zero Percent RH

5.Competitive Sorption of TCE and Water

Competition with water for sorption sites is best evidenced by the decrease in the sorption of TCE for all solids (except for humic acid) as the relative humidity increased. With approximately a monolayer of water (at 40 percent RH) on the surface of alumina, the sorption of TCE was greatly reduced (Figure IV.23). At $P/P_0 <$ 40 percent, the BET type IV isotherm at oven dry conditions became instead a BET type III isotherm at 70 percent RH. Some indication of a type III isotherm can also be seen at 40 percent RH for $P/P_0 <$ 10 percent. The change to a BET type III isotherm suggests the presence of water resulted in a reduction in the attractive forces between TCE and the sorbent. This is indicated by the convex shape as opposed to a concave shape for oven dry alumina (Gregg and Sing, 1982). Probable reasons are that the more active sorption sites were taken up by the water molecules leaving less active sites for TCE. In addition, at 40 percent RH, monolayer coverage by water on the surface of the sorbent is nearly complete, forcing the interaction of TCE molecules with bound water instead of with the mineral surface. The anticipated weak interaction between TCE and bound water molecules would result in a Type III isotherm comparable to that observed by Gammage and Gregg (1972) for the sorption of butane onto calcite with a monolayer of water and Wade (1955) for the sorption of ethylene dibromide onto an organic soil at 50 percent RH.
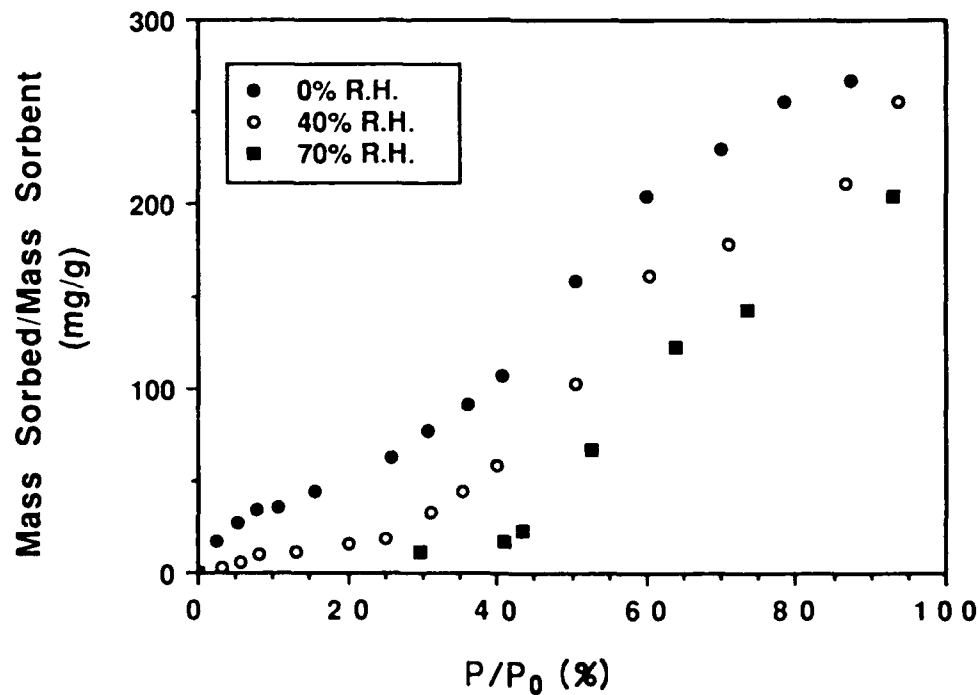
Figure IV.23. Effect of Moisture on Sorption of TCE Vapor onto Alumina

The sorption of TCE was also reduced for coated alumina (Figure IV.24) at a RH of 38 percent and further reduced for a RH of 69 percent. The initial shape of the isotherm at 38 percent RH indicates a type III isotherm. The isotherm has a type IV shape for TCE vapor pressure greater than 30 percent. The change in shape is tentatively attributed to the presence of sufficient TCE coverage to render the sorption more favorable.
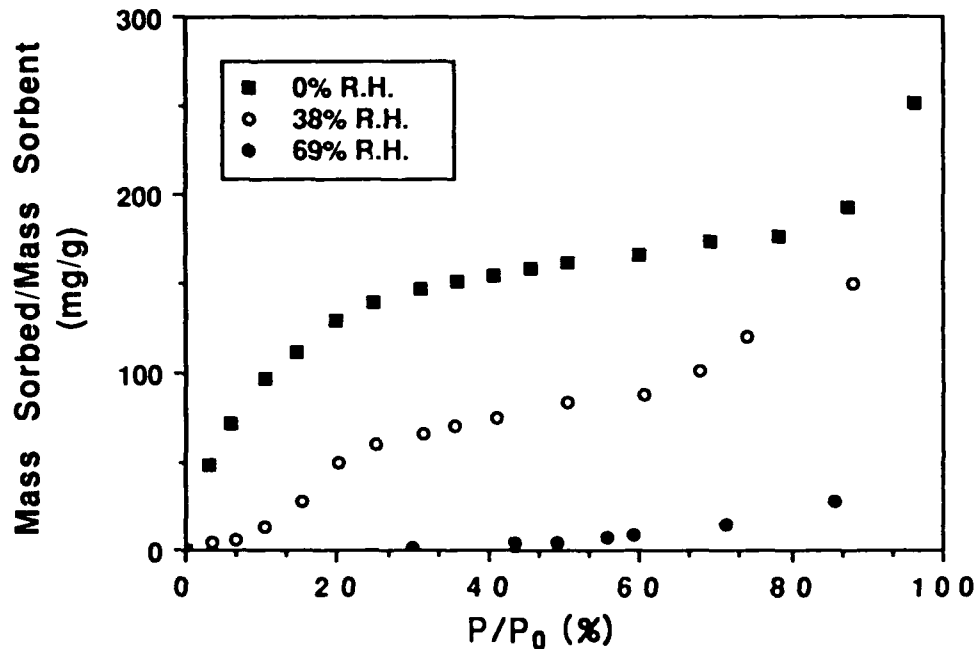
Figure IV.24. Effect of Moisture on Sorption of TCE Vapor onto Coated Alumina

To compare the isotherms at different relative humidities, the amount sorbed was expressed as the volume sorbed by assuming that the density of the sorbates were similar to that of bulk liquid ie. 1.47 g/cm^3 for TCE and 1.00 g/cm^3 for water. The total volume sorbed onto alumina (water and TCE) at 40 percent RH and 70 percent RH was similar to that at 0 percent RH as can be seen by the overlapping of the three isotherms (Figure IV.25) at high relative vapor pressures. A similar result (Figure IV.26) was obtained with coated alumina. In this case the isotherms at 0 and 38 percent RH are coincident from about 15 percent P/P$_0$ and continued in this fashion till 60 percent P/P$_0$ after which some divergence is observed. At 69 percent RH, the TCE vapor sorption isotherm was found to coincide with that at 0 percent RH for P/P$_0$ > 40 percent.

The agreement in isotherms on a volume basis for both alumina and uncoated alumina can be explained by the condensation of vapors in pores. Both solids have internal, small diameter pores. At a given RH, water fills up pores of a size dictated by the Kelvin equation and partially fills up pores that are larger than this size by adsorbing to the walls. At a given P/P$_0$ (sufficiently high to allow condensation), TCE fills the remaining pores whose original diameter is now reduced due to the presence of water. The total volume
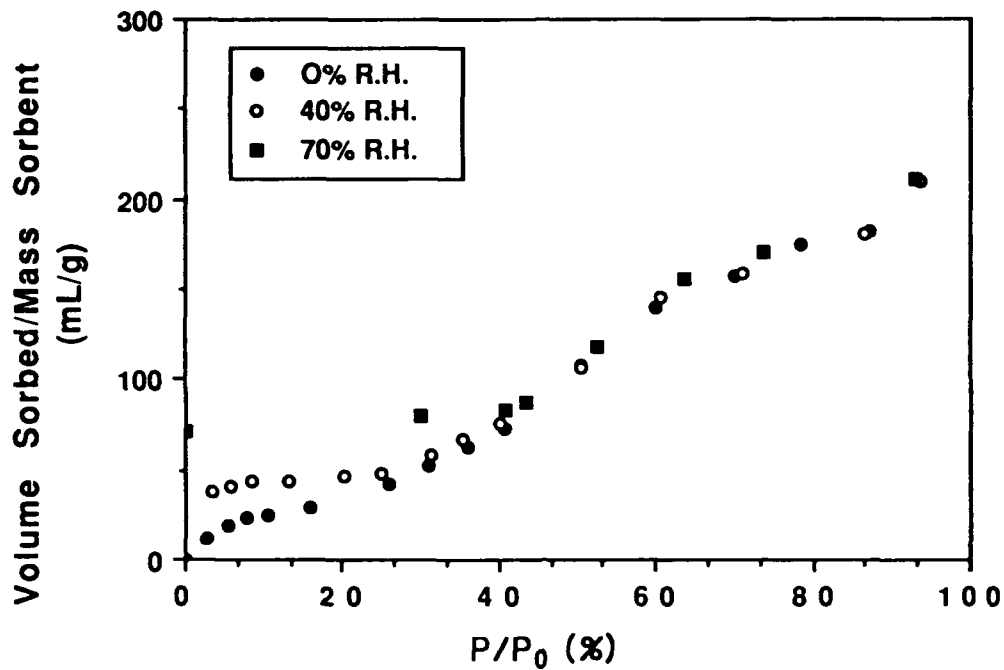
Figure IV.25 Total Volume Sorbed (Water plus TCE Vapor) onto Alumina
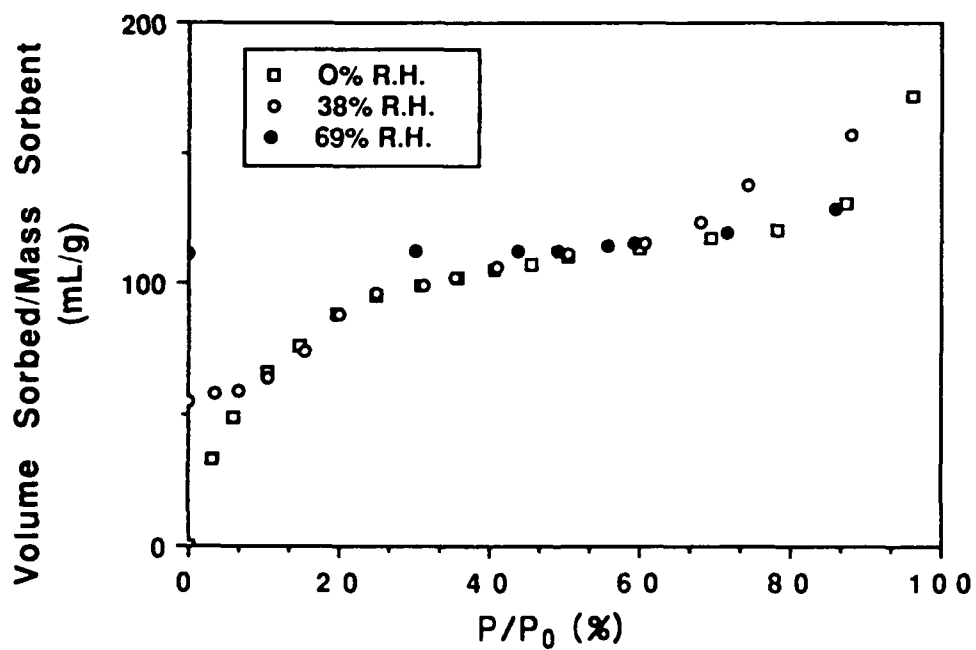
Figure IV.26 Total Volume Sorbed (Water plus TCE Vapor) onto Coated Alumina

113

occupied therefore is the same for several combinations of relative humidity and relative vapor pressure of TCE. Similar limitations in terms of volume sorbed per unit mass were observed by Chiou et al. (1988) for the sorption of organic compounds onto dry humic acid. Emmett and Cines (1947) found that the uptake at saturation of argon, nitrogen and butane onto porous glass was the same when expressed in terms of volume of the liquid sorbed. However, it is stressed that the system studied here consists of a binary mixture of vapors ie. water plus TCE while the studies cited above were based on single vapor. The behavior of the TCE/water mixtures suggests that the two vapors may exist as two separate phases with the water being somewhat strongly bound to the mineral surface.

The case for pore filling is further substantiated when the total volume sorbed does not converge for a nonporous solid like iron oxide. The isotherms for this solid at 0 and 40 percent RH (Figure IV.27 and IV.28) do not overlap and the total volume sorbed at 40 percent RH for high TCE vapor pressures was much lower than that at 0 percent RH.

The coicidence of the data in Figures IV.25 and IV.26 for TCE isotherms under oven dry conditions and at RH ≈ 40 percent and 70 percent sugests a trend which may be extended to higher humidity conditions. It is reasonable to assume that pore filling by water will proceed to a greater extent at high RH and that relatively little pore volume will remain avilable for TCE condensation at the > 99 percent RH conditions found in many unsaturated moist soils. However, TCE uptake may still proceed by sorption at the gas/liquid interface, by dissolution into pore water, and by condensation at high P/P_0.
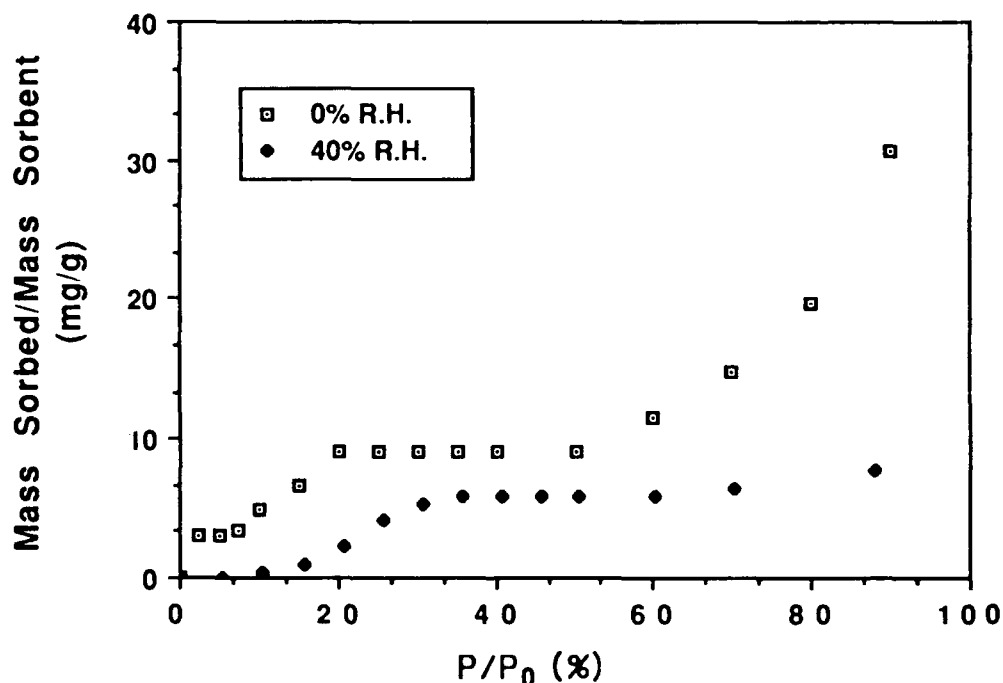
Figure IV.27. Effect of Water Vapor on Sorption of TCE onto Iron Oxide
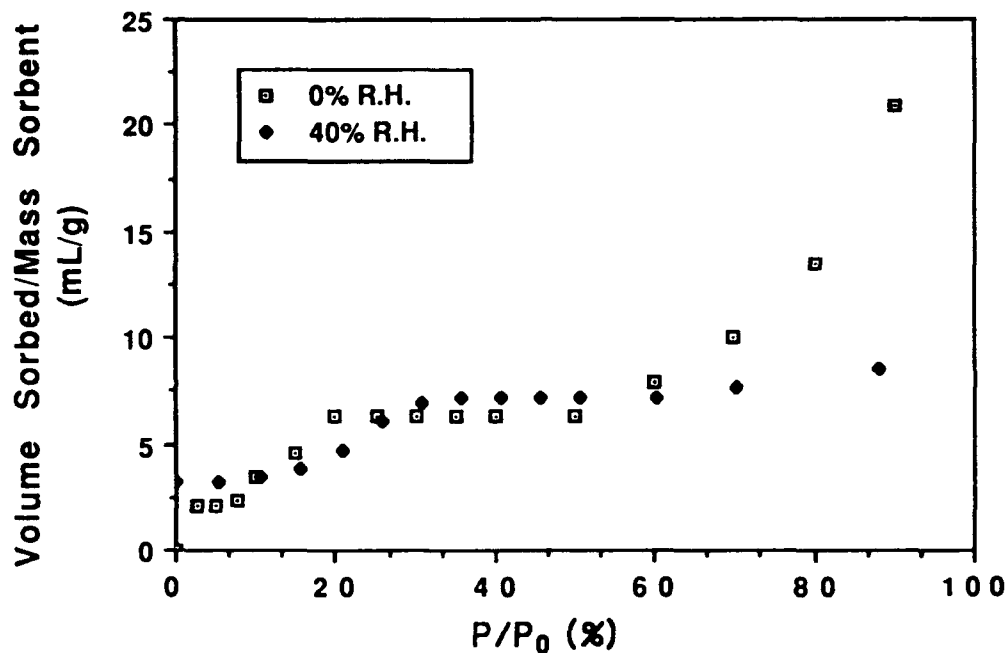
Figure IV.28. Total Volume Sorbed (Water plus TCE) onto Iron Oxide

The effects of water on expanding solids such as montmorillonite and humic acid are illustrated in Figures IV.29 and IV.30. For montmorillonite (Figure IV.29) the mass of TCE sorbed at 40 percent RH is about half of that when the clay was dry. However, when the volume of water sorbed at 40 percent RH was added to the volume of TCE sorbed at this RH, the total volume sorbed was much larger than when the solid is dry (Figure IV.30). This was not observed for non-expanding solids such as alumina and iron oxide. The sorption of water to the interlamellar surfaces of montmorillonite easily accounts for the extra volume adsorbed. However, at 40 percent RH the interlamellar surface may not be available to TCE and the external surface has been wetted, reducing the sorption of TCE relative to that observed at 0 percent RH where the dry external surfaces area is available for the sorption (Figure IV.30). The decrease in the sorption isotherm of TCE at 40 percent RH confirms that the montmorillonite surface has a stronger attraction for polar, amphoteric water molecules than for relatively nonpolar nonionic molecules such as TCE.

In contrast to the behavior of the clay mineral montmorillonite, the swelling of humic acid has the opposite effect on TCE uptake. TCE sorption on the moist humic acid was greater than on the dry solid. As water is sorbed to humic acid more sorption sites for TCE are apparently being made available (Figure IV.31). Also plotted on the same figure is the aqueous sorption (corrected for vapor-phase sorption) of TCE onto humic acid. The saturated partition coefficient of TCE onto aldrich humic acid was 32.1 mL/g (Garbarini and Lion, 1985) and a linear sorption was assumed throughout the full TCE vapor pressure range. The large amount of TCE sorbed at 80 percent RH in comparison to the aqueous
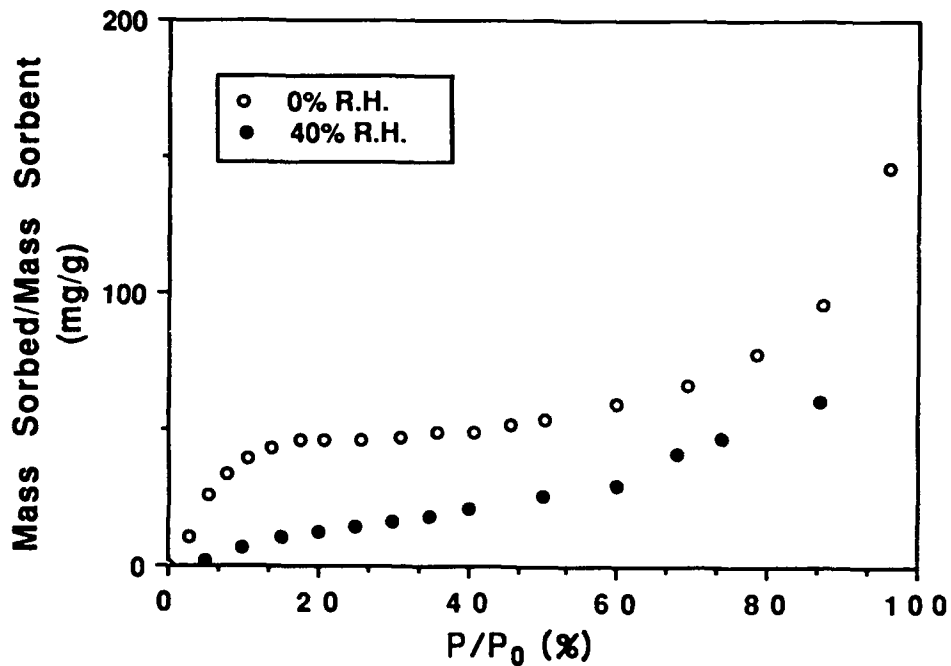
Fig. IV.29   Effects of Water Vapor on Sorption of TCE onto Montmorillonite
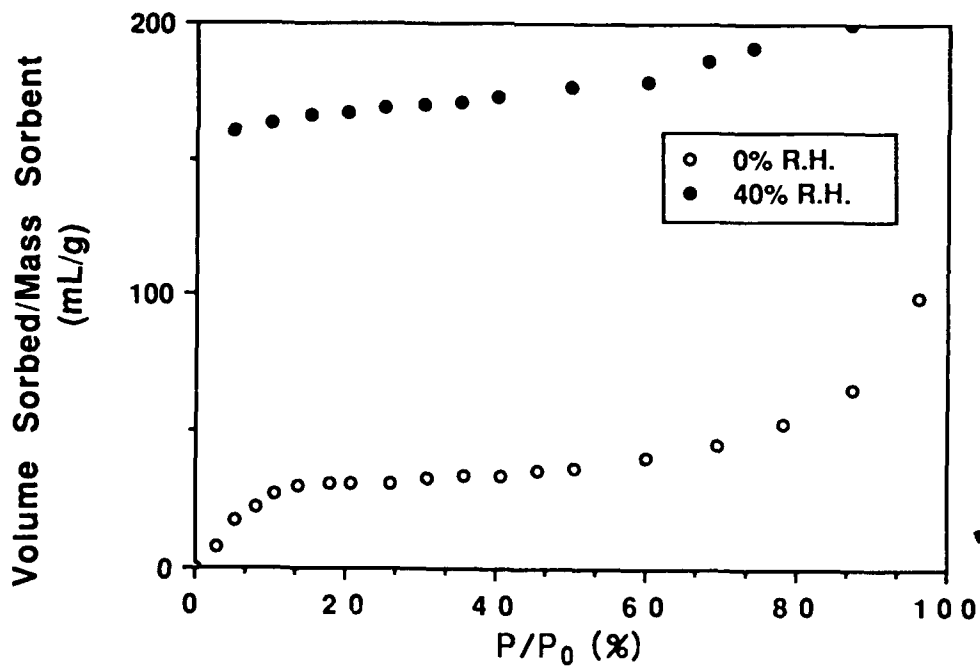
Fig. IV.30   Total Volume Sorbed (Water plus TCE) onto Montmorillonite

116
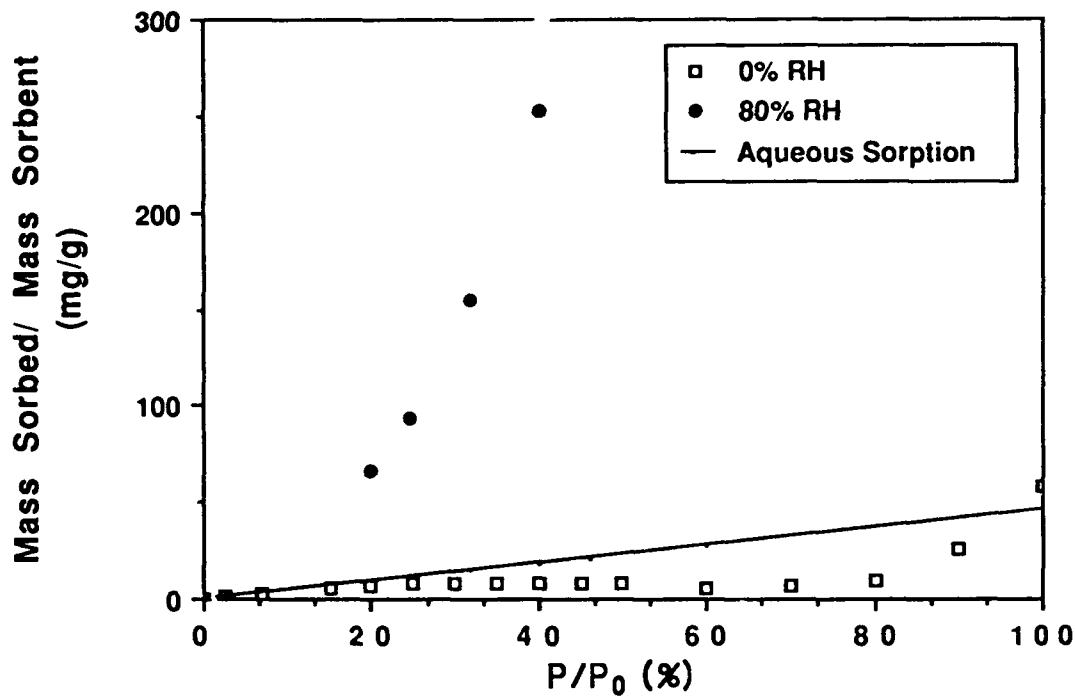
Fig. IV. 31   Effects of Moisture on the Sorption of TCE onto Humic Acid

---

sorption further substantiates the availability of sorption surfaces as the organic matter swells. The impact of dissolution of TCE into soil water at 80 percent RH was found to be negligible. For example, the maximal dissolution of TCE at 50 percent P/P_0, assuming all water associated with the moist humic acid is available, is only 0.22 mg/g. Therefore the sorption capacity of the humic acid at 80 percent RH can not be explained by the sum total of TCE dissolution into water and the saturated partition coefficient for TCE into the humic matrix. It is probable that under saturated conditions, surface "sites" or pore volume that is available at 80 percent RH will be covered (or filled) with water due to mass action, ie., water is present in huge excess compared to TCE (Hayes and Himes, 1986).

D. SUMMARY AND CONCLUSIONS

For all seven sorbents studied, the relative sorption isotherm (dividing the amount of sorbate sorbed with the monolayer capacity) did not converge into a single curve. However, the sorption data were transformed to values that were of the same magnitude. Sorbent specific interaction and the presence of small volume pores are the most likely cause for differences in the relative sorption isotherm. Water sorption isotherms indicated that the coating of alumina with humic acid resulted in a more hydrophobic surface.

Sorption of TCE onto several minerals over the full range of TCE relative vapor pressure and at several relative humidities reveals that sorption of TCE was greatly affected by the presence of water. For solids at 0 percent relative humidity, the relative TCE sorption isotherms were different for each surface, indicating that the surfaces of the sorbents investigated have specific interactions with TCE. It is hypothesized that comparison of the BET surface area based on TCE sorption with the BET surface area found by nitrogen adsorption can serve as a measure of the hydrophobic nature of a sorbent. A large differential between these values is indicative of a hydrophilic surface. For the solids considered in this study, the BET surface area computed from TCE sorption was found to be consistently less than the BET nitrogen surface area.

With increasing amounts of water on the surface of the solids, the amount of TCE sorbed was found to decrease. For porous solids like alumina and humic-acid-coated alumina, converting the amount of water and TCE sorbed to a volume rather than mass basis at different relative humidities resulted in substantial overlap of the isotherms. This result indicates that, at high TCE vapor pressures, vapor condensation plays an important role on porous sorbents in determining the amount of TCE sorbed. In contrast, the TCE isotherms obtained at different relative humidity for a nonporous sorbent (iron oxide) did not converge.

Addition of moisture onto humic acid resulted in sorption of large amounts of TCE in comparison to the humic acid at 0 percent RH and under saturated aqueous conditions. Expansion of the humic acid due to hydration and exposure of internal surfaces/pore volume for sorption/condensation is proposed as a possible explanation for the higher uptake of TCE at high relative humidity (80 percent). Although montmorillonite also expands with the addition of water, its sorption capacity for TCE decreased, indicating that the interlamellar pores were not readily available for the uptake of TCE.

118

SECTION V
EFFECTS OF SOIL PROPERTIES AND MOISTURE
ON THE SORPTION OF TCE VAPOR

By: S.K. Ong and L.W. Lion

A. INTRODUCTION

The sorption of pollutants onto soils in tne subsurface is considered a benchmark abiotic process which determines their environmental fate and transport. Sorption of pollutants is influenced by the high degree of variability of soils both in physical and chemical characteristics, for example in mineral type and content of organic carbon. Current knowledge of the sorption processes of hydrophobic organic compounds (as a class of pollutants) is substantial, but is far from complete. These compounds are nonionic, relatively nonpolar, slightly soluble in water with relatively high octanol-water partition coefficients. Many hydrophobic pollutants, such as the components of fuels and solvents, are volatile. Cosiderable research has focused on the sorption of hydrophobic organic compounds from the aqueous phase of the soil-water system. Studies on the behavior of these pollutants within a three-phase system, ie. soil-water-air are generally lacking. In particular, information on how vapor-phase partitioning depends on sorbent properties would lead to better understanding of the fate of these pollutants in the subsurface.

Sorption of hydrophobic organic vapors is greatly affected by the amount of moisture present in soil (Section III; Call, 1957; Chiou and Shoup, 1985; Spencer et al., 1982). The effect on vapor sorption of other soil properties, such as organic carbon content, specific surface area and cation exchange capacity, is also important. Some early studies which correlated the sorption of organic vapors with soil properties were conducted in the 1950s in response to the use of fumigants for pest control. Wade (1954) investigated the vapor sorption of ethylene dibromide (EDB) onto several soils over the field range of moisture contents, and found that the mass sorbed could be correlated to the organic content of the soil. Several years later, Call (1957) found that the sorption coefficients of EDB vapors on 20 soils at moisture contents corresponding to field capacity could be predicted with reasonable accuracy from their moisture content. [For Call, "field capacity" was defined as the moisture content obtained at a matrix suction potential between 0.1 to 0.3 bar; this corresponds approximately to the moisture retained by a soil drained by gravity.] The studies cited above constitute the available data on the sorption behavior of organic vapors onto soils at moisture contents found in the unsaturated zone.

The unsaturated zone, unlike the saturated zone of the subsurface, has moisture contents which may range from fairly dry to saturation for soils at the surface and the capillary fringe of the water table. For most of the unsaturated zone, it can be assumed that soils are generally at a moisture content corresponding to their ability to retain water. Thus, study of vapor sorption by soils with moisture contents at field capacity is appropriate. Another moisture condition of practical interest is that of surface soils. Soils at the top layer of the ground are generally drier because of exposure to higher temperatures and are subjected to variable relative humidities and changing wind conditions. Organic vapors moving from the subsurface to the surface, spills onto the surface, and even traces of organic vapors in the ambient air can be sorbed by surface soils.

An improved understanding of the factors that affect the sorption of organic vapors would aid prediction of vapor transport in the subsurface and the design of methods used for the remediation of hazardous waste sites. For example, mapping of the pollution plume in the subsurface using soil gas sampling techniques and predictions of the removal of organic vapors by the in-situ volatilization techniques could be enhanced by a better understanding of the behavior and distribution of the pollutants in the soil-water-air system of the unsaturated zone.

In this section, sorption of an organic vapor, trichloroethylene (TCE) onto seven different soils is reported for four different moisture conditions: oven dry at 105°C, air dry at 68 percent relative humidity (RH) and 25°C, field capacity, and saturation. Properties of soils are correlated with the sorption partition coefficients at these moisture contents.

B. METHODS AND MATERIALS

1. Sorbents

To ensure a broad spectrum of physical and chemical properties to which partition coefficients might be correlated, seven soils of different compositions and from a wide range of climatic conditions were used as sorbents. All the soils were air dried and then carefully sieved with a No. 20 mesh sieve (840 μm opening) prior to use.

The seven soils selected for use as sorbents were: Gila silt loam, Bandelier tuff, Rhinebeck loam, Harford loam, Morris loam, Sapsucker Woods silty loam and Columbus aquifer material A summary of the soils and the depths from which the samples were taken is given in Table V.1. All samples were taken from the unsaturated zone.

Gila silt loam and Bandelier tuff are from arid climatic conditions. Gila silt loam, a desert soil from the Central Valley of California, was provided by Dr. W. Spencer, USDA-Agricultural Research Service, Riverside. The soil contains 18.4 percent clay which is predominantly montmorillonite (Spencer and Cliath, 1970). The Bandelier tuff was from Los Alamos National Laboratory, Los Alamos, New Mexico. It is of the Tshirege member consisting of ashflows of rhyolite tuff and was moderately welded with slight deformation of glassy fragments. The tuff was provided by Dr. E.P. Springer of the Environmental Science Group of Los Alamos Laboratory, Los Alamos. The tuff and Gila silt loam are of interest because of the range of dry climatic conditions to which they are exposed. In addition, Los Alamos National Laboratory experiences problems with TCE pollution (Springer, 1986).

The Harford and Rhinebeck soils were taken from sites previously used for alfalfa and dairy production in Tompkins County, New York. The Harford soil was identified as a coarse loam of the mesic family of Aeric Fragiaquepts while Rhinebeck soil is from the mesic family of Aeric Ochraqualfs. The Rhinebeck and Harford soils have been used extensively to investigate the sorption and transport of phenanthrene and atrazine (Magee, 1988; Gamerdinger, 1989). The Harford and Rhinebeck soils were provided by Dr. A. Lemley (Dept. of Textiles and Apparels, Cornell University, Ithaca, NY).

Morris soil is a silty loam taken from a farmland (lodgement till) in Central New York and is reddish in color indicating a high iron content. The Morris soil was obtained from Mr. W. Waltman (Soil Survey, Dept. of Agronomy, Cornell University, Ithaca, NY).

A soil moderately high in organic carbon content was obtained from a swampy lowland area of Cornell University's Sapsucker Woods. The soil sample was obtained from under a cover of plant litter and leaves. Sorption of TCE and toluene by Sapsucker Woods soil has been reported by Garbarini and Lion (1986).

A sandy aquifer material from Columbus Air Force Base, Columbus, Mississippi was selected as a representative low organic material. Columbus aquifer material was provided by Dr. T. Stauffer of the Air Force Engineering and Services Center, Tyndall Air Force Base, Florida.

2. Methods

The organic carbon content, EGME specific surface area, pH, cation exchange capacity and particle density of each soil was analysed using the methods described in Section III. In addition, iron content, was determined for all the soils. Iron oxides have been observed to be a good mineral sorbent for nonionic pollutants (Section III, Stauffer

121

TABLE V.1 DESCRIPTION OF SORBENTS

	Morris loam	Harford loam	Rhine-Beck loam	Bandelier tuff	Sap-sucker soil	Gila silt laom	Columbus aquifer material
Location	Gennesse County, NY	Tompkins County, NY	Tompkins County, NY	Los Alamos, NM	Ithaca, NY	Central Valley, Ca.	Columbus, Miss.
Description	clayey silty loam	silt loam	silty clay loam	volcanic tuff	silty loamy	clayey loam	sand with clay
Depth taken (cm)	56 -112	5 -30	5 -30	2,300-2,350	5	30 -60	150

and MacIntyre, 1986). Total iron of the sorbents was determined by digesting the soil with 48 percent hydrofluoric acid and 70 percent perchloric acid (Jackson, 1958) and evaporating the contents to dryness. The residue from the digestion was then dissolved in 6N sulfuric acid and heated to a temperature of 250°C. The solution was diluted with distilled water and total iron was determined by atomic absorption spectroscopy.

The moisture contents of the samples were determined by weighing the sample before and after equilibrating for 24 hours in a vacuum oven at 105°C. The oven was subjected to 500 mm Hg vacuum which ensured low humidity.

Partition coefficients for TCE vapor sorption were determined at oven-dried conditions at 105°C, at air dried conditions and at field capacity. Saturated partition coefficients for TCE were also determined. Since there are no standards and experimental methods to specify the requirements of an air-dried soil, a consistent criterion was established. After oven drying, all the soils were subjected to an environment of 68 percent relative humidity (RH) at 25°C. Selection of 68 percent RH was based on the average monthly RH for several areas where the soils were obtained. For example, the average monthly RH at Syracuse, NY (representative of the three soils from Central New York) varies between 60 to 74 percent while the RH at Sacremento, California (representative of the climatic conditions for Gila Silt Loam) varies from 57 to 83 percent (Climatological Data National Summary, 1980). By subjecting all the soils to a common RH, ambiguity in the variability of the experimental conditions of the soils was minimized. The 68 percent RH was obtained by exposing the soils within a closed space to a saturated aqueous solution of sodium nitrite. Since soil were oven dried prior to exposure to 68 percent RH, those with hysteresis in their water adsorption/desorption isotherms will have lower moisture contents than if they had been saturated prior to exposure to the 68 percent RH environment.

Moisture level at field capacity was determined by the method of Colman (1946). Instead of a porous plate, a Whatman No. 50 filter paper was used as in Call (1957). In general, a vacuum of 75 mm Hg (0.1 bar) are used for coarse-textured soils, 250 mm Hg (1/3 bar) for medium textured soils, and 380 mm Hg (1/2 bar) for fine-textured soils (Cassel and Nielsen, 1986). All soil samples used were subjected to a vacuum of 250 mm Hg (1/3 bar) except for Columbus (a sandy soil - coarse textured) which was subjected to 75 mm Hg (0.1 bar). The moisture content of the soil was measured when removal of water ceased. This method is an approximate estimate which serves as a measure of the field capacity.

123

The headspace analysis method described in Section III was used to determine the vapor-phase partition coefficients of the soils. Masses used ranged from 0.1 to 30 grams (dry weight) depending on the moisture contents of the soil. All the vials were equilibrated at 25°C between 24 to 36 hours. The headspace concentrations of the vials were analysed with a HP model 5890A Gas Chromatograph using a Flame Ionization Detector. The partition coefficients were found by regressing the following relationship (derived in Sections II and III):

$$\frac{V_B C_B}{V_S C_S} - 1 = K_d' \frac{M}{V_S}$$

<div align="right">V.1</div>

where K_d' is the vapor partitioning coefficient (mL/g)

M is the oven-dry mass of the solids (g)

C_B is the G.C. peak area for a control vial

C_S is the G.C. peak area for a sample vial

V_B is the volume of the blank vial (mL)

V_S is the available gas volume of a sample vial (mL) and is computed from the actual volume of sample vial minus the volume occupied by dry mass minus the volume occupied by water associated with the solids ie. :

$$V_S = V_S' - M/\rho - (\text{Wet Mass} - \text{Dry Mass}\{M\})/\rho_w$$

where: ρ and ρ_w are the density of the solids and water respectively

and V_S' is the empty bottle volume (mL).

For curvilinear isotherms, the linearized Langmuir relationship was used :

$$1/\Gamma = (1/c\Gamma_m)(1/C_S) + 1/\Gamma_m$$

<div align="right">V.2</div>

where Γ_m is the monolayer capacity,

c is a constant related to the binding energy,

and the linear partition coefficient K_d' is given by $c\Gamma_m$.

For saturated sorption studies, the partition coefficients were determined using the method described by Garbarini and Lion (1985). The partition coefficients were found from the slope of the following equation (see Section II):

$$\frac{C_{GB} (\gamma K_H V_{GB} + V_{LB})}{C_{GS} (\gamma K_H V_{GS} + V_{LS})} = K_d \frac{M}{(V_{LS} + K_H \gamma V_{GS})} + 1$$

<div align="right">V.3</div>

where K_H is the Henry's constant, γ is the TCE activity coefficient in the aqueous solution, and the subscripts G, L, B and S denote gas phase, liquid phase, control (blank) and sample vials, respectively.

C. RESULTS AND DISCUSSION

Results of the characterization of all the solids are given in Tables V.2. Table V.3, V.5 and V.6 summarize the partition coefficients for the sorption of TCE under all four moisture conditions, ie. oven-dried, air-dried, field capacity and saturation. Table V.4 provides the correlation coefficients of the vapor-phase partition coefficients of TCE at various moisture contents with the soil properties.

1. Characterization of Sorbents

As shown in Table V.2 the experimental soils ranged from acidic (Morris at pH 4.9) to alkaline (Gila silt loam at pH 8.5). Gila silt loam has the largest specific surface area (EGME method) at 98.5 m²/g while Bandelier tuff has the lowest surface area of 5.48 m²/g. As expected, Sapsucker Woods soil had the highest organic carbon content at 5.2 percent. Both the tuff and Columbus aquifer material have very low organic carbon contents (0.06 percent and 0.03 percent respectively). Surface soils such as Harford and Rhinebeck loams have organic carbon contents that are typical of most "mineral" soils (Brady, 1974). The Morris loam has an iron content of 2.98 percent which is high compared to the other surface soils.

Moisture contents (MC) of the soils exposed to 68 percent RH varied from as low as 0.03 percent for the Bandelier tuff to as high as 3.7 percent for the Sapsucker Woods soil. The average number of monolayers of water molecules ranged from 0.19 for Bandelier tuff to 1.92 for Sapsucker Woods (Table V.2). Monolayer coverages were computed from the EGME specific surface area using a cross sectional area of 10.8 Å² for a water molecule (Livingston, 1949). The measured field capacities varied from 12.5 percent MC for Columbus aquifer material to as high as 48 percent MC for Sapsucker Woods. The sandy Columbus aquifer material did not retain much water while soils with high organic carbon content like the sample from Sapsucker Woods have a tendency to retain a large amount of water (Colman, 1946). The average number of monolayers of water retained at field capacity varied from 11 for Gila silt loam to 25 for Sapsucker Woods (Table V.2). Bandelier tuff was calculated to retain an exceptional 134 monolayers of water attributable to its low surface area and capillary sized pores. The range in the quantity of water at field capacity determined here is approximately the same as that of other reported values which vary from 15 to 20 monolayers of water molecules (Foth, 1978).

125

TABLE V.2 PHYSICAL-CHEMICAL PROPERTIES OF SOILS

	Morris	Harford	Rhine-beck	Tuff	Sap-sucker	Gila	Columbus
Bulk density (g/cm^3)	1.82 †	1.15 §	0.95 §	1.40 ¶	*	*	*
Particle density (g/cm^3)	2.63	2.48	2.45	2.48	2.35	2.53	2.57
pH (H_2O extract)‡	4.9	5.9	6.7	7.2	6.6	8.5	5.4
CEC (meq/100g)‡	6.9	15.0	27.0	1.0	35.2	20.6	3.8
Ca^{2+}	0.2	5.1	14.7	0.5	20.0	35.0	0.5
Mg^{2+}	0.0	0.5	2.5	0.1	2.8	3.3	0.4
Na^+	0.0	0.0	0.1	0.2	0.2	2.0	0.0
K^+	0.0	0.3	0.2	0.0	0.3	1.4	0.0
Percent Organic Carbon‡	0.14	1.64	2.95	0.06	5.20	0.38	0.03
Surface Area (m^2/g) EGME	25.5	44.0	82.5	5.5	66.3	98.5	19.8
Total Fe (percent)‡	2.98	1.91	3.07	1.34	3.22	2.71	0.92
Moisture Content (percent) Air Dried (68 percent RH)	0.71	2.40	3.62	0.03	3.70	2.10	1.03
Avg. Monolayers of H_2O	0.96	1.88	1.51	0.19	1.92	0.73	0.79
Moisture Content (percent) Field Capacity	17.9	25.2	38.0	21.5	48.0	31.6	12.5
Avg. Monolayers of H_2O	24.2	19.7	15.9	134.0	24.9	11.0	21.7

Bulk density measured in the field were from; † - Mr. W. Waltman, Soil Survey, Cornell University, Ithaca, NY, § - Gamerdinger (1989), ¶ - Springer (personal communication, 1987), * were not measured in the field.

‡ tested by the Cornell College of Agriculture & Life Sciences Nutrient Analysis Laboratory, Cornell University, Ithaca, NY

TABLE V.3 TCE VAPOR-PHASE PARTITION COEFFICIENTS (mL/g) (± 95 percent C.I.) FOR OVEN-DRIED SOILS

	$K_d'(c\Gamma_m)$ from Equation V.2	r^2
Morris	850±380	0.85
Harford	2500±360	0.97
Rhinebeck	1440±170	0.98
Tuff	4.7±1.9	0.87
Sapsucker	1180±130	0.99
Gila	4180±90	0.83
Columbus	680±210	0.92

TABLE V.4 COEFFICIENT OF CORRELATION (r^2) FOR PARTITION COEFFICIENTS (mL/g) AT FOUR MOISTURE CONTENTS

	$K_d'(c\Gamma_m)$ (Oven dried)	K_d' (Air Dried)	K_d' (F. Capacity)	K_d (Saturated)
pH	0.57	- 0.03	0.08	0.08
CEC	0.41	0.87	0.90	0.88
OC (percent)	0.01	0.99	1.0	0.99
EGME Surface Area	0.78	0.43	0.48	0.45
Total Iron (percent)	0.33	0.57	0.60	0.57
Moisture Content (percent)	-	0.86	0.91	-

TABLE V. 5 TCE VAPOR-PHASE PARTITION COEFFICIENTS ONTO AIR-DRIED SOLIDS (68 PERCENT RH)

	M.C. (percent)	K_d'(mL/g)	r^2	K_{oc}(mL/g OC)
Morris	0.71	3.50±0.55	0.92	2500
Harford	2.4	11.50±1.50	0.85	700
Rhinebeck	3.62	14.90±1.20	0.98	510
Tuff	0.03	1.50±0.40	0.75	2400
Sapsucker	3.7	25.70±2.20	0.97	495
Gila	2.1	2.80±0.10	0.99	730
Columbus	1.03	2.90±0.75	0.83	9500

2. Sorption of TCE onto Oven-Dried Soils

Curvilinear isotherms were observed for TCE sorption onto oven-dried soils. Partition coefficients (K_d') were determined by Equation V.2 (Langmuir model) and are presented in Table V.3. The partition coefficients K_d' were found to correlate well with the EGME surface area (r^2=0.78, see Table V.4). Organic matter contents which are normally used as an indicator of the extent of sorption could only account for 0.7 percent of the variance of the partition coefficient data under the oven dry condition. Since the mineral fraction of a soil generally contributes significantly towards the total specific surface area (Foth, 1978), the data support the hypothesis that the mineral fraction of a soil plays an important role in the sorption of TCE under oven-dried conditions. This result is consistent with Section III for the sorption of TCE onto minerals and the results of other researchers (Jurinak, 1957; Rhue et al., 1988, Chiou et al., 1986).

3. Sorption of TCE onto Air Dried Soils

The partition coefficients obtained for air-dried conditions ranged from as low as 1.45 mL/g for tuff to as high as 25.72 mL/g for the Sapsucker Woods soil. Regression of these partition coefficients against the properties of the soils (Table V.4) shows that organic carbon content has the highest coefficient of correlation at r^2=0.99. Figure V.1 shows the relationship between organic content and the TCE vapor partition coefficients onto the air-dried soils. Surface area, which was correlated to the partition coefficients with r^2=0.78 under oven-dried conditions, had a coefficient of correlation of 0.43 under air-dried conditions. A possible reason for the change in importance of surface area is that water sorbed onto the mineral surfaces resulted in a decrease in adsorption sites on the minerals. In addition, water sorbed onto organic matter may have resulted in the hydration of its structure, causing swelling (Hayes and Himes,1986) and exposing internal surfaces and "sites" resulting in an enhancement of TCE sorption by soil organic matter relative to that at the oven dry condition (see Section IV). An argument for this case can be made by examining the amount of water sorbed by the soils under the air-dried moisture condition. It is known that the amount of water sorbed onto soils with low organic content is highly dependent on the surface area (Foth, 1978; Brady, 1974). Based on this result, soils with large surface areas such as Gila silt loam would be expected to sorb the most water. Instead, soils with lower surface areas but a larger organic carbon fraction such as Sapsucker Woods soil and Rhinebeck loam were found to sorb the largest amount of water (Table V.5). This observation is supported by the good correlation (r^2=0.86) between the moisture contents at this RH and organic content. The water sorbed over that which is expected on a surface area basis may be taken up by the soil organic fraction (Sections III and IV). Therefore, under air dried conditions, the organic matter fraction may have

expanded sufficiently due to hydration to enhance TCE sorption (Section III and Section IV) while water sorbed onto the mineral surfaces would reduce the sorption of TCE through competition (Section III). Overall, soils with a higher mass fraction of organic matter appear to be a better sorbent for TCE under air-dried moisture conditions. This is illustrated by comparing Sapsucker Woods soil and Gila silt loam. Gila silt loam has a higher partition coefficient ($K_d' = 4180$ mL/g) under oven-dried conditions than Sapsucker Woods soil ($K_d' = 1180$ mL/g). However, at 68 percent RH the Gila silt loam had a lower partition coefficient ($K_d' = 2.79$ mL/g) than the organic-rich Sapsucker Woods soil ($K_d' = 25.7$ mL/g).
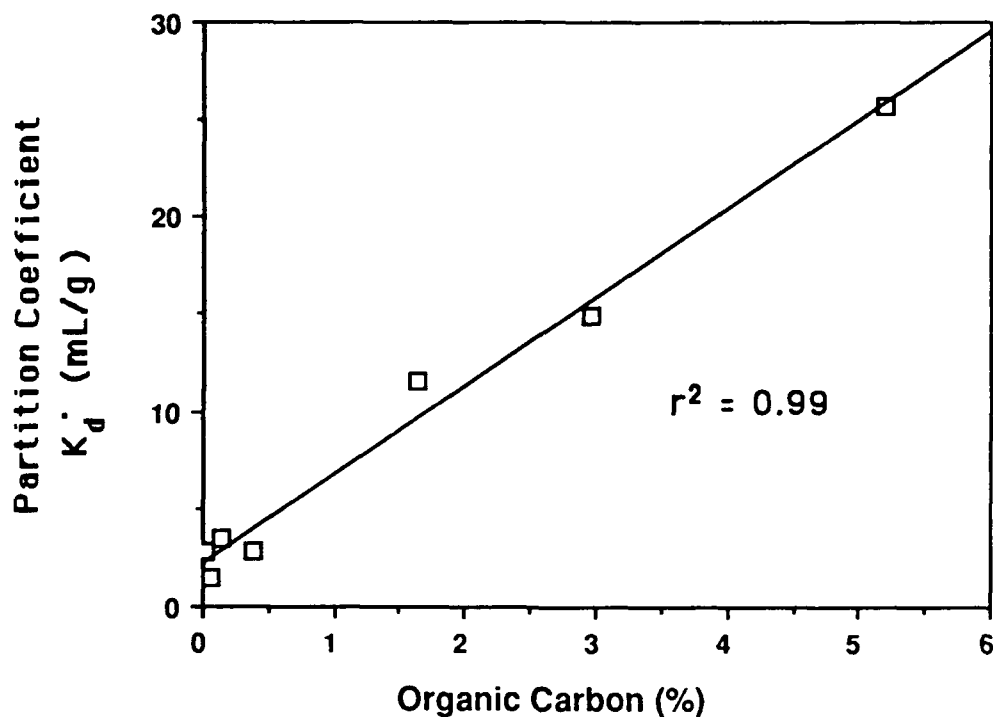
Figure V.1 Relationship between TCE Vapor-Phase Partition Coefficients under Air-Dried Conditions and Organic Carbon Content

Although a good correlation was obtained between the air-dried partition coefficients and organic carbon fraction, the large variation of K_{oc} values for air-dried soils may suggest that sorption of TCE molecules onto the water molecules bound to minerals (as hypothesized in Section III) cannot be excluded. Sorption of TCE to water which is structured or "ice-like" (Grim, 1953) by virtue of its polar attraction to the soil surface at 68 percent RH may contribute significantly to the total mass of TCE sorbed, especially for low organic carbon soils.

Surface soils generally have higher organic carbon weight fractions and also can be drier than soils of a deeper horizon. In the light of the results obtained here surface soils with their larger sorption capacity are likely to act as a barrier to the volatilization loss of organic vapor pollutants.

4. Sorption of TCE Vapor onto Soils at Field Capacity and under Saturated Conditions

Regression of the soil properties with the TCE vapor partition coefficients at field capacity (Table V.5) shows that organic carbon content gave the best coefficient of correlation ($r^2 = 1.00$, see Table V.4 and Figure V.2). This indicates that organic carbon content can be used as a predictor of TCE vapor partition coefficient for soils at field capacity. The partition coefficients were also highly correlated to moisture contents at field capacity ($r^2 = 0.91$) and CEC ($r^2 = 0.90$). This high correlation is due in part to the high correlation of organic matter with CEC and moisture contents at field capacity ($r^2 = 0.89$ and $r^2 = 0.90$ respectively). Call (1957) observed a similar high correlation between the sorption of EDB vapor and moisture contents onto several soils at field capacity.

Partition coefficients under saturated conditions are presented in Table V.6. Table V.4 shows that the saturated partition coefficients were strongly correlated to organic carbon content. This result is consistent with the prior findings of researchers such as Lambert et al. (1965), and Chiou et al. (1979), and Karickhoff et al. (1979).

Under saturated conditions and at field capacity, K_{oc} values for soils with organic carbon contents less than 0.1 percent such as Bandelier Tuff soil and Columbus aquifer material are several times larger (Table V.6) than for soils with a larger organic carbon weight fraction. K_{oc} values for air-dried soils (Table V.5, last column) do not converge to a single value but vary by roughly one order of magnitude. It is interesting to note that the uniformity of K_{oc} values improves as the moisture content is increased. This reflects the hypothesis that organic matter becomes increasingly important as a sorbent medium with increasing moisture content and that, at field capacity, hydrophilic regions of organic matter would be covered with water molecules leaving hydrophobic regions for the uptake of nonpolar organic pollutants (Wershaw, 1986). Organic matter under these moisture conditions could function as a partitioning medium as proposed by some researchers (Chiou et al., 1979).

Iron content was not strongly correlated with the partition coefficients at all four moisture levels. With a saturated partition coefficient of 0.24 mL/g for TCE on iron oxide (Section III), and the small mass fraction of iron in the soil, contribution of iron oxide

130

TABLE V.6 TCE VAPOR PHASE PARTITIONING COEFFICIENTS FOR SOILS AT FIELD CAPACITY AND UNDER SATURATED CONDITIONS

| | SATURATED CONDITIONS | | | | FIELD CAPACITY | | | | |
	K_d (± 95% C.I.) (mL/g)	K_{oc} (mL/g OC)	r^2	K_d/K_H (= K_d') (mL/g)	M.C. (%) (mL/g)	K_d' (± 95% C.I.) (mL/g)	r^2	$(K_d')_{oc}$† (mL/g OC)	K_d' Pred. from eqn. V.4
Morris	0.07±0.037	47.8	0.82	0.16	17.9	0.70±0.09	0.951	180.0	0.59
Harford	0.96±0.042	58.3	0.99	2.28	25.2	2.90±0.23	0.98	140.0	2.88
Rhinebeck	1.45±0.058	49.2	0.99	3.46	38.0	4.80±1.47	0.86	130.0	4.36
Tuff	0.08±0.018	125.0	0.85	0.18	21.5	0.70±0.12	0.96	350.0	0.70
Sapsucker	3.30±0.100	62.7	1.00	7.76	48.0	8.30±0.52	0.99	140.0	8.90
Gila	0.30±0.010	81.6	1.00	0.74	31.6	1.20±0.09	0.99	120.0	1.49
Columbus	0.06±0.050	200	0.78	0.14	12.5	0.50±0.24	0.87	770.0	0.44

† - after subtracting mass of TCE in soil water

131

towards the overall sorption is expected to be low in comparison to that of the organic fraction. However, influence of iron oxide on the sorption of nonpolar compounds may be significant in low organic carbon soils such as aquifer materials (Stauffer et al., 1989).
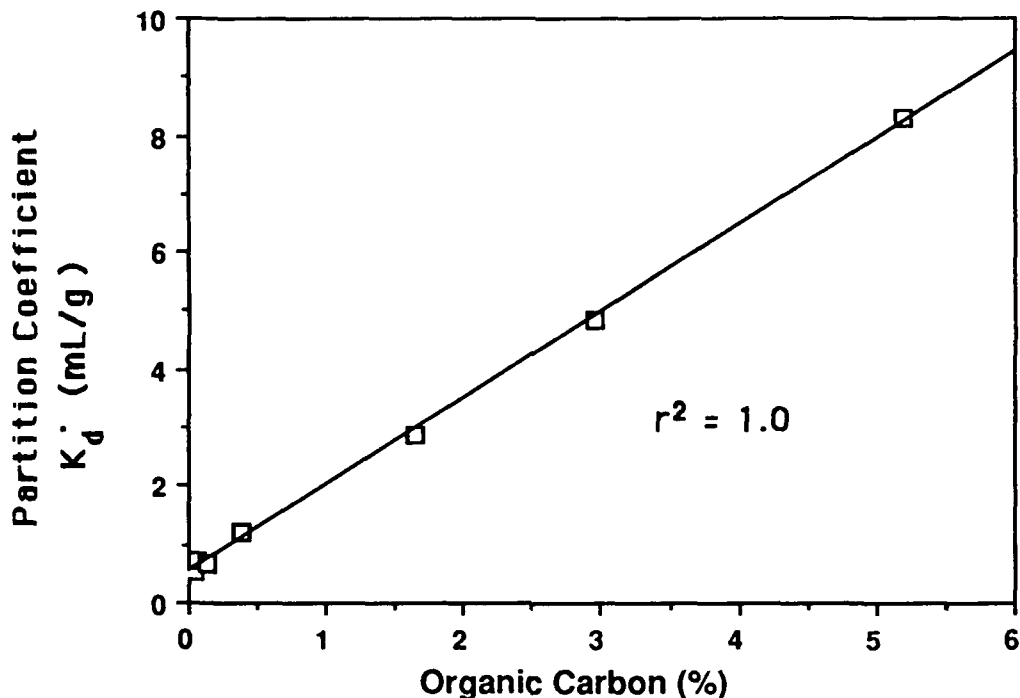
Figure V.2   Relationship Between TCE Vapor-Phase Sorption at Field Capacity and Organic Carbon

5. Distribution of TCE in the Soil-Water-Air System

The relationship developed in Section III (Equation III.10) for high moisture contents is used here to evaluate the vapor-phase partition coefficients and the distribution of TCE in the various phases of moist soils. The relationship is:

$$K_d{}' = K_d/K_H + (\text{Moisture Content \%})/(100\ K_H\ \gamma\ \rho) + \omega/(C_G M) \qquad \text{V.4}$$

where X = mass adsorbed on the soil-liquid interface (g)

K_d = liquid phase partition coefficient (mL/mg)

C_L = TCE concentration in the liquid phase (mg/L)

C_G = TCE concentration in the vapor phase (mg/L)

M = mass of sorbent (g)

γ = aqueous activity coefficient

132

ρ = density of water (g/cm^3)

ω is a lumped parameter which includes the effects of water surface sorption and condensation.

K_H = dimensionless Henry's Constant (0.42 for TCE)

Saturated TCE partition coefficients (K_d) adjusted for vapor-phase sorption (fourth column, Table V.6) were lower than the observed vapor-phase sorption (sixth column, Table V.6). Addition of the mass of TCE in soil water at field capacity to that sorbed at saturation (last column, Table V.6) resulted in predicted values that were similar to the experimental values. Therefore, the amount of TCE vapor sorbed at field capacity can be accounted for by two components, sorption at the solid-water interface and dissolution into the soil water. Contribution of sorption at the air-water interface can be regarded as negligible. This could be due to the insignificant partition coefficients of the TCE sorption for the air water interface and/or the surface area of the interface available for TCE sorption may be small compared to that of the soil water interface and dissolution into soil water. TCE partition coefficients for soils under air-dried conditions cannot be predicted with Equation V.4 indicating that other sorption processes may be contributing towards the total amount sorbed.

To further illustrate the role of accumulation of TCE in the various phases, the vapor-phase partition coefficients of TCE onto Bandelier tuff over a wide range of moisture contents were determined. Plotted on the same figure for the experimental data (Figure V.3) is the predicted partition coefficients based on Equation V.4. The close agreement of the predicted data with the experimental data suggest that the amount of TCE sorbed from the vapor-phase onto this soil can be accounted for by the solid-water sorption and dissolution into soil water at MC > 4 percent.

A basic assumption in many vapor-phase transport models such as those of Jury et al. (1983) and Baehr (1987) is that vapor-phase sorption consists of sorption at the soil-water interface and dissolution in the soil water as controlled by Henry's Law Constant. It is noteworthy that for soils at field capacity the experimental results presented here confirm this assumption. These results are, to the authors knowledge, the first experimental confirmation. However, as noted earlier, this assumption in vapor-phase transport models may not be fully applicable for drier surface soils and soils in the arid and semiarid regions.

133
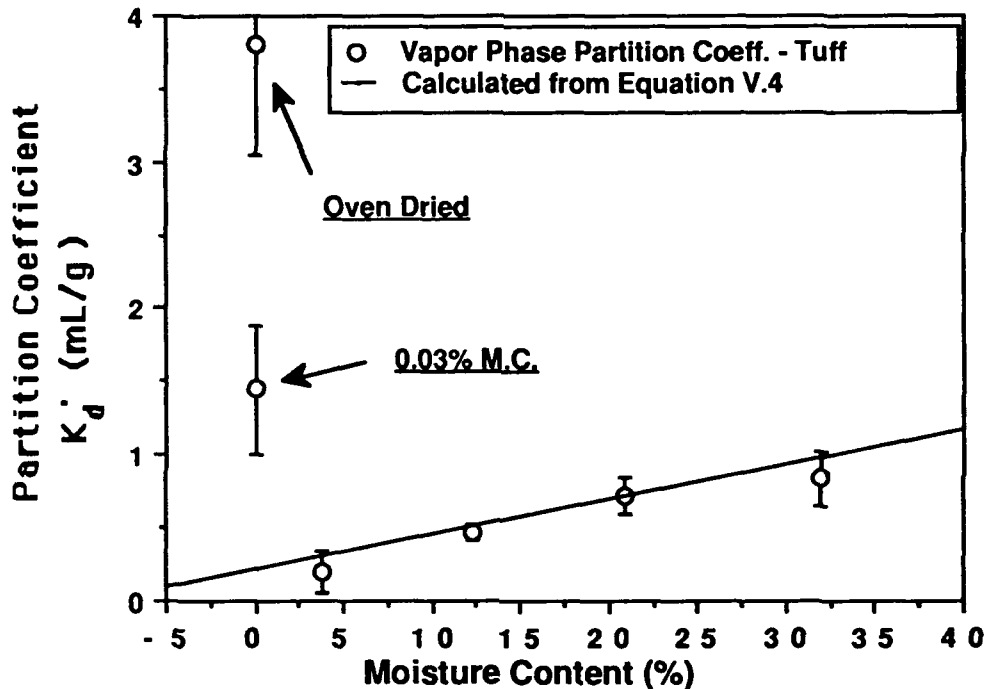
Figure V.3 Change of TCE Vapor-Phase Partition Coeff. on Bandelier Tuff with Moisture
Content (Error Bars = 95 Percent CI)

The importance of dissolution of TCE in soil water to the overall distribution of
TCE vapor in the moist soils can be analysed with the use of Equation V.4 and is illustrated
in Figure V.4. Three moisture contents, ie. 15, 35 and 55 percent are considered for
saturated partition coefficients ranging from 0 to 3.5 mL/g. The high partition coefficient is
representative TCE partitioning in the soils with high organic carbon content such as the
like Sapsucker Woods soil. The amount of TCE dissolution in soil water is expressed as a
percentage of the total amount sorbed from the vapor phase. This percentage is plotted as a
function of the partition coefficient. For low organic carbon soils such as aquifer material
(for example, Columbus; K_d=0.06 mL/g), the contribution of TCE dissolution in the soil
water is about 60 percent for a moisture content of 15 percent. For organic soils
comparable to the Sapsucker Woods (K_d =3.26 mL/g), this percentage reduces to about 10
percent at a moisture content of 35 percent. At least 15 to 35 percent of the total amount
sorbed (at 15 to 55 percent M.C.) can be accounted for by TCE dissolution in soil water for
soils with typical chemical compositions comparable to the Harford and Rhinebeck loams.
These calculations show that for the modeling of vapor-phase transport of a pollutant,
dissolution in the stationary soil water can be substantial contribution to the overall vapor
uptake and may play an important role, especially for low organic carbon soils such as
aquifer materials. Therefore, the use of the saturated sorption partition coefficient as a first

approximation for vapor-phase sorption as suggested by Roy and Griffin (1987) is most likely to be valid for soils with moderately high organic carbon.
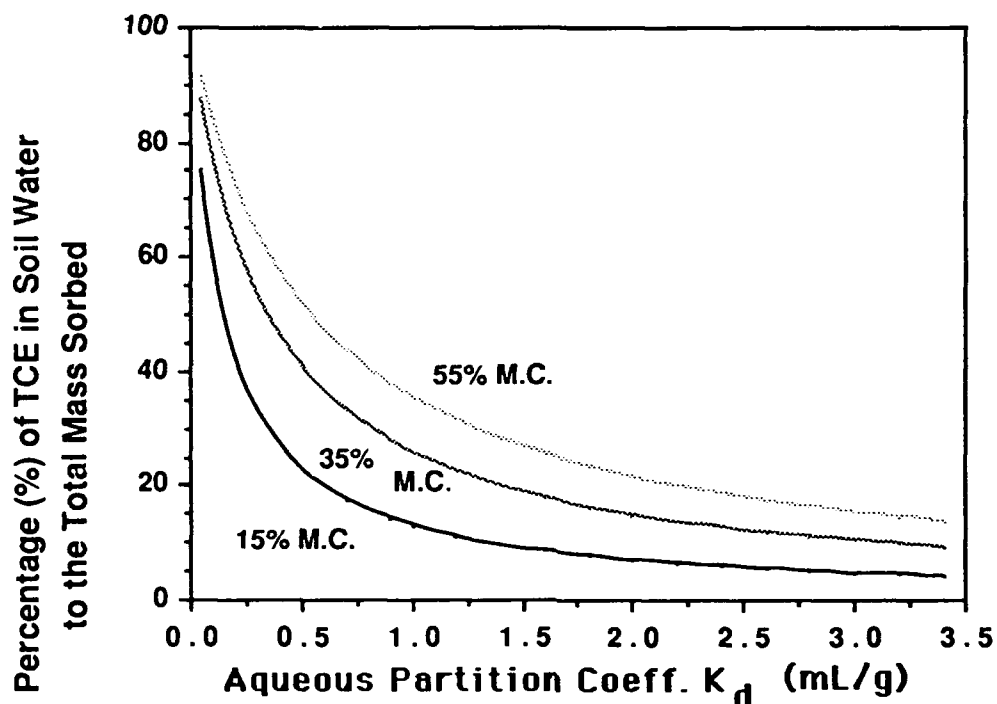
Figure V.4 Percentage of TCE Sorbed in Soil Water as function of Aqueous Partition Coefficient of TCE

D. SUMMARY AND CONCLUSIONS

As expected, vapor-phase partition coefficients (K_d') of TCE onto soils under oven-dried conditions were found to correlate well with the specific surface area, indicating that surface area can be used as a measure of the amount sorbed.

TCE vapor partition coefficients of seven soils under air-dried conditions and at field capacity were found to correlate well with organic carbon content of the soils. The partition coefficients under air-dried conditions were about three times larger than the partition coefficients at field capacity. The vapor-phase partition coefficient of the seven soils at field capacity can be accounted for by two components: TCE dissolution into soil water, and TCE sorption at the soil-water interface. However, the higher sorption partition coefficients under air-dried conditions cannot be accounted for by these components. This result indicates that TCE uptake processes other than vapor dissolution and saturated partitioning may be occurring at air-dried conditions. Soil organic matter is believed to

135

swell in response to varying moisture contents. Under air-dried conditions such swelling may be adequate to reveal internal regions for binding of TCE. When more moisture is added as at field capacity, hydrophilic regions will be covered with water leaving hydrophobic regions for the sorption of TCE. Under these moisture conditions, organic matter could function as a partition medium.

Contribution of TCE dissolution into soil water can be significant for soils with low organic matter contents such as aquifer materials. Use of the saturated partition coefficients as an approximation for vapor-phase sorption is valid only for soils that have moderately high organic contents and with moisture contents around field capacity. For example for a soil with 1.6 percent organic carbon, TCE dissolution in soil water would contribute about 15 percent to the total amount sorbed from the vapor phase at field capacity.

SECTION VI
PARAMETRIZATION OF ADSORPTION ISOTHERMS TO DATA COLLECTED BY ADSORBATE CONCENTRATION DIFFERENCE

By: S.R. Lindner, S.J. Schwager and L.W. Lion

A. INTRODUCTION

Since the introduction of the nonlinear Langmuir adsorption isotherm in 1918, various curve-fitting techniques have been used to estimate the two parameters most frequently used to describe vapor-solid distribution, the monolayer capacity, Γ_m, and the adsorption affinity constant, c. Although graphically fitting a straight line by eye to a linearized form of this equation (as proposed by Langmuir) is still useful today, recent work by Kinniburgh and others has addressed regression techniques for parameterizing adsorption isotherms. Kinniburgh (1986) advocated using weighted nonlinear regression to overcome the difficulty of finding, or choosing, a linearized form of an isotherm equation, if such a linear form exists. Part of the argument for using weighted nonlinear least squares was that whenever possible, regression analysis should be performed directly on the data rather than on calculated quantities (as is necessary when an equation is linearized), to avoid uneven propagation of experimental error (Cabaniss and Shuman, 1988). Calculated quantities may also be introduced into regression analyses when the extent of adsorption is computed from concentration-level differences. This calculation is common in practice when extraction of adsorbate from the adsorbent phase is experimentally difficult.

This section examines the effectiveness and reliability of parameter estimation by nonlinear regression and compares it with an alternate numerical technique. In addition, isotherm equations have been rewritten in a form where the response variable, Γ, the amount of adsorption per gram sorbent, has been replaced by a concentration ratio. Replacing Γ by a concentration ratio was found to improve parameter estimation and is shown to be useful for data where the extent of adsorption is inferred from the difference between a reference concentration and the equilibrium value.

B. THEORETICAL CONSIDERATIONS

The difficulties in parametrizing isotherm equations are well known (see for example Dowd and Riggs, 1965; Harter, 1984; and Low and Batley, 1988). The pitfalls of linear regression may be illustrated by the Langmuir adsorption isotherm. For adsorption of a gas, the equation for the Langmuir isotherm can be written as:

$$\Gamma = \frac{c \, \Gamma_m \, \phi}{1 + c \, \phi}$$

VI.1

where Γ_m = the mass of gas required to form a monolayer per gram adsorbent (g/g)

c   = a dimensionless affinity constant related to the vapor binding energy

Γ = the mass of gas adsorbed per gram adsorbent (g/g)

ϕ = adsorbate vapor concentration normalized by the concentration of the saturated vapor at the experimental temperature and pressure.

In this equation, Γ_m and c are parameters, whose values remain fixed, while the quantities Γ and ϕ may vary as different cases are observed. The Langmuir model is appropriate if Equation VI.1 is satisfied by every observed pair Γ and ϕ, when these are measured with perfect accuracy (i.e., without error).

The Langmuir equation has at least three linear transformations:

$$\Gamma = \Gamma_m - \frac{\Gamma}{c\phi}$$

VI.2

$$\frac{\phi}{\Gamma} = \frac{1}{c \, \Gamma_m} + \frac{\phi}{\Gamma_m}$$

VI.3

$$\frac{1}{\Gamma} = \frac{1}{c \, \phi \Gamma_m} + \frac{1}{\Gamma_m}$$

VI.4

All three of these equations are equivalent to VI.1, so all of the Equations VI.1 to VI.4 represent the Langmuir model.

In practice, there are two complications with use of Equations VI.1 through VI.4: the values of the Langmuir model parameters Γ_m and c are not known, and the pair Γ and ϕ cannot be observed with perfect accuracy. Thus, the ith experimental observation consists of a pair of values Γ_i and ϕ_i that make Equations VI.1 to VI.4 hold approximately (but not exactly). Estimates of the Langmuir isotherm equation parameters Γ_m and c can be obtained from a regression analysis of a set of n observations, using one of the Equations VI.1 to VI.4. If the regression is based on one of the equations VI.2 to VI.4, Γ_m and c can be estimated from the slope and intercept of the best line drawn through the transformed data. Statistical research on this problem has focused on determining which transformation gives the most reliable parameter estimates. Some of the leading work in this area may be found in regard to the Michaelis-Menten equation in the field of enzyme kinetics (Dowd and Riggs, 1965), which has the same hyperbolic form as the Langmuir equation (Lineweaver and Burk, 1934).

138

Each linear transformation shown above suffers from an apparent drawback. The first two equations are deficient, as noted by Dowd and Riggs (1965), in that the same variable appears on both sides of the equation (Γ in Equation VI.2 and ϕ in Equation VI.3), creating a correlation between the plotted variables. Equation VI.4 is also problematic because the reciprocal of Γ tends to emphasize small values, which are known with the least accuracy. Using synthetic data, Dowd and Riggs (1965) found that Equation VI.3 gave the most reliable parameter estimates for unweighted data and was far superior in this respect to the double reciprocal, or Lineweaver-Burk method (Equation VI.4) regardless of the error structure assumed. Paradoxically, Equation VI.4 created the line with the best visual appearance even though its ability to estimate the true parameters was poorest. In addition, it was found that the linear transformations having high correlation coefficients on the predictors and narrow confidence intervals for the parameters did not show superior ability to estimate parameter values correctly. In fact, linear transformations that highlighted outliers and resulted in broader 95 percent confidence intervals proved better at judging parameter estimates than transformations that obfuscated errors (Dowd and Riggs, 1965).

Harter (1984) showed, by use of examples, that both a linear appearance of a linearized Langmuir plot and a high value of the correlation coefficient were obtainable even when the data clearly did not fit the Langmuir model. This was apparent to the observer when the data was plotted without linearization along with the fitted curve. He concluded that linearity of a Langmuir plot derived from one of the Equations VI.2 - VI.4 did not sufficiently justify choosing the Langmuir model. He showed that several curves with different shapes could produce straight line plots using Equation VI.3 with high correlation coefficients. Small errors in the data could throw the prediction of the adsorption maximum off by as much as 50 percent. Harter concluded that, even when correlation coefficients are high, it is important to plot the data along with the fitted curve to check the fit. Absence of data in the high concentration range, precludes validation of the predicted adsorption maximum.

1. The Application of Regression Analysis

Although the methodology for parameter estimation in regression models is highly developed, confusion may still result when regression analysis is applied to adsorption data, because of the nature of the adsorption experiments and the complexity of the isotherm equations. Important questions include which transformations of the isotherm equation and data are appropriate, how to avoid gross errors in parameter estimates due to extraneous variables, how to use weighted regression, how uncontrolled variations in experimental conditions can be handled, and whether the added complexities of approaches avoiding these difficulties are justified.

The derivation of the regression analysis equations involves four critical assumptions regarding the statistical properties of the data. Because departure from the assumptions inherent in regression models can lead to bias in parameter estimation and other difficulties, the four assumptions of regression are briefly reviewed.

Regression analysis relates the value of a response variable Y to the corresponding value of the predictor variable X. (The discussion here is restricted to regression with a single predictor variable, which suffices for the models considered in this report. It can be extended in straightforward fashion to the case of several predictor variables; see Draper and Smith, 1981.) The first assumption is that for every possible value of the predictor variable X there is a normal distribution of the dependent variable Y. The second assumption is that the values of X are known without error, or with negligible error. The third assumption is that the mean and the variance of the distribution of Y conditional on X are related to the value of X by known functional forms. It is often assumed that the variance of Y given X is the same for all X; however, this standard assumption can be relaxed by using weighted least squares, which allows unequal variance problems to be recast as problems in which there are equal variances. The fourth assumption is that observations of the dependent variable Y are jointly independent (i.e., one measurement of Y_i does not affect any other).

To summarize, the four assumptions are: Y given X has a normal distribution; the values of X are measured without error; the distribution of Y given X has mean and variance of known form; and observations are independent. Point estimation of the parameters can be performed with less restrictive assumptions, e.g., dropping the requirement of normality and replacing independence of the Y's by the weaker assumption that the Y's are pairwise uncorrelated. However, the four assumptions as specified above are needed to obtain confidence intervals and test hypotheses. These assumptions are incorporated into the general model:

$$Y_i = \Gamma(X_i, \Gamma_m, c) + \varepsilon_i \qquad \text{for } i=1,2,\ldots,n, \qquad \text{VI.5}$$

where: $\Gamma(X_i, \Gamma_m, c)$ is the expectation function, of known mathematical form, evaluated at the value of the predictor variable, X_i,

and ε_i is the random error term, which is normally distributed with mean zero and variance given by a function $q(X_i, \Gamma_m, c)\sigma^2$ of known form. [If the variances of all observations are equal, the variance function reduces to σ^2.]

2. Plotting and Analyzing Adsorption Data

Since equations can often be written in many equivalent forms, e.g., Equations VI.1 - VI.4, a pressing problem is deciding which arrangement to use. Because of the first assumption of regression analysis, it is important to resolve the relationships between the variables. Some variables are controlled by the experimenter and some are not because they are the result of the phenomenon that the experimenter is attempting to study. Here we will refer to the experimental results as the response variable, or dependent variable. Similarly we will refer to what is varied in a controlled manner by the investigator as the predictor variable, or independent variable. Note that the same variable may be either a response variable or a predictor variable depending on the experimental design.

Wherever possible, the isotherm equation should be arranged, and plotted, so that the response variable is expressed as a function of the predictor variables and the parameters. When the experimenter ignores this suggestion, by plotting on a different set of axes, he or she inevitably introduces correlation between the x and y variables. The form of the isotherm equation plotted will depend on the experimental method chosen, to reflect the diverse roles of variables in different experimental protocols. With the experiments described here, equilibrium concentration is the response variable and sorbent mass is the predictor variable. Instead, if the experiment were performed by controlling the initial amount of sorbate and measuring the equilibrium concentration, under conditions where sorbent mass was held constant, then equilibrium concentration would be the response variable and initial concentration the predictor variable. The experimentally based rearrangement of the isotherm equation, once found, forms the basis of the analysis and requires no further manipulation before regression analysis (Kinniburgh 1986). This work focuses on the equations pertaining to a protocol where mass of adsorbent is chosen by the investigator and concentration is measured relative to a control level. This analysis may easily be adapted to other protocols.

The headspace analysis technique for vapor sorption will be used to illustrate the effect of experimental protocol on data analysis. Details of the headspace analysis technique, used here and by Peterson et al. (1988) to measure vapor sorption, are given in the materials and methods section.

In the headspace analysis technique the investigator starts by choosing a level of sample mass to weigh into an experimental bottle. Thus the sample mass in a bottle is the independent or assigned variable and will be referred to as the predictor. The equilibrium vapor concentration, estimated by gas chromatography, is then the dependent or measured variable, or the response variable, because it is a function of the mass of sample present. Sample mass is a good choice for the independent variable, because it may be measured

141

with a precise analytical balance (±0.0002g) and therefore best satisfies the assumption of regression analysis that the predictor variable is known without error. In the headspace procedure, as in many other experimental protocols, the amount of adsorption is not measured directly. Instead vapor concentration is measured and adsorption is inferred by mass balance from an initial vapor concentration. The amount of vapor adsorbed per gram, therefore, is viewed not as a variable in its own right, but as a quantity calculated from the values of other system variables.

If the choice of sample mass and gas concentration as predictor and response variables is ignored, one can construct the same plot as that used by experimenters where adsorption is measured directly (hereafter referred to as the conventional method), that is, a plot of the adsorption density (the mass of vapor adsorbed per gram of solid) versus equilibrium concentration. Analysis of headspace data by the conventional approach is complicated because both plotted variables are subject to errors, instead of solely the response variable as the regression model assumes. Excessive error propagation occurs with the conventional method since the errors occurring in the predictor and response variables are negatively correlated, shifting data points perpendicular to the true isotherm. For instance, a slightly larger estimate of the equilibrium concentration will produce a correspondingly lower estimate of adsorption. Conversely, a slightly lower estimate of concentration will result in a slightly greater estimate of adsorption. Because a unique distribution of Y for a given level of X is not guaranteed, and because errors occur in both the X and Y variables when the data are plotted as amount adsorbed per gram versus concentration, this approach is avoided here. An alternate equation form is proposed, which avoids the negative correlation of the variables and obeys the first regression assumption. The approach (derived below), which satisfies these criteria, is extended from the linear isotherm equation to the Langmuir and B.E.T. isotherms.

3. Adsorption Isotherms

Linearity of adsorption isotherms is commonly observed when relatively few molecules of adsorbate are present in the company of a large excess of adsorbent. This condition occurs at the low concentration range of the isotherm. Many experimental isotherms are linear over some range, especially those for partitioning of nonionic pollutants onto soils. Within the linear range of an isotherm, the relationship between the amount adsorbed and the concentration can be expressed via a single constant, K'_d.

In a typical vapor adsorption experiment the amount adsorbed is inferred by comparison of the equilibrium concentrations in a control (no adsorbent) vessel and a sample (with adsorbent) vessel. To the degree possible the same initial mass of adsorbate

is added to each vessel. Assuming a linear partitioning process, the equation for mass balance over controls and samples can be equated as:

$$V_B C_B = \Gamma_i M_i + V_i C_i \qquad \text{VI.6}$$

where: V_B = the average volume of the control bottles (cm^3)
C_B = the average concentration of the controls (g/cm^3),
M_i = the sample mass (g),
V_i = the volume of the sample bottle (cm^3),
C_i = the concentration measured for the sample bottle (g/cm^3).

If vapor density is measured by gas chromatography, then concentration is proportional to G.C. signal area:

$$C_B = \Phi_B z/B \text{ and } C_i = \Phi_i z/B, \qquad \text{VI.7}$$

where:

Φ_B = the average signal area of the control bottles,
Φ_i = the measured signal area of the sample bottle,
z = the density of the saturated vapor (g/cm^3)
B = the signal area equivalent of the saturated vapor or $\Phi_B/(V_G/V_B)$, where
(V_G/V_B) = a volume dilution factor, and
V_G = the volume of the source syringe (cm^3).

Approximation of gas concentration by G.C. signal area allows Equation VI.6 to be written as:

$$\frac{V_B \Phi_B z}{B} = \Gamma_i M_i + \frac{V_i \Phi_i z}{B}. \qquad \text{VI.8}$$

When a direct relationship exists between the amount adsorbed, for a given mass of adsorbent, M_i, and the relative concentration of the sorbate, ϕ, where $\Phi_i/B = \phi_i$, a linear isotherm (Equation VI.9) may be substituted for Γ_i in Equation VI.8.

$$\Gamma_i = K \Phi_i/B = K'_d z\Phi_i/B \qquad \text{VI.9}$$

where K is the dimensionless parameter to be fitted,
and K'_d has dimensions of cm^3/g.

143

Equation VI.8 can then be arranged to put the dependent variable (Φ_i) that is measured on the left hand side, keeping the independent variable (M_i) and the parameter to be fitted (K) on the right:

$$\frac{V_B \Phi_B}{V_i \Phi_i} = K \frac{M_i}{V_i z} + 1$$

VI.10

Equation VI.10 may also be derived by observing that Γ_i may be expressed as:

$$\Gamma_i = \frac{z(V_B \Phi_B - V_i \Phi_i)}{M_i B}$$

VI.11

and substituting into Equation VI.9.

Defining for observation i (i=1,2, . . .,n),

$$Y_i = \frac{V_B \Phi_B}{V_i \Phi_i} \quad \text{and} \quad X_i = \frac{M_i}{V_i z}$$

VI.12

transforms Equation VI.10 into $Y_i = KX_i + 1$. If the assumptions of the model VI.5 are satisfied at least approximately [the linear isotherm is the simplest form of Equation VI.5 where $K = f(\Gamma_m c)$], this model can be used to analyze the observations (X_i, Y_i). The expectation function ($KX_i + 1$) gives the linear model:

$$Y_i = K X_i + 1 + \varepsilon_i \qquad \text{for } i=1, 2, \ldots, n, \qquad \text{VI.13}$$

with ε_i representing an error term, required whenever observations of Y_i are not exact. As will be seen below, for the experimental data presented here, an exponential function best explained the squared deviation of Y_i from the expected value of Y_i ($\hat{Y}_i$). Details of the model used for the variance of the observations, and the manner in which the variances were examined, are given in the data analysis and results and discussion sections.

It is possible, of course, that no choice of the variance function will make a linear model suitable for a given set of observations. This will be the case if the assumption of a linear partitioning process is not satisfied. In this situation, an alternate model may be more consistent than the linear model (VI.9) with the observations. Two nonlinear models, the Langmuir and the B.E.T. equations, will now be treated.

144

4. Fitting Nonlinear Models: The Langmuir and B.E.T. Equations

The model connecting a response variable Y and a predictor variable X can lead to a regression analysis of varying degrees of complexity. The simplest case is the linear regression model of Equation (VI.9). A more general case is the regression model of Equation (VI.5), which does not require the function Γ to be linear in the parameters.

It is possible that X and Y satisfy a physical law that does not allow an explicit solution for Y as a function of X and the parameters. If X and Y could both be measured without error, all observed X,Y pairs would satisfy a relationship of the form:

$$f(X,Y; \{\theta\}) = 0 , \qquad\qquad VI.14$$

where $\{\theta\}$ denotes the set of parameters in the model. The Redlich-Peterson isotherm is an example of an equation which satisfy Equation VI.14 but not Equation VI.5. The crucial point is that regression methods can still be applied in spite of the inability to solve for Y explicitly as was done in Equation VI.5.

For specified values of X and the parameter set $\{\theta\}$, the value(s) of Y that satisfy Equation VI.14 can be determined. Thus, even if Y can not be explicitly solved for, $f_Y(X;\{\theta\})$ can be defined implicitly as the value of Y that satisfies VI.14 for a given X and $\{\theta\}$. To reflect the fact that Y is observed with error, an error term is incorporated in the relation between Y and $f_Y(X;\{\theta\})$.

$$Y = f_Y(X;\{\theta\}) + \varepsilon. \qquad\qquad VI.15$$

Although f_Y is an implicit rather than an explicit function, Equation VI.15 can be solved numerically as needed and the results used to obtain a regression analysis of the data. Even when it is possible to solve explicitly for Y, such as with the Langmuir isotherm, it may still be advantageous to use an implicit solution to a nonlinear adsorption isotherm to avoid possible colinearity in the coefficient matrix for the parameters which may occur under nonlinear regression on Equation VI.1.

a. The Langmuir Equation

Langmuir derived a model isotherm (VI.1) for an adsorption process in which adsorption proceeds to a monomolecular film because at most one molecule is allowed to occupy a given adsorption site. Brunauer, Emmet, and Teller (1938) extended Langmuir's equation to allow adsorbate molecules to form multiple layers by relaxing this assumption.

The B.E.T. equation, as their relationship came to be known, assumes that a dynamic equilibrium (similar to that described by the Langmuir equation) explains adsorption for each successive layer. Both Langmuir and Brunauer, Emmet and Teller originally developed their isotherms to describe the adsorption of gases by solids.

The data analysis for the Langmuir and B.E.T. model equations is similar to that for the linear model and involves the same variables X and Y (defined in Equation VI.12). As was the case with the linear isotherms, it is dimensionally expedient to normalize the measured adsorbate concentration (or G.C. signal area) by the saturated vapor pressure concentration (i.e., the G.C. signal area expected at that concentration).

$$\Gamma = \frac{\Gamma_m c \, \dfrac{\Phi_i}{B}}{1 + c \dfrac{\Phi_i}{B}} \qquad\qquad\qquad VI.16$$

where Γ_m = mass of adsorbate corresponding to monolayer coverage per gram of adsorbent,

   c = the Langmuir affinity parameter,

   Γ = mass of vapor adsorbed per gram adsorbent.

Substitution of Equations VI.12 and VI.16 into Equation VI.8 yields:

$$Y_i = X_i \, \frac{c \, \Gamma_m}{1 + c \, Z_i \, Y_i^{-1}} + 1 + \varepsilon_i \qquad\qquad \text{for } i = 1, 2, \ldots, n \qquad VI.17$$

where $Z_i = V_G/V_i$, V_G is the volume of the source syringe (cm^3), and the subscript i refers to individual observations.

For the Langmuir equation an implicit relationship, as in Equation VI.15, between X and Y was chosen as the basis for analysis. An error term ε_i is incorporated into Equation VI.17 to reflect the random variability in Y_i. This reflects the fact that several observations with identical values of X_i will result in distinct values of Y_i. Regression analysis can still be performed, despite the occurrence of the Y_i^{-1} on the right-hand side of Equation VI.17, when a numerical procedure is used to calculate values for Γ_m and c that minimize the residual sum of squares (RSS). The details of fitting the parameters and incorporating the error in the observations is developed in the data analysis section.

b. The B.E.T. Equation

The form of the B.E.T. isotherm used here is:

$$\Gamma = \frac{\Gamma_m c \dfrac{\Phi_i}{B}}{\left(1 - \dfrac{\Phi_i}{B}\right)\left\{1 + (c-1)\dfrac{\Phi_i}{B}\right\}} \quad \text{for } i = 1,2,\ldots,n \qquad \text{VI.18}$$

where terms are defined as in Equation VI.16. This can be treated as the Langmuir equation was previously, to form an equation in X and Y of Equation VI.12, by substituting for Γ in Equation VI.18 by Equation VI.11:

$$Y_i = X_i \frac{\Gamma_m c}{\left[1 - \dfrac{Z_i}{Y_i}\right]\left[1 + (c-1)\left(\dfrac{Z_i}{Y_i}\right)\right]} + 1 + \varepsilon_i \qquad \text{VI.19}$$

The equation used for the B.E.T. isotherm, as was the case with the Langmuir isotherm, is an implicit function of Y_i in terms of X_i and the parameters when the extent of adsorption is not independently measured. Equation (VI.19), like Equations VI.13 and VI.17, includes an error term ε_i to reflect the random variability in Y_i. Regression analysis may proceed despite the implicit nature of the function for Y_i as described in the data analysis section which follows.

5. Weighting Data for Regression

Having identified the dependent variable in the system, it is appropriate to examine the issue of equality of variances. Frequently some observations in a regression analysis are "less reliable" than others. The variances of the observations will hence be unequal, and weights corresponding to these variances must be assigned to the observations. Analysis of these weighted observations involves transforming them to a set of variables to which we can apply the usual (unweighted) regression analysis. A detailed treatment of weighted least squares regression is given by Draper and Smith (1981).

To understand the variance structure of the observations, it is useful to identify potential sources of error. For instance, in this work, in which vapor concentration was measured, error was likely attributable to the difficulty of measuring low concentrations on the G.C. relative to the blanks, which were used to set the signal range. This error was compounded by the division operation (i.e., calculation of Y_i), especially as the divisor

approached zero. In general there is no method of knowing *a priori* how the variance of a random variable will behave over its entire range. It is good practice, therefore, to conduct replicate experiments so that errors may be quantified. In absence of a sizable pool of replicates, it may be appropriate to assume a functional relationship for the variance in the response variable based on the magnitude of the response or predictor variable. Common assumptions of this type are discussed by Kinniburgh (1986). The model used for the variance of vapor sorption data is described in the Results and Discussion section below.

6. Fitting the Intercept

The model forms of the linear, Langmuir, and B.E.T. isotherms (Equations VI.13, VI.17, and VI.19, respectively) share a common intercept of 1.0. The fitting routine used here forced the linear model through the theoretical value of the intercept. Poor fit indicated that an alternate model should be chosen. Forcing the intercept through the theoretical value was necessary to make different forms of the linear model equivalent. Intercepts of the nonlinear models were not forced.

C. DATA ANALYSIS

1. The Langmuir Equation

Although equations VI.17 and VI.19 may be solved explicitly, an implicit solution may also be employed. We elected to solve the equation implicitly for Y_i, in attempt to improve parametrization by nonlinear regression. The values of the parameters Γ_m and c that minimize the RSS were found by using a numerical minimization algorithm. The numerical procedure was simplified by the fact that the Langmuir equation is linear in the parameter Γ_m. This made it possible to treat only c iteratively, rather than the pair (c, Γ_m). For any given value of c, the usual linear regression methods can be applied to find the value of Γ_m that minimizes the RSS for the data and the specified value of c. We proceeded by iterating on c, finding for each value of c the minimizing value of Γ_m and the resulting minimum RSS. In summary, the residual sum of squares was the objective function minimized and c was the decision variable.

Minimization was performed by Golden Section search which is described in detail by Press et al. (1986), and Wagner (1969). This method begins with the value of c bracketed in an initial interval [a,b], specified by the user. With each iteration, the function is evaluated at two interior points, C_1 and C_2. The points C_1 and C_2 are chosen according to golden ratio to optimize convergence. They divide the bracketing interval into three sections. By looking at the value of the objective function at the interior points C_1 and C_2, one of the end sections of the bracketing interval is discarded. The process continues until

the interval around the c that minimizes the RSS is tolerably small, as described by the following algorithm:

set $C_0 = a$

       $C_3 = b$

       $C_1 = 0.618a + 0.392b$ *and* $RSS_1 = RSS(C_1)$

       $C_2 = 0.392a + 0.618b$ *and* $RSS_2 = RSS(C_2)$

Do the following loop while the absolute value of $(C_3 - C_0)$ is greater than the tolerance:

    If RSS_2 is less than RSS_1 then

         $C_0 = C_1;$ *and* $RSS_0 = RSS_1$

         $C_1 = 0.392C_0 + 0.618C_3;$ *and* $RSS_1 = RSS(C_1)$

         $C_2 = 0.618*C_0 + 0.392*C_3;$ *and* $RSS_2 = RSS(C_2)$

    else

         $C_3 = C_2$ *and* $RSS_3 = RSS_2$

         $C_2 = 0.392*C_3 + 0.618*C_0$ *and* $RSS_2 = RSS(C_2)$

         $C_1 = 0.618*C_3 + 0.392*C_0$ *and* $RSS_1 = RSS(C_1)$

End

For each specified value of c, the value of Γ_m minimizing RSS (Equation VI.29) was determined from the linear regression equation with no intercept:

$$U_i = X_i \Gamma_m + \delta_i \qquad \text{for } i = 1, 2, \qquad\qquad VI.20$$

where δ_i is a random error term and U_i is defined as the function of Y_i:

$$U_i = (1/c) [Y_i + c\, Z_i(1 - Y_i^{-1}) - 1] \qquad\qquad VI.21$$

Equation VI.21 is obtained from Equation VI.17 by moving all terms involving Y_i to the left-hand side while keeping all occurrences of X_i and Γ_m on the right-hand side. We assume in VI.20 that the n observations are independent and that the random error term δ_i has a normal distribution with mean zero and variance given by:

$$Var(U_i) = Var\{(1/c)[Y_i + c\, Z_i(1 - Y_i^{-1}) - 1]\} \qquad\qquad VI.22$$

The variance can be approximated by the standard result, based on a first-order Taylor series expansion assuming the variance of Z_i is negligible (see Kendall and Stuart, 1969):

$$\text{Var}(g(Y_i)) \approx (d\ g(Y)/dY)^2\ |_{Y=Y_i}\ \text{Var}(Y_i). \hspace{2cm} \text{VI.23}$$

Applying this to the function $U_i = g(Y_i) = c^{-1}[Y_i + c\ Z_i(1 - Y_i^{-1}) - 1]$ gives:

$\text{Var}(U_i) \approx d_i\ \text{Var}(Y_i)$, where d_i is defined by:

$$d_i = c^{-2}\ (1 + (c\ Z_i)\ Y_i^{-2})^2. \hspace{2cm} \text{VI.24}$$

The technique of weighted least squares may now be used to estimate the parameter Γ_m in VI.20, where the weight of each observation is proportional to the reciprocal of its variance. For a discussion of weighted least squares regression see Draper and Smith, (1981).

Examination of the data obtained in the vapor sorption experiments reported here suggested that the variance of Y_i can be modeled as a function of $\hat{Y}_i$, the expected value of Y given the value of X_i, where h is approximately equal to the variance of the blanks and Q is a power constant. The choice of this particular function for modeling the variance will be justified in the discussion of results.

$$\text{Var}(Y_i) = h\ \hat{Y}_i^{\ Q} \hspace{2cm} \text{VI.25}$$

The weights used with Equation (VI.20) are derived from Equation (VI.25) as in Draper and Smith (1981). The variance of U_i is calculated from the variance of Y_i as:

$$\text{Var}(U_i) = \frac{\sigma^2}{w'_i} \approx d_i\ hY_i^Q \hspace{2cm} \text{VI.26}$$

yielding the weights applicable to estimation of the parameter Γ_m of Equation VI.20,

$$w'_i = \frac{\sigma^2}{h\ Y_i^Q}\ . \hspace{2cm} \text{VI.27}$$

Then
$\hat{\Gamma}_m$ is given by weighted linear regression (Draper and Smith, 1981):

$$\hat{\Gamma}_m = \frac{\sum\limits_{i=1}^{n} w'_i\, X_i\, U_i}{\sum\limits_{i=1}^{n} w'_i\, X_i^2} = \frac{\sum\limits_{i=1}^{n} \dfrac{X_i\, U_i}{d_i\, Y_i^Q}}{\sum\limits_{i=1}^{n} \dfrac{X_i^2}{d_i\, Y_i^Q}}.$$ VI.28

This is the $\hat{\Gamma}_m$ that minimizes the weighted RSS for the data (X_i, Y_i), i=1,2, . . .,n, and the given c. The RSS is given by:

$$RSS(c, \hat{\Gamma}_m) = \sum\limits_{i=1}^{n} w_i\, (Y_i - \hat{Y}_i)^2 = \sum\limits_{i=1}^{n} w_i\, R_i^2$$ VI.29

where residuals $R_i = Y_i - \hat{Y}_i$ are calculated using Equation VI.34 given below. The variance of Y_i is given by Equation VI.25, and setting this equal to σ^2/w_i (Draper and Smith, 1981) gives:

$$w_i = \frac{\sigma^2}{h\, Y_i^Q}.$$ VI.30

Therefore:

$$RSS(\hat{c}, \hat{\Gamma}_m) = \sum\limits_{i=1}^{n} w_i\, (Y_i - \hat{Y}_i)^2$$ VI.31

The residuals are calculated as the difference between Y_i and $\hat{Y}_i$ where $\hat{Y}_i$ is the value for Y predicted using the estimated values of Γ_m and c, denoted by $\hat{\Gamma}_m$ and $\hat{c}$. The positive root to the quadratic equation:

$$Y_i^2 + (\hat{c}\, Z_i - X_i\, \hat{\Gamma}_m\, \hat{c} - 1)\, Y_i - \hat{c}\, Z_i \approx 0$$ VI.33

gives the predicted value for Y, $\hat{Y}_i$, of Equation VI.17, as:

$$\hat{Y}_i = \frac{1}{2}\left[\hat{c}\hat{\Gamma}_m X_i - \hat{c}Z_i + 1 + \sqrt{\hat{c}^2 Z_i^2 - 2\hat{c}^2\hat{\Gamma}_m X_i Z_i + 2\hat{c}\hat{\Gamma}_m X_i + 2\hat{c}Z_i + (\hat{c}\hat{\Gamma}_m X_i)^2 + 1} \right]$$

VI.34

2. The B.E.T. Equation

Data analysis for the B.E.T. equation was similar to the Langmuir equation except that solving for $\hat{Y}_i$ resulted in a cubic expression that was evaluated as described by Abramowitz and Stegun (1972). In the case of the vapor sorption data the determinant was negative, implying three real roots. The first root was the desired solution, the second root being negative and the third less than 1.0.

Like the Langmuir equation, the B.E.T. equation is linear in the parameter Γ_m. A similar numerical analysis was therefore applied. A value for c was chosen and weighted linear regression (the left-hand portion of Equation VI.28) was used to solve for Γ_m. The regression equation resulting from (VI.19) was

$$T_i = X_i \Gamma_m + \delta_i \quad \text{for } i=1, 2, 3, \ldots, n \qquad \text{VI.35}$$

where δ_i is a random error term and T_i is defined as:

$$T_i = g(Y_i) = (1/c)(Y_i + a_1 + a_2 Y_i^{-1} + a_3 Y_i^{-2}) \quad \text{for } i=1, 2, 3, \ldots, n \qquad \text{VI.36}$$

where

$$a_1 = (c - 2)Z_i - 1, \qquad \text{VI.37}$$

$$a_2 = -(c - 2)Z_i - (c - 1)Z_i^2, \qquad \text{VI.38}$$

$$a_3 = (c - 1)Z_i^2, \qquad \text{VI.39}$$

This is obtained from Equation VI.19 by moving all terms involving Y_i to the left-hand side while keeping all occurrences of X_i and Γ_m on the right-hand side. As with the Langmuir equation, we assume that the n observations are independent and that the random error term δ_i has a normal distribution with mean zero and variance given by:

$$\text{Var} (T_i) \approx \text{Var}\{(1/c)[Y_i + a_1 + a_2 Y_i^{-1} + a_3 Y_i^{-2}]\}. \qquad \text{VI.40}$$

The analysis proceeds as before to estimate the variance of T_i from the variance of Y_i using a first-order Taylor series approximation:

$$\text{Var}(T_i) = g_i \, bY_i^Q \qquad\qquad\qquad \text{VI.41}$$

where:

$$g_i = \frac{1}{c^2} \left[1 - a_2 \, Y_i^{-2} - 2a_3 \, Y_i^{-3} \right]^2. \qquad\qquad \text{VI.42}$$

Equations VI.41 and VI.42 are used to calculate the weights for the regression model for the B.E.T. Equation (VI.35) using an equation similar to VI.19.

The same method is used to calculate the residual sum of squares, including the same weights as in the case of the Langmuir equation. The RSS minimizing value of c was likewise found by golden section. Once predictions of Γ_m and c were obtained, $\hat{Y}_i$ was the solution of:

$$\hat{Y}_i^{\,3} + a_1 \hat{Y}_i^{\,2} + a_2 \hat{Y}_i + a_3 = 0 \quad \text{for } i=1, 2, \ldots, n. \qquad \text{VI.43}$$

The fitting of both the Langmuir and the B.E.T. isotherms was done in FORTRAN on the Cornell IBM 4381 mainframe computer.

3. Results

Several approaches to data analysis were compared for 25 synthetic data sets for the linear and Langmuir isotherms generated with the SAS statistical computing program. Synthetic data allowed parameter estimates obtained in each analysis to be compared to the exact or "true" values. A value of one was chosen for the slope of the linear model and a value of eleven for the parameter c in the Langmuir model with Γ_m equal to one eleventh. Sample mass, assumed to be assigned without error, was allowed to have seven values ranging from five to thirty-five. Two replicates were used at each level of mass. Given the mass, the corresponding value of Φ was calculated for each of two models, the linear and the Langmuir. Φ_B was set equal to one. Two kinds of error structures were assumed: a) error of constant magnitude and b) constant percentage error. Error of constant magnitude was modelled by adding to Φ_i a random variable with mean equal to zero and $\sigma = 0.0005$. Constant percentage error was incorporated by multiplying Φ_i by a random variable with mean equal to one and $\sigma = 0.03$. For the linear model, two forms of linearization were compared for each error structure, Equations VI.9 and VI.13. The Langmuir model was fit to the synthetic Langmuir data by two linearizations, Equations (VI.3) and (VI.4), by

nonlinear regression on Equation VI.1, and by the Golden Section numerical approach on Equation VI.17. Weighting was used in all cases as the reciprocal of the variance given in Equation VI.23. Parameterization methods were compared using the computed sum of squared normalized differences between the true values and the estimates. Methods were tested for systematic bias with frequency diagrams (Figures VI.1-VI.8).
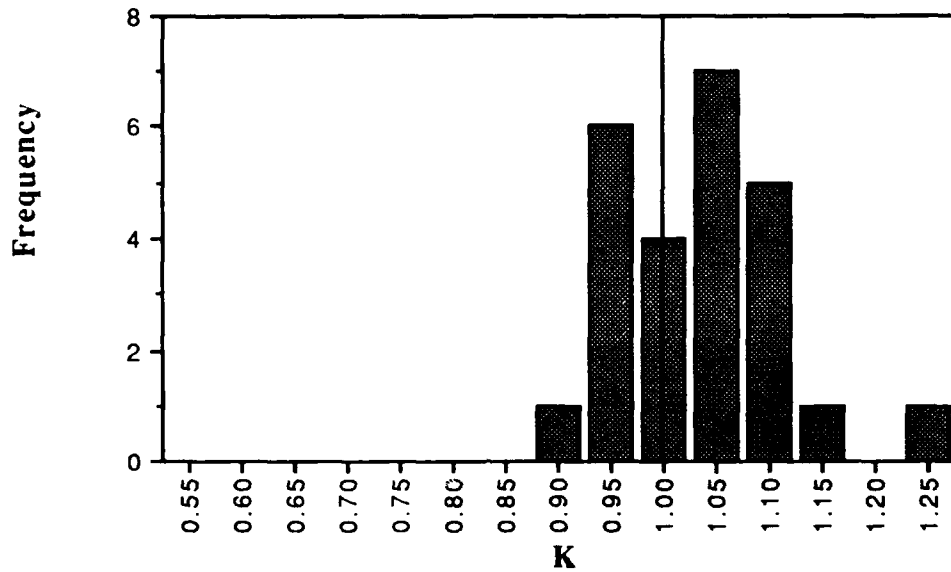
Figure VI.1.   Frequency Distribution using Equation VI.9 on Data with Relative Error.
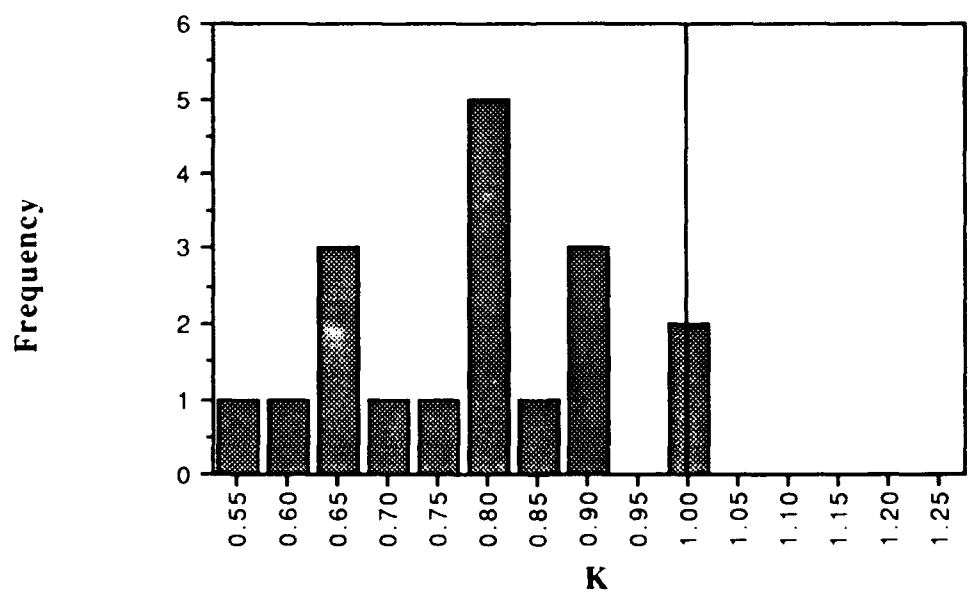
Figure VI.2.   Frequency Distribution using Equation VI.9 on Data with Absolute Error.
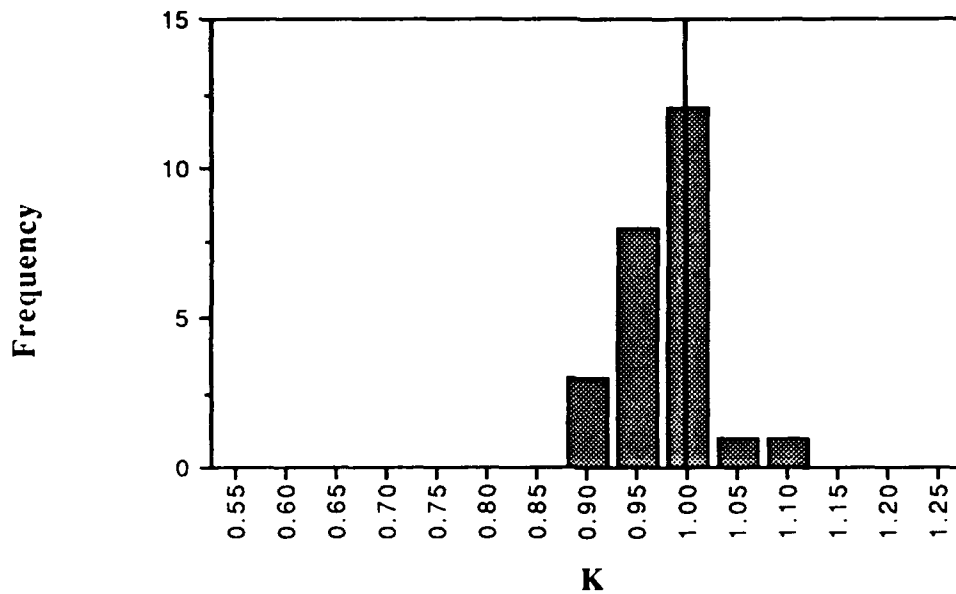
Figure VI.3. Frequency Distribution for K using Equation VI.13 on Data with Relative Error.
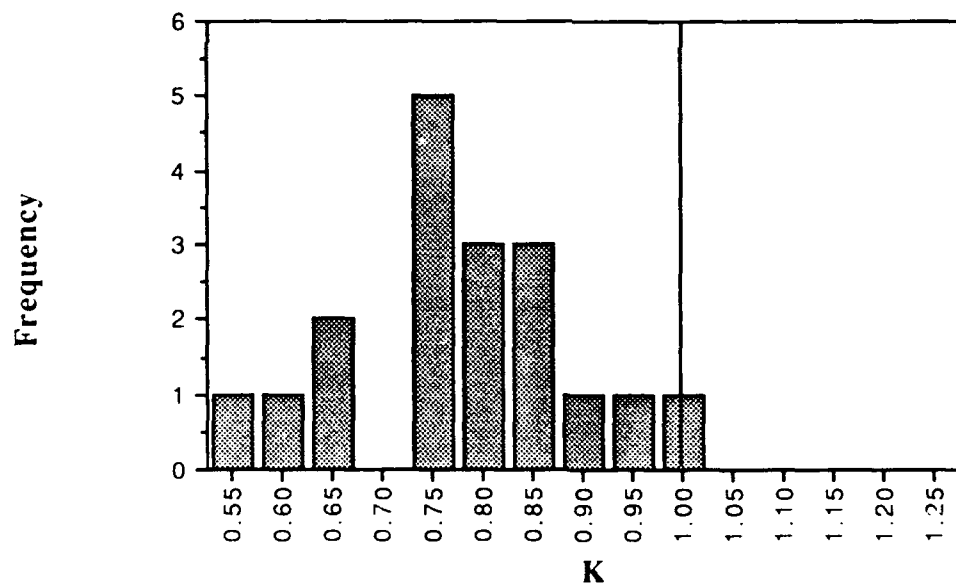
Figure VI.4. Frequency Distribution for K using Equation VI.13 on Data with Absolute Error.

155
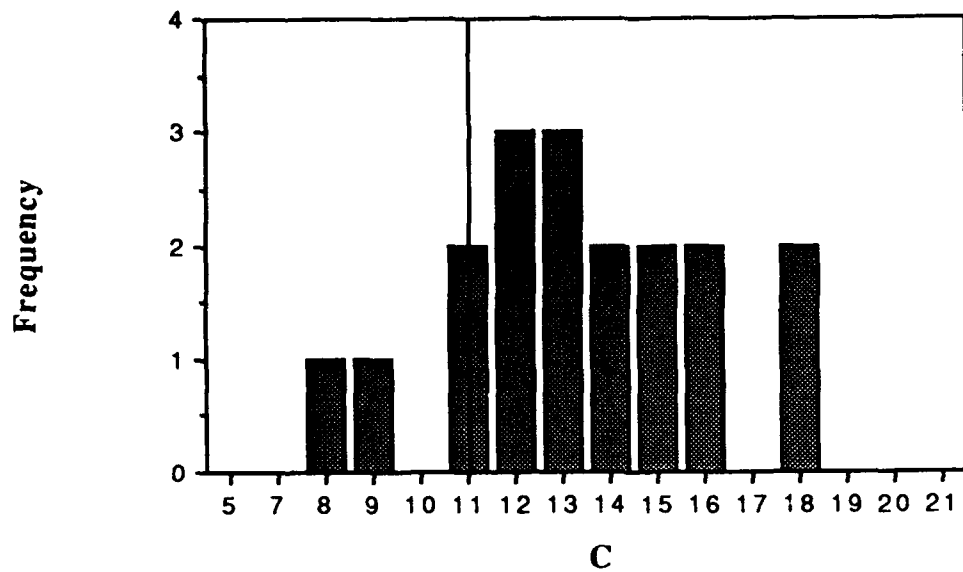
FigureVI.5. Frequency Distribution for c using Equation VI.3 on Data with Relative Error.
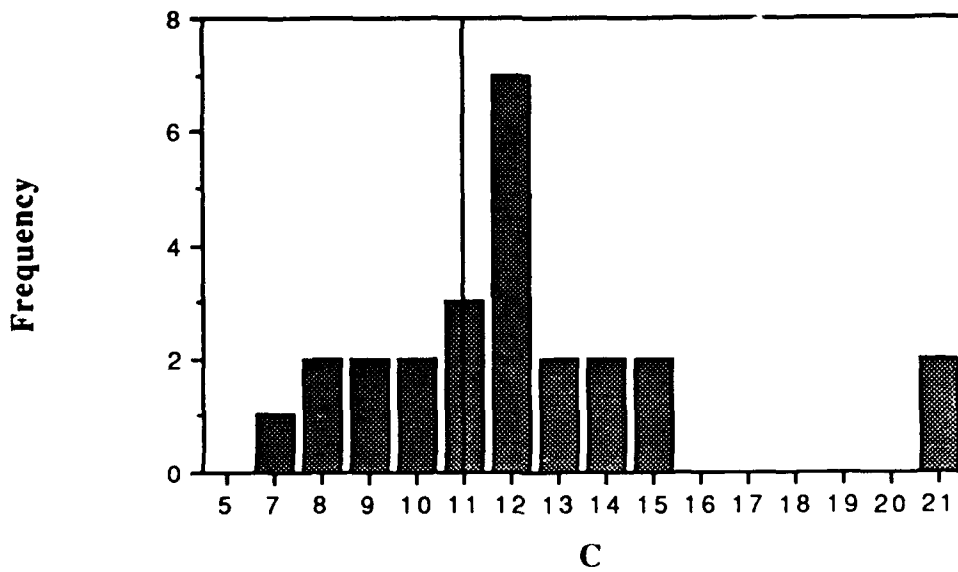
Figure VI.6. Frequency Distribution for c using Equation VI.3 on Data with Absolute Error.
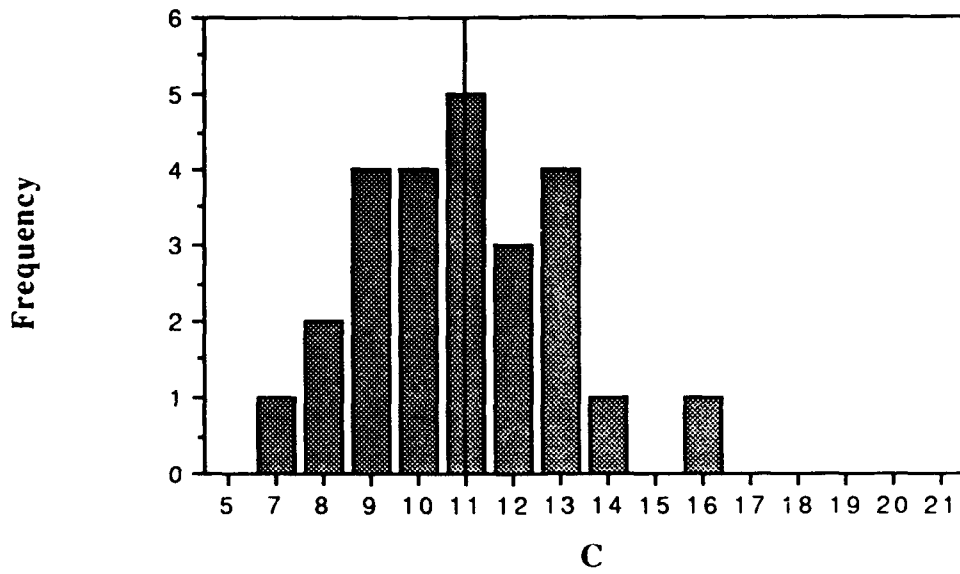
Figure VI.7. Frequency Distribution for c using Equation VI.17 on Data with Relative Error.
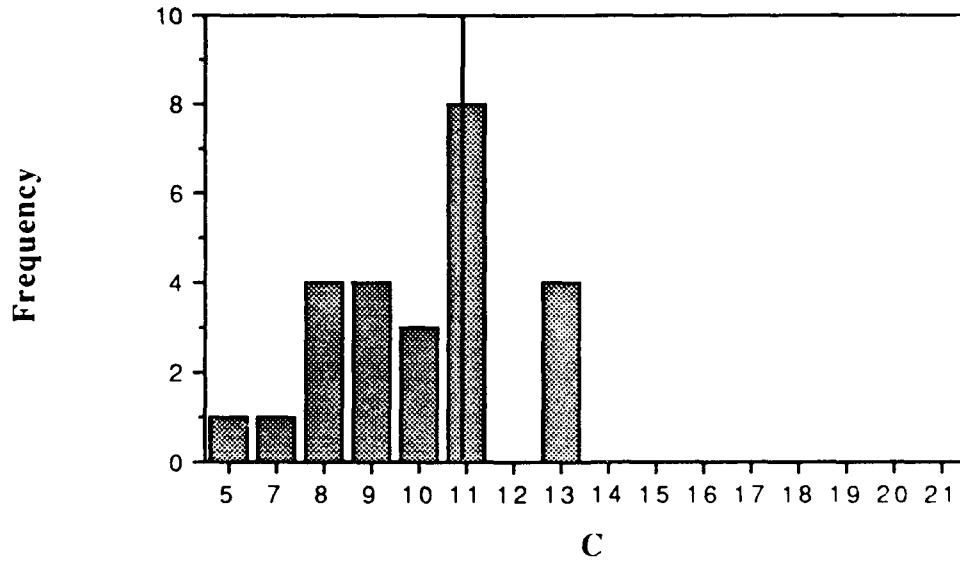
Figure VI.8. Frequency Distribution for c using Equation VI.17 on Data with Absolute Error.

157

Results of the data analysis comparison study are shown in Table VI.1. For both the constant magnitude and constant percentage error synthetic data sets, Equation VI.13, on the average, gave better estimates than Equation VI.9, although for the constant magnitude error the two methods performed virtually identically (due to the weighting). Equation VI.3 outperformed the method of nonlinear regression on Equation VI.1. The method of Golden Section was superior to both nonlinear regression and linearization by Equation VI.3. As found by Dowd and Riggs (1964), Equation VI.3 did better than Equation VI.4. The frequency diagrams illustrate that data with constant magnitude error tends to lead to underprediction of the slope of the linear equation. Considerably less bias was observed in the estimate of parameters from data with constant percentage error. Equation VI.3 for the Langmuir isotherm tended to overestimate the value of the parameter c as opposed to Golden Section which was more likely to underestimate it. Results for Γ_m, not shown, were negatively correlated with c. [Also not shown are the frequency diagrams for nonlinear regression (Equation VI.1) and linearization of the Langmuir equation by Equation VI.4 because both methods gave inferior results to those which are shown.] The methods for fitting the B.E.T. equation could be compared in a similar manner. Since there is no reason to believe that there would be a difference, this comparison is not provided here. In conclusion, the methods advocated in this work are proven for their ability to estimate parameters of synthetic data sets. Experimental data (see below) show that, for the Langmuir and B.E.T. equations, Golden Section was the most practical approach.

TABLE VI.1 SUMS OF SQUARED NORMALIZED ERRORS IN PREDICTIONS

	Constant Magnitude error	Constant percentage error
Linear Eqn (VI.9)	1.13	0.17
Linear Eqn. (VI.13)	1.11	0.064
Langmuir Eqn.(VI.3)	1.89	2.84
Langmuir Eqn.(VI.4)	28900	47.9
Nonlinear Regression Eqn. (VI.1)	4040	123
Golden Section Eqn. (VI.17)	1.14	1.80

D. MATERIALS AND METHODS

Six organic vapors were chosen to represent two classes of volatile pollutants found in aquifers: chlorohydrocarbon solvents and degreasers, and fuel hydrocarbons. Sorption of each vapor was followed in a separate experiment. The experimental compounds included chloroform (CF), methylene chloride (DCM), and 1,1,1-trichloroethane (1,1,1-TCA) from Fischer Scientific Co. perchloroethylene (PCE) and 1,1-dichloroethylene (1,1-DCE) from Aldrich Chemical Co. and toluene from Malinkrodt Chemical Co. All compounds were certified reagent grade.

Chromatographic adsorption alumina, 80-200 mesh size, (Fischer Scientific) was chosen for use as a sorbent because of its large surface area, well-characterized particle size distribution, and known chemical composition (Table VI.2). In some experiments the alumina was coated with humic acid (Aldrich Chemical Co.) using the procedure of Garbarini and Lion (1985). The purpose of the humic acid coating was to provide a surrogate organic phase for natural soil organic matter. Specific surface area was measured by B.E.T. nitrogen adsorption. Particle density was measured by the pycnometer method (ASTM, 1958). Pore size distributions were obtained by mercury porisimetry and from the nitrogen desorption curve (Lowell and Shields, 1984). Carbon content was determined by wet combustion with $Cr_2O_7^{-2}$ (Allison, 1960).

TABLE VI.2 PROPERTIES OF SOLIDS INVESTIGATED

Property	humic acid coated alumina	uncoated alumina
N_2 surface area (m²/g)	189.3	143.2
mean pore size, N_2 (Å)	20	20-30
organic carbon (percent)	0.45	0.02
particle density (g/cm³)	2.57	2.98

In the headspace analysis technique, used here and by Peterson et al. (1988), the sorbent is exposed to a controlled amount of sorbate vapor in a vial until equilibrium is established. The equilibrated vapor in the headspace was analyzed by gas chromatography (Hewlett Packard Model 5890) using a flame ionization detector. The column was 100/180 mesh Supelcoport® coated with 20 percent SP-2100 and 0.1 percent Carbowax 1500. The signal areas obtained were compared to the average signal area measured for the controls (no sorbent). Masses of sorbent in the vials, in the experiments on dry alumina, were varied at five levels of three replicates each ranging typically between 0.05 and 1.0 grams.

Vapors were transferred to and from the vials with valved gas-tight syringes (Precision Sampling). One mL of saturated (25°C) vapor was used for all vapors except PCE (2.0 mL) and p-xylene (5.0 mL). The source for vapor was a 150 mL vessel containing roughly ten mL of liquid product in equilibrium with the airspace. Here as in the sample vessel, seal was provided by Teflon®-backed rubber septa (Supelco Chromatography Supply) with tear-away aluminum crimp seals. Five source bottles were used in rotation to ensure a constant source vapor concentration. In the experimental protocol, vapor was delivered to the open sample vessel with the syringe needle placed deep within the bottle. Septum integrity was preserved by leaving the cap ajar during vapor delivery. Incubation

periods at 25°C ranged between 12 and 24 hours, sufficient to allow equilibration based on preliminary experiments.

The experiment on p-xylene employed seventy-seven replicates and was used to define the structure of the variance associated with Y_i. Coated alumina, used in this study, was moistened by mechanical incorporation of distilled water to a moisture content of roughly 20 percent. Masses of moist coated alumina varied by eight levels (0.25, 0.5, 1.0, 2.0, 3.0, 5.0, 8.0, and 10.0 grams). Each of the eight mass levels was replicated in seven blocks. To each block was added three controls to form a total of eleven replicates per block. The replicates in each block were randomized.

E. RESULTS AND DISCUSSION

1 . Variance Model and Weighting

Replication within the sorption experiment on p-xylene allowed the error associated with the measurement of Y to be examined. Differences in moisture content, an important variable (Chiou et. al., 1985 and Chiou et. al., 1988) occurred between the blocks (Table VI.3). Such differences were incorporated into the sorption model using the following relationship:

$$Y_i = X_i (b_1 G_i + b_2) K + \varepsilon_i \qquad \text{for } i=1,2, \ldots ,n \qquad \text{VI.44}$$

where G_i is the percent moisture content of sample i (g/g) and b_1 and b_2 are parameters and ε_i is the error of sample i. The average of the term in parentheses is equal to one. This relationship allowed K to be computed for any moisture content, within the range of those investigated, so that moisture content differences could be included in the analysis. For p-xylene this relationship was:

$$Y_i = X_i (0.0130 - 0.0005653 G_i) K \qquad R^2=0.92. \qquad \text{VI.45}$$

TABLE VI.3 RESULTS OF LEAST SIGNIFICANT DIFFERENCE (LSD) ANALYSIS

Grouping*				Mean	Block
A				20.96	1
	B			20.55	2
	B	C		20.46	3
	B	C		20.34	4
		C		20.13	5
			D	19.70	6
			E	19.18	7

*Mean moisture contents with the same letter are not significantly different at 95 percent.

The variance in Y is shown in Figure VI.9. The graph suggests that a log linear relationship of the form of Equation VI.25 may be used to describe the variance of Y. [Data points at log(Y) = 1 constitute blanks and are not well fit by the model.] The moisture content correction was used to adjust observed values of Y before fitting to Equation VI.25 (Figure VI.9). Incorporation of moisture content effects reduced the slope, Q, from 3.104 ± 0.111 to 2.621 ± 0.159 when all moisture contents were corrected to 20.4 percent. The variance structure observed in the p-xylene experiment was compared to that observed in the experiments on the six organic vapors where Q was 2.621 ± 0.159 (see Figure VI.9.) Because values of Q were the same at the 95 percent confidence level, it was concluded that a single value of Q could be used throughout. Thus for all data analysis a value of $Q=2.687\pm0.017$ was used. This value was based on a compilation of eight experiments, (including the p-xylene data) including a total of 57 groups of three or more replicates of the level of sample mass. The relationship explained over 92 percent of the variation in the variance. It is assumed that this exponential relationship is adequate to explain the variance for the purpose of data weighting in regression. Experiments in the variance study included those on coated as well as uncoated alumina, dry as well as moist samples, chlorohydrocarbons as well as hydrocarbons. The relationship, which employs a single power constant Q and the variance of the controls, can be used for all experiments regardless of whether there were replicates. It states that variance increases rapidly from the value observed for the controls as larger sample masses drive the vapor concentration down and the signal area ratio up.

The relationship of Equation VI.25 was also used to fit the linear, Langmuir and B.E.T. isotherms to the sorption on dry adsorption alumina. An example of these results is shown for toluene in Figure VI.10.
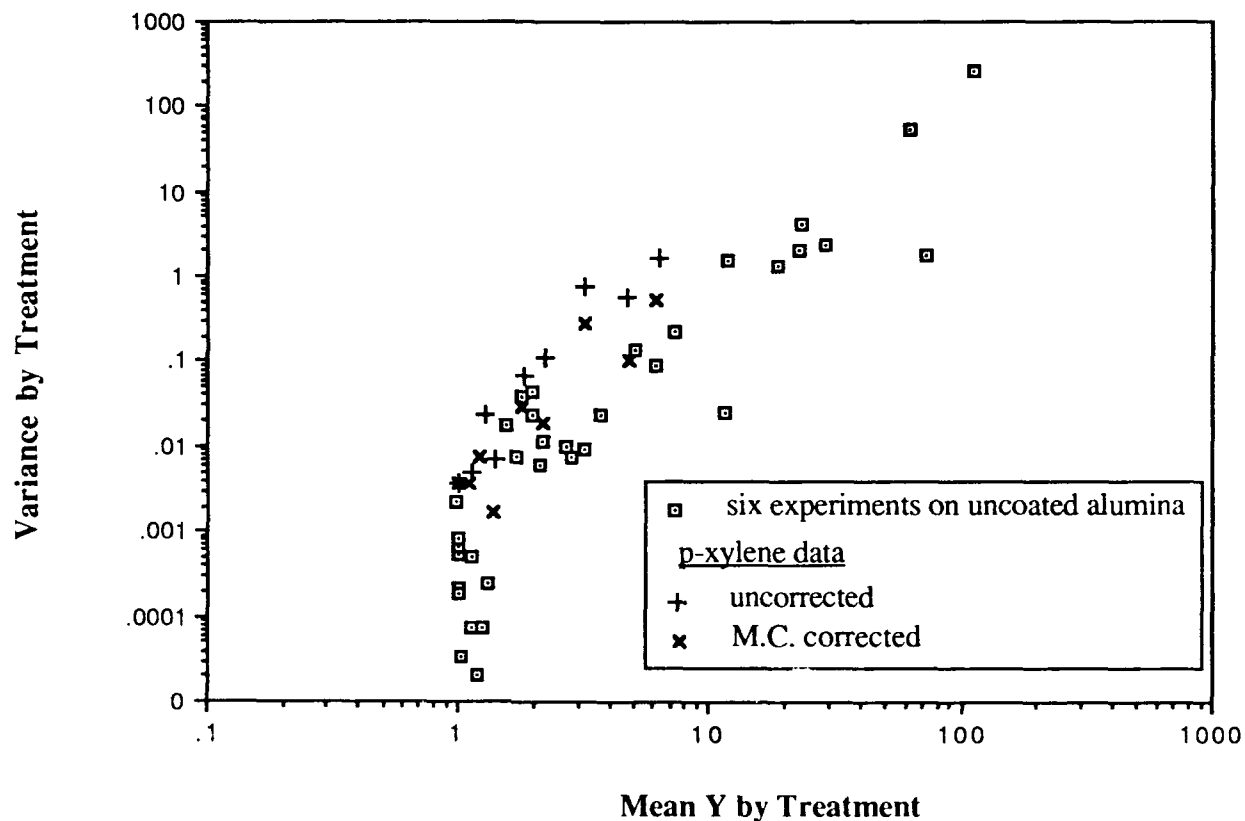
Figure VI.9. Data Used to Fit Equation VI.25, the Variance Model Used for Weighting Laboratory Data.

[Shown are the variances observed for each treatment in six experiments on dry alumina. The dry alumina data is compared to data for p-xylene sorption on coated alumina at 20.4 percent moisture content. The p-xylene data lies on top of the combined data for the dry alumina. After a moisture content correction, the p-xylene data are compatible with the other data.]

162
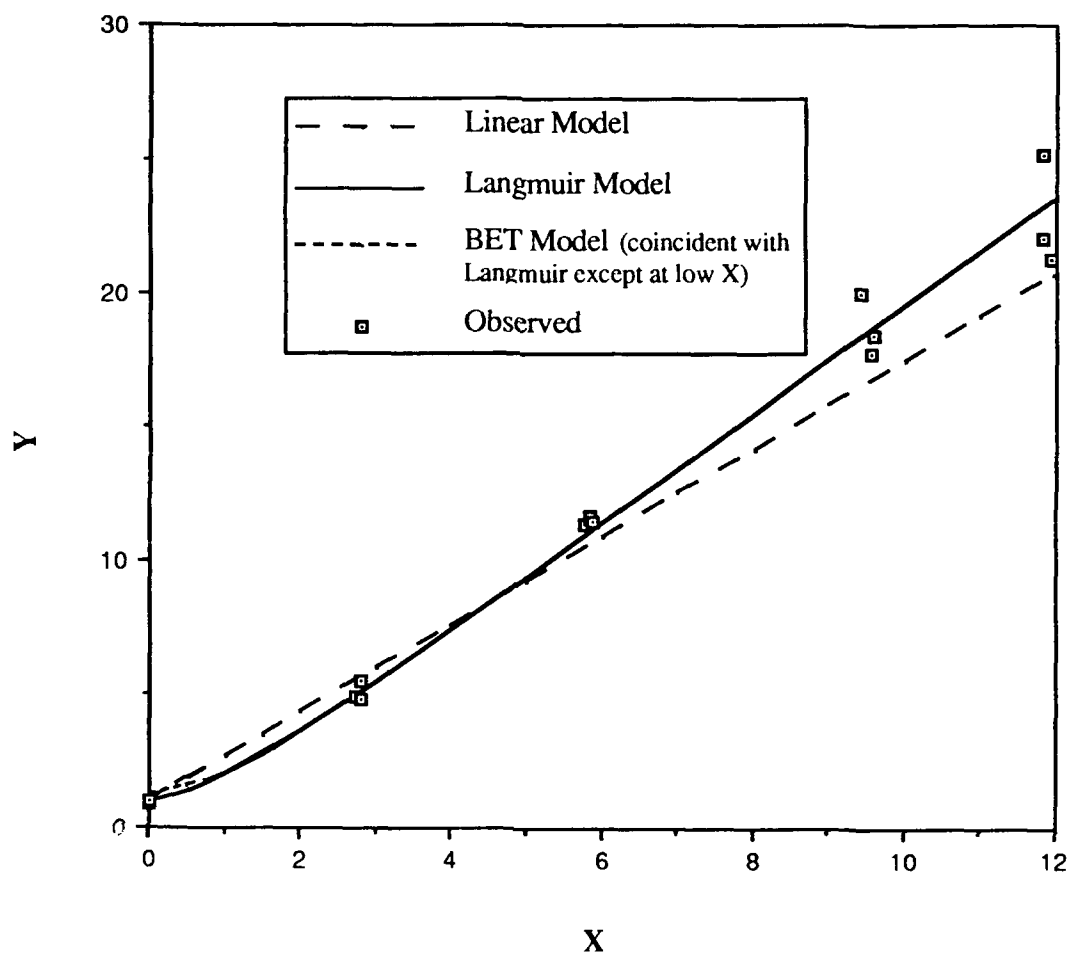
Figure VI.10. Typical data Showing the fit of the Langmuir and B.E.T. Models for Adsorption of Toluene on dry Alumina.

2. Vapor Sorption onto Dry Alumina: Model Comparison Study

Sorption isotherms measured by the headspace technique for chloroform, 1,1-dichloroethylene, methylene chloride, perchloroethylene, 1,1,1-trichloroethane, and toluene were fitted to the three models (linear, Equation VI.13; Langmuir, Equation VI.17; and B.E.T., Equation VI.19) as described under theoretical considerations. Values obtained for the fitted parameters and the correlation coefficients are provided (Table VI.4). This work focussed on the statistical analysis of nonlinear isotherms for adsorption concentration data using the Langmuir and B.E.T. models as examples. Because both these nonlinear models both have the same number of adjustable parameters, the weighted residual sums of squares provided sufficient basis for comparison.

163

TABLE VI.4   FITTED PARAMETERS FOR THE LINEAR, LANGMUIR, AND B.E.T.
ISOTHERMS ON DRY ADSORPTION ALUMINA

	Linear		Langmuir			B.E.T.		
Vapor	K'_d	r^2	c	Γ_m (mg/g)	r^2	c	Γ_m (mg/g)	r^2
CF	2925	0.874	276.4	12.06	0.98	282.0	11.86	0.99
1,1-DCE	120.1	0.955	137.0	1.90	0.99	142.7	1.84	0.99
DCM	208.5	0.885	387.7	4.78	0.94	385.1	4.77	0.94
PCE	1158	0.871	149.9	19.74	0.97	156.5	19.13	0.98
1,1,1-TCA	711.3	0.935	140.1	9.93	0.98	144.4	9.67	0.98
toluene	11670	0.978	122.8	118.5	1.00	125.2	116.2	1.00
TCE	1040	0.998	57.7	19.73	1.00	60.46	18.86	1.00

Equivalent fits were obtained with the Langmuir and B.E.T. equations for the range of vapor concentrations investigated. Figure VI.10 illustrates typical results. Similar values of the parameters Γ_m and c were predicted by the Langmuir and B.E.T. models. Neither the Langmuir equation nor the B.E.T. equation proved better at fitting the sorption isotherms for dry adsorption alumina for the six compounds investigated. Likely this is due to the fact that the influence of multilayer sorption was negligible at the vapor concentrations used.

Although the B.E.T. model, despite its increased complexity, did not outperform the Langmuir, based on r^2 the two nonlinear models fitted better than the linear case (Table VI.4). The parameter Γ_m was lower than predicted for TCE in Section IV. The value of c was correspondingly higher than that given in Section IV for TCE. The difference in the values could be explained by the existence of a small number of high affinity sites in the low P/P_0 portion of the isotherm which is the region accessible to the bottle experiments described here. Based on the surface area of the alumina and assuming an approximate molecular surface area of 30Å, the value of Γ_m should be about 100 mg/g. Most values for Γ_m in Table VI.4 are about 20 percent of this maximum value.

Unrealistic estimates were obtained of the parameters c and Γ_m when nonlinear regression or linearization by Equation VI.3 was applied. Golden Section is a more robust nonlinear regression technique because small perturbations in the data are less likely to misdirect the numerical minimization algorithm. Since the effects of each parameter on the RSS can be separated more effectively by Golden Section, many of the disadvantages of nonlinear regression are eliminated (eg. colinearity in the coefficient matrix used to estimate the parameters). When adsorption is measured indirectly through concentration differences,

the method proposed here will provide better estimates of the fitting parameters than nonlinear regression.

F. SUMMARY AND CONCLUSIONS

Fitting adsorption data to adsorption isotherms allows hypotheses about the nature of the adsorption process to be tested. When the extent of sorption is inferred from the concentration difference before and after the sorption process, isotherm fitting approaches must reflect the pattern of error expected in this type of data. Errors may be large, especially when the concentration difference observed, as well as the mass of sorbent, are small.

The Golden Section approach provides a method of using weighted least squares to incorporate the pattern of errors commonly observed for adsorption measurements made by concentration difference. Instead of a difference as the response variable (Equation VI.11), a ratio Y (Equation VI.12) is used to compare the concentration after adsorption to a reference concentration, representing what was present initially before adsorption. Nonlinear equations for the Langmuir and B.E.T. isotherms were fitted to the data using a weighted nonlinear numerical optimization procedure. Weights, based on an exponential model for the variance, were derived from a separate experiment. The same values for the two parameters, Γ_m and c, were predicted for both the Langmuir and B.E.T. isotherms. This result is expected for data in the low vapor concentration range which was examined here.

Current nonlinear regression practices for fitting the parameters of complex adsorption isotherms are questioned for the data in the low concentration range of the isotherm. When data in the linear, or near linear range is measured by concentration level difference, the linear isotherm (Equation VI.13) was better suited for regression analysis because concentration became the regressor. Likewise this approach allows the variable known with the least error, sorbent mass, to function as the predictor. Overall, slightly better parameter estimates were obtained with Equation VI.13 than Equation VI.9.

Since nonlinear regression was hampered by correlation between the parameters, the Golden Section method was superior for parametrizing isotherms to experimental data. Golden Section did the best job at parametrizing a synthetic data set compared to linearized Equation VI.3 and nonlinear regression (Equation VI.1). Weighting the data allowed the fitted curves and parameters obtained to reflect what is known about the level of certainty at each data point. Weighting improved the consistency of predictions by each method by correcting for the effect of transformations on the Y values. Weighting was unable,

however, to control for the errors which occur in the predictor variables X, which explains why linearizations of the Langmuir equation (Equation VI.3) and nonlinear regression on Equation VI.1 did not perform as well as the Golden Section method. The agreement between the Langmuir and the B.E.T. isotherm fits for these data also supports the validity of the Golden Section regression method.

G. FINAL COMMENTS

Two choices confront the researcher preparing to analyze adsorption data: 1) whether to use a linear or nonlinear (eg, Langmuir, B.E.T., etc.) isotherm; and 2) once a particular model is chosen, deciding which form of the model equation to use. Both of these issues have been addressed by Kinniburgh (1986) for the case of adsorption data collected at a fixed sorbate concentration. Kinniburgh, however, discussed cases where the amount adsorbed per gram is measured directly rather than calculated from the observed adsorbate concentration difference, as is often the case.

For the first issue, ie. that of whether to fit a one or two parameter model, Kinniburgh (1986) suggested the following equation to test whether or not to remove a parameter from the model. This equation applies to comparisons between concentric models, ie. where the model with fewer parameters is a limiting case of the model with more parameters.

$$F(p_2 - p_1, m - p_2) = \frac{(RSS_1 - RSS_2) / (p_2 - p_1)}{RSS_2 / (m - p_2)} \qquad \text{VI.46}$$

where $F(p_2 - p_1, m - p_2)$ is the F statistic with $(p_2 - p_1, m - p_2)$ degrees of freedom,

p_1 =   the number of parameters in the limiting model, ie. $p_1 = 1$ for the linear isotherm,

p_2 =   the number of parameters in the more complex model, ie. $p_2 = 2$ for the Langmuir model,

m =   the number of data points or observations taken,

RSS_1 =   the residual sum of squares of the limiting model, and

RSS_2 =   the residual sum of squares of the more complex model.

For the second issue (which is the focus of the discussion in this section), Kinniburgh (1986) showed that all forms of the Langmuir isotherm equation resulted in essentially the same values for the parameter estimates, when weighted linear regression was used (provided the weights were assigned correctly). Kinniburgh (1986) gives proper weights for a variety of different isotherms, including the Langmuir and B.E.T. isotherms. Many

adsorption isotherms, however, such as the Redlich-Peterson isotherm, are more complex than the Langmuir or B.E.T. isotherms. For the complex isotherms, involving more than two fitting parameters, Kinniburgh advocated using nonlinear regression.

The weights given by Kinniburgh, unfortunately, are not always sufficient for analysis of the adsorption data where the amount of adsorption is inferred from adsorbate concentration difference. This was the case in the headspace analysis technique in this study. Data collected by the headspace analysis technique, or other techniques where adsorbate concentration difference is measured, produce errors associated with both the predictor variable (adsorbate concentration) and the regressor variable (amount of adsorption). The weighting approach advocated by Kinniburgh accounts only for errors in the response variable. When adsorption is measured by concentration difference, it is therefore necessary to express the equations for the Langmuir and B.E.T. isotherms in a form where the standard weighting equations used by Kinniburgh are valid. Since the variables were not separated in the resulting equations, a Golden Section search routine was employed for their solution. Analysis of synthetic data (Table VI.1) demonstrated that the weights suggested by Kinniburgh performed poorly for Equation VI.1 and Equation VI.4. Therefore, it is suggested that the Langmuir equation be linearized by Equation VI.3 or that the golden section approach be used on Equation VI.17. Additionally, for fitting linear data, it is suggested that Equation VI.13 be used rather than Equation VI.9. Figures VI.1-VI.8 compare parameters estimates by several of the best approaches. The data analysis methods presented here are used to aid in the comparison of the sorption of different vapors both as individual compounds and as mixtures in Sections VII and VIII.

SECTION VII

PREDICTION OF VAPOR SORPTION PARTITIONING PARAMETERS FOR VOLATILE ORGANIC COMPOUNDS: A REGRESSION APPROACH

By: S.R. Lindner and L.W. Lion

A. OVERVIEW

The tendency of volatile organic compounds (VOCs) to partition between the vapor phase and a surrogate soil system, consisting of moisture, organic matter, and a hydrophilic aluminum oxide surface, has been investigated for 15 components of fuels and solvents. Sorption partition coefficients obtained in the analysis have been related to four sorbate properties: vapor pressure, VP, solubility, S, Henry's law constant, H_c, and the logarithm of the octanol water partition coefficient, $\log K_{ow}$. In addition, properties calculated from molecular configuration such as the first-order molecular connectivity index, $^1\chi$, and the polarizability index of Nirmalakhandan and Speece (1988), $\overline{\Phi}$, were employed in the analysis. Regression equations show a change in vapor property dependencies as the moisture content of aluminum oxide is increased from oven dry to 1.9 percent. Sorption of different vapors on moist coated alumina was well described by the logarithm of the aqueous solubility and Henry's law constant. On the moist solid, compounds with high solubility and low Henry's law constants sorbed to a greater extent than those with low solubility and high Henry's law constants.

B. BACKGROUND

Creation and use of organic compounds in modern society has been called man's boldest experiment. As a result of this activity, organic chemicals are increasingly detected in groundwater aquifers as they leak from improperly designed landfills and faulty underground storage tanks. Many of these compounds are volatile, yet because they are often not near the soil/atmosphere interface, there is little potential for them to escape into the atmosphere other than by diffusing to the surface.

Plumb and Pitchford (1985) found a vast diversity of volatile hydrocarbons and chlorinated hydrocarbons in a survey of over 500 hazardous waste sites. Due to the sheer numbers of hydrocarbon and chlorinated hydrocarbon species found at such sites, there is a need to correlate sorptive behavior with readily available chemical or structural properties. The attractiveness of the partitioning concept lies in its ability to generalize to many different congeneric compounds and soils based on relatively few measurements. A broad

view of partitioning is taken in this section through the use of structure-activity relationships which are used to predict the behavior of diverse compounds.

Partitioning concepts based on log K_{ow}, the distribution coefficient between the concentration of the compound in water and the concentration of the compound in octanol, have met with great success in describing environmental partitioning processes (Karickhoff et al., 1979; Dzombak and Luthy, 1984; Briggs, 1981). A direct correlation has also been found between the sorptive partition coefficient, K_d, of soils normalized by the organic carbon content, f_{oc}, and K_{ow} (Karickhoff, 1981; Karickhoff et al., 1979; Abdul et al., 1987). This fact has been used to support the theory that organic chemicals partition into soil organic matter (Lambert et al., 1965; Chiou, 1981; Chiou et al., 1987). Predictions of sorptive partitioning based on K_{ow} provide order of magnitude estimates of sorption partition coefficients. However, caution must be exercised when applying K_{ow} relationships to sorption in low carbon soils because sorption may be influenced to a greater or lesser extent by mineral surfaces (Minglegrin and Gerstl, 1983; Stauffer et al., 1989). Even if partitioning into organic matter is the predominant sorptive mechanism, differences in the sorption by different types of soil organic matter will be expected to occur (Garbarini and Lion, 1986; Gauthier et al., 1987). Nevertheless, use of K_{ow}- K_d/f_{oc} relationships provides a good prediction for partitioning of different nonionic compounds for saturated soils with organic matter contents greater than 0.1 percent (Schwarzenbach and Westall, 1981).

Vapor partitioning, that is the distribution of organic pollutants between the vapor phase and soil, is complicated by its dependence on moisture content. Under dry conditions, sorbent surface area (versus organic content) is likely to be a major parameter which influences partitioning (see Section III). Under wet conditions dissolution of vapors into soil moisture may play an important role in vapor partitioning (see Section III). In addition to uncertainties with regard to the sorbent, the dependencies of vapor partitioning on sorbate properties have not been evaluated. For sorption of vapors there is presently no relationship comparable to that of K_d with K_{ow} in saturated soils.

Equilibrium distribution of compounds between several phases occurs when the fugacities, or escaping tendencies, of the compound in each phase are equal (Atkins, 1978; Mackay, 1979; Mackay and Paterson, 1982). The ability of a phase to accumulate a sizable amount of a pollutant compound is expressed by its fugacity capacity (Mackay, 1979). In this section we are concerned with how the fugacity capacity, or "binding" is influenced by the properties of VOCs. It is the differences in the fugacity capacities of the phases for the various VOCs that will account for differences in the observed distribution coefficients for a series of volatile organic compounds.

The observations of many investigators (Karickhoff et al., 1979; Rao and Davidson, 1980; Schwarzenbach and Westall, 1981; Chiou et al., 1979, 1987; Abdul et al., 1987) show the distribution of nonionic compounds from aqueous solution onto soils is strongly influenced by the organic content of the sorbent. Therefore, the distribution coefficient is related to the relative fugacity capacities, Q, of the aqueous and organic carbon fraction of the sorbent (Karickhoff, 1981; MacKay, 1979).

$$K_{OC} = \frac{Q_{OC}}{Q_S} = \frac{\gamma^S F_0^S}{\gamma^{OC} F_0^{OC}}$$

VII.1

where: Q_{OC} is the fugacity capacity of the organic carbon phase (inversely proportional to Karickhoff's (1981) fugacity coefficient),

Q_S is the fugacity capacity of the aqueous solution,

γ^S and γ^{OC} are activity coefficients for the pollutant compound in the aqueous and organic carbon phases, respectively, and

F_0^S and F_0^{OC} are reference fugacities at an arbitrary standard state.

Karickhoff (1981) and Rao et al. (1985) indicate that the most important difference between compounds in Equation VII.1 is through the diversity of interactions within the aqueous phase. The interactions of various hydrophobic organic compounds with the organic carbon phase are expected to vary relatively little between compounds (Karickhoff, 1981; Rao et al., 1985). Activity corrections are far more important in aqueous solutions of hydrophobic pollutants than they are when organic carbon is the solvent. The solute-solvent interactions for hydrophobic organic compounds in aqueous solution vary to a greater extent from compound to compound (ie. by several orders of magnitude) than do the solute-solvent interactions of hydrophobic organic compounds in organic matter solutions, such as represented by pollutant partitioning into soil organic matter (Karickhoff, 1981). Therefore the magnitude of the activity correction for the aqueous solution in Equation VII.1, is the principle factor that describes the influence of sorbate properties on sorption (ie., $K_{OC} \propto \gamma^S$). Since γ^S is inversely proportional to aqueous solubility (Karickhoff, 1981), the partition coefficients of hydrophobic organic pollutants from saturated solution are observed to increase as compound solubility decreases.

The argument for partitioning of organic vapors into unsaturated soils is similar in that differences between compounds are expected due to aqueous solution activity effects. In the case of partitioning into unsaturated soils, partitioning occurs between the vapor and a non-vapor phase, consisting for simplicity of soil moisture, organic carbon, and a soil mineral.

$$K = Q_{nv}/Q_v$$

VII.2

170

where: Q_{nv} is the fugacity coefficient in the non-vapor phase,

and Q_v is the fugacity coefficient in the vapor phase.

Because there are no activity corrections in the vapor phase, and, in addition, no major (>10x) differences in the fugacity capacity of organic matter for different compounds, the most important vapor property effects are likely to be found with regards to the aqueous solution phase (as before). In Equation VII.2 the aqueous solution effects occur in the numerator, which results in an expected direct correlation of K for vapor sorption with solubility, a trend reciprocal to that found in the case of sorption from solution. Since the fugacity capacity of an aqueous solution for a vapor is inversely related to its Henry's law constant (Mackay, 1979), an inverse correlation of vapor-phase partition coefficient with H_c is also expected. This discussion applies to sorption on moist soils. Upon drying, vapor sorption is influenced to a greater degree by the mineral surface and insufficient water will be available for the aqueous solution effects described above.

In this section a semi-empirical approach is employed to examine the sorption of a range of organic vapors. Observed partition coefficients are fitted to the vapor properties which are expected (based on theoretical considerations) to best describe sorption. The hypothesized dependencies presented above are tested by examining the statistical relationship between vapor properties and vapor partition coefficients.

C. MATERIALS AND METHODS

1. Volatile Organic Compounds

Fifteen volatile organic compounds were chosen for the study. They represent the two major classes of volatile pollutants found in aquifers: chlorinated hydrocarbon solvents and the hydrocarbon components of fuels. The basis for selection of compounds for this study was: (1) frequency of detection as groundwater pollutants, (2) to span a range of chemical properties and characteristics including Henry's law constant, solubility, vapor pressure, and structural indexes, and (3) to form homologous series where possible. The compounds selected included: trichloroethylene, 1,1,1-trichloroethane, chloroform, methylene chloride, decane, hexane, p-xylene, and toluene (from Fischer Scientific), octane, heptane, mesitylene, methylcyclohexane, and cyclohexane (from Fluka Chemical Corp.) and, perchloroethylene and 1,1-dichloroethylene (from Aldrich Chemical Co.). All compounds were reagent grade.

Chemical properties chosen for examination as predictors of sorptive behavior included: log K_{ow}, the polarizability index of Nirmalakhandan and Speece (1988, 1989) $\overline{\Phi}$,

Henry's law constant (dimensionless), vapor pressure (mm Hg), log solubility (mol/L), the first order molecular connectivity index $^1\chi$, and the valence connectivity index $^1\chi^v$. Chemical properties are listed in Table VII.1.

TABLE VII.1 CHEMICAL PROPERTIES OF SORBATES

vapor	log K_{ow} [1]	$\overline{\Phi}$[2]	H_c	V_p[3]	log S[3]	$^1\chi$[4]	$^1\chi^v$[2]
				mm Hg	mol/L		
perchloroethylene	2.60	-0.453	0.716[6]	18.6	-2.97	2.643	2.51
trichloroethylene	2.29	-0.368	0.397[6]	72.8[5]	-2.08	2.270	2.07
1,1-Dichloroethylene	2.63*	-0.319	1.050[6]	598	-2.38	1.732	1.64
1,1,1-trichloroethane	2.49	0.233	0.688[6]	124	-2.22	2.000	2.20
chloroform	1.97	-0.104	0.147[6]	192	-1.17	1.732	1.96
methylene chloride	1.25	-0.037	0.087[6]	438	-0.65	1.414	1.60
decane	5.12*	3.130	282[3]	1.31	-6.59	4.914	4.41
octane	4.03*	2.456	132[2]	14.1	-5.24	3.914	3.91
heptane	3.49*	2.119	83[2]	45.8	-4.57	3.414	3.41
hexane	2.97*	1.782	74[2]	151.5	-3.93	2.914	2.91
mesitylene	3.42	1.176	0.234[2]	2.46	-3.26	4.182	3.23
p-xylene	3.15	0.839	0.257[2]	8.78	-2.78	3.788	2.82
toluene	2.73	0.502	0.275[2]	28.5	-2.25	3.394	2.41
methylcyclohexane	2.88*	1.407	17.8[2]	46.4	-3.81	3.394	3.39
cyclohexane	2.35*	1.070	7.9[2]	95.3	-3.15	3.000	3.00

*Calculated from log S using relationships given by Chiou et al. (1982) for alkyl halides and alkanes.

$$\log K_{ow} = -0.819 \log S + 0.681 \qquad \text{(for alkyl halides)}$$
$$\log K_{ow} = -0.808 \log S - 0.201 \qquad \text{(for alkanes).}$$

[1] Hansch and Leo (1979); [2] Nirmalakhandan and Speece (1988); [3] Mackay and Shiu (1981); [4] Sabljic (1987); [5] Verschueren (1983); [6] Gossett (1985)

Polarizability and the molecular connectivity indexes are nonexperimental parameters calculated from molecular structure. The ability of $^1\chi$ to predict soil sorption characteristics (K_{om}) of polycyclic aromatic hydrocarbons (PAHs) and chlorinated hydrocarbons has been demonstrated by Sabljic (1984, 1987). The physical basis for the

strong predictive ability given by Sabljic was the correlation of $^1\chi$ with the molecular surface area, specifically the area occupied by the non-hydrogen skeleton of the molecule (Sabljic, 1984, 1987).

To the extent that vapor sorption occurs as a surface reaction, it is reasonable to expect that it is influenced by the surface area of both the sorbent and the sorbate. There is, however, some disagreement about the direction of the influence of the surface area of the sorbate because the direction of the effect will depend on the nature of the sorptive process. Sabljic (1984,1987) found that aqueous sorption of a series of organic compounds was positively correlated with $^1\chi$, which he attributed to the importance of van der Waals effects such as in the attraction between two charged plates. A direct relationship between hydrocarbon surface area and the saturated partition coefficient has also been noted by Dzombak and Luthy (1984) and Rao et al. (1985).

Minglegrin and Gerstl (1983) and Kyle (1981) also assert the importance of sorption at surfaces of minerals and surfaces of organic matter coatings. Physical adsorption onto solid surfaces may occur even under saturated conditions (Kyle, 1981) and may be described as inversely related to sorbate size by a modification of the Polanyi equation (Manes and Hofer, 1969) for adsorption from aqueous solution (Chiou and Reucroft, 1977). For physical adsorption of multiple layers of sorbate, the mass of sorbate adsorbed depends on both the affinity of the surface for the sorbate and the molar volume of the sorbate, the latter being directly related to surface area and $^1\chi$. Thus, wherever there is condensation into a liquid film or into pores an inverse relationship for sorption with $^1\chi$ is expected because of packing considerations.

Where the differential sorption of VOCs is controlled by dissolution into soil moisture, an inverse trend in $^1\chi$ is also expected. This is due to the observation that smaller molecules and molecules with more branching tend to be more soluble than large straight chain molecules (McAuliffe 1966). It is expected that the sorption mechanisms of physical adsorption, or condensation into pores will more likely predominate in the case of dry samples or those with a limited coverage (< 4 to 8 monolayers) by water. In the case of wetter samples, a negative trend in $^1\chi$ would be more readily explained by solubility effects.

Connectivity indexes are calculated from the identities of the atoms and their connections in the structural formula. Regression analysis is used to relate the values of the connectivity indexes to molecular properties. After a predictive relationship has been well established, connectivity indexes may be used as a surrogate to measured molecular

properties in subsequent regression analyses. As described by Kier and Hall (1986), the identities of the atoms and their connections make up what is called the topology of the molecule. For example, $^1\chi$, an extension of the Randic branching index in alkanes (Randic, 1975), is calculated from the molecular skeleton, or the molecular structure minus the hydrogen atoms (Kier and Hall, 1976). Adjacency values, or the number of non-hydrogen atoms adjacent to each of the two molecules connected by a bond, are used to calculate $^1\chi$. The final value is computed by summation of the product of the adjacency values taken to the -0.5 power or:

$$^1\chi = \Sigma(\delta_i\delta_j)^{-0.5} \hspace{3cm} \text{VII.3}$$

where: δ_i is the number of adjacent nonhydrogen atoms for the ith nonhydrogen atom of the pair,

and δ_j is the number of adjacent nonhydrogen atoms of the jth nonhydrogen atom.

Randic noted that in alkanes $^1\chi$ decreased in magnitude as the degree of branching increased. Kier and Hall (1986) demonstrated a positive correlation between molecular surface area and $^1\chi$.

In addition to the relative degree of branching and the molecular surface area, $^1\chi$ has been related to molar refraction, polarizability, water solubility, molar volume, chromatographic retention time, and various thermodynamic properties (Kier and Hall 1986). The usefulness of $^1\chi$ (Equation VII.3) is limited, however, in that it depends on the structure of the molecule solely, without respect to the specific ions involved. The valence molecular connectivity index, $^1\chi^V$, of Kier and Hall (1976, 1977), which can distinguish different types of atoms and double bonds, was included in the analysis described here. $^1\chi^V$ is calculated in a similar manner to equation VII.3 except δ_i and δ_j are replaced by δ_i^V and δ_j^V, the valence deltas. δ^V values are calculated as:

$$\delta^V = (Z^V - h) / (Z - Z^V - 1) \hspace{3cm} \text{VII.4}$$

where: Z^V is the number of valence electrons,

h is the number of hydrogens,

and Z is the atomic number of the atom.

Nirmalakhandan and Speece (1988) employed the "polarizability" index, $\overline{\Phi}$, as a predictor of vapor properties. $\overline{\Phi}$ is calculated using a model proposed by Ketelaar (Horvath 1982):

$$\overline{\Phi} = A(\# \text{ of H}) + B(\# \text{ of C}) + C(\# \text{ of Cl}) + \ldots + A_1(\# \text{ of double bonds}) \hspace{1cm} \text{VII.5}$$

174

The constants in Equation VII.5 were optimized by Nirmalakhandan and Speece (1988) so that $\overline{\Phi}$ and $^1\chi^v$ could, in combination, give the best predictive equation for H_c.

2. Solids

The solids chosen for the experiments (Table VII.2) were Fischer adsorption alumina and Fischer adsorption alumina that had been coated with Aldrich humic acid using the procedure of Garbarini and Lion (1985). The aluminum oxide represents a mineral surface with a well characterized surface area and pore size distribution. The purpose of the humic acid coating was to provide an organic phase as a surrogate for natural soil organic matter. Moisture content of the sorbents was established by measuring distilled water into oven-dried materials and mechanically mixing. The moist sorbent was allowed to equilibrate in a sealed container overnight to promote water distribution. In addition, moist samples were mixed frequently during sample bottle preparation.

TABLE VII.2 PROPERTIES OF SOLIDS INVESTIGATED

Property	coated alumina	uncoated alumina
B.E.T. N_2 surface area (m^2/gm)	189	143.2
mean pore size $(\text{Å})^*$	20	20-30
organic carbon (percent)[**]	0.45	<0.03
particle density $(gm/cm^3)^\dagger$	2.98	2.57

[*]from N_2 desorption curve
[**]wet combustion (Allison 1960)
[†]pycnometer method (ASTM, 1958)

3. Experimental Procedure

Vapor sorption was measured by the headspace analysis procedure described by Peterson et al. (1988). Briefly, a controlled amount of vapor sorbate is sealed with the sorbent, at a constant temperature, until equilibrium is established. The resulting equilibrium vapor concentration was analyzed by an HP 5890 gas chromatograph with a flame ionization detector (column: 20 percent SP2100, 0.1 percent Carbowax 1500 on 100/80 mesh Supelcoport). The signal areas obtained were compared to the average signal area measured for the controls (no sorbent). Equilibration periods, based on preliminary kinetic testing, ranged between 12 to 24 hours with the longer times used for the experiments on moist alumina. All experiments were performed at 25°C.

D. DATA AND ANALYSIS

1. Overview

Sorption of seven organic chemicals was tested on oven-dry alumina, and five solvent vapors were tested on alumina at 1.9 percent moisture content. In addition, sorption of nine fuel hydrocarbons and five chlorinated solvents was tested on coated alumina at average moisture contents ranging between 43 and 54 percent. Vapor sorption for moist solids was described by the linear adsorption partition coefficient (Tables VII.3 and VII.6) estimated by weighted linear regression (Section VI). Sorption onto oven-dry alumina did not obey a linear isotherm and was fitted to the Langmuir isotherm as described in Section VI. Partition coefficients were subsequently compared to vapor properties (Table VII.1). Statistical analysis was performed using SAS Version 5 using standard regression procedures.

a. Choice of Regressor Variable

The partition coefficient K has the same units as Γ and Γ_m, and is "dimensionless" if units for Γ are grams sorbed per grams sorbent. K may be calculated from K_d' by multiplying by the saturated vapor density in g/cm^3. Log K was used as a regressor rather than log K_d' because using a dimensionless parameter facilitated comparison of vapors. Log K was used instead of K for purposes of consistency since log K is commonly used for regression in saturated systems. Sorption isotherms for oven-dry alumina were nonlinear. Hence the logarithm of the product of the parameters Γ_m and c of the Langmuir isotherm was used as the regressor for the oven-dry experiments.

b. Weighting of Data

Weighting was applied based on the discussions of Kinniburgh (1986) and deLevie (1986) to account for the logarithmic transformation and the apparent structure of the variance. It was assumed, based on the observed widths of confidence intervals, that the values of K_d' for coated alumina at approximately 45 percent moisture content (Table VII.7) had constant magnitude error and values of K_d' for sorption onto dry or partially dry alumina (Table VII.3) had constant percentage error. The data at 45 percent moisture content were weighted by the partition coefficient K, in units of (g/g), to correct for the logarithmic transformation (Equations VI.23 and VI.27; see "Choice of Regressor Variable" above). No weighting was used for the dry and semi-dry data because transformation and variance weights cancelled.

c. Adjusted r^2

Adjusted r^2 (Equation VII.4) was used as a measure of the reduction in the mean square error due to multiple regression. This statistic, unlike r^2 which will equal one if enough parameters are included in a model, tends to stabilize to a value less than one when an adequate set of variables is chosen. Adjusted r^2 is calculated as:

$$\text{adjusted } r^2 = 1 - (1 - r^2)\left[(n - 1)/(n - m - 1)\right] \qquad \text{VII.4}$$

where: n is the number of observations in the data set, and

m is the number of regression parameters, excluding the intercept.

2. Linear Partition Coefficients for Dry and Partially Dry Alumina

Table VII.3 shows partition coefficients obtained for sorption of six chlorinated solvents and toluene on oven-dry alumina. Also shown are partition coefficients for five solvents on alumina at 1.9 percent moisture content (M.C.). Because the data sets contained a maximum of six partition coefficients, it seemed reasonable to consider regression models with at most one variable as the predictor of log K. It is important to retain sufficient error degrees of freedom in the analysis to guard against chance correlations. Several single variable models of the form $\log K_i = BX_i + C$, were tested, where B is the parameter estimate, C is the intercept, and X_i is the value of the predictor variable in the model (from Table VII.1). Results are given for sorption of solvents on oven-dry and partially-dry alumina in Table VII.4. It is useful to examine the difference between the model prediction and the actual observation using the error sum of squares, SSE, also shown in Table VII.4. Error sum of squares decreases in magnitude as the model fit improves.

TABLE VII.3 DIMENSIONLESS EXPERIMENTAL LINEAR PARTITION COEFFICIENTS ON ALUMINA

vapor	$c\Gamma_m$ (oven dry) (mg/g)	r^2	K (1.9 percent M.C.) (mg/g)	r^2
perchloroethylene	2,959	0.97	66±13	0.92
1,1-dichloroethylene	260	0.99	125±7	0.99
1,1,1-trichloroethane	1,391	0.98	187±8	0.99
chloroform	3,333	0.98	314±16	0.99
methylene chloride	1,853	0.94	189±7	1.00
trichloroethylene	1,138	1.00		
toluene	14,550	1.00		

TABLE VII.4 REGRESSIONS FOR ONE VARIABLE MODELS OF THE FORM Y=BX$_i$+C FOR SORPTION PARTITION COEFFICIENTS ON ALUMINA

Adjusted r^2	Oven-dry Alumina SSE	C	B	X$_i$	Adjusted r^2	1.9 percent M.C. Alumina SSE	C	B	X$_i$
-.17	2.01	3.37	-0.0002	log S	-.29	0.248	2.14	0.00019	VP
0.35	1.13	3.85	-1.07	H$_c$	-.02	0.195	2.83	-0.32	$^1\chi^v$
0.37	1.08	3.37	0.95	$\overline{\Phi}$	0.20	0.154	2.40	-0.39	H$_c$
0.39	1.05	1.13	1.06	$^1\chi^v$	0.28	0.138	2.28	0.65	$\overline{\Phi}$
0.46	0.94	3.71	-0.002	VP	0.41	0.114	2.97	-0.41	$^1\chi$
0.47	0.92	2.15	0.52	$^1\chi$	0.49	0.098	2.598	0.21	log S

Table VII.4 shows that sorption of vapors on the alumina at 1.9 percent M.C. is unlike sorption on oven-dry alumina because both the ordering of the best predictors and the signs of their coefficients differ for sorption at these two moisture contents. Vapor pressure is one of the best predictors of sorption for the oven-dry alumina, yet it is a poor predictor, and shows the opposite direction of effect, for the alumina at 1.9 percent M.C. This could be due to the filling of some small pores, in the case of the dry alumina, which would explain the inverse trend with vapor pressure. Even if vapor concentrations are below those necessary for condensation, greater affinity presumably exists between molecules with a lower liquid vapor pressure.

The decrease in sorption of organic vapors with increasing moisture content of the sorbent is particularly evident in Table VII.3 and provides further evidence for the importance of polar interactions in the sorption of vapor on relatively dry surfaces.

3. Partition Coefficients for Coated Alumina at 45 Percent Moisture Content

Linear partition coefficients for coated alumina are shown in Table VII.5 for 14 vapors. Partition coefficients for cyclohexane and methylcyclohexane were negative, and were excluded from the regression analysis of log K. A negative partition coefficient may indicate exclusion of the vapor from the pore space, and water, of the solid. Cyclohexane and methylcyclohexane do not have the surface area of a straight chain molecule, such as n-hexane, which would contribute to entropy driven sorption, nor do they have efficient packing ability necessary for forming physically adsorbed surface films due to their cage-like structure (Gavezzotti, 1985).

Because data were available for twelve vapors, regression models of up to three parameters were considered reasonable. Typically connectivity relationships are used as surrogates for physico-chemical properties (Grovers et al. 1984). Therefore, multiple regressions were examined involving $\overline{\Phi}$, $^1\chi$ and $^1\chi^V$ as one set of predictors and regressions involving log S, log K_{ow}, log VP, and log H_c as another. Since the calculated parameters $\overline{\Phi}$, $^1\chi$, and, $^1\chi^V$ are used as predictors of measured properties such as H_c (Nirmalakhandan and Speece, 1988) it is reasonable to expect that the parameters in these two sets are highly correlated. Therefore calculated and measured parameters were not mixed in the multiple correlations.

a. Comparing Trends in Connectivity Indexes and Polarizability Index

The values of r^2 for all possible multiple regressions on the three connectivity indexes are shown in Table VII.6. Adding the third parameter significantly reduced sum of squares error and improved the adjusted r^2. Based on adjusted r^2, the three parameter model was considered best.

TABLE VII.5   EXPERIMENTAL LINEAR PARTITION COEFFICIENTS FOR
COATED ALUMINA AT ≈ 45 PERCENT MOISTURE CONTENT

vapor	$K \times 10^4$ (dimensionless)	r^2	percent moisture content (dry weight basis)
perchloroethylene	1.15±0.31	0.74	50.27±0.31
trichloroethylene	17.28±4.53	0.74	48.56±0.30
1,1,1-trichloroethane	3.17±1.23	0.56	50.44±0.39
chloroform	36.56±2.75	0.97	50.59±0.36
methylene chloride	8.00±0.44	0.98	50.21±0.31
decane	0.24±0.04	0.89	43.00±2.91
octane	0.51±0.36	0.28	46.71±0.27
heptane	1.06±0.76	0.34	52.28±1.61
hexane	10.87±2.31	0.85	45.72±1.43
mesitylene	0.85±0.09	0.96	49.22±1.68
p-xylene	1.88±0.21	0.94	48.04±0.44
toluene	3.04±0.62	0.85	55.07±1.85
methylcyclohexane	-0.29±0.10	0.33	48.60±5.70
cyclohexane	-3.27±0.97	0.37	56.30±2.90

TABLE VII.6 REGRESSIONS FOR LOG K ON COATED ALUMINA AT 45 PERCENT MOISTURE CONTENT FOR PREDICTORS Φ, $^1\chi$, AND $^1\chi^v$

# Vars.	r^2	Adjusted r^2	SSE	Intercept (C)	$\overline{\Phi}$	$^1\chi$	$^1\chi^v$
1	0.274	0.201	2.507	-2.393	-0.434		
1	0.789	0.768	0.728	-0.602			-0.959
1	0.848	0.833	0.523	-1.211		-0.669	
2	0.853	0.821	0.506	-1.046		-0.531	-0.218
2	0.870	0.841	0.450	0.108	0.381		-1.350
2	0.870	0.841	0.448	-1.043	0.168	-0.769	
3	0.905	0.870	0.326	-0.356	0.316	-0.410	-0.712

Physical adsorption by accumulation onto water films, if it occurs, is expected to be inversely proportional to the first order molecular connectivity index, a measure of molecular surface area. The calculated regression results are consistent with this expectation. In addition, an indirect trend with the connectivity indexes could be due to their relationship with solubility (Nirmalakhandan and Speece, 1989). Except for the insignificant trend in the single parameter model, the polarizability index was directly proportional to log K.

b. Trends Observed in One-Parameter Regressions using Measured Parameters

One-parameter regressions on the data in Table VII.5 against measured parameters showed that the logarithm of the octanol water partition coefficient, and logarithm of vapor pressure predicted log K better than did logarithm of solubility and Henry's law constant for the combined solvent and fuel data (Table VII.7). Although the most significant relationships were with log K_{ow} and log VP, it is interesting to note that the signs in front of the other coefficients are consistent with sorption driven by hydrophillic (polar) interactions. In general the sorptive partition coefficients increased with increasing solubility and decreasing Henry's law constant. The direct dependency on solubility, and the corresponding indirect relationship with log K_{ow}, may result from the importance of vapor dissolution into water in the partitioning process for the more soluble VOCs (see Section III) as well as the relationship between solubility and polarizability, which may assist in the formation of surface films in the case of the less soluble compounds as well as in binding to polar mineral surfaces.

The Henry's law constant was expected to explain vapor-sorptive behavior in partially saturated systems because it is a measure of the distribution of a volatile compound between the solution and vapor phases. All other things being equal, compounds with high H_c will tend to reside in the vapor phase (vs. aqueous phase). For compounds with high Henry's law constants, a substantial increase in vapor density will result in but a small increase in fraction of the total mass contained in solution. Lower partition coefficients are expected for such compounds. As expected, based on dissolution effects (Equation III.10), a reverse proportionality with Henry's law constant was found for the solvents and fuel components for sorption to coated alumina at 45 percent M.C.

Sorption of both fuel components and solvents was directly proportional to vapor pressure. This result is counter intuitive since organics with high vapor pressures would be expected to reside in the vapor phase, all other factors being equal. This result may be explained, in part, by the normalization by vapor density that was applied to the partition coefficients. For the same value of K_d', compounds with higher vapor densities will have a larger log K. Regressions without this normalization were statistically insignificant.

TABLE VII.7   REGRESSIONS FOR LOG K ON COATED ALUMINA AT 45 PERCENT MOISTURE CONTENT FOR PREDICTORS LOG S, LOG K_{ow}, LOG H_c, AND LOG VP

# Vars.	r^2	Adjusted r^2	SSE	Intercept (C)	log H_c	log S	log VP	log K_{ow}
1	0.435	0.378	1.952	-2.690	-0.392			
1	0.740	0.714	0.899	-1.907		0.397		
1	0.840	0.824	0.552	-4.962			1.078	
1	0.860	0.845	0.485	-1.213				-0.685
2	0.880	0.853	0.415	-0.866	0.143			-0.827
2	0.911	0.891	0.308	-2.985			0.534	-0.394
2	0.912	0.893	0.302	-4.697	-0.180		0.915	
2	0.916	0.898	0.288	-3.892		0.187	0.727	
2	0.929	0.913	0.245	-0.680	0.757	0.948		
3	0.915	0.883	0.294	-3.920	-0.107		0.737	-0.176
3	0.936	0.912	0.220	4.208	2.089	-1.879	-1.125	

c. Multiple Regressions on Solvents and Fuels Together

The multiple-regression models with the highest values of adjusted r^2 in Tables VII.6 and VII.7 were:

$$\log K = 0.948 \log S + 0.757 \log H_c - 0.680 \qquad \text{VII.8}$$
$$r^2 = 0.929, \text{ Adjusted } r^2 = 0.913, \text{ SSE}=0.244, \text{ F}=59.0, \text{ n}=12$$

$$\log K = -0.7117 \ ^1\chi^v - 0.4095 \ ^1\chi + 0.3162 \ \overline{\Phi} - 0.3555 \qquad \text{VII.9}$$
$$r^2 = 0.905, \text{ Adjusted } r^2 = 0.870, \text{ SSE}= 0.326, \text{ F}=25.6, \text{ n}=12$$

The statistics for Equations VII.8 and VII.9 show that both models are highly significant [probability of a greater F statistic (p value for F) less than 0.0001 for Equation VII.8 and 0.0002 for Equation VII.9]. Equation VII.8 was considered superior because the coefficients in front of the parameters were highly significant (probability of a greater t statistic <0.0001 for log S and <0.0008 for log H_c) as compared to p values for t $\approx$ 0.1 in Equation VII.9 (a p value greater than 0.05 indicates that the coefficient in front of that parameter is not significant at the 95 percent level). Finally, Equation VII.9 suffered from problems with an influential outlier, namely methylene chloride. Equation VII.8 had some trouble describing hexane, but was better able to describe methylene chloride. In addition, Equation VII.8 had less of a problem with colinearity (as indicated by examination of the eigen values in the correlation matrix) than Equation VII.9.

Given the correlation between log S and log K_{ow} (Karickhoff et al., 1979), it might be anticipated that a regression involving log K_{ow} and log H_c would also be successful. The coefficient for log H_c in the regression with log K_{ow}, however, was not significant based on its p value. Equation VII.8 also did better with two parameters (based on r^2) than Equation VII.9 did with three. One may conclude that connectivity indexes are not as adept at predicting sorptive behavior as the measured properties for which they are surrogate.

d. Regressions on Solvents and Fuel Components by Compound Type

The solvents and fuel components were compared separately to observe whether the same trends could be observed for a subset of the compounds. Separate regressions for the solvents and fuels (Table VII.8) are given in Equations VII.10 and VII.11 for the models in Table VII.8 with the highest values of adjusted r^2.

For solvents:

$$\log K = -1.253 \log H_c - 3.4323 \qquad \text{VII.10}$$
$$r^2 = 0.912, \text{ adjusted } r^2 = 0.882, \text{ SSE}=0.135, \text{ F}=31.0, \text{ n}=5$$

For fuel components:

$$\log K = -1.561 \log K_{ow} - 0.4801 \log S - 0.2578 \qquad \text{VII.11}$$
$$r^2 = 0.879, \text{ adjusted } r^2 = 0.818, \text{ SSE}=0.043, \text{ F}=14.5, \text{ n}=7$$

When separate regressions are performed on the components of solvents and fuels by compound type (Table VII.8), the single parameter regressions show that log H_c was a better predictor of log K for the solvents than for the fuels where the regression ($r^2=0.27$) was not significant. Some of this effect may be due to the fact that Henry's constant was estimated from vapor pressure and solubility for the fuel components. More likely, the strong dependence with log H_c in Equation VII.10 is due to the importance of solvent partitioning into sample moisture because solvents generally had lower Henry's law constants than the fuel components. Sorption of solvents decreased with increasing log H_c. A reverse, but not statistically significant, trend was observed with the fuel components. Sorption of the fuels and solvents remained directly proportional to vapor pressure. Observed and predicted values of log K as given by Equation VII.8 and either VII.10 or VII.11 are shown in Table VII.9.

e. Correction of Sorption Partition Coefficients for Dissolution into Sample Moisture

Sorption partition coefficients were corrected to account for dissolution into the sample moisture based on a modification of Equation III.10 (shown as Equation VII.12 below). Equation VII.12 was utilized in a similar form by Culver (1989) to correct partition coefficients of Swanger (1990) and Gustafson (1986) for inclusion in groundwater transport models.

$$K_d^* = K_d{'} - \text{M.C.}/(100 \, \rho \, H_c) \qquad \text{VII.12}$$

where: K_d^* is the corrected partition coefficient,

M.C. is the moisture content (percent by mass),

H_c is the dimensionless Henry's law constant, and

ρ is the density of water.

TABLE VII.8 REGRESSIONS FOR LOG K ON COATED ALUMINA AT 45 PERCENT M.C. BY SOLVENTS AND FUEL COMPONENTS

SOLVENTS

# Vars.	r^2	Adjusted r^2	SSE	Intercept (C)	$\log H_c$	$\log S$	$\log VP$	$\log K_{ow}$
1	0.818	0.757	0.279	4.811			1.028	
1	0.821	0.761	0.274	-1.213				-0.686
1	0.900	0.866	0.153	-1.721		0.585		
1	0.912	0.882	0.135	-3.432	-1.253			
2	0.840	0.677	0.247	-2.958			-0.365	0.506
2	0.912	0.824	0.135	-3.387	-1.221	0.0155		
2	0.912	0.824	0.135	-3.368	-1.302		-0.0445	
2	0.914	0.830	0.131	0.301		0.947	-0.681	
2	0.915	0.830	0.130	-3.093	-1.074			-0.112
3	0.914	0.658	0.131	0.129	-0.064	0.902	-0.652	
3	0.918	0.673	0.125	-2.398	-1.227		-0.279	-0.207

FUELS

# Vars.	r^2	Adjusted r^2	SSE	Intercept (C)	$\log H_c$	$\log S$	$\log VP$	$\log K_{ow}$
1	0.008	-0.190	0.350	-3.47		-0.048		
1	0.267	0.120	0.258	-3.515	0.198			
1	0.412	0.294	0.207	-0.831				-0.807
1	0.813	0.776	0.066	-4.519			0.693	
2	0.852	0.779	0.052	-4.679	-0.110		0.852	
2	0.853	0.779	0.052	-4.209		0.110	0.743	
2	0.855	0.782	0.051	-1.037	0.744	0.853		
2	0.862	0.793	0.049	-3.369			0.595	-0.320
2	0.876	0.814	0.044	-0.510	0.268			-1.008
3	0.864	0.728	0.048	30.76	8.197	8.399	-7.454	
3	0.880	0.760	0.042	2.062	0.505		-0.537	-1.625

TABLE VII.9   COMPARISON OF OBSERVED AND PREDICTED VALUES OF
             LOG K ON COATED ALUMINA AT 45 PERCENT MOISTURE
             CONTENT

vapor	log K (g/g) (experimental)	log K predicted (Eqn. VII.8)	(Eqns. VII.10,VII.11)
perchloroethylene	-3.94	-3.62	-3.25
trichloroethylene	-2.76	-3.08	-2.93
1,1,1-trichloroethane	-3.50	-3.06	-3.23
chloroform	-2.44	-2.63	-2.39
methylene chloride	-2.10	-2.36	-2.10
decane	-4.48	-4.91	-5.08
octane	-4.30	-4.08	-4.03
heptane	-3.97	-3.63	-3.51
hexane	-2.96	-3.21	-3.00
mesitylene	-4.07	-4.13	-4.03
p-xylene	-3.70	-3.72	-3.84
toluene	-3.52	-3.31	-3.44
methylcyclohexane	n.a.	-3.49	-2.92
cyclohexane	n.a.	-3.17	-2.41

Examination of the corrected partition coefficients suggests that most sorption of both fuel and solvent vapors onto the moist ($\approx$ 45 percent M.C.) coated alumina occurred primarily as partitioning into the sorbent moisture (Table VII.10). All solvents except trichloroethylene and perhaps perchloroethylene, showed no more sorption than would be anticipated by dissolution into liquid water.

While sorption of solvents was generally less than expected based on simple vapor dissolution, sorption of all the fuel components exceeded the amount that could be accounted for by vapor dissolution. The normal alkanes had high Henry's law constants precluding a significant contribution from dissolution in the aqueous phase. Two other modes of accumulation are possible for the n-alkanes. They may either sorb to the humic organic coating of the aluminum oxide or accumulate at the air/water interface. The first case, involving sorption to organic matter, is considered most likely due to the high K_{ow} values of these compounds. Sorption at the air/water interface, however, cannot be excluded as a sorptive mechanism. The likelihood of accumulation at the air/water interface is less in the case of the solvents, because of high solvent vapor pressures.

TABLE VII.10 COMPARISON OF K_d' AND K_d' CORRECTED FOR DISSOLUTION INTO SAMPLE MOISTURE (K_d^*) FOR COATED ALUMINA AT APPROXIMATELY 45 PERCENT MOISTURE CONTENT

Vapor	K_d'(mL/g)	r^2	percent M.C.	K_d^*(mL/g)
perchloroethylene	0.70±0.19	0.74	50.27±0.31	-0.004
trichloroethylene	3.36±0.88	0.74	48.56±0.30	2.13
1,1,1-trichloroethane	0.36±0.14	0.56	50.44±0.39	-0.375
chloroform	2.92±0.22	0.97	50.59±0.36	-0.532
methylene chloride	4.02±0.22	0.98	50.21±0.31	-1.77
decane	2.39±0.40	0.89	43.00±2.91	2.39
octane	0.59±0.42	0.28	46.71±0.27	0.59
heptane	0.43±0.31	0.34	52.28±1.61	0.42
hexane	1.55±0.33	0.85	45.72±1.43	1.54
mesitylene	6.51±0.67	0.96	49.22±1.68	4.40
p-xylene	3.75±0.41	0.94	48.04±0.44	1.88
toluene	2.16±0.44	0.85	55.07±1.85	0.15
methylcyclohexane	-.12±0.04	0.33	48.6±5.70	-0.15
cyclohexane	-.74±0.22	0.37	56.3±2.90	-0.81

The four best single parameter regressions on the data in Table VII.10 are shown in Table VII.11. Notice that the most successful predictors are solubility and log K_{ow}. Stronger sorption is observed for those compounds with higher log K_{ow}, and lower solubility, once the effects of dissolution into the sample moisture are removed. This finding is consistent with the observation that aqueous sorption of diverse pollutants is highly correlated with their octanol water partition coefficients (Kenaga, 1980).

TABLE VII.11 REGRESSIONS MODELS FOR CORRECTED K_d^* OF TABLE VII.10

r^2	Adjusted r^2	SSE	Intercept (C)	Parameter Estimates (B_i)			
				H_c	S	log S	log K_{ow}
0.156	0.071	27.70	-0.795	0.025			
0.665	0.632	10.98	-2.173			-1.159	
0.748	0.723	8.27	-4.146				1.971
0.844	0.828	5.13	1.342		-1.68E-4		

E. SUMMARY AND CONCLUSIONS

The impact of sorbate properties on sorption of organic vapors onto unsaturated soils was examined to quantify the direction and magnitude of the expected vapor property effects. The study involved examination of sorption under both dry and moist conditions. The differences in sorption under dry conditions between the study compounds were explained best by an inverse trend with vapor pressure, due perhaps to condensation in small pores. Log solubility was the best predictor for sorption at 1.9 percent moisture content. Therefore, the relative sorption behavior of the sorbate is influenced by the presence of water molecules even at partial water film coverage.

Differential vapor sorptive abilities of the chlorinated hydrocarbons and hydrocarbon components of fuels on the moist coated alumina sorbent was inversely related to their Henry's law constant and directly related to solubility. The dependency on solubility was consistent with predictions based on a conceptual analysis of the role of aqueous phase activity in the sorption of organic vapors. Since vapor uptake includes dissolution into soil water, vapor partition coefficients are anticipated to be directly proportional to solubility. This is the inverse of the solubility dependency observed for saturated partition coefficients.

The dissolution of vapors in the solid solution was adequate for describing uptake of the more soluble compounds but was not always sufficient to explain sorption of the n-alkanes. When the effects of dissolution into the moisture of the solid were removed, log K_{ow} emerged as an important predictor of relative sorptive strength.

In summary, sorption of VOCs in unsaturated soils appears to be a dual process controlled by polar attraction to mineral surfaces (under very dry conditions), dissolution into soil moisture as well as sorption within organic carbon. The relative importance of these processes for any given compound will depend on its solubility and octanol-water partition coefficient.

SECTION VIII

VAPOR COMPETITION AND SORPTION ENHANCEMENT AT LOW SORBATE CONCENTRATION

By: S.R. Lindner and L.W. Lion

A. INTRODUCTION

Pollutants frequently exist as mixtures, yet researchers such as Rao and Lee (1987), Nkedi-Kizza et al. (1985), Fu and Luthy (1986a;1986b), Woodburn et al. (1986), MacIntyre and deFur (1985), and Staples and Geiselmann (1988), have only addressed composition affects on sorption of organic compounds. Rao et al. (1985) classified sorption experiments into four categories based on sorbate-solvent combinations: (1) single sorbate - single solvent, (2) multiple sorbates - single solvent, (3) single sorbate - mixed solvents, and (4) multiple sorbates - mixed solvents. These classifications are useful for describing saturated aqueous-phase sorption; yet, in the case of vapor sorption at low moisture contents, the distinction between sorbate and solvent inevitably breaks down. For instance, at high moisture contents the mixed sorbate system may be thought of as type (2). However, upon drying, a type (2) system may proceed to type (3) if all organics other than the one of interest are considered as an organic cosolvent.

Because the system type may change upon drying, the process of interaction between sorbates, if any, may be strongly influenced by moisture content. Vapor sorption experiments have the obvious advantage, over saturated sorption experiments, in that they allow investigation of the effect of moisture content on sorption. Several types of sorption processes, ranging from absorption, or partitioning, (under moist conditions) to adsorption (under dry conditions), may therefore be examined for the same mixture of vapors.

In saturated systems, sorbate competition is virtually unknown (Lee et al., 1988; Rao and Lee, 1987). The experiments that lead to this conclusion include work by Chiou et al. (1983) where the sorption of 1,3-dichlorobenzene was not effected by the presence of 1,2,4-trichlorobenzene on Woodburn soil. Rao et al. (1986) observed that the sorption isotherms for naphthalene, toluene, diuron, atrazine, and carbofuran were identical when compared as a single sorbate and in ternary mixture. MacIntyre and deFur (1985) found only slight affect of mixture for the sorption of 16 hydrocarbon components of JP8 jet fuel. They concluded that sorption coefficients obtained for single compounds can be used to predict the sorption of complex hydrocarbon mixtures.

The ability of multiple compounds to partition freely into a phase of organic matter is one reason given for the the absence of competition observed in saturated sorption experiments (Chiou et al., 1983). The fact that that the presence of an organic cosolvent reduces sorption has also been used to support the concept that hydrophobic sorbates partition into organic matter (Chiou et al., 1988). Since differential sorption in saturated soils is controlled by the solubility of the sorbate in the aqueous solution (Rao et al., 1985), it appears that the activity of sorbates in bulk aqueous solution is not substantially affected by trace amounts of other sorbates. In addition, little effect is expected on the activity of sorbates in the organic carbon phase (Karickhoff, 1981).

Moisture content is variable in the vadose zone, and the fact that there are some moisture conditions where sorbate interaction is negligible, eg. saturated soils, does not guarantee that vapors will sorb independently at all moisture contents. The strength of vapor sorption at low moisture contents (Spencer and Cliath, 1972; Chiou et al., 1987) suggests that sorption processes different from those occurring at saturated conditions predominate at lower moisture. In particular, at low moisture contents the increased orientation of water films, by polar attraction to mineral surfaces, may enhance interfacial accumulation of nonpolar organic compounds by "squeezing" them out of solution (Valsaraj, 1988). At constant concentration of sorbate vapors, competition effects are expected to intensify at low moisture contents because of the increasing importance of the mineral surface, which acts as an adsorption medium rather than a partitioning medium. For example, it is possible that sorbates may compete for sites left unoccupied when surface coverage by water is incomplete. Wetting and drying cycles within the root zone will permit a spectrum of sorptive processes, some of which may produce sorbate mixture effects. At low moisture contents, increased mixture effects may also be observed due to the limited capacity of the aqueous phase to dissolve organic vapors without alterations in their aqueous activity coefficients.

B. THEORETICAL CONSIDERATIONS

1. Competitive Langmuir Adsorption Model

Effects of multiple sorbates may be expected when the adsorptive capacity of the surface can be exhausted, for instance when adsorption at mineral surfaces governs uptake and sorbates compete for surface sites. This is most likely to occur at very low moisture contents or on sorbates with very low carbon contents, ie. where mineral surfaces govern uptake. Since mineral surfaces are always present in soils, there will always be some competition occurring between sorbates in soils. However, the low adsorptive capacity of

mineral surfaces, relative to organic matter, often allows such competition to go unobserved.

In an adsorption process, adsorbates compete with water and, by extension, other organic adsorbates for adsorption sites. The Langmuir equation governs adsorption proceeding a maximum of monolayer surface coverage, which makes it relevant to the description of the competition for sites on mineral surfaces. Competition may still occur in systems where adsorption proceeds beyond a monolayer, however, an equation to describe sorption of mixtures under such conditions is presently unavailable. The competitive Langmuir equation (Weber, 1972) for two adsorbates **a** and **b** is given by:

$$\Gamma_a^m = \frac{\Gamma_{max}^a \, c_a \, \phi_a}{1 + c_a\phi_a + c_b\phi_b}; \quad \Gamma_b^m = \frac{\Gamma_{max}^b \, c_b \, \phi_b}{1 + c_a\phi_a + c_b\phi_b} \qquad \text{VIII.1}$$

where:

Γ_a^m, Γ_b^m = the mass of vapor **a** and **b** adsorbed per gram of adsorbent, in a binary mixture

$\Gamma_{max}^a, \Gamma_{max}^b$ = adsorption monolayer capacities for vapors **a** and **b**,

c_a, c_b = adsorption affinity constants for vapors **a** and **b**,

ϕ_a, ϕ_b = relative vapor concentrations of **a** and **b**,

The competitive Langmuir equation implies that adsorption isotherms for vapors are nonlinear. Inspection of Equation VIII.1, shows that, as the concentrations of *both* adsorbate **a** and adsorbate **b** increase, adsorption of adsorbate **a** will increase to an "apparent" maximum, G^a_{max}, somewhat less than Γ^a_{max}, because some of the adsorption sites will be occupied by adsorbate **b**.

$$G_{max}^a = \frac{\Gamma_{max}^a c_a\phi_a}{c_a\phi_a + c_b\phi_b} \qquad (\text{assuming } c_a\phi_a + c_b\phi_b \gg 1) \qquad \text{VIII.2}$$

An additional term in the denominator of Equation VIII.1 versus the ordinary Langmuir equation (compare to Equation VI.1.) results in a reduction of adsorption of each component for binary mixtures. Greater reduction in G^a_{max} will occur for coadsorbates with higher affinities, c_b. If ϕ_a and ϕ_b are equal, the ratio of the apparent adsorption maximum G^a_{max} for binary mixtures to that for single vapors is given by the quantity:

190

$c_a/(c_a + c_b)$. Therefore, if vapors **a** and **b** have equal affinities, then the apparent adsorption maximum G^a_{max} achieved when $\phi_a = \phi_b$ should be one half of the value for vapors adsorbing alone. The ratio of $G^a_{max} : \Gamma^a_{max}$, should show greater deviation from unity for competing vapors with high affinity coefficients. The competitive Langmuir equation (Equation VIII.1) is used below to evaluate the adsorption behavior of vapors on dry sorbents.

2. A Solvophobic Sorption Model for Organic Vapors

The concept of sorption as driven by hydrophobic interactions explains the behavior of sorbate mixtures when another sorbate or mixture of sorbates is present in sufficient quantity to alter the activity of the aqueous phase or to create a separate immiscible phase. Simply stated, this concept indicates that hydrophobic organic compounds tend to "seek refuge", from polar solutions, by partitioning into an organic phase, which may consist of soil organic matter, dissolved humic materials, or, in the case of heavily contaminated soils, an immiscible organic cosolvent. Generally it is assumed that the organic phase into which sorbates partition has a large capacity. Because it is expected that there will be little change in free energy of the organic phase upon addition of sorbate molecules (Karickhoff, 1981; see Section VII), negligible influence of sorbate mixtures on the partitioning into an organic phase is presumed. The question arises as to the nature of conditions in which cosorption effects (ie. the alteration of the behavior of a sorbate due to its presence as a component of a mixture) might appear.

When there is sufficient moisture to form over 4 to 8 monolayers, solubility of sorbates in the aqueous solution films contributes greatly to the sorption of soluble organic vapors (See Sections III and V). Partitioning from the gaseous phase into aqueous films as governed by Henry's law may be influenced by the presence of other organics (Yurteri et al., 1987). These effects can be handled by empirical activity corrections, which have a strong dependence on species composition (Yurteri et al., 1987). The solvophobic model of Rao et al. (1985) offers an alternative, more mechanistic, understanding of vapor sorption processes which are influenced by partitioning of cosorbates into the aqueous phase.

The solvophobic model of Rao et al. (1985) relates the relative sorptive strength of hydrophobic pollutants to changes in the activity of the pollutant in the aqueous phase (see Section VII). The decrease in aqueous sorption with increasing cosolvent concentration which has been observed by many investigators (Rao and Lee, 1987; Nkedi-Kizza et al., 1985; Fu and Luthy, 1986; Woodburn et al., 1986) is predicted by this model.

When dissolution into water films contributes significantly to vapor sorption, changes in solution composition may lead to vapor-solution partitioning behavior not well described by Henry's law. In the case of vapor partitioning in unsaturated soils, the aqueous phase is less extensive and thereby more susceptible to activity effects caused by the presence of dissolved organic compounds. As noted in Section VII, any influence on the activity of the compound within the film of condensed water will affect the compound's sorptive partition coefficient. A modification of the solvophobic sorption model of Rao et al. (1985) is derived below to describe the sorption of organic vapor mixtures in unsaturated soils.

As described in Section VII, the sorption of a vapor proceeds until equilibrium is reached between the fugacity of the sorbate in the vapor phase and the fugacity of the sorbate in the non-vapor, or sorbed, phase:

$$F_o^g \gamma_g C_g = F_o^{nv} \gamma_{nv} C_{nv} \qquad\qquad \text{VIII.3}$$

where F_o^g, F_o^{nv} are the reference state fugacities of the sorbate in the vapor and sorbed phases, γ_g, and γ_{nv} are activity coefficients and C_g and C_{nv} are the concentrations in the vapor and sorbed phase.

Since, under saturated conditions, the partitioning of the same compound in several soils is determined by the fraction of organic carbon (f_{oc}), Rao et al. (1985) suggested that the saturated partition coefficient normalized by organic carbon content was proportional to the ratio (γ_s/γ_{oc}) where γ_s is the sorbate activity coefficient in the solution phase and γ_{oc} is the sorbate activity coefficient in the organic carbon phase.

In the case of vapor partitioning the "non-vapor" phase is made up of both organic carbon and aqueous solution (assuming negligible sorption at the air/water interface), therefore, equilibrium is established between all three phases: solution, vapor and organic carbon.

$$F_o^g \gamma_g C_g = F_o^s \gamma_s C_s = F_o^{oc} \gamma_{oc} C_{oc} \qquad\qquad \text{VIII.4}$$

where superscripts and subscripts g, s, and oc refer to vapor, water, and organic carbon respectively and concentrations are in grams per gram. Given the moisture content, M.C., (percent dry weight basis), the concentration in the non-vapor phase is defined as:

$$C_{nv} = \frac{M.C. \, C_s}{100} + f_{oc}C_{oc}.$$

VIII.5

For vapor partitioning the concentration in the sorbed or "non-vapor" phase is related to the concentration in the vapor phase through the partition coefficient as:

$$C_{nv} = KC_g$$

VIII.6

where,

$$K = F_o^g \, \gamma_g \left[\frac{M.C.}{100F_o^s \, \gamma_s} + \frac{f_{oc}}{F_o^{oc} \, \gamma_{oc}} \right].$$

VIII.7

Therefore, the partition coefficient reflects the fact that the activity coefficient for the solute in the nonvapor phase is influenced by contributions from both the aqueous and organic carbon phase. Karickhoff (1981) has suggested that γ_s may vary by four orders of magnitude as the solute changes from benzene to pyrene, due to the dissimilarity of the interactions between the sorbate and water molecules, while γ_{oc} varies only by a factor of four. Therefore, the activity of the solute in the aqueous phase γ_s was considered by Rao and co-workers to be the primary factor influencing the saturated partition coefficient (Rao et al., 1981). By extension, the same factor will potentially dictate cosorption effects in vapor partitioning onto moist soils. Cosorption effects are anticipated to be most pronounced in soils with low organic fractions, f_{oc}, that is, when the second term in Equation VIII.7 is small.

Equation VIII.7 shows a proportionality between the partition coefficient and the activity coefficient, γ_s, in the solution phase:

$$K \propto 1/\gamma_s.$$

VIII.8

Therefore, as shown in Section VII, an inverse relationship exists between the activity correction in aqueous solution and the vapor partition coefficient. This effect is the opposite of that anticipated when partitioning is from saturated solution. The activity coefficient in the aqueous solution is defined by (Atkins, 1978):

$$\log(\gamma_s) = \log(X^w)^{ideal} - \log(X^w)^{experimental}$$

VIII.9

193

where X^w is the mole fraction aqueous solubility and the superscripts refer to the ideal and experimentally measured aqueous solubility. The activity coefficient, therefore, represents the experimentally observed deviation from ideal solution behavior. Substitution of Equation VIII.9 into Equation VIII.8 yields:

$$\log K \propto \log(X^w)^{experimental} - \log(X^w)^{ideal} \qquad \text{VIII.10}$$

The relationship between log K and log solubility is apparent from Equation VIII.10 and suggests a regression relationship (Equation VIII.11) similar to that used by Karickhoff (1981, 1984). In the case of vapor partitioning, there is a modification of the sign due to the reciprocal relationship between K and γ^s in Equation VIII.8. Following the approach of Karickhoff (1981, 1984), the ideal mole fraction solubility for a crystalline solid is employed in Equation VIII.11. As will be shown below, the reference state used for the ideal mole fraction solubility is immaterial since it will drop out of the final equation:

$$\log K = \alpha \ln X^w + (\Delta S_f/RT)(T_m - T) + \beta \qquad \text{VIII.11}$$

where α and β are parameters for regression and

$$\log(X^w)^{ideal} = - (1/2.303) (\Delta S_f / RT) (T_m - T). \qquad \text{VIII.12}$$

In Equation VIII.12, ΔS_f is the entropy of fusion (kJ/mol °K), T_m is the melting point (°K), T is temperature (°K), and R is the gas constant (kJ/mole °K). The relation of the mole fraction solubility of a compound in binary mixture X^m to its mole fraction solubility in water has been provided by Yalkowsky et al. (1975,1976):

$$\ln X^m = \ln X^w + f^c \sigma^c. \qquad \text{VIII.13}$$

Here X^m is the solubility of an organic solute in a binary mixture of water and organic cosolvent, f^c is the volume fraction of organic cosolvent, and σ^c is given by:

$$\sigma^c = \frac{(\Delta\lambda^c \, HSA) + (\Delta\varepsilon^c \, PSA)}{k \, T} \qquad \text{VIII.14}$$

where:

T = temperature (°K)

k = the Boltzmann constant (kJ/°K)

HSA = the hydrocarbonaceous surface area of the sorbate

PSA = the polar surface area of the sorbate

$\Delta\lambda^c = \lambda^w - \lambda^c$

$\Delta\varepsilon^c = \varepsilon^w - \varepsilon^c$

λ^c = the interfacial free-energy (kJ/nm^2) at the interface between the HSA and the organic cosolvent

λ^w = the interfacial free-energy (kJ/nm^2) at the interface between the HSA and the aqueous phase

ε^c = the interfacial free-energy (kJ/nm^2) at the interface between the PSA and the organic cosolvent

ε^w = the interfacial free-energy (kJ/nm^2) at the interface between the PSA and the aqueous phase

The term σ^c in Equation VIII.13 reflects the energy to form a "cavity" in the mixed solvent. This energy depends upon the surface tension at the interface between the solvent and the solute as well as the solute molecular surface area (Yalkowsky, 1975). The deltas in Equation VIII.14 result from the summation of terms describing the pair-wise interfacial interactions of each solvent (water and each cosolvent) with the hydrocarbonaceous and polar surfaces of the solute. Yalkowsky (1975) calculated the hydrocarbonaceous surface area (HSA) from the total surface area (TSA) by subtracting the polar surface area (PSA), which is obtained from the summed contributions of the individual polar moieties. The total surface area (TSA) was determined using the hard sphere model of Herman (1972). By extension of Equation VIII.12 to binary sorbate mixtures:

$$\log K^m = \alpha \ln X^m + (\Delta S_f / RT)(T_m - T) + \beta \qquad \text{VIII.15}$$

where K^m is the distribution coefficient observed for the organic compound when other compounds are present. Substitution of Equation VIII.13 into Equation VIII.15 gives:

$$\log K^m = \alpha \ln X^w + \alpha\, f^c \sigma^c + (\Delta S_f / RT)(T_m - T) + \beta. \qquad \text{VIII.16}$$

Subtraction of Equation VIII.11 from Equation VIII.16 results in Equation VIII.17. (Note that the entropy of fusion for a crystalline solid cancels out in this step; so that the reference state is not a factor in Equation VIII.17.)

$$\log (K^m/K) = \alpha \, f^c \sigma^c. \qquad \qquad \text{VIII.17}$$

This result for vapor-phase partitioning is identical to that obtained by Rao et al. (1985) for saturated systems except for the sign. In the application of Equation VIII.17 to unsaturated soils the distinction between cosorbate and cosolvent is effectively lost. Equation VIII.17 can be extended to multiple sorbate interactions by summing over the fractions of the various cosorbates as:

$$\log (K^m/K) = \alpha \, \Sigma f^c \sigma^c. \qquad \qquad \text{VIII.18}$$

When hydrophobic interactions are dominant, Equation VIII.14 can be simplified [see Nkedi-Kizza et al. (1985)] as:

$$\sigma^c \approx \Delta \lambda^c \text{HSA}/(kT) \qquad \qquad \text{VIII.19}$$

The modified solvophobic model of Equation VIII.18 may be used to explain the hydrophobic sorbate interactions observed in the vapor-phase sorption experiments on moist soils. The term σ^c in Equation VIII.14 is expected to be positive for the vapors used in this study because the interfacial free energy between a liquid sorbate and water, λ^w, is about 25 dynes cm^{-1} for each sorbate (Horvath, 1982). Additionally, because solvent mixtures and fuel mixtures, such as the ones investigated in this research, are infinitely miscible, the parameter λ^c is expected to be much less than λ^w resulting in a positive value for $\Delta \lambda^c$ and a positive value for σ^c. Therefore, it is expected that the vapor-phase sorption coefficient for a compound sorbing in mixture will tend to increase with increasing concentration of other sorbates in the aqueous phase. In effect, organic cosolvents compete with the soil organic matter for the organic sorbate (Equation VIII.7). Additionally from Equation VIII.19, the effect of one sorbate on another is expected to be related to the hydrocarbonaceous surface area of the former. It is evident from Equation VIII.18 that compounds that are scarcely sorbed (f^c small) will not influence the sorption of others ($K \approx K^m$).

The solvophobic sorption model explains hydrophobic sorbate interactions to the exclusion of other types of sorbate interactions. It is hypothesized, in calculating the interactions by Equation VIII.14, that the cosolvent and water molecules display no preferential locations at the film/air or sorbent/film interface. This approximation may not always be valid in the case of vapor sorption at intermediate moisture contents (between 1 to 8 monolayers) because of the importance of sorption at both of these interfaces (see

Section III). Additionally it is hypothesized that activity changes in the aqueous phase are the primary determinant of sorption for systems consisting of vapor, water, and organic carbon phases. Systems containing a condensed nonpolar organic liquid phase, such as that which may occur at the air/water interface may display substantial activity changes in the nonpolar organic liquid phase. Compositional activity effects in the nonpolar phase have been found to influence the partitioning of hydrocarbon mixtures to a greater extent than such effects in the aqueous phase (Leinonen and Mackay, 1973; Banerjee, 1984; Burris and MacIntyre, 1985; Fu and Luthy, 1986; and Muntz and Roberts, 1988). These effects, however, are only expected to be important for systems containing a nonpolar organic condensed liquid phase. Such systems are not described by the hydrophobic sorption model.

The modified solvophobic model depends on the assumption that, at low moisture content, sorbates are present in sufficiently high concentrations within the thin film of water comprising the aqueous phase to alter the aqueous-phase activity coefficient. In this case, dissolution of sorbates is taken as a primary influence in uptake from the vapor phase. There is also some evidence to suggest that low solubility nonpolar organic compounds may accumulate at the air/water interface (Valsaraj, 1988). Given the expected orientation of water molecules relative to a polar mineral surface, and the ability of structured water to exclude nonpolar organics, the aqueous solubilities of sorbates may be reduced, resulting in their accumulation at the gas liquid interface. If accumulation at the gas/liquid interface were to occur, it is likely that it will be governed by a physical adsorption process with low heats of adsorption (for binding of nonpolar organics to a water film). A Type III isotherm shape (convex to the x-axis at all sorbate concentrations) is expected for vapor uptake which is driven by weak physical adsorption. The shape of a Type III isotherm would guarantee that sorption will increase in greater than linear fashion as the amount of adsorption increases. Therefore, an expectation for interfacial accumulation is that it will be enhanced in sorbate mixtures. This analysis indicates that predictions of enhanced sorption in mixtures are not restricted to reasoning based on the modified solvophobic model.

3. Summary

Depending upon moisture content, sorption of a vapor is likely to be governed by processes ranging from adsorption (on dry surfaces) to partitioning (on moist surfaces). The competitive Langmuir isotherm provides a basis for interpretation of vapor competition in an adsorption process while the solvophobic model for partitioning (as modified above) provides a basis for interpretation of vapor sorption by moist soils. Figure III.11 (repeated here as Figure VIII.1) indicates the manner in which organic vapor sorption is influenced by moisture content. In the region of lower moisture content below monolayer coverage

197

(Region 1), sorption of an organic vapor rapidly decreases due to addition of moisture (Chiou and Shoup, 1985). Within this moisture domain, competition for sorption sites is indicated as the mechanism responsible for the moisture content dependencies (see Section III). Organic vapors presumably may also compete with one another for surface sites. Water is strongly preferred by the sorbent over the organic vapors (Chiou et al., 1987). Therefore, as fewer positions on the mineral surface are available for organic vapors, the effects of sorbate vapor competition should be minimized because the sites unoccupied by water will account for a small percentage of the total. The result is that, although sorbate mixture effects are expected to occur at all moisture contents within region 1, they are expected to dampen as moisture content increases.
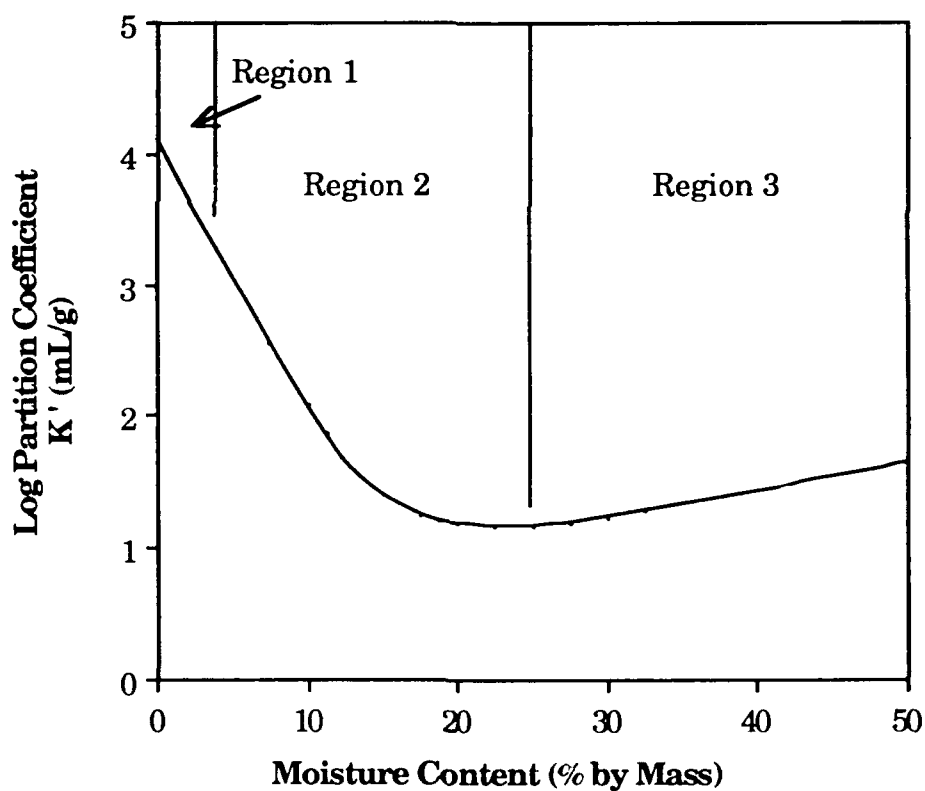

Figure VIII.1 Influence of Moisture Content on the Sorption of TCE on Coated Alumina.

198

Region 2 (5-20 percent M.C., on the aluminas used in this study) represents a zone of transition where sorption may occur on the water interface with the soil surface and the soil air. Minimal dissolution of nonpolar organic compounds into the bound water layer is expected in this region due to the orientation of water molecules relative to the mineral surface. This has the net effect of displacing nonpolar molecules from the water films in a manner similar to the salting out effect observed when an electrolyte is added to bulk solution. The association of the water molecules with the surface inhibits their ability to arrange themselves around the nonpolar molecule and hence solubility of the nonpolar compound is reduced. Thus, polar and nonpolar molecules will tend to be segregated within Region 2. Activity changes due to compositional effects in the nonpolar phase may influence the partitioning equilibrium, ie. sorption. If a nonpolar "phase" of accumulated hydrocarbons exists at the air/water interface it is also possible that activity effects in such a phase may play a large role in the observed compositional effects on sorption.

In Region 3, where sorption is predominantly determined by dissolution into bound water (versus partitioning from the aqueous phase into soil organic matter), sorption enhancement due to the presence of soluble cosorbates may occur, according to the solvophobic model for vapor sorption. This is likely to occur on sorbents with low carbon content such as aquifer materials and for cosolvents with high aqueous solubility, such as methanol and acetone. With increasing moisture content, soil water will tend to behave more and more like bulk solution. Most hydrocarbons, and chlorinated hydrocarbons, have low aqueous solubilities ($<10^{-3}$M). Therefore hydrocarbons in hydrocarbon saturated bulk water solutions tend to obey Henry's law (Munz and Roberts, 1986). That is the infinite dilution activity coefficient is expected to apply, in saturated soils, regardless of solution composition because hydrocarbon molecules are not associated in solution. This may also apply in unsaturated soils; however, given a limited number of monolayers of water, some of which are oriented by polar interactions with a mineral surface, the net effect of many solutes at low concentrations on aqueous-phase activity is unclear.

The experiments described below were conducted at a range of moisture contents to evaluate the extent to which vapors compete and the consistency of observed competition with the expectations described above.

C. MATERIALS AND METHODS

1. Experiments on Oven Dry and Moist Surfaces

The headspace analysis procedure described in Sections VI and VII was used to measure sorption. In competitive sorption experiments, several vapors were introduced simultaneously through separate gas tight syringes before the sample bottles were capped. Samples from the bottles were analyzed by gas chromatography (GC). The G.C. column was 20 percent SP-2100 0.1 percent Carbowax 1500 on 100/80 mesh Supelcoport. The output from the flame ionization detector from the Hewlett Packard 5890 GC was monitored by an HP 3392A integrator. The one mL splitless injections to the G.C. were taken directly from the sample bottles using a valved gas-tight syringe (Precision Sampling). The bottle seal was provided with Teflon®-backed rubber septa. Incubation periods were at least 16 hours. Preliminary experiments showed this period to be sufficient for attaining equilibrium. All experiments were performed at 25±1°C, and temperature was controlled by circulating water bath.

Vapor pairs chosen for the study included chloroform (CF) and 1,1,1-trichloroethane (TCA); methylene chloride (DCM) and perchloroethylene (PCE); and trichloroethylene (TCE) and toluene. Also included was the ternary mixture: CF, TCE, and toluene. Vapor pairs were selected to achieve good peak separation and to observe the effects of two very different vapors, such as TCE and toluene versus solvent pairs. The sorbent was oven dried 80-200 mesh adsorption alumina (Fischer Scientific).

To test the validity of Equation (VIII.1) for the dry alumina, data were reduced by fitting the Langmuir isotherm and the B.E.T. isotherms for single sorbates by weighted Golden Section minimization as described in Section VI. The parameters, Γ_m and c, were compared to those given for single vapors in Section VI (Table VI.4).

In order to study the effects of moisture content on the influence of sorbate mixtures, the experiment on chloroform and TCA on oven-dry adsorption alumina was repeated at 12.6 percent moisture content. This moisture content was achieved by placing the adsorption alumina in a circulating water bath at 25°C±2°C for 2 days. As noted in Section VII, the presence of water on adsorption alumina reduces sorption of both chloroform and TCA.

2. Factorial Experiments

Two separate factorial experiments were conducted on the components of fuels and solvents. Factorial experiments are an efficient statistical design that allows simultaneous investigation of the influence of several factors (in this case sorbate vapors) as well as the interactions among them. Both binary (one factor and response variable) and ternary (two factors and response variable) interactions were considered for coated alumina at 20 percent M.C. A binary interaction which resulted in an increase in sorption (synergism) would be interpreted as consistent with a positive $\Delta\lambda^c$ term in Equation VIII.19 of the solvophobic model, ie. a decrease in free energy upon addition of the cosorbate. A binary interaction resulting in reduced sorption (antagonism) would not be explained by the solvophobic model but by some other type of interaction. Ternary interactions result when the presence of a third sorbate influences the synergism or antagonism between two other vapors, for instance by making two vapors that originally were synergistic compete. In general it is expected that if both vapor **a** and vapor **b** individually enhance the sorption of vapor **c**, the effects of the simultaneous presence of **a** and **b** should be additive. When the effects are more than additive, a ternary interaction between **a** and **b** is said to have occurred. For the purpose of this study the 90 percent level was taken as the cut-off for significance. For an interaction to be considered significant, the p value (probability of a more extreme effect) was required to be < 0.10.

Each set of observations was collected as a full factorial, that is, single vapors plus all possible combinations of two vapors, three vapors, etc. up to six were investigated. Two replicates were used at each combination. Each sample bottle contained two grams of sorbent, therefore, only two levels of each factor were used, presence or absence of the sorbate vapor. Replicates were divided into eight blocks based on standard experimental design procedures (Barker, 1985). Replicates within each block were randomized. Each experiment had 128 replicates total, however, the GC peaks for chloroform and methylene chloride could not be separated; thus half of the replicates were not used in the factorial experiment with solvents. A one mL syringe was used to deliver vapor to the bottles except for perchloroethylene and 1,3,5-trimethylbenzene where a two mL syringe was used. The coated alumina was prepared in quantity as needed. One hundred grams of coated alumina were weighed into a container to which 20mL of water was added by volumetric pipette. The sealed containers were allowed to stand overnight to allow moisture to permeate the alumina. The coated alumina was well mixed before use and during bottle preparation.

Compounds selected for the solvent study included 1,1,1-trichloroethane (TCA), perchloroethylene (PCE), 1,1-dichloroethylene (DCE), trichloroethylene (TCE), chloroform (CF), and methylene chloride (DCM). The factorial experiment on fuels included methylcyclopentane (MCP), cyclohexane (CH), methylcyclohexane (MCH), toluene, p-xylene (PXYL), and 1,3,5-trimethylbenzene (TBENZ). The DCM, CF, PXYL, ·~ TCA were from Fischer Scientific. TCE was from Aldrich Chemical Co.; all other compounds were from Fluka Chemical Co. All compounds were reagent grade.

Samples in mixtures were analyzed by GC using a temperature ramp from 100°C to 160°C. Equilibration periods were at least 24 hours and extended up to a week for some blocks due to GC malfunction. All experiments were performed at 25±1°C.

Although the experiment was laid out as a six-way factorial, the data were analyzed as a set of six five-way factorial designs. In each of the six factorial analyses, the signal area from a different vapor functioned as the dependent variable. Simple presence or absence of each of the other five vapors supplied the factors to be investigated for their effect on the signal area of the vapor serving as the dependent variable. Half of the sample bottles were excluded from each of the six analyses because they did not contain the vapor that was of concern in that analysis. The model used to reduce the data (Equation VIII.20) seeds to explain any deviation observed from the mean signal area of the vapor serving as the dependent variable by the presence of absence of one to five other vapors and their combinations.

$$\Phi_{jk} = \mu_j + \beta_{j1} + \beta_{j2} + \ldots + \beta_{j5} + \left(\beta_{j1}*\beta_{j2}\right) + \left(\beta_{j1}*\beta_{j3}\right) + \ldots + \varepsilon_{jk} \qquad \text{VIII.20}$$

where:
- Φ_{jk} = the GC signal area of compound j in observation k, j = 1, 2, . . ., 6, and k = 1, 2, . . ., 64,
- μ_j = the mean signal area for compound j,
- β_{j1} = the influence of the first vapor on the signal area of compound j,
- β_{j2} = the influence of the second cosorbate on the signal area of compound j, etc.,
- $\beta_{j1}*\beta_{j2}$ = one of many binary or higher-order interaction terms, and
- ε_{jk} = the error term.

Although it is not explicitly shown in equation VIII.20, all 31 possible combinations of one or fore of the five factors were included in the factorial analysis. By including all combinations in the model, the error sum of squares directly reflected the

variability between the replicates at each vapor combination. Because this test was performed to identify possible mixture effects, rather than to accurately determine the β coefficients in Equation VIII. 20, this test constituted an initial screening. The 90 percent confidence level was used to better ensure that all effects of potential importance would be identified.

D. EXPERIMENTAL RESULTS

1. Sorbate Vapor Competition on Dry Alumina

Parameters $\hat{\Gamma}_m$ and $\hat{c}$ were obtained by fitting the Langmuir equation for single sorbates to the data (Table VIII.1 and Figures VIII.2-VIII.5). Since the equation fitted to the data was for single vapors, and ϕ_a increased with ϕ_b, the fitted values of the adsorption maxima for binary adsorption isotherms approximated $G^a{}_{max}$, an "apparent" adsorption maximum somewhat less than $\Gamma^a{}_{max}$ due to occupation of the surface by sorbate **b**.

TABLE VIII.1   FITTED PARAMETERS TO THE LANGMUIR ISOTHERM FOR VAPORS ALONE AND IN MIXTURE

Vapor	Single Vapor $\hat{\Gamma}_m$ (mg/g)	$\hat{c}$	Binary Mixture $\hat{G}_m$ (mg/g)	$\hat{c}$	Ternary Mixture $\hat{G}_m$ (mg/g)	$\hat{c}$
TCE	19.73	57.7	14.02	62.4[1]	8.98	17.6
toluene	30.07	264.7	41.50	139.1[2]	16.86	242.8
chloroform	12.06	276.4	5.75	162.3[3]	2.83	134.9
TCA	9.93	140.1	4.89	130.2[4]		
DCM	4.78	387.7	2.49	285.3[5]		
PCE	19.74	149.9	11.64	121.5[6]		

1. with toluene 2. with TCE 3. with TCA 4. with chloroform 5. with PCE 6. with DCM

Sorption was reduced in both binary and ternary mixture as was expected based on the competitive Langmuir equation (VIII.1). As expected, the fitted parameter for the capacity of the surface, $\hat{G}_m$, in binary mixture is reduced relative to $\hat{\Gamma}_m$ and to even a

203

greater extent in ternary mixture for sorption onto oven-dry alumina (Table VIII.1). Due to the experimental design, the concentration of the vapor and its competitor increased simultaneously which produced the observed reduction in the fitted parameter $\hat{G}_m$. In general, the linear region for isotherms of binary vapor mixtures ended at lower concentrations than did isotherms for the single vapor which indicates a capacity driven process (ie. competition for surface sites) rather than partitioning into the cosorbate.

Less sorption was observed for TCE when in mixture with toluene (Figure VIII.2). Toluene sorption was affected only slightly by the presence of TCE (Figure VIII.3). This was expected because the affinity coefficient for toluene is over 4 times greater than the value of the affinity coefficient for TCE. Also shown in Figures VIII.2 and VIII.3 are the predictions of the competitive Langmuir isotherm using the parameters obtained for single vapor adsorption of TCE and toluene. The competitive Langmuir model was able to predict the influence of toluene on TCE sorption and the influence of TCE on toluene sorption. This indicates that sorption of toluene and TCE on the dry alumina surface is truly competitive.
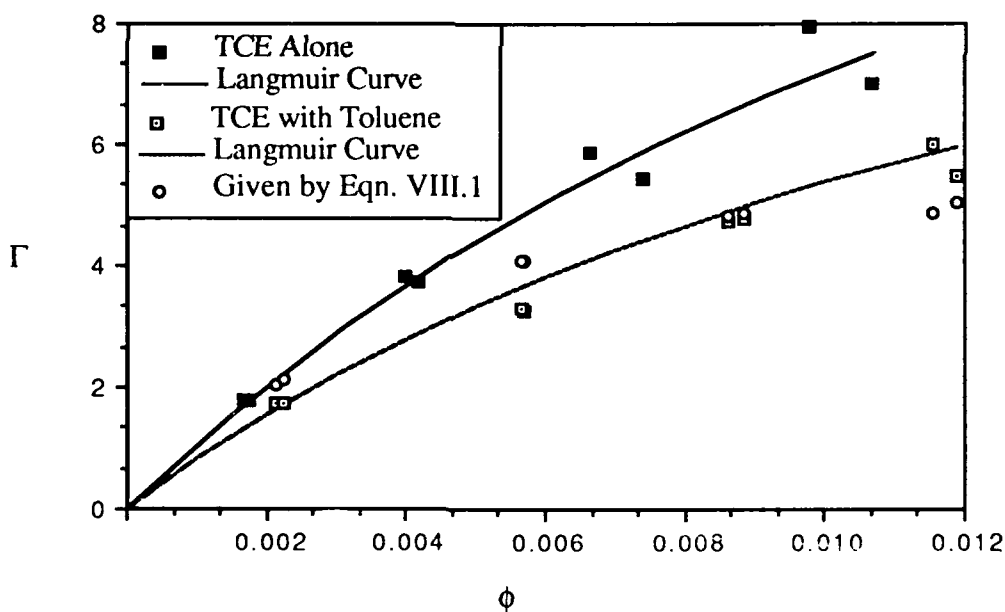

Figure VIII.2   Sorption of TCE on Oven-Dry Alumina Alone and in Binary Mixture with Toluene.
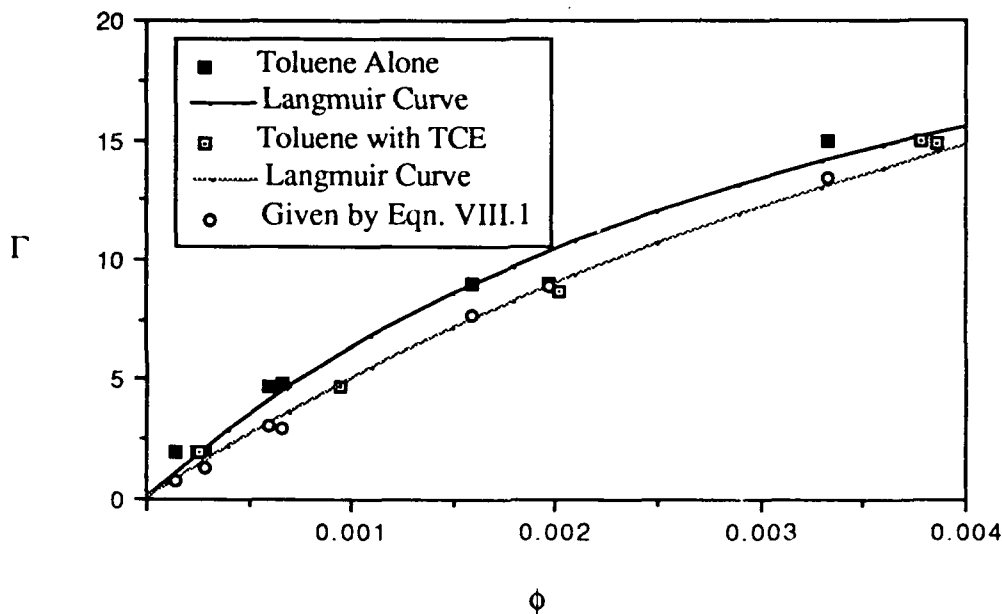
Figure VIII.3 Sorption of Toluene Alone on Dry Alumina and in Binary Mixture with TCE

The apparent sorption capacity $\hat{G}_m$ of both CF and TCA was reduced by about one half in mixture (Figures VIII.4 and 5). Because CFs fitted affinity coefficient was about twice that of TCA, equations VI.1 and VIII.1 indicate that its $\hat{G}_m$ in binary mixture would be reduced by only a third instead of by half. It was also expected that the weakly sorbing TCA should have a greater reduction in sorption than CF, which has a higher affinity for the surface.

The sorption of both PCE and DCM was also reduced in binary mixture (Figures VIII.6 and VIII.7). DCM did not reduce the sorption of PCE as greatly as expected based on the competitive Langmuir Equation. The parameter $\hat{G}_m$ was reduced in binary mixture as predicted by the competitive Langmuir isotherm.

In the ternary experiment on dry adsorption alumina, sorption of all three vapors (TCE, CF, and toluene) was reduced by competition (Figures VIII.8, 9, and 10). Toluene had the highest affinity coefficient (c), and its apparent affinity coefficient increased in the ternary mixture. The affinity constants of the other vapors were reduced in ternary mixture. The isotherm for TCE, the sorbate with the lowest c value, is nearly linear, which may indicate "partitioning" of TCE into adsorbed CF and toluene.

Figure VIII.4   Sorption of Chloroform on Oven-Dry Alumina Alone and in Binary Mixture with TCA.
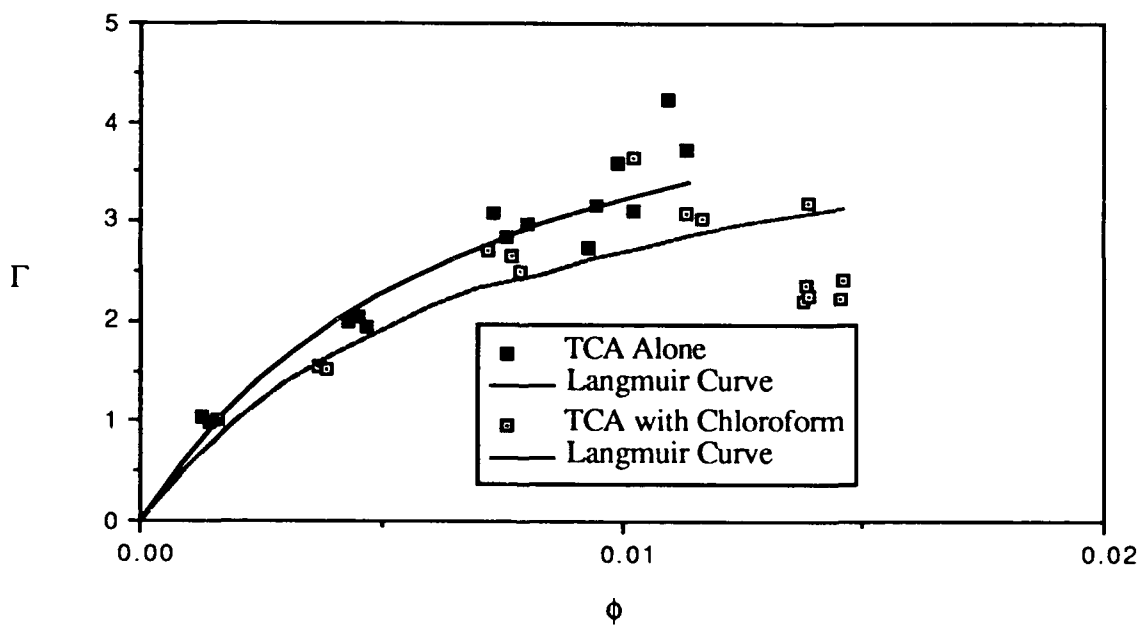
Figure VIII.5 Sorption of TCA Alone and in Binary Mixture With Chloroform.

206
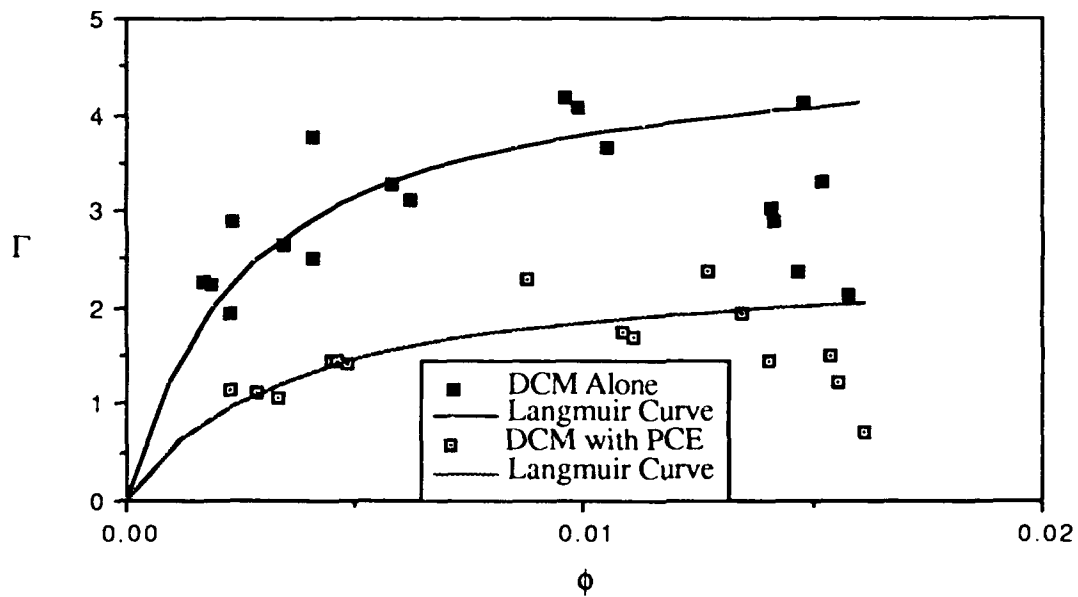
Figure VIII.6   Sorption of DCM on Oven-Dry Alumina Alone and in Binary Mixture with PCE.

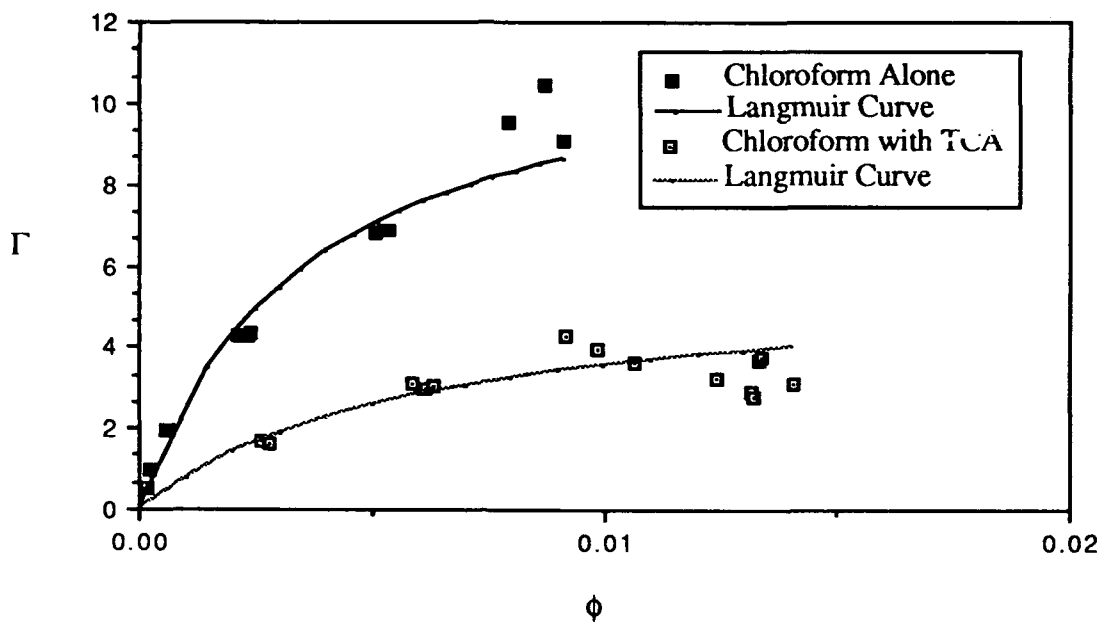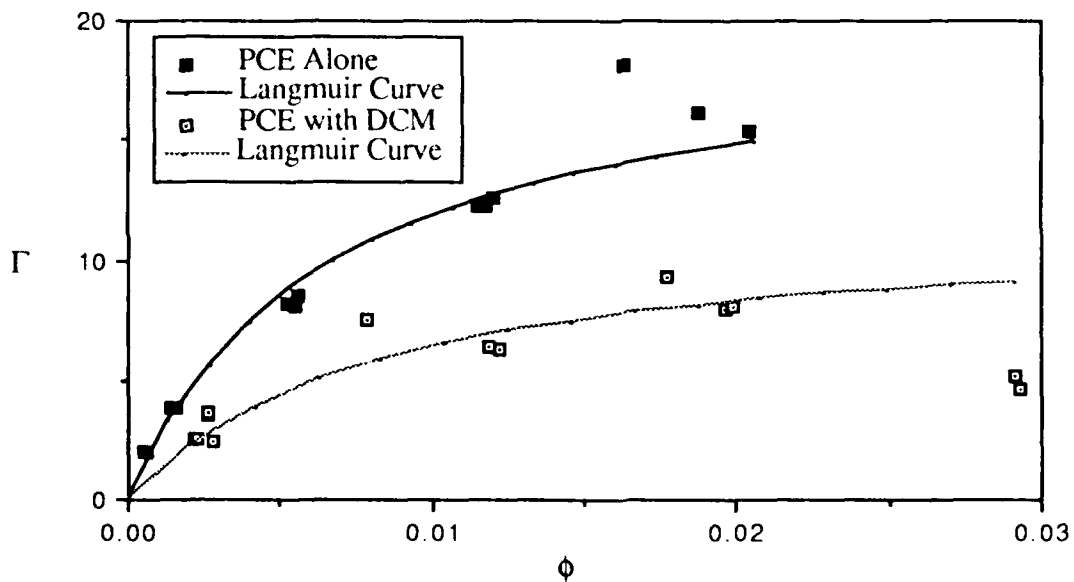Figure VIII.7   Sorption of PCE on Oven-Dry Alumina Alone and in Binary Mixture with DCM.
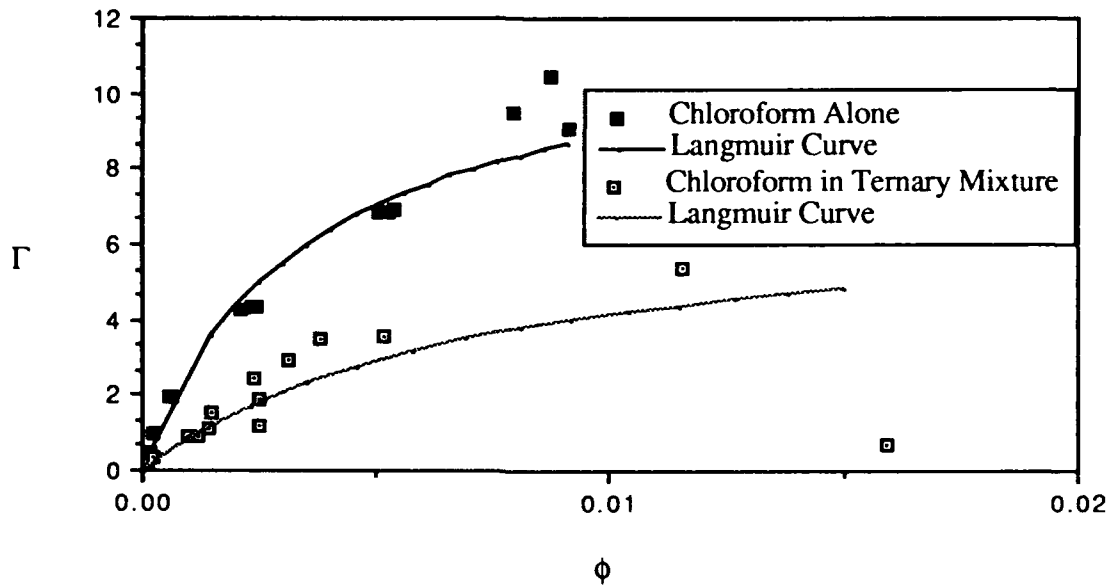
Figure VIII.8   Sorption of CF on Oven-Dry Alumina Alone and in Ternary Mixture with
TCE and Toluene.
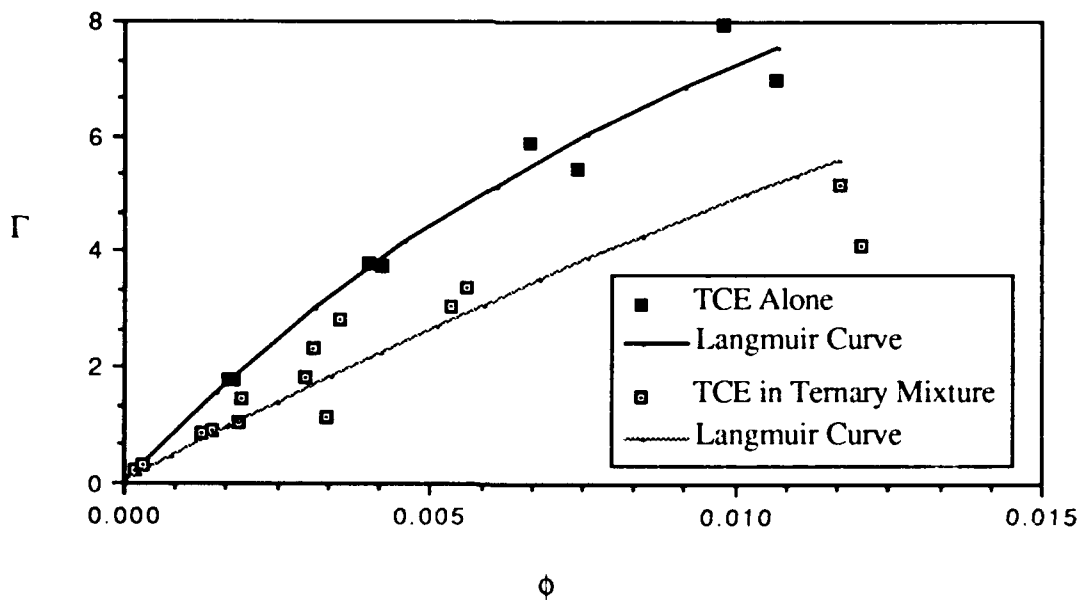
Figure VIII.9   Sorption of TCE on Oven-Dry Alumina Alone and in Ternary Mixture
with CF and Toluene.
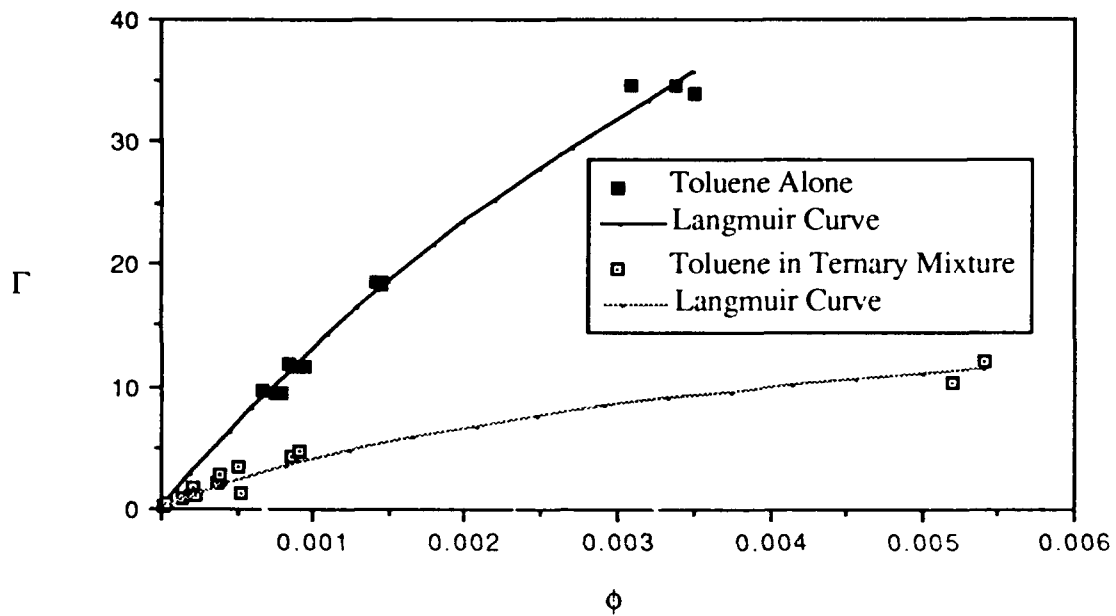
Figure VIII.10   Sorption of Toluene on Oven-Dry Alumina Alone and in Ternary Mixture with CF and TCE.

2. Influence of Moisture Content on the Sorption of Chloroform and 1,1,1-Trichloroethane on Uncoated Alumina

A summary of the partition coefficient estimates is shown in Table VIII.2 for chloroform and TCA by themselves and in mixture for sorption on uncoated alumina at 12.6 percent moisture content.

In this experiment a diminished effect of sorbate mixture was expected due to the overall reduction in sorption at 12.6 percent moisture content. Less sorption of both chloroform and TCA occurred in mixture. The effect of mixture on chloroform was greater than on TCA. This was also observed in the experiment on dry alumina where the effect of mixture on both vapors was more pronounced. However, because the 95 percent confidence intervals overlap between the single sorbate and binary sorbate experiments at 12.6 percent M.C. there is no assurance that the parameter estimates for the partition coefficients are actually different. Partition coefficients are much lower for the moist sorbents, which makes small differences more difficult to distinguish from experimental noise.

209

TABLE VIII.2 SUMMARY OF BINARY SORPTION EXPERIMENT CHLOROFORM
AND 1,1,1-TRICHLOROETHANE AT 12.6 PERCENT M.C.

Single Sorbate	$K*10^3$(dimensionless)	95 percent CI	r^2(weighted)
chloroform	19.97	(17.32, 22.61)	0.929
1,1,1-trichloroethane	13.69	(12.23, 15.15)	0.953
Binary Sorbate			
chloroform	17.38	(14.38, 20.39)	0.885
1,1,1-trichloroethane	12.69	(11.27, 14.12)	0.948

From the preceding discussion it is apparent that sorbate vapors can display competition in the dry moisture content region of the simulated soil water regime. The competition is reduced, and perhaps eliminated, by increasing moisture content due to the fact that the surface is covered by continuous layers of water.

3. Factorial Studies on Solvents and Fuels

a. Results for Solvents

According to Equation VIII.18 an increase in sorption, by aqueous-phase partitioning, is expected with increasing concentrations of cosorbate present in the aqueous phase, due to a modification to the aqueous activity coefficient. Although substantial agreement with model predictions was obtained in the factorial studies, in following discussion will show that binary mixtures did not always display enhanced sorption. Reduced sorption for some compounds in some mixtures was also observed. This may have occurred due to intermolecular interactions that are not solvophobic in nature, and are not accounted for by the solvophobic model.

The effects of individual cosorbates over all the mixtures tested (termed "main effects") are described in Table VIII.3 for each sorbate vapor. Tabulated p-values (probability of a more extreme effect) are given, and must be less than 0.10 to be considered statistically significant. The statistical procedure compared the mean signal areas of the sorbate (dependent variable) between bottles with and without each of the 5 cosorbate vapors. The arrows in Table VIII.3 show whether sorption was increased or decreased, over all, by the cosorbate for the cases that were significant at the 90 percent confidence interval. For instance, Table VIII.3 is read to mean that sorption of TCE, on

210

the average, was greater for bottles containing CF. Also the sorption of CF is enhanced by PCE and reduced by DCE.

TABLE VIII.3   p-VALUES FOR MAIN EFFECTS OF SORBATE COVAPORS
(Arrows indicate the direction of the effect)

Sorbate:	Cosorbates: DCM	TCE†	CF	PCE	TCA	DCE
DCM	N.A.	0.2	0.7	0.2	0.2	*
TCE	0.6	N.A.	0.07↑	0.6	0.4	0.3
CF	0.6	0.4	N.A.	0.002↑↑	0.7	0.002↓↓
PCE	0.3	0.0001↑↑	0.1	N.A.	0.09↑	0.6
TCA	0.1	0.03↑↑	0.3	1.0	N.A.	0.5
DCE	*	0.2	0.9	0.1	0.9	N.A.

N.A.= not applicable

* not measured

† Effect of cosorbate is confounded with experimental blocking

↑ significant at the 90 percent level

↑↑ significant at the 95 percent level

The sorbates in Table VIII.3 are arranged in order of decreasing oven-dry partition coefficient (Table VII.3). DCE (not in Table VII.3) was expected to sorb poorly based on its predicted partition coefficient (Table VII.4) and is therefore listed last. In general, sorption of strongly sorbing sorbates such as DCM and TCE, was unaltered by the presence of cosorbates in the mixture. This is evidenced by the fact that, with the exception of the effect of CF on TCE, the top two rows of Table VIII.3 contain relatively large p-values (ie. greater than 0.10), which shows that the behavior of DCM and TCE was generally unaffected by other sorbates. When sorbates compete strongly sorbing sorbates occupy the sorption space to the exclusion of other sorbates, mitigating their effect. Also, significant solvophobic effects are anticipated for cosorbates that increase f^c. Therefore, molecules with low solubilities are less likely to alter f^c and to influence sorption. In summary, when sorption is influenced by the presence of other sorbed compounds, either by competition or enhancement, it may be anticipated that sorbates with low solubilities, such as DCE, TCA, and PCE, will rarely affect the sorption of other sorbates in mixture. This is evidenced by the fact that the p-values in the last column, for DCE, are large. Since

DCM was the sorbate with the smallest molecular surface area, based on Equations VIII.18 and VIII.19, it should have less affect as a cosorbate on the sorption of other vapors. As the first column in Table VIII.3 indicates, this predicted effect was observed. Negligible affect of DCM, in a sorption column study on the sorption of binary mixtures with kepone, was also observed by Staples and Geiselmann (1988), although they found that ethanol, methanol, 2-propanol, and butanol enhanced the concentration of kepone in the aqueous phase.

Given the data in Table VIII.3, one would expect that CF would sorb better in bottles containing PCE than bottles containing PCE and DCE. It would follow that if sorption were enhanced five units by PCE and reduced two units by DCE that the effect of adding both would be three units increase in sorption. In other words the main effects might be expected to be additive. The computation of ternary interactions in the factorial study disclosed exceptions to additivity. These exceptions are discussed below. At any combination where higher level effects could not be described by summation of main effects, an "interactic " was said to have occurred. Because most of the significant main effects were consi ent with the solvophobic model, sorption of vapor combinations which did not show a significant interaction were, for the most part, also consistent with predictions of the solvophobic model. Exceptions (ie., interactions) were examined for consistency with the solvophobic model for vapors (Equation VIII.18) by determining whether more sorption or less sorption occurred than was predicted by the main effects.

The interactions between the sorbates observed in this study were classified into 2 types as shown in Figure VIII.11: (1) sorption was enhanced (ie., vapor concentration was reduced) by the two cosorbates acting alone but was reduced by the same two sorbates when mixed together; (2) sorption was reduced by each sorbate acting alone but was enhanced by these same sorbates when mixed together. In the case of the last type of interaction, more sorption was observed than expected for the mixtures containing both vapors, an observation consistent with the solvophobic model. To study ternary interactions the data were divided into replicates containing one or more of three factors (organic compounds). The results in Figure VIII.11 involve smaller sets of observations than those in Table VIII.3 and, therefore, will not agree in all cases.

Type 1 interaction

TCA

DCM

PCE

Also:
PCE:DCM*TCE
PCE:CF*TCA
TCA:DCM*TCE

Type 2 interaction

TCA

CF

PCE

Also:
TCA:CF*TCE
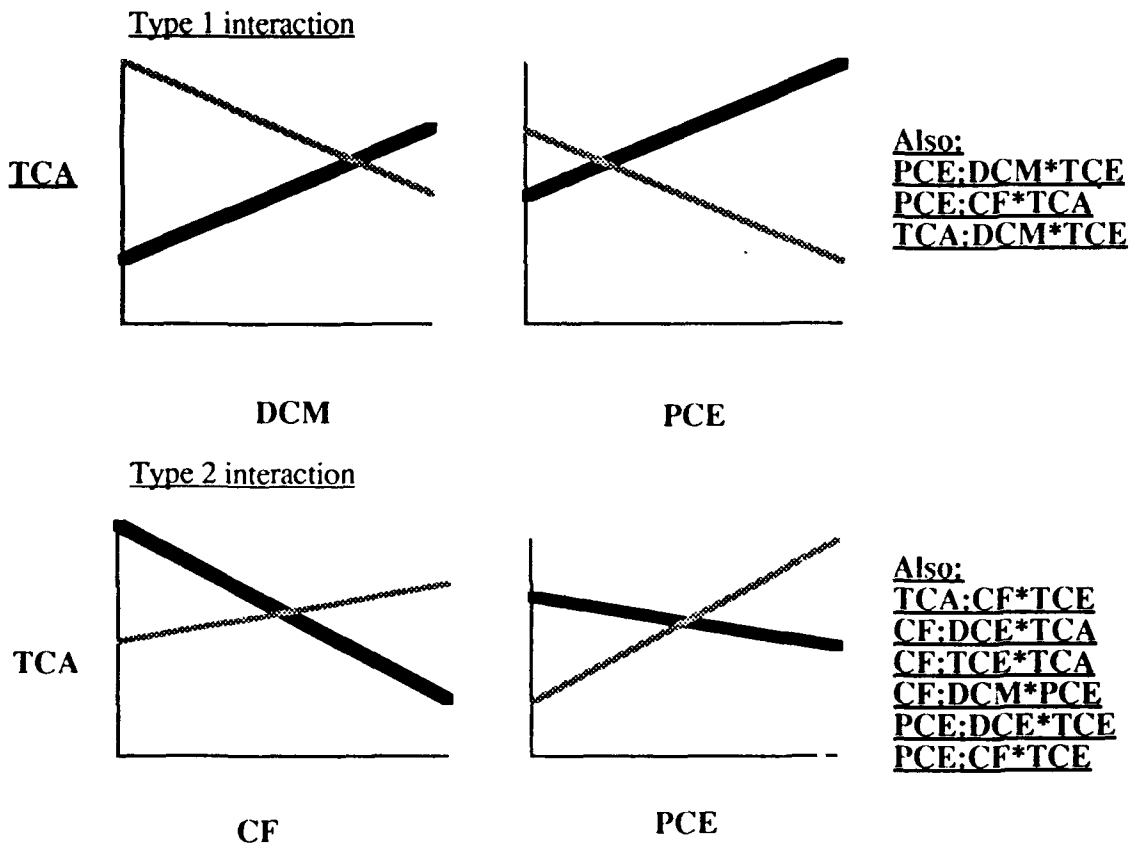CF:DCE*TCA
CF:TCE*TCA
CF:DCM*PCE
PCE:DCE*TCE
PCE:CF*TCE

Figure VIII.11. Example of Two Types of Ternary Interaction. [Light lines are for binary mixtures; dark lines are for ternary mixtures. Shown are equilibrium concentrations in the vapor phase.]

Chloroform sorption displayed three ternary vapor interactions of Type 2 (Figure VIII.11). The sorption of CF was reduced by DCE, and TCE acting alone (Type 2 interaction) but was not reduced by the DCE or TCE when TCA was present. Table VIII.3 shows that CF sorption was enhanced as a main effect by PCE. For the remaining Type 2 interaction, slight, yet significant at the 90 percent level, enhancement of CF sorption by PCE was observed in bottles without DCM. The enhancement of CF sorption by PCE, however, was especially evident in bottles containing DCM. When PCE was absent from the mixture, sorption of CF was reduced by competition with DCM.

Sorption of TCA was increased in binary mixture by the strongly sorbing vapors DCM and TCE (Type 1 interaction). Introduction of PCE, however, reduced the gains in sorption made upon addition of DCM or the addition of TCE, despite the observed enhancement of the sorption of DCM and TCE by PCE. Type 1 interactions are not explained by the solvophobic model.

Recall that CF enhanced the sorption of TCE (Table VIII.3). Therefore, TCE and CF together were more effective in enhancing the sorption of TCA (Type 2 interaction). The combination of PCE and DCE was also more effective than PCE alone in enhancing TCA sorption but this effect was confounded with the block design of the experiment. The combination of CF, and PCE (Type 2 interaction) was more effective than either CF or PCE alone in enhancing the sorption of TCA because CF sorption was enhanced by PCE (Table VIII.3).

Enhanced sorption of PCE was observed in combination with CF or TCA, exclusively, or DCM or TCE, exclusively; but little gain in sorption was observed when both members of either pair were present (Type 1 interaction). Sorption of PCE was enhanced by TCE (Table VIII.3), and to an even greater extent if the TCE was combined with DCE or CF (Type 2 interaction), although DCE and CF overall had no significant main effect on PCE sorption as shown in Table VIII.3.

Sorption of DCM was enhanced by TCA and PCE acting alone (Type 1 interaction) but this effect was confounded by the experimental block design. PCE enhanced the sorption of DCM to a greater extent when CF was present (Type 2 interaction).

Sorption of TCE was enhanced by the presence of CF. This main effect (Table VIII.3), however, was the only significant effect observed for TCE, ie. no interactions were observed.

214

Out of a possible 28 main effects, 6 were significant at the 90 percent level and 5 of the 6 resulted in increased sorption as predicted by the solvophobic model. Of the 48 possible ternary interactions, 11 were significant and 7 of these enhanced sorption . Thus the solvophobic model may have overall use for predicting the sorption of mixtures, but may be limited to predictions for specific vapors because of intermolecular interactions and accumulation at interfaces which are not described by the model.

b. Results for Fuel Components

Sorptive interactions were observed for the fuels used in the factorial study, namely MCP, CH, MCH, toluene, PXYL, and TBENZ. Inspection of the main effects (Table VIII.4) reveals the relative influence of each cosorbate. p-values in Table VIII.4 indicate the statistical significance of the various interactions. Low p-values ($p<0.10$) indicate significance at the 90 percent level. The effect on the sorption of each vapor in the first column by each cosorbate is shown across the row. Binary and ternary interactions with p-values less than 0.10 are discussed below.

TABLE VIII.4 p-VALUES FOR BINARY INTERACTIONS BETWEEN FUEL COMPONENT PAIRS (Arrows show the direction of the effect)

Sorbate:	Cosorbate: MCP	CH	MCH	toluene	PXYL[†]	TBENZ
MCP	N.A.	0.004↑↑	0.4	0.09↓	0.0001↑↑	0.08↑
CH	0.0002↑	N.A.	0.9	0.2	0.0001↑↑	0.0001↑↑
MCH	0.0001↑	0.07↑	N.A.	0.003↑↑	0.0001↑↑	0.0001↑↑
toluene	0.4	0.0001↑	0.3	N.A.	0.0001↑↑	0.02
PXYL	0.3	0.04↑	0.4	0.99	N.A.	0.9
TBENZ	0.1	0.02↑	0.9	1.0	0.0001↑↑	N.A.

N.A.= not applicable

[†] Effect of cosorbate is confounded with experimental blocking

↑ significant at the 90 percent level

↑↑ significant at the 95 percent level

In general, interactions (ie. ternary mixture effects) involving the sorption of fuels were less complicated than those observed for the solvents because few sorbates competed. Instead, cosorbate vapors tended to enhance sorption as is expected based on the solvophobic model. From the main effects shown (Table VIII.4), it is clear that the vapor most influenced by the presence of others is MCH because its sorption was enhanced by the presence of all of the other vapors (as seen by the low p-values in the row for MCH). In addition, p-values in the MCH column were all large, indicating that MCH had little, if any, overall influence on the sorption of other mixture components. Recall that the sorption reported for MCH in Section VII was very low. As previously discussed, the solvophobic model indicates that a vapor with low sorption is not expected to have a large enhancement effect on the sorption of others.

Binary mixtures of PXYL and the other vapors were confounded by the blocks used in the experiment. The large p-values in the column under PXYL, therefore may not be reliable, since variability in the experimental setup may have contributed, in part, to the observed effects.

CH enhanced the sorption of several other vapors including TBENZ, toluene, MCP, and MCH. CH sorption was enhanced by these same four vapors.

Toluene reduced the sorption of MCP. CH, TBENZ, and potentially PXYL enhanced the sorption of toluene. Adding both CH and PXYL had a more than additive effect, in other words, a significant Type 2 ternary interaction was observed. Sorption of MCP was enhanced by CH, TBENZ and potentially PXYL.

Twelve ternary interactions for the fuel components resulted in enhanced sorption for sorbates in combination (Type 2 interactions). The interactions that were significant at the 90 percent level and not confounded by the experimental block design are listed in Table VIII.5.

TABLE VIII.5   TERNARY INTERACTIONS BETWEEN FUEL COMPONENTS

MCP:TOL*MCH	MCH:CH*TBENZ
MCP:CH*PXYL	MCH:CH*PXYL
CH:TBENZ*MCH	TOL:TBENZ*MCH
CH:TBENZ*PXYL	TOL:CH*PXYL
MCH:MCP*CH	TBENZ:TOL*MCH
MCH:MCP*TOL	PXYL:CH*TOL

c. Influence of Moisture Content on Sorbate Competition

In general, increasing moisture content will reduce mixture effects through alterations in the aqueous activity coefficients as the water films thicken and begin to mimic bulk solution. A series of experiments was conducted on coated alumina with the three aromatic compounds toluene, PXYL and TBENZ at two moisture contents, 40 and 16 percent. Before comparisons could be made at 16 percent M.C., a moisture content correction was applied based on the observed M.C. variation between replicates within the experiment. The moisture content correction was necessitated to allow comparison of the data from different experiments within this highly sensitive moisture regime. The correction was applied to the linear isotherm by multiplying each observation, X_i, by a factor which normalized it to the average moisture content. The factor was, on the average, equal to 1.0.

$$Y_i = X_i \, (bW_i + a) \, K + 1 + \varepsilon_i \qquad\qquad VIII.21$$

where W_i is the percent moisture content of the sample and ε_i is the error term. The parameters to be fitted are b, a, and K. The model was solved as:

$$Y_i = X_i \, K(b(W_i - W) + 1) + 1 + \varepsilon_i \qquad\qquad VIII.22$$

for b and K using weighted nonlinear regression, where W is the average moisture content used in an experiment. The parameter a was solved for as:

$$a = 1 - bW \qquad\qquad ViII.23$$

based on the specification that the average of the M.C. correction terms is 1.0.

At 40 percent M.C. vapor competition effects were virtually absent for binary and ternary sorption experiments (Table VIII.6). Of the three vapors, only p-xylene had its partition coefficient reduced (at the 95 percent confidence level) in binary and ternary mixture. At 16.1 percent M.C. (Table VIII.7), however, several mixture effects were observed after the moisture content correction as follows. The sorption of toluene was reduced by both PXYL and TBENZ. PXYL was reduced by TBENZ, which was in turn reduced by PXYL. It appears that the larger sorbates, based on molecular surface area, can reduce the sorption of the smaller sorbates, eg. toluene. Additionally, the larger sorbates, PXYL and TBENZ, are preferred over toluene (see Section VII) which gives them further competitive advantage. The more strongly a compound is sorbed the more potential it has to affect others.

217

TABLE VIII.6   SORPTION OF MIXTURES OF TOLUENE, P-XYLENE AND
TBENZ AT APPROXIMATELY 40 PERCENT M.C.

	M.C.	95 % Confidence Interval	$K*10^3$ (dimensionless)	95% Confidence Interval	r^2 (weighted)
Single vapor					
toluene	55.1	(53.2,56.9)	3.92	(3.32,4.51)	0.998
p-xylene	56.5	(54.9,58.1)	2.21	(2.08,2.34)	0.997
TBENZ	48.6	(47.5,50.9)	0.783	(0.629,0.937)	0.996
Binary vapor					
toluene	39.6	(39.4,39.8)	4.57	(4.15,4.98)	0.999
p-xylene			1.78	(1.66,1.90)	0.999
toluene	38.5	(38.3,39.0)	2.10	(-.20,4.40)	0.977
TBENZ			0.646	(0.584,0.708)	0.997
p-xylene	38.4	(38.3,38.6)	1.74	(1.39,2.09)	0.997
TBENZ			0.610	(0.520,0.700)	0.998
Ternary Vapor					
toluene	36.2	(36.1,36.4)	5.01	(3.54,6.48)	0.987
p-xylene			1.60	(1.45,1.76)	0.999
TBENZ			0.740	(0.661,0.819)	0.997

TABLE VIII.7   SORPTION OF MIXTURES OF TOLUENE, P-XYLENE AND 1,3,5-
TRIMETHLYBENZENE CORRECTED TO 16.1 PERCENT M.C.

	M.C.	95% Confidence Interval	$K*10^3$	95% Confidence Interval
Single vapor				
toluene	16.37	(16.20,16.55)	7.89	(6.63,9.15)
p-xylene	16.55	(16.42,16.68)	8.70	(6.74,10.66)
TBENZ	17.10	(16.65,17.55)	5.44	(3.84,7.04)
Binary vapor				
toluene	15.82	(15.73,15.91)	4.74	(4.18,5.29)
p-xylene			6.37	(5.67,7.07)
toluene	15.17	(14.56,15.77)	3.99	(3.03,4.96)
TBENZ			2.83	(0.72,4.94)
p-xylene	16.15	(15.48,16.83)	2.53	(1.05,4.01)
TBENZ			2.15	(1.20,3.10)
Ternary vapor				
toluene	16.10	(16.04,16.18)	5.35	(5.07,5.63)
p-xylene			8.59	(7.63,9.54)
TBENZ			7.47	(4.06,10.88)

E. SUMMARY AND CONCLUSIONS

Vapor competition was explored for four different moisture regimes: oven dry, 12-16 percent M.C., 20 percent M.C. and 40 percent M.C. On oven-dry sorbent, vapor competition occurred between mixed sorbates. This may be anticipated based on the observed competition of water with organic sorbates under the conditions of incomplete surface coverage (see Section III). As more water is added, there are fewer sites remaining over which the organic vapors may compete, therefore mixture effects on sorption become less obvious. The trend of decreasing competition with increasing moisture content continues well beyond monolayer coverage as observed for the experiments involving toluene, PXYL, and TBENZ at 16 percent M.C. and CF and TCA at 12.5 percent M.C. There may be intense competition over the few remaining sites under partially dry conditions, yet the net effect of this competition may not be readily observable if the sites involved account for only a small portion of total sorption.

After sufficient water is present to allow significant vapor dissolution, vapor sorption may be enhanced as well as impeded by other vapors due to intermolecular interactions not described by Henry's law. This was evident from the factorial screening experiments on solvents and fuels. Factorial experiments at 20 percent M.C. revealed complex binary and ternary interactions. Sorption of most individual components of a fuel mixture, at this moisture content, was enhanced by the presence of the other components in the fuel. The factorial studies on solvents showed that sorption could be either reduced or enhanced by cosorbates, depending on the sorbate combinations. From Section III, 20 percent moisture content is near the boundary of the region where Henry's law begins to control sorption for both the alumina and coated alumina used in this study. Yurteri et al., (1987) used factorial experiment similar to the one employed here to study the effect of composition on Henry's law. They found that dissolution of compounds into water by Henry's law was influenced by solute mixture and that solutes display complex interactions such as those observed in the factorial experiments of this study.

The coated alumina at 16 percent M.C. and the uncoated alumina at 12.6 percent moisture content showed very little influence of sorbate mixture. Within this moisture content region dissolution of vapor is thought not to play a major role in sorption since water films at this moisture content are anticipated to be highly structured (Grim, 1968) and will tend to exclude nonpolar organic compounds. In addition, the moisture content correction that best described this data bore no resemblance to a Henry's law correction. Within this moisture region, sorption is controlled neither by competition for an exposed surface nor dissolution into water films. Accumulation of nonpolar compounds as an

organic film at the air/water interface may be the primary cause of cosolvent effects at these moisture contents. Interactions between organic molecules sorbed at the air/water interface may approximate those attributed to activity effects in the hydrocarbonaceous phase. The large effect of the activity coefficient in the hydrocarbon phase on the dissolution of hydrocarbon mixtures was reported by Burris and MacIntyre (1985), Banerjee (1984), Groves (1988), and Leinonen and Mackay (1973).

Partitioning of vapors at higher moisture contents, such as the 40 percent M.C. used for the three aromatics, toluene, PXYL and TBENZ, showed no affect of cosorbates at the 99 percent confidence level. This may be due to the fact that there is enough water present to accommodate all the sorbates without activity effects. By extension of the solvophobic theory, vapor competition effects may perhaps be more readily observable at this moisture content at higher cosorbate concentrations.

SECTION IX

TRANSPORT OF ORGANIC VAPORS IN THE SUBSURFACE

By: S.K. Ong, T.B. Culver and L.W. Lion

A. INTRODUCTION

Volatilization from the soil surface has long been recognized as one of the important pathways for the movement and attenuation of organic pesticides in the subsurface (ex. Spencer et al., 1973). Recently, with the discovery of gross contamination of groundwater by volatile organic compounds (VOCs) such as solvents and fuels, knowledge regarding the movement of organic vapors in the subsurface has been extended to consideration of transport and the interphase distribution of these compounds. The importance of organic vapor movement in the subsurface is evidenced by the successful use of shallow soil-gas sampling techniques to estimate the extent of groundwater pollution (Marrin and Kerfoot, 1988) and the use of venting techniques to remediate contaminated aquifers (Baehr et al., 1989).

A variety of models to predict the movement of VOC's have been developed. Several of the currently available vapor-phase transport models are described in Table IX.1. The physical-chemical and biological features incorporated in each model are summarized. The capabilities and limitations of different modelling approaches are discussed below.

The early models developed by soil physicists to estimate movement of organic compounds predicted the loss of pesticides from the soil surface by volatilization (ex. Hamaker, 1972; Mayer et al., 1973). These models may be classified as emission models. Subsequent model development has provided greater flexibility in that spatial concentrations within the subsurface and biological and chemical processes that affect the fate of the organic vapors have been incorporated. Jury et al. (1983) developed a one dimensional analytical screening model that included linear solid-liquid partitioning, liquid-vapor partitioning (Henry's Law), and biodegradation within a uniform soil moisture profile. Adsorption was assumed to attain instantaneous equilibrium while gas phase advection and effects of vapor density gradients were not considered. In this model, the retardation of pollutants is through aqueous phase partitioning effects. Vapor-phase adsorption studies by Peterson et al. (1988) and as described in Section II, III and V have shown that sorption reactions other than that occurring in the aqueous phase (ex., vapor sorption at the water-air interface and direct sorption of vapors to mineral surfaces) may be important under certain moisture conditions.

TABLE IX.1 VAPOR TRANSPORT MODELS

REFERENCE / Features:	1	2	3	4	5	6	7	8	9	10	11	12	13	14	15
Mohsen et al., 1980	2	√	√										√		
Weeks et al., 1982	1	√	√			√	√						√		
Jury et al., 1983	1	√		√	√	√	√			√					
Stephanatos, 1985	2	√	√	√	√	√						√	√		
Abriola and Pinder, 1985	1	√	√		√	√	√					√	√	√	√
Pinder and Abriola, 1986	2		√		√	√	√	√				√	√	√	√
Springer, 1986	2		√			√	√								
Baehr & Corapcioglu, 1987	1	√	√		√	√	√	√			√		√	√	
Baehr, 1987	2	√	√		√	√	√	√					√	√	
Metcalfe & Farquhar, 1987	2	√	√		√	√							√		√
Shoemaker et al., 1990	2		√		√	√	√	√	√		√				
Sleep & Sykes, 1989	2	√	√	√	√	√				√		√	√	√	√
Culver et al., 1989	2		√		√	√	√	√	√				√	√	√
Hutzler et al., 1987	1	√	√	√	√	√	√			√					

List of Features:

1 - Dimensions
2 - Multicomponent (pollutant)
3 - Diffusion, vapor phase
4 - Advection, vapor phase
5 - Diffusion, aqueous phase
6 - Advection, aqueous phase
7 - Dissolution (Henry's Law)
8 - Sorption at solid-liquid interface
9 - Vapor sorption other than 7 & 8
10 - Mass transfer effects
11 - Biodegradation
12 - Variable moisture contents (precipitation)
13 - Spatial heterogeneity
14 - Immiscible phase
15 - Density dependent gas flow

223

Peterson et al.(1988) utilized Jury's screening model by adjusting the value of the solid-liquid partition coefficient to account for enhanced sorption of vapors. These calculations showed greater retardation of volatile pollutants due to the effect of vapor-solid partitioning. This work was extended by Shoemaker et al. (1990) who included a separate partition coefficient for vapor sorption and developed a two-dimensional analytical solution. In a sensitivity analysis, vapor-phase parameters such as vapor diffusion coefficient, Henry's Law constant and sorption from the vapor phase were found to be important with regard to transport. The recent work of Culver (1989) extended the conceptual consideration of vapor partition coefficients to a numerical model and allowed the moisture dependence of this parameter to be included.

Other models such as the two-dimensional finite-difference model developed by Stephanatos (1985) for the unsaturated zone included advection for the aqueous and vapor phase while dissolution of organic vapor was governed by Henry's Law (assuming instantaneous equilibrium) but sorption at the solid-liquid interface and vapor-phase sorption effects were neglected. Transport of organic vapors were found to be strongly affected by the vapor-phase diffusional parameters. Similar results by Weeks et al. (1982) and Springer (1986) showed that, in arid regions, vapor diffusion is an important transport mechanism. The one-dimensional transport model of Weeks et al. (1982) verified tortuosity values for the diffusion of chlorofluorohydrocarbons which were calculated using theoretical and empirical relationships. However, Weeks et al. (1982) found that the computed tortuosity was dependent on the solid-liquid partition coefficient used. In their study, a uniform solid-liquid partition coefficient was assumed for the entire soil profile. Springer (1986) developed a two-dimensional finite-element model that predicted the vapor-phase movement of a pollutant. This model incorporated the apparent vapor diffusion coefficient as defined by Weeks et al. (1982).

A multi-component hydrocarbon mixture transport model was developed by Baehr and Corapcioglu (1987). This one-dimensional finite-difference model included biodegradation and aqueous-phase transport of pollutants in the presence of a constant vertical water flux and uniform moisture content. The model was extended to a two-dimensional system by Baehr (1987). Abriola and Pinder (1985) developed a one-dimensional finite-difference model which included immiscible organic flow and equilibrium interphase transfer between three phases ie. the vapor phase, water phase and the immiscible organic phase. Pinder and Abriola (1986) extended this work to two dimensions and included solid-liquid sorption.

The common assumption that gas phase advection is negligible for modeling vapor-phase transport was questioned by Pinder and Abriola (1986). Kell (1987) observed that

advective transport may be significant in laboratory studies. However, work by Kreamer et al. (1988) suggested that vapor-phase advection is small and can be neglected unless air pumping is present or unless there is a rapidly fluctuating water table.

Most models have assumed that instantaneous equilibrium is achieved between the solid, liquid, and gas phases for the interphase transfer of volatile hydrocarbons. Work by Vilkner and Parnas (1986) discussed the need to consider mass transfer between phases as a possible rate limiting step in the transport of organic hydrocarbons in the subsurface. However, good prediction of vapor fluxes from column studies with an equilibrium-based model has implied that non-equilibrium mass transfer may not be significant (Baehr et al., 1989). A recent model, which accounts for the two above assumptions ie. vapor advection and nonequilibrium transfer, was recently developed by Sleep and Sykes (1989). Their simulations showed that the rate of partitioning between the liquid and gas phases significantly affected the transport predictions. Sorption processes were not considered in the model.

Although many models of vapor transport are available, verification of these models on a laboratory- or on a field scale is lacking. Furthermore, information on physical chemical processes affecting the movement of organic vapors, such as the rates of vapor-phase partitioning reactions and/or mass transfer rates of vapors, are limited. Equilibrium results of sorption of various organic vapors onto a variety of minerals and soils (Section II, III and VIII) show that vapor-phase partitioning onto soils is a function of moisture content and that, in the presence of mixtures, interactions resulting in enhancement or suppression of vapor sorption may occur. Below eight monolayers of water (as in semiarid regions or some surface soils), vapor sorption can be significant. Values two to four orders of magnitude larger than those observed at higher moisture contents (such as field capacity) can be attained.

In this section, we incorporate the equilibrium sorption results obtained in the previous chapters to investigate their impact on the transport of organic vapors. The calculations are limited to the impact of variable vapor sorption on movement of organic vapors since predictive equations for incorporating the effects of vapor interaction have not been developed. A two-dimensional transport model that includes variable soil moisture content is employed. The importance of the vapor transport and the effect of various chemical parameters in attenuating transport are discussed.

B. DESCRIPTION OF TRANSPORT MODEL

Movement of organic vapors in the subsurface was calculated using the two-dimensional transport model VOCWASTE (Culver, 1989). This model is a modification of the finite-element model developed by Yeh (1987 and 1988). vapor-phase transport along with variable vapor sorption were incorporated as a modification to the original model. This model is presently the only numerical code which specifically considers the sorption reactions of vapors and their dependence on moisture content.

The original contaminant transport model consisted of two parts: FEMWATER and FEMWASTE. The FEMWATER program (Yeh, 1987) predicts the changes in the potential heads and in volumetric water contents due to water fluxes in variably saturated systems. Since VOCWASTE assumes advection occurs only in the aqueous phase, no fundamental changes were needed in FEMWATER. Volumetric water contents and Darcy's velocities computed by FEMWATER are used as inputs to the contaminant transport model FEMWASTE (Yeh, 1988). FEMWASTE describes the movement of the contaminant in the aqueous phase for both saturated and unsaturated zones. Aqueous-phase sorption and biodegradation of the contaminant are included in the model. However, FEMWASTE does not include any vapor transport, and the code was extensively modified to include vapor-phase transport and sorption. The modifications and simulations which employ VOCWASTE have been described by Culver (1989) and Culver et al. (1990). A brief overview of FEMWATER and VOCWASTE is presented here.

Water flow in a variably saturated media is described in FEMWATER by:

$$\frac{d\Theta}{dh}\frac{\partial h}{\partial t} = \nabla \cdot \left[K(\Theta) \cdot (\nabla H) \right] + q \qquad \text{IX.1}$$

where h = pressure head (L)

H = $h + z$ = total head (L)

$K(\Theta)$ = hydraulic conductivity tensor (L/T)

Θ = volumetric water content (L^3/L^3)

q = source/sink (L^3/L^3-T)

$\dfrac{d\Theta}{dh}$ = specific moisture capacity (L^{-1})

Assumptions made for this equation are that the soil matrix and the carrier fluid are incompressible.

226

The modified equation for contaminant movement in VOCWASTE which includes vapor-phase movement is given by:

$$\frac{\partial C_T}{\partial t} = - \frac{\partial V_z C_T / R_L}{\partial z} - \frac{\partial V_x C_T / R_L}{\partial x}$$

$$+ \frac{\partial}{\partial x}\left(\Theta D_{Hxx} \frac{\partial C_T / R_L}{\partial x} + \Theta D_{Hxz} \frac{\partial C_T / R_L}{\partial z} \right)$$

$$+ \frac{\partial}{\partial z}\left(\Theta D_{Hzx} \frac{\partial C_T / R_L}{\partial x} + \Theta D_{Hzz} \frac{\partial C_T / R_L}{\partial z} \right)$$

$$+ \frac{\partial}{\partial x}\left(a D_G \frac{\partial C_T / R_G}{\partial x} \right) + \frac{\partial}{\partial z}\left(a D_G \frac{\partial C_T / R_G}{\partial z} \right) + M \qquad \text{IX.2}$$

where C_T = $\Theta C_L + a C_G + C_L K_d \rho_b + C_G K_{SG} \rho_b$ = total mass of contaminant in a volume of soil

C_T = $R_{SL} C_{SL} = R_L C_L = R_G C_G = R_{SG} C_{SG}$

R_L = $\rho_b K_d + \Theta + a K_H + \rho_b K_H K_{SG}$

R_G = $\rho_b K_d / K_H + \Theta / K_H + a + \rho_b K_{SG}$

R_{SG} = $\rho_b K_d / K_H K_{SG} + \Theta / K_H K_{SG} + a / K_{SG} + \rho_b$

R_{SL} = $\rho_b + \Theta / K_d + a K_H / K_d + \rho_b K_H K_{SG} / K_d$

C_L = aqueous concentration (M/L^3)

C_G = gaseous concentration (M/L^3)

C_{SL} = mass sorbed per unit mass of sorbent due to aqueous sorption (M/M)

C_{SG} = mass sorbed per unit mass of sorbent other than aqueous sorption and dissolution into soil water eg. vapor-liquid sorption, and condensation

K_d = saturated soil-water partitioning coefficient (L^3/M) = $K_{oc} f_{oc}$ = C_{SL}/C_L

K_{oc} = aqueous partitioning coefficient normalized with respect to organic carbon

f_{oc} = weight fraction of organic carbon in soil (M/M)

K_{SG} = vapor sorption coefficient (a variable function of the water content) = C_{SG}/C_G (L^3/M)

K_H = Henry's Law constant (dimensionless)

a = volumetric air content (L^3/L^3)

ρ_b = soil bulk density (M/L^3)

V_i = the Darcy's velocity in the ith direction (L/T)

D_{Hij} = the ij-th component of the hydrodynamic dispersion tensor including aqueous diffusion (L^2/T) = $D_{Mij} + D_L$

D_{Mij} = the ij-th component of the mechanical dispersion tensor (L^2/T)

D_L = aqueous-phase coefficient of molecular diffusion (L^2/T)

$$D_G = \text{vapor-phase coefficient of molecular diffusion } (L^2/T)$$

and M = source/sink input term $(M/L^3\text{-}T)$.

The vapor sorption term K_{SG} accounts for sorption other than at the liquid-solid interface and dissolution into soil water. As observed in Sections III and IV, sorption other than these two processes may occur depending on the moisture content of the soil and the vapor concentrations. Multivapor interactions, as observed in Section VIII, are not included in the model. The model assumes all partition equilibria obey local equilibrium. K_{SG} is computed from the following equation which is a rearrangement of Equation III.10:

$$K_{SG} = K_d{}' - K_d/K_H - (\text{Moisture Content } \%)/(100 \; K_H \; \gamma \; \rho) \qquad \text{IX.3}$$

The Millington and Quirk (1961) equations were used to calculate the coefficients of diffusion through a porous media D_L and D_G:

$$D_L \, (\Theta) = \frac{\Theta^{10/3}}{\phi^2} \, D_{Lwater} \qquad \text{IX.4}$$

$$D_G \, (\Theta) = \frac{a^{10/3}}{\phi^2} \, D_{Gair} \qquad \text{IX.5}$$

where D_{Lwater} = aqueous diffusion coefficient in pure water (L^2/T)

D_{Gair} = diffusion coefficient in pure air (L^2/T)

and ϕ = $a + \Theta$ = porosity (L^3/L^3).

The coefficients for mechanical dispersion tensor were estimated by the following formulas (Bear, 1975):

$$D_{Mxx} = \frac{\alpha_T \, \bar{V} + (\alpha_L - \alpha_T) \left[\dfrac{V_x^2}{\bar{V}} \right]}{\Theta} \qquad \text{IX.6}$$

$$D_{Mzz} = \frac{\alpha_T \, \bar{V} + (\alpha_L - \alpha_T) \left[\dfrac{V_z^2}{\bar{V}} \right]}{\Theta} \qquad \text{IX.7}$$

228

$$D_{Mxz} = D_{Mzx} = \frac{(\alpha_L - \alpha_T)\dfrac{V_x V_z}{\bar{V}}}{\Theta}$$

<div align="right">IX.8</div>

where α_T = transverse dispersivity (L)

α_L = longitudinal dispersivity (L)

and $\bar{V}$ = $(V_x^2 + V_z^2)^{1/2}$.

Equation IX.2 was solved numerically using the Galerkin finite-element method with bilinear basis and weighting functions for each node. Finite-element equations and the computer algorithms for the transport model can be found in Culver (1989).

C. VOC TRANSPORT SIMULATIONS

Two transport simulations are presented below to illustrate the impact of vapor sorption on vapor transport and the attenuation of organic pollutants in the vadose zone. For the simulations, a region of contaminated soil is assumed to be present at either 4 or 10 meters below the ground surface and the domain is 15 meters deep ι is illustrated in Figure IX.1). The initial area of contaminated soil is assumed to be 2 meters square. Both simulations, therefore, approximate soils contaminated by underground storage tanks, or abandoned landfills. Boundary conditions for the domain of study (Figure. IX.1) are: a rainfall-seepage-volatilization boundary at the ground surface, and Neumann boundary conditions on all other sides. A grid of 575 elements was employed, consisting of 624 nodes.

In the first simulation, the effect of vapor-phase sorption on the transport of TCE is considered. The vapor sorption data for TCE obtained in Section II and III were empirically summarized with a regre sion model based on the specific surface area of the solids and the average number of monolayers of water coverage. As in section III, vapor-phase sorption is considered significant for moisture contents that provide less than eight monolayers but negligible for moisture contents that provide more than eight monolayers. The sorption data is illustrated in Figure IX.2 and the regression equation for the vapor sorption data is given below ($r^2 = 0.78$). Data from the sorption of TCE onto montmorillonite were excluded from the regression since the specific surface area of this mineral is not accurately known due to expansion of the clay.

<div align="center">229</div>

$$\ln (K_{SG}/S.A.) \; = \; -0.417 - 0.755 \ln \text{(layers of water)} - 0.28 \, [\ln \text{(layers of water)}]^2$$

$$- 0.304 \, [\ln \text{(layers of water)}]^3 \qquad\qquad \text{IX.9}$$

$$\text{for} \;\; 0.025 < \text{monolayers of water} \le 8$$

$$K_{SG} \; = \; 0 \qquad\qquad\qquad\quad \text{for} > 8 \text{ monolayers of water}$$

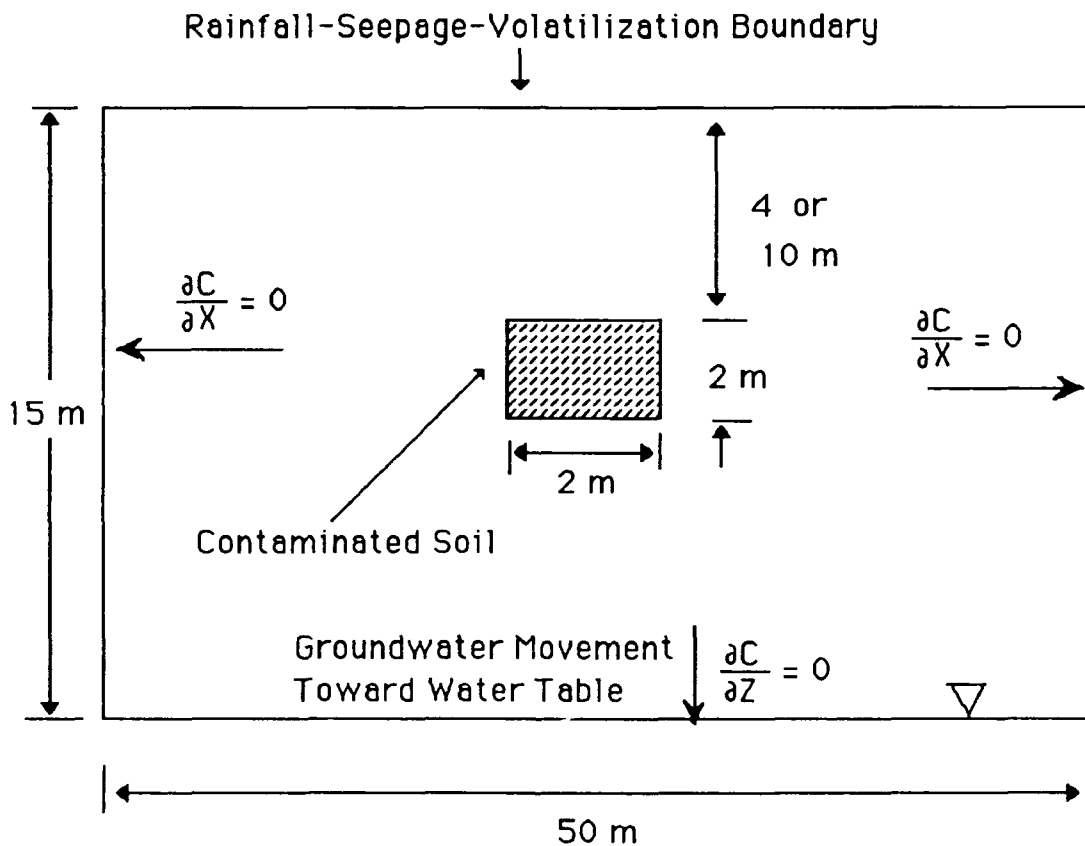where S.A. is the specific surface area of the solid.

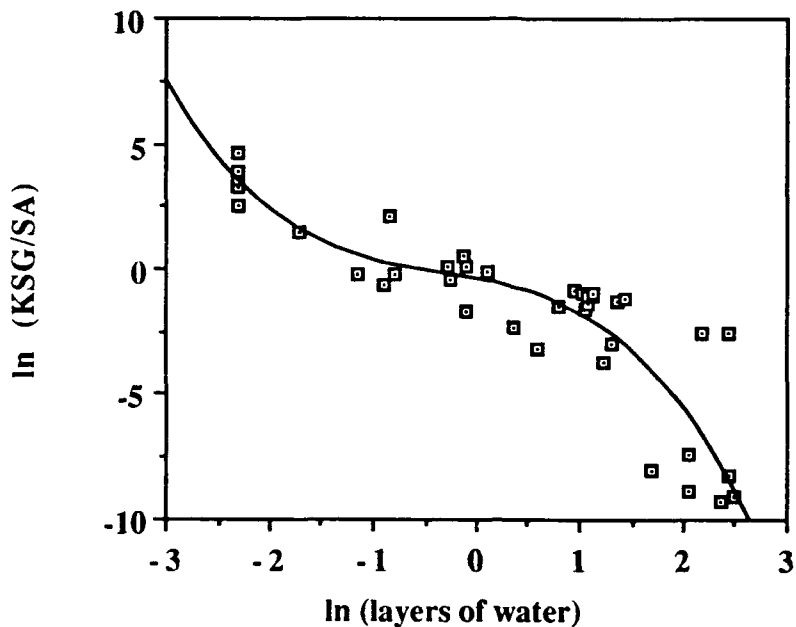Figure IX.1 Simulation Area and Boundary Conditions

Figure IX. 2 Sorption Data as a Function of the Average Number of Monolayers Of Water

The first simulations illustrate the impact of vapor-phase sorption under two different climatic conditions: (1) a humid environment where the soils are moist at about field capacity and (2) a dry environment, typical of a drought season, where soil close to the ground surface is fairly dry. A rainfall rate (above evaporation) of 0.2 cm/day (2.36 ins/month) is used for the humid condition while for the dry condition a rainfall of 0.02 cm/day (0.236 ins/month) is used. In one calculation an additional wet climatic condition with a rainfall rate of 0.4 cm/day was also used. The input parameters for the soil moisture characteristic curves were adjusted appropriately for each region. Input data for computer simulations are summarized in Tables IX.2 and IX.3.

The second set of computer simulations illustrate the sensitivity of transport of VOCs in the vadose zone to several physical-chemical properties of contaminants. Here, four common components of gasoline will be modeled ie., benzene, toluene, o-xylene and octane. A study domain similar to the first simulation is used (Figure IX.2) and it is assumed that the climatic condition is humid with a rainfall of 0.2 cm/day.

231

Table IX.2 SOIL INPUT PARAMETERS FOR COMPUTER SIMULATION

Symbol	Definition	Units	Value	References
ϕ	porosity	cm^3/cm^3	0.45	
ρ_b	soil bulk density	g/cm^3	1.35	
f_{oc}	soil organic content	g/g	0.0125	
K_{sxx}	xx-component of saturated conductivity	cm/day	100.2	US Dept. of Interior (1981)
K_{szz}	zz-component of saturated conductivity	cm/day	100.2	US Dept. of Interior (1981)
K_{sxz}	xz-component of saturated conductivity	cm/day	0.0	
Θ_{sat}	saturated volumetric water content	cm^3/cm^3	0.45	
Θ_r	residual water content	cm^3/cm^3	0.00	
α_T	transverse dispersivity	cm	40	
α_L	longitudinal dispersivity	cm	100	
d	depth of surface boundary layer	cm	0.475	Jury et al. (1983)
SA	surface area of soil	m^2/g	80.0	
ha	pressure head scaling factor	cm		
	wet region		3500	
	humid region		3200	
	dry region		2100	
β	characteristic curve exponent			
	wet region		1.2	
	humid region		1.0	
	dry region		0.5	

Characteristic Curves

$$\Theta\,(h) = \Theta_{sat} - (\Theta_{sat} - \Theta_r)\,(-h/ha)^{\beta} \qquad \text{if } h < 0.0 \text{ cm}$$
$$= \Theta_{sat}, \qquad \text{otherwise}$$
$$K\,(\Theta) = K_s\,[\,(\Theta - \Theta_r)/(\Theta_{sat} - \Theta_r)]^{\,4}$$

TABLE IX.3 PHYSICAL-CHEMICAL PARAMETERS OF VARIOUS VOCs

Symbol	Definition	Units	TCE	benzene	toluene	o-xylene	n-octane
D_{Gair}	diffusion coeff. in pure air	cm^2/day	7030	7460	6570	5980	4910
D_{Lair}	diffusion coeff. in pure water	cm^2/day	0.8304	0.095	0.084	0.075	0.064
K_H	Henry's Law Const.	-	0.397	0.222	0.270	0.200	121
K_{oc}	partition coeff.normalized with organic carbon	cm^3/g	61.1	65	259	691	73000
K_d	Saturated soil-water sorption coefficient	cm^3/g	0.76	0.8125	3.237	8.64	912
$C_{sat.}$	saturated aqueous solubility (20°C)	mg/L	1100	1780	515	175	0.7
$C_{vapor\,sat}$	saturated vapor concentration (20°C)	mg/L	432	319	110	40.7	86.5
	vapor pressure	mm Hg	60	76	22	7	13.9
ρ_L	liquid density (20°C)	g/mL	1.4655	0.8765	0.8669	0.8802	0.70
Am	molecular cross-sectional area	Å	30.67	30.53	34.34	37.36	45.6

D. RESULTS AND DISCUSSION

1. Effects of Vapor-Phase Partitioning

The moisture profiles generated by FEMWATER for the two different rainfall conditions are shown in Figure IX.3. Under dry climatic conditions (0.02 cm/day), the volumetric moisture content ranges from 0.08 cm^3/cm^3 (18 percent saturation) at the ground level to about 0.36 cm^3/cm^3 at 15 meters (80 percent saturation). For a soil with a specific surface area of 80 m^2/g, the number of monolayers of water at 0.8 cm^3/cm^3 volumetric moisture content is approximately 2.6. For a rainfall of 0.2 cm/day, the

moisture content at the ground level is ≈ 0.22 cm^3/cm^3 (49 percent saturation or ≈ 7 monolayers) and increases to about 0.44 cm^3/cm^3 at 15 meters (98 percent saturation). The moisture content profiles generated by FEMWATER are illustrative for the purposes of this example.
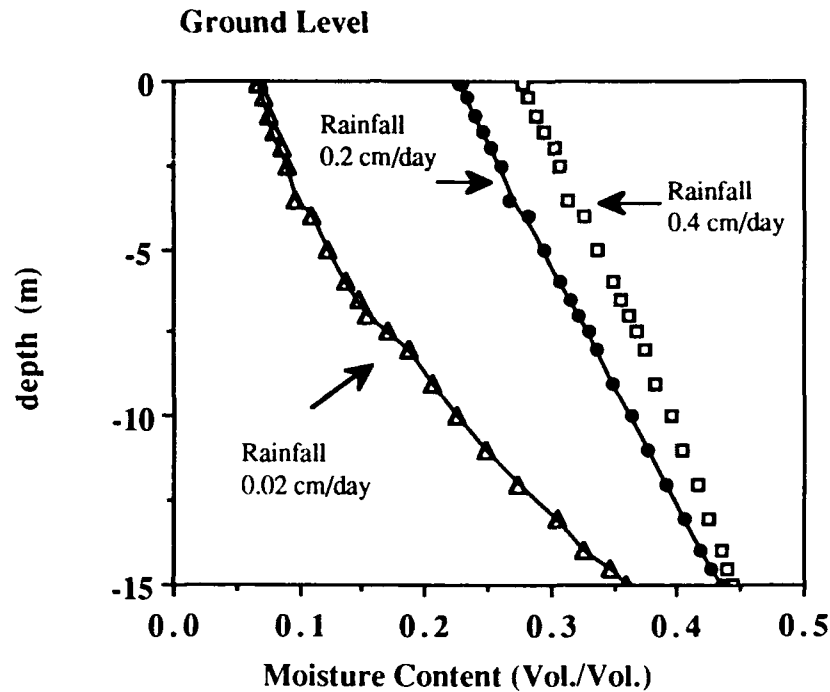
Ground Level

Figure IX. 3 Volumetric Moisture Content Profile

With TCE contaminated soil assumed to be 10 meters below the surface, volatilization of TCE over a period of 8 years was computed for the two different climatic conditions. Figure IX.4 shows that the amount of TCE which is volatilized under dry conditions is less than that under wetter conditions. The 10 meters of relatively dry soil between the source and the volatilization flux at the surface acts a "buffer" from the volatilization loss. This result indicates that enhanced vapor-phase partitioning in a deep, dry, soil profile can play an important role in the retardation of organic pollutants in the subsurface. The above result is similar to that reported by Culver (1989).
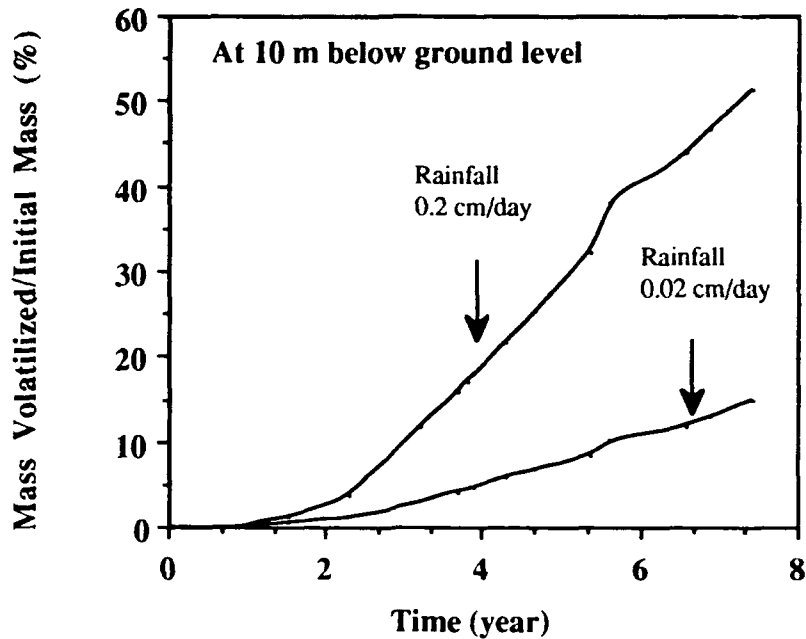
Figure IX. 4   Volatilization Loss for a 10-Meter Deep Source of TCE Under Different
Field Conditions

The volatilization simulations were repeated for a 4 year period with the source located at 4 m below the surface (Figure IX.5). Comparison of Figures IX.4 and IX.5 reveals that the total volatilization at a given time is greater for the shallow source since the upper region of the soil profile are strongly influenced by the volatilization flux. Contrary to the results when the source is deep, volatilization under dry conditions was greater than that under wet conditions for the 4 m deep source. Even though vapor-phase partitioning still occurs, the dominant physical parameter controlling volatilization in the upper soil is vapor diffusion. Vapor diffusion is much greater in a dry soil than a moist soil where it is restricted by soil moisture (see Equation IX.5). The increased partitioning from vapor sorption in the case of the 4 m deep source is not strong enough to counterbalance vapor diffusion and the impact of volatilization near the surface.
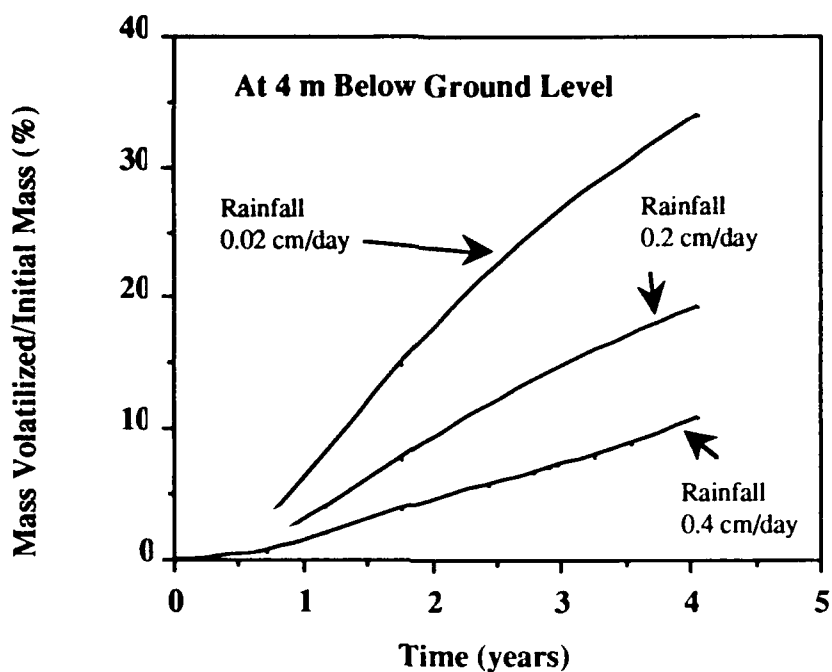
235

Figure IX. 5   Volatilization Loss for a 4-Meter Deep Source of TCE Under Different
Field Conditions

2.Effects of Physical-Chemical Parameters on Volatilization

Two of the important physical chemical parameters of pollutants which influence their loss by volatilization are Henry's constant and the aqueous-phase partition coefficient. Even though the diffusion of VOCs in the vapor-phase is about four orders of magnitude larger than that in the aqueous phase, the diffusion coefficients for most organic vapors are of similar magnitude. Therefore, although the magnitude of the vapor-phase diffusion coefficient indicates that the movement of pollutant in the vapor phase is important, differences in the transport between vapors do not result primarily from differences in their diffusion coefficients. For the following simulations, the contaminated soil was placed at 4 meters below ground level and the rainfall was 0.2 cm/day. At these moisture levels, vapor-phase sorption is negligible and was not a factor in the simulations.

To illustrate the effects of Henry's constant, two organic pollutants having similar K_{oc} values but differing K_H values were selected: TCE (K_{oc} = 61.1, K_H = 0.397) and Benzene (K_{oc} = 65, K_H = 0.222). As expected, the organic pollutant with the larger K_H value ie. TCE had the greater loss by volatilization from the soil. This result is shown in Figure IX.6

Three organic compounds with similar Henry's Constant but different K_{oc} values were used to illustrate the effect of aqueous-phase partitioning on volatilization. Aqueous-phase sorption reduces the mass fraction of pollutants in the aqueous phase and subsequently the vapor phase, from which volatilization occurs. The three compounds used in this simulation were: Benzene ($K_{oc} = 65$, $K_H = 0.222$), Toluene ($K_{oc} = 259$, $K_H = 0.270$) and o-xylene ($K_{oc} = 690$, $K_H = 0.20$). Results for volatilization of all three compounds are shown in Figure IX.7. As anticipated, o-xylene, which has the largest K_{oc} value, was found to volatilize the least in comparison with the other two compounds. This effect is similar to the chromatographic effect commonly observed for the transport of organic pollutants under saturated conditions.

The physical chemical characteristics of pollutants have an aggregate effect on their transport in the vadose zone and should not be treated individually in assessing fate. Simulation runs with n-octane, which has large K_H and K_{oc} values (121.1 and 73000 respectively), predicted less volatilization than o-xylene. The reason for this low rate is that most of n-octane (over 99.9 percent) was calculated to be sorbed from the aqueous phase, in spite of the large Henry's constant which would favor loss of this pollutant by volatilization.
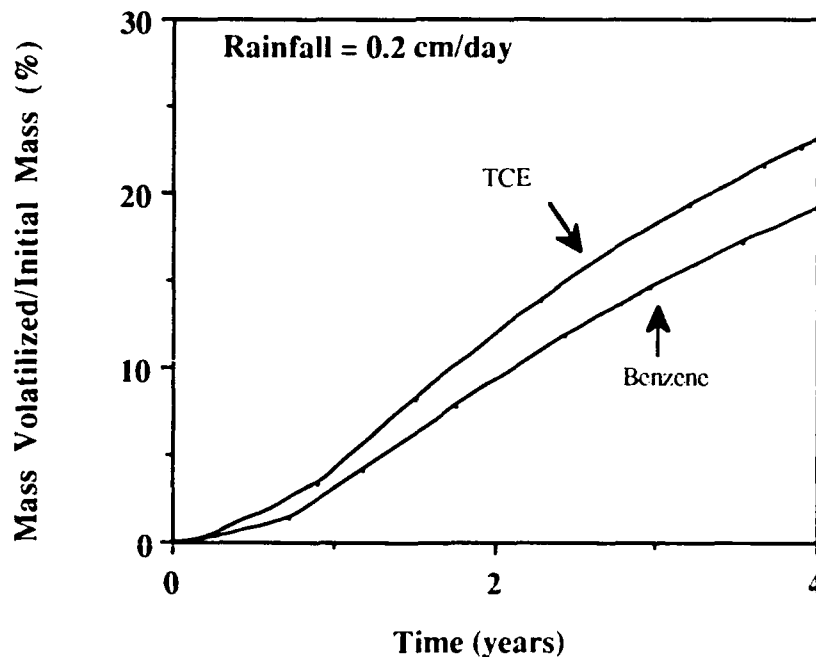

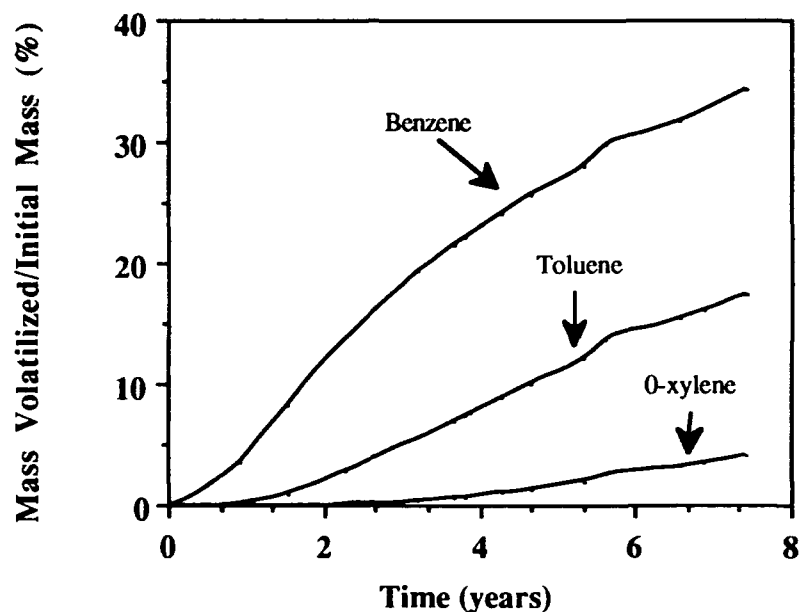Figure IX.6 Effect of Henry's Constant on Volatilization of VOCs.

Figure IX. 7 Effect of K_{oc} on the Volatilization of Selected Organic Compounds

---

E. CONCLUSIONS

Vapor-phase transport of organic pollutants is one of the important pathways in the distribution and attenuation of volatile organic compounds in the vadose zone. Simulation studies performed in this Section show that under dry conditions, vapor-phase partitioning of the organic pollutants may have a prominent effect on the transport of the pollutants. This result implies that it is possible for drier soils to act as a reservoir of VOCs. The partitioning of the pollutants between the three phases found in the vadose zone, ie. solid-liquid (aqueous-phase partitioning) and liquid-vapor (as governed by Henry's Law), was found to influence the movement of VOCs. Because of the interaction between sorption and volatilization, the influence of individual physical-chemical properties of vapors should not be considered in isolation. The overall effect of several properties including K_{oc}, and K_H should be taken into consideration in a.tempts to assess the movement of a particular pollutant.

SECTION X

CONCLUSIONS

The objective of this research was to characterize the sorption behavior of organic vapors onto unsaturated soils and soil minerals. Major conclusions are listed at the end of each Section of the report and are summarized here.

A. SECTION II

The effect of moisture content variations on the sorption of volatile organic compounds from the vapor phase was evaluated in Section II. Moisture profiles were established using laboratory columns packed with well-characterized sorbents consisting of oxide mineral phases with and without a coating of humic-type organic material. In addition, an unsaturated soil core profile was obtained in the field and characterized with respect to its sorptive characteristics.

Variation in the partition coefficients for TCE and toluene sorption on silica and humic-coated alumina versus moisture content showed the same pattern. Partition coefficients decreased sharply with increasing moisture, then gradually approached the value attained at saturation.

There was little correlation between partition coefficients and ambient moisture contents in individual samples from the unsaturated soil core profile. This was attributed to the sandy nature of the core (low specific surface area) and because it was obtained from a moist geographical region where unsaturated soils are likely to be near field capacity. Samples from the core profile showed variability in parameters other than moisture content and this obscured dependencies of partition coefficients on moisture levels. Removal of the surface sample in the profile from the statistical analyses increased correlation coefficients between the partition coefficients and moisture content.

Of the soil core parameters measured, the highest correlations were obtained between partition coefficients and organic carbon content, and partition coefficients and specific surface area. The limited range of soil parameters and partition coefficients in the soil core (below the surface sample) restricted inferences regarding the influence of specific soil properties on vapor sorption.

239

B. SECTION III

In Section III, the influence of variation in moisture content was further evaluated by measurement of partition coefficients for TCE vapor onto several common soil minerals at low TCE vapor pressure. Partition coefficients of oven-dried solids were usually several orders of magnitude higher than when the solid was moist. With oven-dried solids, surface area was found to be an important indicator of the sorptive capacity of TCE vapor. Observations of partition coefficients and thermodynamic data as a function of moisture content resulted in the identification of three distinct regions of vapor behavior. Sorption mechanisms were hypothesized for each region based upon known surface coverage by water, the observed enthalpy change for TCE partitioning relative to that for TCE condensation or dissolution, and the ability of saturated partition coefficients and TCE dissolution into water to explain the observed data.

Below a monolayer coverage by water, direct sorption of TCE vapor on the solid surface is postulated to occur in competition with water. This hypothesis is supported by (1) the ability of sorbent surface area to remove most of the variance in oven dry partition coefficients, and (2) the observation that water was the preferred sorbate resulting in a rapid decline in the partition coefficients for TCE vapor with increasing mineral moisture content. This is consistent with the behavior which is anticipated based on the relative polarities of water and TCE sorbates and the hydrophilic nature of mineral surfaces.

Between a monolayer to 4- to 8 monolayers surface coverage of water molecules, it is proposed that TCE sorbs onto bound water on the surface of the soil. This is supported by enthalpy data for TCE sorption which are below values for TCE condensation or dissolution into bulk water. Since the water on the surface of minerals is reported to be highly structured within the moisture regime covered by this region, dissolution of TCE is either prohibited (TCE dissolution at one monolayer coverage by water is not possible by definition of the process) or impaired by salting-out effects.

From 4- to 8 monolayers of water molecules coverage to the water retention capacity of the sorbent, the dissolution of TCE into condensed water along with water-solid interface sorption is postulated to dominate TCE uptake. TCE sorption at the water-air interface was not detectable for most solids used in this study and TCE dissolution plus the saturated partition coefficient could account for all the observed partitioning within the uncertainty (95 percent confidence interval) of the data. Enthalpy data were comparable in magnitude to the values expected for TCE dissolution.

Application of Henry's Law to model TCE interaction with water condensed on the solid surface is possible only after 4- to 8 monolayers of water have formed. This condition may not be hold for soils in arid or semiarid regions or for the top surface soil layer in temperate regions on a seasonal basis.

C. SECTION IV

In Section IV, the sorption of TCE at high relative vapor pressures was evaluated onto a representative suite of porous and nonporous soil mineral phases in the presence and absence of water vapor. Sorption of TCE was greatly affected by the presence of water. For solids at 0 percent relative humidity, the relative TCE sorption isotherms were different for each surface, indicating that the sorbent surfaces have specific interactions with TCE. With increasing amounts of water on the surface of the solids, the amount of TCE sorbed was found to decrease. For porous solids like alumina and humic-acid-coated alumina, converting the amount of water and TCE sorbed to a volume rather than mass basis at different relative humidities resulted in substantial overlap of the isotherms. This result indicates that, at high TCE vapor pressures, vapor condensation plays an important role on porous sorbents in determining the amount of TCE sorbed. In contrast, the TCE isotherms obtained at different relative humidities for a nonporous sorbent (iron oxide) did not converge.

Addition of moisture onto humic acid resulted in sorption of large amounts of TCE in comparison to the humic acid at 0 percent RH and under saturated aqueous conditions. Expansion of the humic acid due to hydration and exposure of internal regions/pore volume for sorption/condensation is proposed as a possible explanation for the higher uptake of TCE at high relative humidity (80 percent). Although montmorillonite also expands with the addition of water, its sorption capacity for TCE decreased, indicating that the interlamellar pores were not readily available for the uptake of TCE.

D. SECTION V

In Section V, sorption of TCE was evaluated onto seven different soils selected to represent a broad spectrum of physical/chemical properties. Vapor-phase partition coefficients of TCE onto soils under oven-dried conditions were found to correlate well with the specific surface area, indicating that surface area can be used as a measure of the sorptive capacity under extremely dry conditions.

TCE vapor partition coefficients under air-dried conditions (68 percent relative humidity) and at field capacity were found to correlate well with organic carbon content of

the soils. The partition coefficients under air-dried conditions were about three times larger than the partition coefficients at field capacity. The vapor-phase partition coefficient of the seven soils at field capacity could be accounted for by two components: TCE dissolution into soil water, and TCE sorption at the soil-water interface. However, the higher sorption partition coefficients under air-dried conditions could not be accounted for by these components. This result indicates that TCE uptake processes other than vapor dissolution and saturated partitioning may be occurring at air-dried conditions. Soil organic matter is believed to swell in response to varying moisture contents. Under air-dried conditions such swelling may be adequate to reveal internal regions for binding of TCE. When more moisture is added as at field capacity, hydrophilic regions will be covered with water leaving hydrophobic regions for the sorption of TCE. Under these moisture conditions, organic matter could still function as a partition medium.

Contribution of TCE dissolution into soil water can be significant for soils with low organic matter contents such as aquifer materials. Use of the saturated partition coefficients as an approximation for vapor-phase sorption is valid only for soils that have moderately high organic contents and with moisture contents around field capacity. For example in a soil with 1.6 percent organic carbon, TCE dissolution in soil water would contribute about 15 percent to the total TCE uptake from the vapor phase at field capacity.

E. SECTION VI

Section VI considers the statistical difficulties that arise when fitting parameters to linear and nonlinear isotherms when adsorption is inferred from concentration differences. When the extent of sorption is determined from the concentration difference before and after the sorption process, isotherm fitting approaches must reflect the pattern of error expected in this type of data. Errors may be large, especially when the concentration difference observed, as well as the mass of sorbent, are small.

Current nonlinear regression practices for fitting the parameters of complex adsorption isotherms are questioned for the data in the low concentration range of the isotherm. When data in the linear, or near-linear, range are measured by concentration level difference, the isotherm expressed in terms of a concentration ratio is better suited for regression analysis, because concentration becomes the dependent variable and sorbent mass (which is known with high precision), acts as the predictor.

Nonlinear regression is hampered by correlation between the dependent and independent parameters conventionally used for the isotherm equation. A Golden Section method was shown to be superior for parametrizing nonlinear isotherms to experimental data. Weighting the data allowed the fitted curves and parameters obtained to reflect what

is known about the level of certainty at each data point. Weighting improved the consistency of predictions by each method by correcting for the effect of transformations on the dependent variable. Weighting was unable, however, to control for the errors which occur in the predictor variables, which explains why linearizations of the Langmuir equation and nonlinear regression on the isotherm equation did not perform as well as the Golden Section method. The agreement between the Langmuir and the B.E.T. isotherm fits for experimental data also supports the validity of the Golden Section regression method.

F. SECTION VII

The impact of sorbate properties on sorption of organic vapors onto unsaturated soils was examined in Section VII. The study involved examination of sorption under both dry and moist conditions. The differences in sorption under dry conditions were explained best by an inverse trend with the vapor pressure of the sorbates which were studied, perhaps because of vapor condensation in small pores. Log solubility was the best predictor for sorption at low (1.9 percent) moisture content. Therefore, the relative sorption behavior is influenced by the presence of water molecules even at partial water coverage of the sorbent.

The vapor-phase sorption of chlorinated hydrocarbons and the hydrocarbon components of fuels on moist humic-coated alumina was inversely related to the Henry's law constant of the vapor and directly related to its aqueous solubility. The dependency on solubility was consistent with predictions based on a conceptual analysis of the role of aqueous phase activity in the sorption of organic vapors. Since vapor uptake includes dissolution into soil water, vapor partition coefficients are anticipated to be directly proportional to solubility. This is the inverse of the solubility dependency observed for saturated partition coefficients.

The dissolution of vapors in the solid solution was adequate for describing uptake of the more soluble compounds but was not always sufficient to explain sorption of the n-alkanes. When the effects of dissolution into the moisture of the solid were removed, the octanol-water partition coefficient emerged as an important predictor of relative sorptive strength.

Sorption of VOCs in unsaturated soils appears to be a dual process controlled by polar attraction to mineral surfaces (under very dry conditions), dissolution into soil moisture, and sorption to soil organic matter. The relative importance of these processes for any given compound will depend on its solubility and octanol-water partition coefficient.

G. SECTION VIII

The influence of vapor mixtures on sorption was evaluated in Section VIII. Vapor interaction was explored for four different moisture regimes: oven dry, 12-16 percent moisture content, 20 percent moisture content and 40 percent moisture content. On oven-dry sorbent, competition occurred between mixed sorbates. This may be anticipated based on the observed competition of water with organic sorbates under the conditions of incomplete surface coverage (see Section III). A trend of decreasing competition with increasing moisture content was observed.

The coated alumina at 16 percent moisture content and the uncoated alumina at 12.6 percent moisture content showed very little influence of sorbate mixture. Within this moisture content region, dissolution of vapor is thought not to play a major role in sorption since water films at this moisture content are anticipated to be highly structured and will tend to exclude nonpolar organic compounds. In addition, the moisture content correction that best described this data bore no resemblance to a Henry's law correction. Accumulation of nonpolar compounds as an organic film at the air/water interface may be the primary cause of cosolvent effects at these moisture contents.

After sufficient water is present to allow significant vapor dissolution, vapor sorption may be enhanced as well as impeded by other vapors due to intermolecular interactions not described by Henry's law. This was evident in factorial screening experiments on solvents and fuels. Factorial experiments at 20 percent moisture content revealed complex vapor interactions. Sorption of most individual components of a fuel mixture, at this moisture content, was enhanced by the presence of the other components in the fuel. A comparable evaluation of solvents showed that sorption could be either reduced or enhanced by cosorbates, depending on the sorbate combinations.

Partitioning of vapors at higher moisture contents, such as the 40 percent moisture content used for the three aromatics, toluene, p-xylene and 1,3,5 trimethylbenzene, showed no affect of cosorbates at the 99 percent confidence level. This may attributable to the absence of activity effects. By extension of the solvophobic theory, vapor competition effects may be more readily observable at this moisture content at higher cosorbate concentrations.

H. SECTION IX

In Section IX, a numerical transport model was utilized to evaluate the potential impact of vapor-phase sorption on the transport of organic vapors in the unsaturated zone.

Simulation studies performed in this Section show that, under dry conditions, vapor-phase partitioning of the organic pollutants may have a prominent effect on transport. This result implies that it is possible for drier soils to act as a reservoir of VOCs. The partitioning of the pollutants between the three phases found in the vadose zone, ie. solid-liquid (aqueous-phase partitioning) and liquid-vapor (as governed by Henry's Law), influences the movement of VOCs. Because of the interaction between sorption and volatilization, the influence of individual physical-chemical properties of vapors should not be considered in isolation. The overall effect of several properties should be taken into consideration in attempts to assess the movement of a particular pollutant.

APPENDIX A. SUPPLEMENTARY BACKGROUND INFORMATION: SOIL MOISTURE REGIMES, REACTIONS OF VAPORS AND SORPTION MODELS

By: J.L. Swanger and L.W. Lion

A. INTRODUCTION

In this Appendix we discuss the range of moisture conditions which can be encountered in the vadose zone and consider the reactions which may result in uptake of volatile pollutants. Models which may be used to describe the adsorption equilibria of nonionic organics as vapors and as solutes are reviewed. This information serves as a background for discussion through out the report. Additional background material is provided in each section or the report as needed.

B. SOIL MOISTURE

Soil moisture is anticipated to be a major variable which affects the sorption of organic vapors. The factors influencing the moisture content of soils are briefly discussed here. The amount of moisture in a particular soil depends on the type of soil, the position relative to the water table and climatic conditions at the soil/air interface. Groundwater occurs in unsaturated and saturated zones below the soil surface (Figure A.1). In the saturated zone, virtually all soil pores are filled with water. The upper bound of the saturated zone in an unconfined aquifer is the water table, which is the surface of atmospheric pressure. The lower boundary is typically some underlying impermeable strata such as clay beds or bedrock. In the unsaturated zone, soil pores are partially occupied by air and partially by water.

The unsaturated zone can be further divided into three regions. The soil water zone extends from the surface down through the region occupied by roots. It varies in thickness depending on soil type and vegetation. The intermediate or vadose zone lies between the soil water zone and the capillary zone, described below. The intermediate zone can be nonexistent to 100 meters deep, depending upon the depth of the water table. The capillary zone extends from the water table up to the limit of capillary rise of soil water. The capillary rise depends on soil or rock particle size and on chemical composition of the soil pore water and the hydrophilic nature of the pore wall. It can range in thickness from a centimeter or less in gravel to 25 centimeters in a medium sand to 100 centimeters in clay (Todd, 1980).

Three different mechanisms control water in the unsaturated zone. Hygroscopic water is adsorbed from the air and forms a tightly held layer several molecules thick on soil particles. This hygroscopic or adhesion water is always present in the normal soil, but can be removed by oven-drying. Capillary water is held in small pores by surface tension. Gravitational water is water in excess of the other two types, and drains through the soil by gravity.
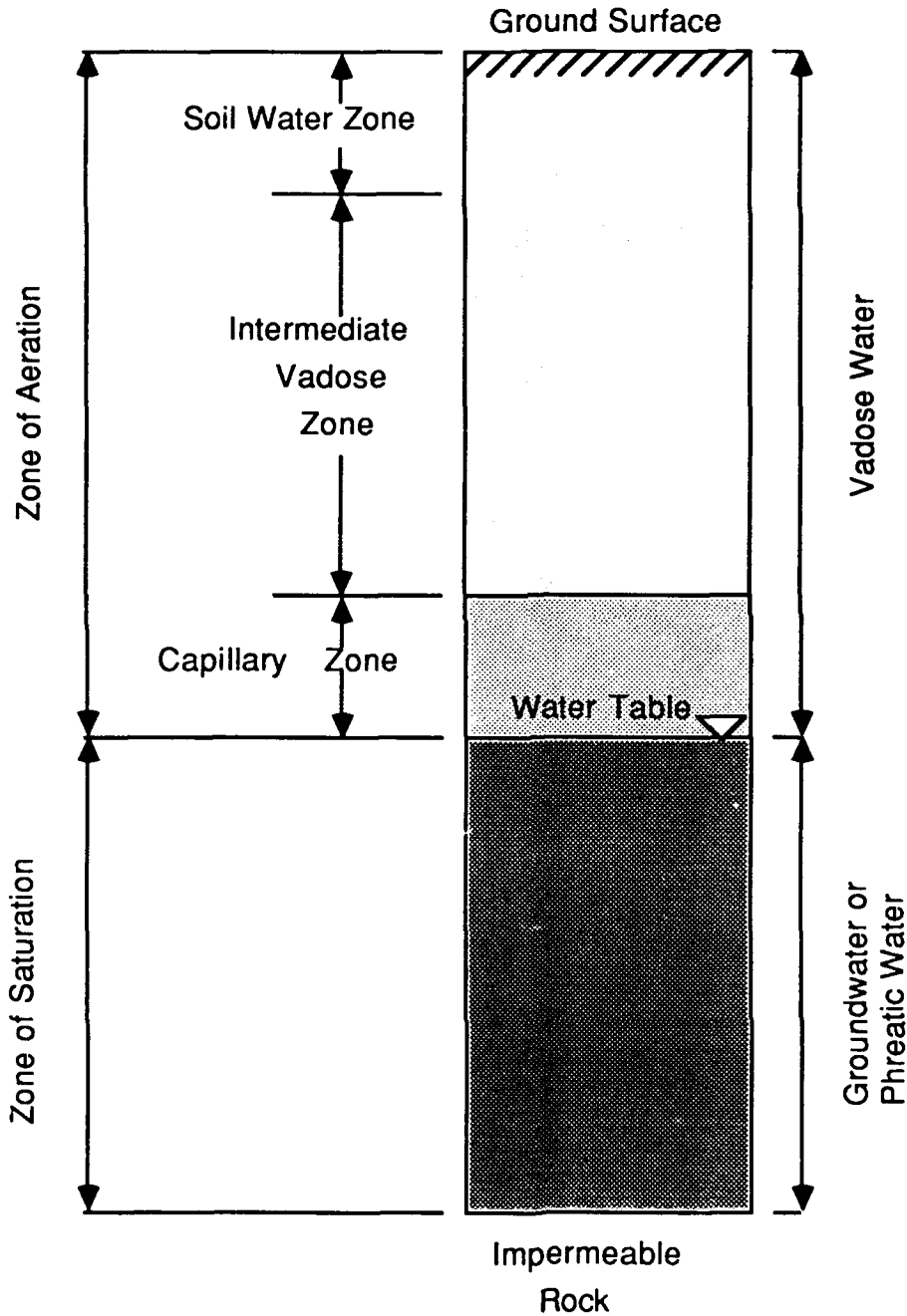

Figure A.1. Divisions of Subsurface Water (from Todd, 1980)

Moisture content in unsaturated soils is a function of the adhesive and capillary forces. A measurement of these forces, expressed in energy or pressure terms, is the matric potential of the soil. The matric potential is a negative pressure potential (relative to atmospheric pressure) because the capillary and adhesive forces that bind the water to soil lower its potential energy relative to that of bulk water. Matric potential is zero at and below the water table, where total water potential is positive due to hydrostatic forces. Soil moisture characteristic curves (Figure A.2) show the relationship between water content and matric potential for several soil types (Hanks and Ashcroft, 1980).
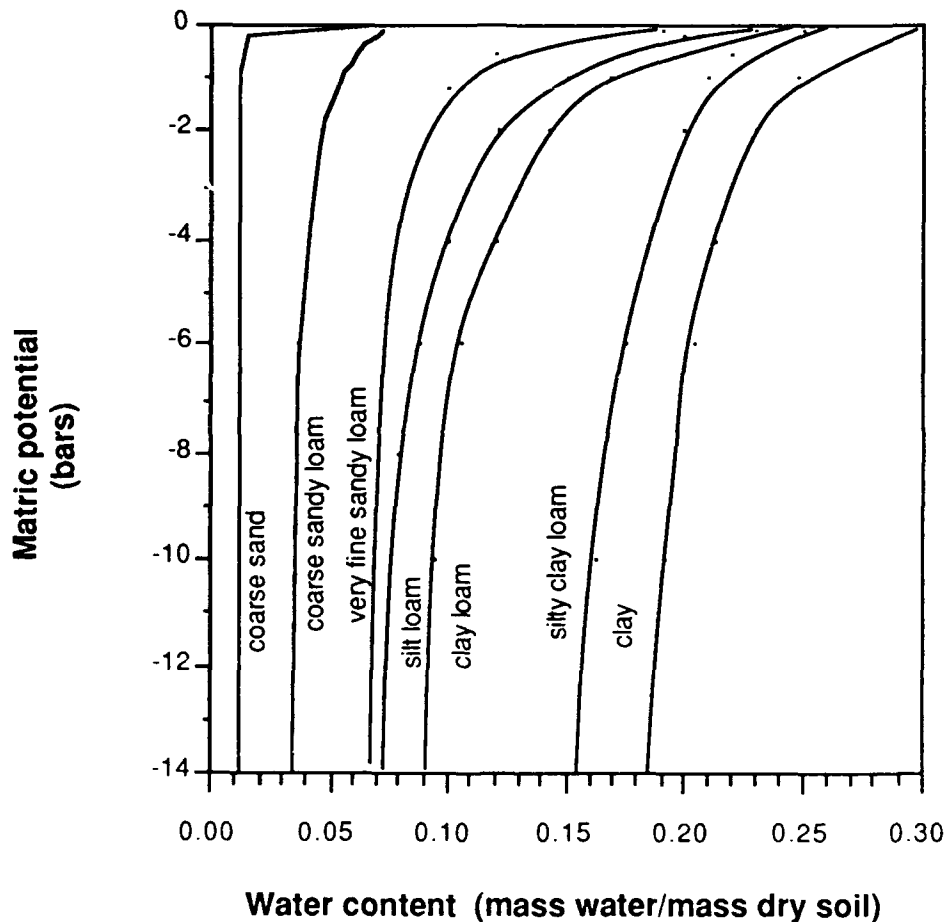

Figure A.2. Soil Moisture Curves for Several Types of Soil (from Hanks and Ashcroft, 1980).

When matric potential is low (near - 0.5 bars), a small change in matric potential causes a large change in water content, representing the emptying of larger pores as negative pressure is applied. As the soil dries, the matric potential needed to remove

additional water increases dramatically. The asymptotic nature of the curves at high matric potentials reflects the presence of hygroscopic water. For a well-aggregated, medium-textured soil, Foth and Turk (1972) reported that hygroscopic water was reached at a matric potential of -31 bars, and oven-dry soil at -10,000 bars. Figure A.2 shows that moisture content is largely a function of the soil components.

C. REACTIONS OF VOLATILE ORGANIC COMPOUNDS IN SOIL

There are many possible reactions for a volatile organic compound released below ground, as shown in Figure A.3. Because the compound is volatile, it will exist both in solution in soil moisture and in the vapor phase in the gas spaces in the unsaturated zone. The equilibrium between liquid concentration and gaseous concentration is governed by the Henry's Constant (H_c) for the compound. Sorption to the soil particles can occur from both the liquid phase and, the vapor phase, and under some circumstances, is governed by linear partition coefficients (K_d and K_d', respectively). The VOC can also partition into components dissolved in the soil water such as humic type molecules (Carter and Suffet, 1982). Another possible fate is the degradation of the VOC via microorganisms or chemical reactions in the soil.

The research presented in this report focuses on the abiotic reactions of sorption and volatilization. Other possible abiotic reactions include chemical degradation of organics through hydrolysis or oxidation-reduction reactions. Hydrolysis may or may not occur depending on the organic structure, and if it does occur, is likely to be very slow (Donigian and Rao, 1986). Abiotic oxidation-reduction reactions involving organics in the soil have not been well documented (Valentine, 1986).

Biological transformation of the test compounds TCE and toluene were not included as part of this st dy. TCE is not normally degraded by microorganisms under aerobic conditicns. TCE can be degraded aerobically by methanogenic organisms, but these are not present unless methane gas is available to stimulate their growth (Ghiorse and Wilson, 1988). TCE degradation under anaerobic conditions has been observed both in the field (Ghiorse and Wilson, 1988) and in laboratory studies (Vogel and McCarty, 1985). Toluene does degrade under aerobic conditions (Wilson et al., 1981; Ghiorse and Wilson, 1988), but this was not a factor in experiments performed in this study (see Section II).
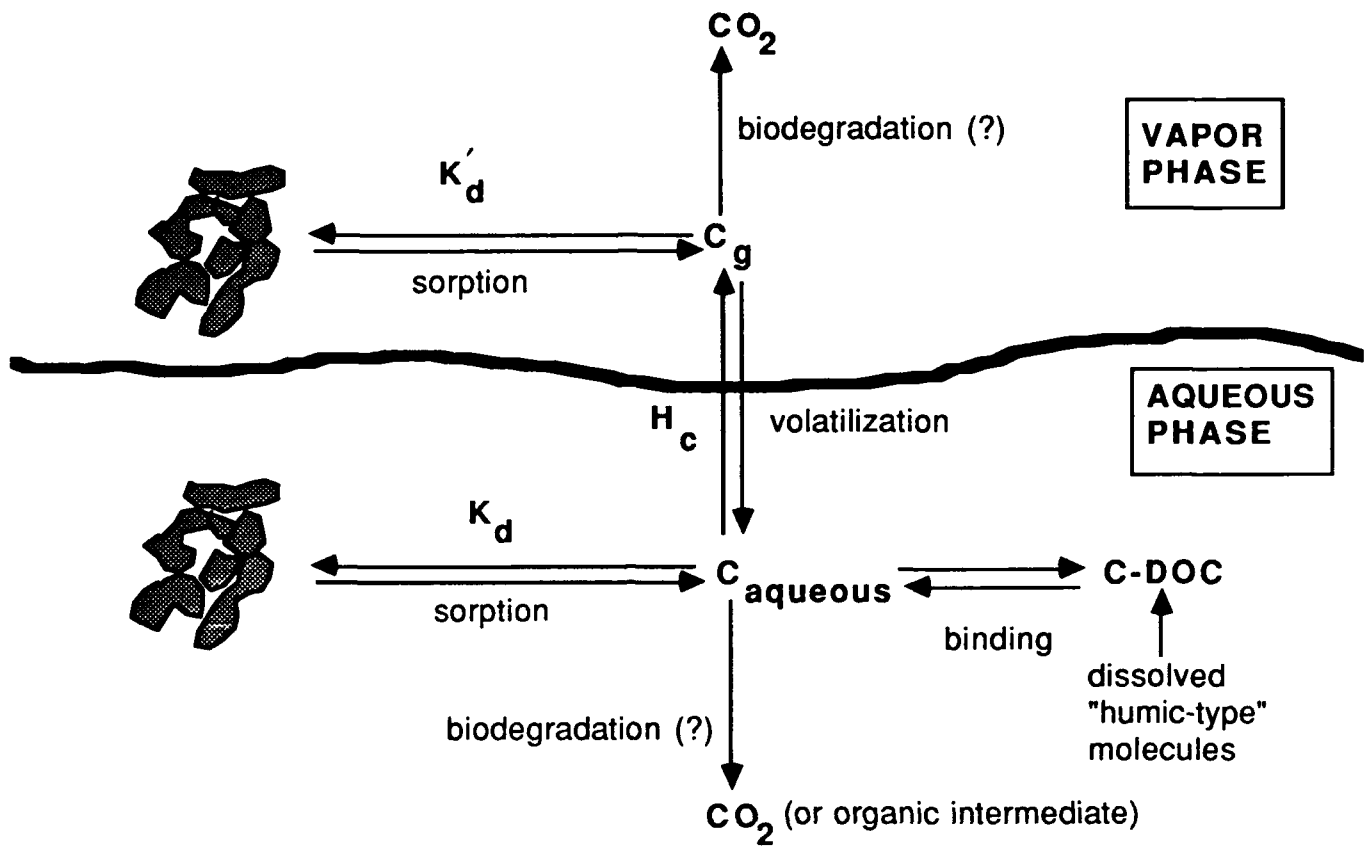
Figure A.3. Potential Reactions of a Volatile Organic Pollutant in Unsaturated and Saturated Aquifer Zones.

1.Volatilization

Volatilization in the soil environment is often defined as the loss of chemicals from surfaces into the vapor phase followed by movement to the atmosphere. Examined in this context, volatility is influenced by chemical properties of the compound in question, and by soil and environmental conditions affecting the rate of movement to the evaporating surface and into the atmosphere. (Spencer et al., 1973).

The scope of this study extends only to equilibrium conditions in the unsaturated zone, and not to transfer of pollutants to the atmosphere. Therefore, a narrower definition of volatilization is used. At equilibrium, volatilization relates to the partitioning between vapor and solution as described by Henry's Law:

$$C_G = H_c C_L \qquad\qquad\qquad A.1$$

where C_G is the concentration in gaseous phase (mass/volume)

              H_c is Henry's Constant (dimensionless)

              C_L is the concentration in the aqueous phase (mass/volume).

Another common form of Henry's Law is:

$$H = \frac{P_G}{C_L} \qquad\qquad\qquad A.2$$

where   H is Henry's Constant of the solute (m^3-atm/mol)

              P_G is the partial pressure of the gas (atm)

              C_L is the aqueous concentration (mol/m^3).

These two forms of Henry's Constants are interrelated by the Gas Constant, R, and absolute temperature, T :

$$H_c = \frac{H}{RT} \qquad\qquad\qquad A.3$$

Henry's Constants are characteristic of individual compounds, and can be measured experimentally or obtained from the literature (Mackay and Shiu, 1981; Lyman et al., 1982; Lincoff and Gossett, 1984). All other factors being equal, the higher the Henry's Constant, the larger the fraction of the compound that will occur in the gaseous phase.

2. Sorption

Sorption is the accumulation of gaseous or dissolved substances by solids. The solid phase is called the sorbent, and the gas or liquid is the sorbate. When the accumulation occurs on the solid surface, the process is adsorption. If molecules do not remain at the surface, but penetrate into the structure of the solid, the process is known as absorption. The term sorption encompasses both adsorption and absorption and is often used if the exact mechanism of interaction between sorbate and sorbent is unknown. In unsaturated soils, if the "solid" is any stationary immobile phase, then soil moisture is included. If this definition is used, then the sorption of vapors will include the contribution of their solubility in soil moisture such as water condensed in small pores.

Sorption has traditionally been divided into two categories (physical and chemical) based on strength of the attractive forces between sorbate molecules and the solid surface. Physical sorption refers to the attraction of sorbate molecules to sorbent through weak van

251

der Waals forces. Physically sorbed substances are free to move on the surface of the sorbent, and can form multiple layers. Physical sorption is considered to be completely reversible.

Chemical sorption (chemisorption) occurs as a result of a chemical reaction between the sorbate and sorbent. Because a chemical bond is formed, chemical sorption is much stronger than physical sorption, and is sometimes considered irreversible. Chemically sorbed molecules are thought not to move on the surface, and are limited to monolayer thickness. In the case of nonionic volatile organic compounds, coulombic attractions do not need to be considered (Voice and Weber, 1983).

Physical adsorption is usually characterized by a relatively low heat of adsorption, on the order of 1 to 10 kcal/mol for small molecules (Adamson, 1967). Heats of adsorption ranging from 15-50 kcal/mole indicate chemical adsorption (Voice and Weber, 1983). Physical and chemical sorption also differ in the specificity of the processes. Because of the chemical reaction, chemisorbed substances are bound to fixed sites on the sorbent. Physical sorption is nonspecific, in that it proceeds on all surfaces, with the extent dependent on temperature and pressure (Cerny, 1970). In some cases, distinguishing between types of sorption can be difficult, especially when dealing with the heterogeneous surfaces of natural sorbents. Actual sorption processes probably involve varying degrees of all types of interactions. In the absence of soil organic matter, physical sorption is considered the prevalent mechanism for adsorption of volatile nonionic organics, and will be examined in more detail below.

C. SORPTION MODELS

The conventional form for presenting sorption is to equate the quantity of sorbate taken up by a sorbent at equilibrium as a function of sorbate concentration or pressure. Because the extent of sorption is also a function of temperature, temperature is generally held constant, and the resulting relationship is called a sorption isotherm. Several models have been developed to describe the relationship between material sorbed and sorbate concentration or pressure, because no one model has been found to be generally applicable to experimental data from different conditions. Five different shapes of adsorption isotherm were proposed by Brunauer et al. (1940) and are illustrated in Figure A.4. Each shape reflects some unique condition described in the discussion which follows.
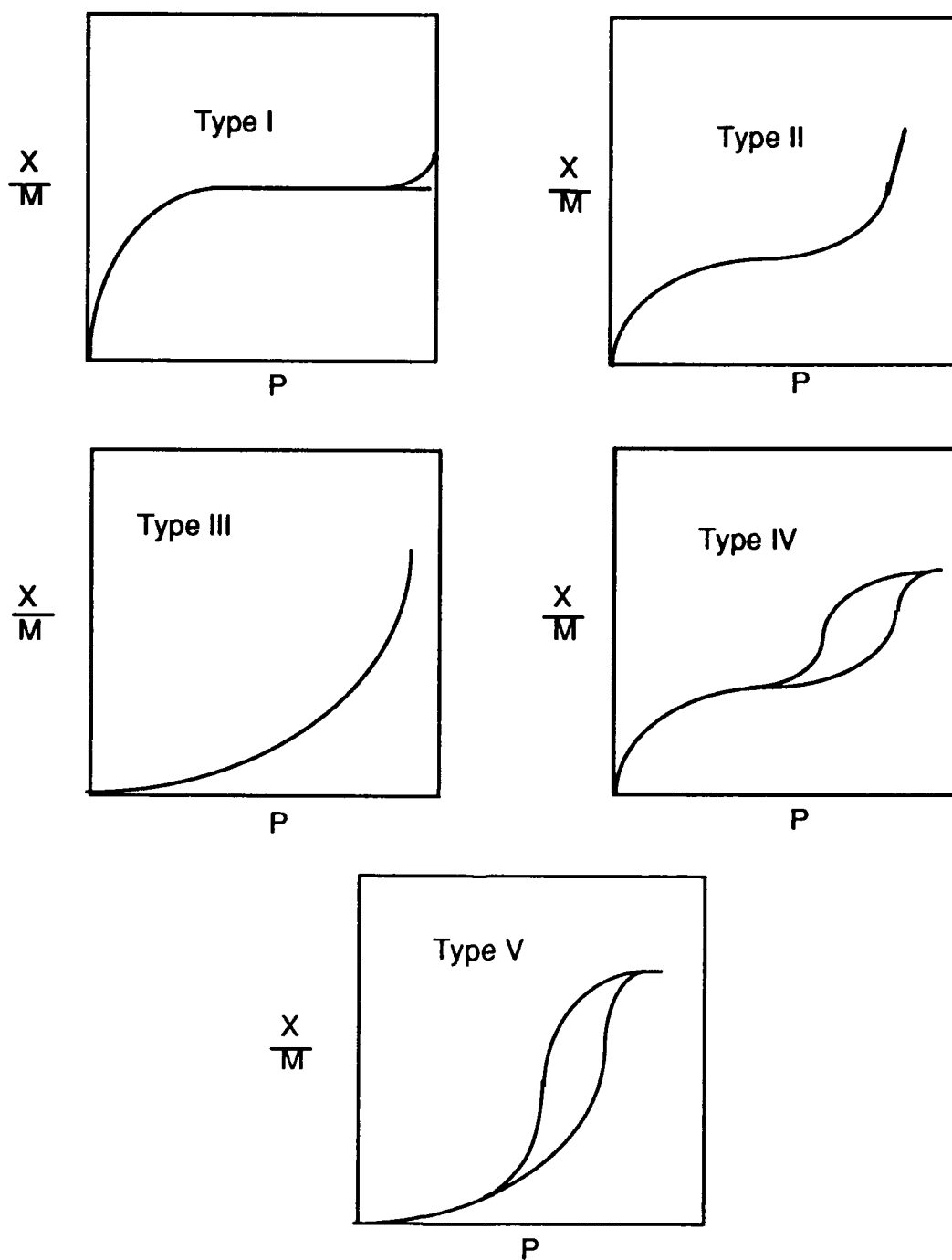
Figure A.4. Five Types of Adsorption Isotherm (after Brunauer et al., 1940). The Parameter, P, Represents Equilibrium Concentration Which May be Expressed in a Variety of Ways Including as the Pressure or Relative Pressure of Vapors.

253

The earliest sorption model was developed by Langmuir (1918) to describe the sorption of gases onto solids. The Langmuir equation assumes the following: energy of adsorption is constant and independent of surface coverage, adsorption occurs only on localized sites with no interaction between adsorbate molecules, and the maximum adsorption possible is a complete monolayer. These assumptions make the Langmuir equation most applicable to the process of chemisorption rather than physisorption, unless these assumptions are relaxed. The Langmuir equation may be written as:

$$\frac{X}{M} = \frac{(X/M)_{MAX} \, K \, C}{1 + K \, C} \qquad\qquad A.4$$

where:

      X = mass of sorbate sorbed

      M = sorbent mass

      K = constant

      C = equilibrium concentration.

      $(X/M)_{MAX}$ = maximum theoretical mass of sorbate per gram of

                    sorbent at monolayer coverage

A plot of equation A.4 results in a Type I isotherm (see Figure A.4). The general equation can be linearized in several ways to determine K and $(X/M)_{MAX}$:

$$\frac{1}{X/M} = \frac{1}{(X/M)_{MAX}} + \frac{1}{K(X/M)_{MAX}C} \qquad\qquad A.5$$

$$\frac{C}{X/M} = \frac{1}{K(X/M)_{MAX}} + \frac{C}{(X/M)_{MAX}} \qquad\qquad A.6$$

$$\frac{X}{M} = (X/M)_{MAX} - \frac{(X/M)}{K\,C} \qquad\qquad A.7$$

All the linearized forms are equivalent, but one form may be more desirable depending on the range and spread of data (Weber, 1972).

The monolayer assumption limits the applicability of the Langmuir isotherm for gaseous phase adsorption because multilayer adsorption is a common form of physical adsorption. The Langmuir equation, however, is often used to describe chemical sorption.

The BET equation (Brunauer et al., 1938) is an extension of the Langmuir equation to account for multilayer adsorption. Like the Langmuir isotherm, the BET isotherm assumes that adsorption sites are energetically uniform, and that adsorption at one site does not

affect adsorption at neighboring sites. The derivation of the BET equation assumes that the Langmuir equation applies to each layer. The initial layer is adsorbed to the surface. Subsequent layers are bound by forces that are the same as those acting in the condensation of vapors. The general form of the BET equation is:

$$V = \frac{V_m \, c \, P}{(P_o - P)\left[1 + (c-1)\left(\frac{P}{P_o}\right)\right]}$$ A.8

where:

V = volume of sorbate sorbed per mass of sorbent

V_m = volume sorbed at monolayer coverage per mass of sorbent

P_o = saturated vapor pressure

P = vapor partial pressure

c = constant

This volumetric form of the BET equation is most commonly cited, but it can also be expressed on a mass basis. A linear form that can be used to graphically determine V_m and C from experimental data is:

$$\frac{P}{V(P_o - P)} = \frac{1}{V_m c} + \frac{(c-1)P}{V_m c P_o}$$ A.9

The presence of the V_m term shows one of the most useful attributes of the BET theory. The volume of molecules in a monolayer can be determined experimentally despite the fact that one monomolecular layer is never actually formed. Physically, multiple layers start to form before the first layer is complete because energetic differences exist between sites. These differences are due to chemical heterogeneity or surface irregularities (Lowell and Shields, 1984). From the V_m term plus the sorbate molecular size, a measurement of sorbent surface area can be made. Despite criticism of some of its assumptions, use of the BET theory for surface area determination has continued because of its simplicity and applicability to many situations.

A plot of Equation A.8 gives a Type II isotherm (Figure A.4), representative of multilayer adsorption. The BET equation assumes that the number of layers of sorbate molecules is not limited. If limited to monolayer coverage, the BET equation reverts to the Langmuir equation (Equation A.4).

If the sorbent has narrow pores, and layering is restricted to some finite number, n, the BET equation is modified to :

255

$$V = \frac{V_m c \frac{P}{P_o}}{\left[1 - \frac{P}{P_o}\right]} \left[\frac{1 - (n+1)(P/P_o)^n + n (P/P_o)^{n+1}}{1 + (c-1)(P/P_o) - c (P/P_o)^{n+1}}\right] \qquad \text{A.10}$$

The value of the constant c affects the shape of the isotherm curve. The higher the value of c, the more pronounced the bend in the curve. The parameter c incorporates the heat of adsorption and adsorbate heat of vaporization from the liquid state. For c values greater than 2, a Type II isotherm results. For c values $\leq$ 2, Type III isotherms are obtained (Gregg and Sing, 1982). In the type III isotherm, adsorption increases with increasing partial pressure because adsorbate interaction with an adsorbed layer is greater than the interaction with the adsorbent surface. This isotherm shape is termed "unfavorable" and is rare.

Type IV and V isotherms are modifications of Types II and III, respectively, due to the presence of pores. Instead of approaching P/P_o asymptotically, isotherm types IV and V turn towards the pressure axis (see Figure A.4). These shapes suggest that complete or almost complete filling of the pores and capillaries of the sorbent occurs at a pressure lower than the vapor pressure of the sorbate. This will be discussed in more detail below.

Both the Langmuir and BET equations can be derived from either kinetic or thermodynamic considerations, but sometimes neither adequately describes the sorption which is observed. Another sorption model, the Freundlich isotherm, is empirical in nature and takes the following form:

$$\frac{X}{M} = K C^{1/n} \qquad \text{A.11}$$

where K and n are data-derived constants. A linear form to determine the values of the constants K and n comes from taking the log of both sides:

$$\log\left(\frac{X}{M}\right) = \log K = \frac{1}{n} \log C \qquad \text{A.12}$$

The shape of the Freundlich isotherm comes from the value of n. If n < 1, the curve follows the Type I shape, and is called "favorable" because high adsorption occurs at low vapor pressure. The curve is linear if n $=$ 1, and is unfavorable if n > 1.

The simplest isotherm model is that of linear adsorption or constant partitioning:

$$\frac{X}{M} = K_d C \qquad \text{A.13}$$

where K_d is the adsorption coefficient, sometimes called the distribution coefficient, and C is sorbate concentration. This model has gained widespread acceptance for its description of sorption because of its mathematical simplicity. The use of the linear isotherm must be justified, however, as the relationship is often not valid over wide ranges of concentration (Voice and Weber, 1983).

Under certain conditions, all the alternative isotherm models discussed above reduce to the linear isotherm. The denominator of the Langmuir isotherm (Equation A.⁄) approaches a value of 1 at low concentrations or pressures, and $[(X/M)_{max} K]$ becomes a coefficient of linear partitioning (Brunauer et al., 1967). At low concentrations with much less than monolayer coverage, the BET equation reduces to the Langmuir equation, and so at still lower concentrations it also becomes linear. As mentioned above, the Freundlich isotherm is linear when n = 1, a condition that is frequently found in sorption studies with saturated soil at low solution concentrations.

D. SORPTION FROM THE AQUEOUS PHASE

The sorption of organic chemicals from the aqueous phase onto soils was studied initially as an aspect of pesticide activity. The recent threat of aquifer contamination has renewed and extended the interest in aqueous sorption to other organic pollutants, and to sediments as well as soils. Sorption is one of the major abiotic processes controlling the behavior of organic pollutants in the saturated zone.

The linear sorption isotherm fits experimental data for nonionic organic pollutants particularly well at the concentrations encountered in the saturated zone. Karickhoff (1980) defines those concentrations as less than 1 ppm or below half of the aqueous phase solubility, which ever is lower. The linear isotherm (Equation A.13) allows the characterization of the sorption process through the partition coefficient K_d.

The ability to predict the partition coefficient and thus the degree of sorption has been of great importance to modeling the fate and transport of organic chemicals. Characteristics of the sorbent and the compound have been examined to determine their predictive value.

In aqueous systems, the characteristic of soils that overwhelmingly controls sorption of neutral organic compounds is the organic carbon content (Karickhoff et al., 1979; Means et al., 1980; Schwarzenbach and Westall, 1981). The inorganic fraction of the soil appears to be relatively inert to neutral organic compounds in soil-water systems, presumably because of its strong dipole interactions with highly polar water. This

precludes an active association of neutral organic compounds with the inorganic portion of the soil (Chiou et al., 1983). Because of the importance of organic carbon in sorption, a normalized partition coefficient with respect to organic carbon, K_{oc}, has been defined:

$$K_{oc} = \frac{K_d}{f_{oc}}$$

A.14

where f_{oc} is the fraction of organic carbon in the soil.

K_{oc} has been shown to remain relatively constant for a particular organic compound, and to be valid for soils with organic carbon values ranging from 0.1 to 40 percent (Chiou, 1981).

Sorption from the aqueous phase is also a function of the solubility (S) of the sorbate in water. Many nonpolar organic pollutants are considered hydrophobic (having a water solubility $< 10^{-3}$ M). Lambert (1968) suggests that the role of soil organic matter is similar to that of an organic solvent in solvent extraction and that the partitioning of a nonpolar organic compound between soil organic matter and water should correlate well with its partitioning between water and an immiscible organic solvent. The organic solvent-water partition coefficient often used is the octanol-water partition coefficient, K_{ow}. Correlation between soil uptake and low water solubility or high K_{ow} is thus expected (Mingelgrin and Gerstl, 1983). Both S and K_{ow} have been used to estimate K_{oc}, typically via a linear regression equation of the form:

$$\log K_{oc} = \alpha \log S + \beta$$

A.15

or $\qquad \log K_{oc} = \alpha \log K_{ow} + \beta$

A.16

where α and β are data-fitted coefficients (Karickhoff, 1984). Table A.1 gives values from several studies and shows the diversity of results. Predictions of K_{oc} from K_{ow} or S for different compounds using various equations are often only within a factor of two and can differ by an order of magnitude (Mingelgrin and Gerstl, 1983).

TABLE A.1. DATA-FITTED COEFFICIENTS FOR EQUATIONS A.15, AND A.16 FROM DIFFERENT STUDIES.

Sorbate Property	α	β	Reference
S			
	-0.54	0.44	Karickhoff et al. (1979)
	-0.686	4.237	Means et al. (1980)
K_{ow}			
	1.00	-0.21	Karickhoff et al. (1979)
	0.72	0.49	Schwarzenbach and Westall (1981)
	2.00	-0.317	Means et al. (1980)
	1.04	-0.88	Abdul et al. (1987)

Although soil organic carbon is generally thought to "control" sorption of hydrophobic organic compounds, the variability in K_{oc} estimates indicate that other factors contribute to sorption. The use of K_{ow} and S to calculate K_{oc} implies that these sorbate characteristics are solely responsible for the degree of sorption, and use of f_{oc} implies that soil organic matter (reduced to organic carbon for analytical considerations) is a uniform material that invites nonpolar organic sorption because of its hydrophobic nature. The treatment of soil organic matter as a generic organophilic phase may be an oversimplification because it is, in fact, extremely variable, complex, and poorly defined (Jury, 1986). Organic matter in soil consists of humic substances with identified components of resins, waxes, fats, proteins, pigments, carbohydrates, and polymeric acids (Chiou, 1981). Recent studies have suggested that further examination of sorption by different components of organic matter is needed (Mingelgrin and Gerstl, 1983; Chiou et al., 1983; Garbarini and Lion, 1986; Stauffer and MacIntyre, 1986).

The emphasis on K_{oc} does not necessarily imply that organic chemicals will not sorb onto soil minerals free of organic mater. Expanding clays with their large surface areas can cause higher K_{oc}s than calculated from f_{oc} (Khan et al., 1979). Means et al. (1980) and Banerjee et al. (1985) found that mineral contributions to sorption began at an expanding clay mineral content to organic carbon content ratio of 60. Karickhoff (1984), working with the limited data available, presented a model to calculate K_d based on organic carbon content and mineral content.

Sediment particle size is of secondary importance in the sorption of hydrophobic chemicals on natural sediments. Karickhoff et al. (1979) examined sorption on different

particle size fractions, and found that K_{oc} was reduced for sand sized particles relative to K_{oc} for sediment fines. Weber et al. (1983) suggested that variation in sorption between different size fractions is not due to particle size differences per se. but is mostly a reflection of their respective organic carbon content. The majority of soil organic carbon is in the fines. Horzempa and DiToro (1983) found little correlation between PCB sorption and sediment specific surface area.

The correlation between organic carbon and partition coefficients holds until organic carbon levels drop below approximately 0.1 percent (Schwarzenbach and Westall, 1981; Banerjee et al.,1985; Miller and Weber, 1986; Mackay et al., 1986; Mehran et al., 1987). This is significant because many very permeable sand or gravel aquifers may have less than that amount of organic matter (Cherry, 1984). If factors other than organic carbon content act to control sorption on low carbon soils, new predictive equations for partition coefficients must be proposed for modeling pollutant behavior in many aquifers. For two low carbon soils (<0.1 percent) and three inorganic solids, Schwarzenbach and Westall (1981) found that experimentally determined partition coefficients for sorption of four chlorinated benzenes were generally larger than partition coefficients calculated from K_{ow} and f_{oc} values. Specific surface area did not seem to influence sorption, as evidenced by the fact that partition coefficients for large surface area sorbents were not proportionally larger than partition coefficients for low surface area sorbents. Miller and Weber (1986) did not see any consistency between observed and calculated partition coefficients for lindane and nitrobenzene sorption on soils of various carbon content. Ratios of (estimated K_d/observed K_d) varied from 9.00 to 0.33 for low carbon soils (organic carbon range 0.10 to 0.13 percent).

Mehran et al. (1987) measured partition coefficients for TCE sorption onto five saturated clays with TOC values ranging from 0.34 percent down to 0.022 percent. Theoretical partition coefficients calculated from K_{ow}, S, and K_{oc} were comparable to measured values except for the low carbon clay (TOC < 0.1 percent), which had a K_d higher than expected from calculations.

Mackay et al. (1986) studied sorption of tetrachloroethylene (PCE) onto twenty 10 cm increments of a low carbon aquifer sand core. Normalized to bulk sample values, partition coefficients showed larger variation (range 0.3 to 3.2) than organic carbon (range 0.8 to 1.2) or specific surface area (range 0.8 to 1.6). Multiple regression of K_d as a function of organic carbon and specific surface area gave a poor coefficient of determination ($r^2 = 0.2$, n = 20). Mackay et al. (1986) speculated that observed sorption may be related to the amount and distribution of an as yet unidentified mineral phase. Banerjee et al. (1985), on the other hand, found that variations in total organic carbon (TOC) in deep, low carbon

samples of a soil core were not accompanied by changes in partition coefficients for o-dichlorobenzene sorption. They suggested that carbon found in subsurface rather than surface soils is older and, as a result, has been exposed to more intensive and varied diagenetic and microbial alteration. Because of this, it was suggested that the carbon in a subsurface environment may be distributed differently, perhaps more widely dispersed or in thinner films, making it less available to the sorbate or less able to compete with other sorbing surfaces.

In summary, organic compound sorption from the aqueous phase can generally be predicted from the octanol-water partitioning coefficient and the organic carbon content of the sorbent. These empirical relationships hold until the organic carbon content drops below 0.1 percent. At organic carbon contents below 0.1 percent, soil minerals and surface area may play an important role in the control of sorption.

E. SORPTION FROM THE VAPOR PHASE

Saturated soil can be viewed as one end point on the spectrum of possible soil moisture contents, with the other end point being oven-dry soils containing little or no moisture. This section begins with a discussion of organic vapor sorption onto dry soils, and then reviews what is known about sorption at various moisture contents.

The sorption of vapors is frequently described by the BET equation (Equation. A.8). The sorption of water vapor and organic chemicals onto various dry soils and clays typically show Type II isotherms (Call, 1957; Jurinak, 1957; Chiou and Shoup, 1985; Rao et al. 1988). The use of a linear isotherm model is valid in the very low pressure range of the isotherm. The linear isotherm model for vapor sorption is of the form:

$$\frac{X}{M} = K_d' C_G \qquad\qquad A.17$$

where K_d' is the vapor phase partition coefficient (mL/g), and C_G is the gaseous phase concentration.

One complicating factor in vapor sorption is the effect of sorbent pores on sorbate condensation. This was mentioned briefly above to explain isotherm Types IV and V, where the presence of interstitial pores changed the shape of the isotherm at high P/P_0 values. Condensation normally occurs at pressures greater than compound vapor pressure, but when pores are present, vapors can condense at partial pressures that are less

than the compound vapor pressure. Early condensation is the result of the curved meniscus formed inside very small pores. According to the Laplace equation:

$$\Delta P = \frac{2\sigma}{R}$$ A.18

where:

    σ = surface tension
    R = radius of curvature of surface

a fluid with a curved meniscus, such as that in a pore, has a lower vapor pressure relative to the bulk fluid phase.

Differential filling and emptying of pores is observed in porous sorbents and is termed hysteresis. A hysteresis loop, shown on a Type II isotherm (Figure A.5), can have a variety of shapes, but in all cases, results in at least two quantities of adsorbed material for each equilibrium pressure in the hysteresis range. The lower branch of the loop which corresponds to adsorption (increasing pressure) displays less adsorption than the desorption branch (Hiemenz, 1986).
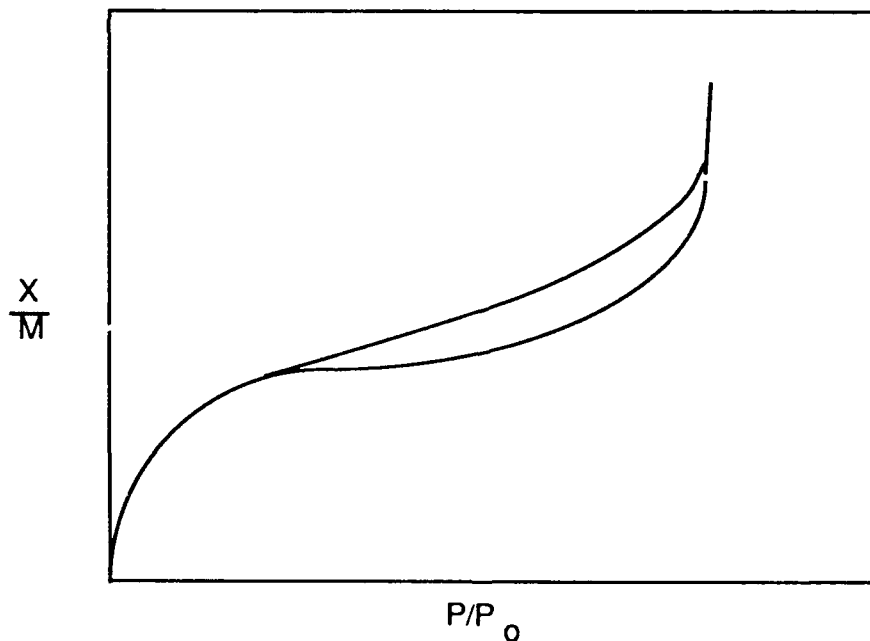

Figure A.5 Type II Isotherm with Hysteresis Loop

The "ink bottle effect", referring to the nonuniform geometry of some soil pores, is often cited as an explanation of hysteresis. A pore shaped roughly like an ink bottle

262

(Figure A.6) has a relatively wide void of radius R, which is accessible only through a narrow neck of radius r. In a sorption, the partial pressure at which condensation occurs is governed by the larger pore radius R. Once the pore fills, the controlling radius for emptying the pore is r, so emptying occurs at a lower P/P_o. The geometry used in this explanation, even including voids joined by narrow passages, seems too specialized to account for the widespread occurrence of hysteresis. Other explanations, based on contact angle and multilayer adsorption, are also not completely satisfactory explanations of this complex phenomena (Hiemenz, 1986). One functional explanation offered for hysteresis of water adsorption in soil is that, due to entrapped air in the soil, true equilibrium is not reached before measuring adsorption. Another functional explanation is that the wetting and drying history of the soil, causing swelling, shrinking and aging, can differentially change soil structure so different conditions exist for adsorption and desorption (Hillel, 1982).
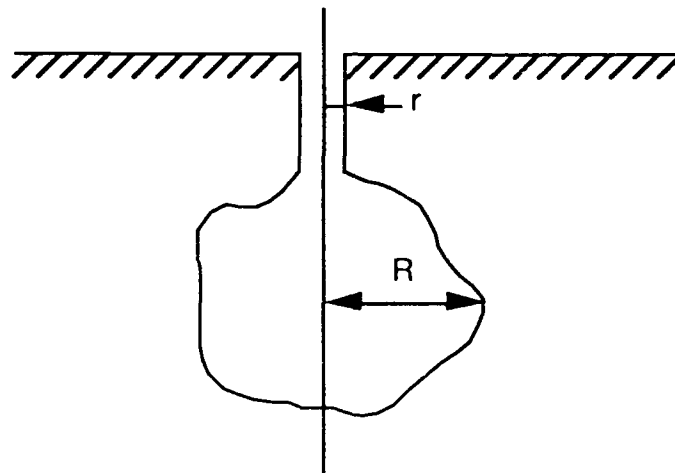

Figure A.6 Conceptualization of an "Ink Bottle" Pore

Sorption of organic compounds onto oven-dried soils has been part of several studies (Call, 1957; Jurinak, 1957; Mackay et al., 1986). Even though this degree of dryness does not occur naturally, use of oven-dry sorbent allows the study of organic compound sorption in the absence of competition for surface sites by water. Oven-dry conditions can also be conceptually viewed as an end member to the spectrum of possible moisture conditions in soil, with water-saturated soil defining the other end of the range (Peterson et al., 1988). As expected, the amount of sorption on dry soils varies depending on the composition of the soil and the sorbate. For oven-dried soils, sorption is higher onto mineral soils than organic soils (Harris, 1964). Sorption of Ethylene

dibromide (EDB) vapor onto four different soils was inversely proportional to their organic carbon content, but proportional to clay content. EDB vapor sorption onto a peaty loam (30.6 percent organic matter, 30.9 percent clay) increased threefold when the organic matter was removed (Call, 1957). The predominant soil clay mineral influenced sorption of the fumigant 1,2-dibromo-3-chloropropane, with montmorillonite soils sorbing more at low P/P_0 than kaolinitic or illitic soils (Jurinak, 1957). Under dry conditions, the internal surfaces of swelling clays would presumably not be available for sorption, so differences in sorption among clay types would not be as striking as when they are wet.

When volatile organic chemicals are present in the unsaturated zone, the system is more complex than in the single vapor case. Even with only one VOC present, a binary system exists due to the presence of water vapor. Because of "early" condensation in pores, water or the organic can also be present in liquid form. Call (1957) found that when soil was at field capacity (the amount of water retained after initial rapid drainage), sorption of EDB was due to solution in the soil water and sorption at the water interfaces.

Calvet (1984) described four possible mechanisms for pesticide/water sorption on soils. Mechanisms were divided into two categories according to the nature of adsorption sites. In the first category, pesticide molecules and water molecules are assumed to have different sorption sites. This may be the case in low carbon soils, for example, where there are mineral sites as well as hydrophobic organic matter sites available. In Mechanism 1, pesticide adsorption is from the vapor phase onto a dry or partially hydrated surface. Mechanism 2 is pesticide molecule sorption from solution on a hydrated surface, as might occur with hydrophobic sites. In the second category, pesticide molecules and water molecules are assumed to have the same sorption sites. Here, adsorption from the vapor or solution takes place by exchange on a specific sorption site between water molecules and pesticide molecules. In Mechanism 3, adsorption sites are on the adsorbent surface. In Mechanism 4, sorption sites are adsorbed water molecules.

In binary vapor systems with soil as the sorbent, strongly polar water vapor molecules seem to out compete weakly polar and neutral organics for adsorption sites. Ethylene dibromide (EDB) sorption on four soils decreased as relative humidity increased. The Type II isotherms shown at 0 percent humidity flattened with increasing humidity, and two of the four soils began to show a Type III shape at 50 percent relative humidity (Call, 1957). The same isotherm shape change was shown for benzene, m-dichlorobenzene, and 1,2,4-trichlorobenzene sorption onto a soil as relative humidity was raised from 0 to 90 percent (Chiou and Shoup, 1985).

Trace amounts of moisture on a dry soil determine the amount of mineral surface covered by water molecules. Spencer and Cliath (1970) and Yaron and Saltzman (1972)

•

264

observed that lindane and parathion vapor density (and hence adsorption by implication) did not change until the soil water content was below the equivalent of a monolayer on the soil surface. Hance (1977) fitted isotherms of atraton and monuron sorption on two soils with Freundlich isotherms, and plotted the Freundlich K values versus moisture content (Figure A.7). He attributed the flattening of the curve to monolayer coverage by water. Chiou and Shoup (1985) found that at 90 percent relative humidity, the sorption capacities of benzene compounds became comparable to those in aqueous systems. The relative humidity of most soils is commonly in excess of 99 percent.

The approach used by Yaron and Saltzman (1972), Hance (1977) and Chiou et al., (1985) to study sorption at different relative humidities involved replacing air in the three phase air-water-organic system with an immiscible organic solvent. This allowed use of standard batch equilibrium techniques to generate isotherms, although applicability to field situations may be limited (Calvet, 1984).

Chiou et al., (1985) used nonpolar solvents to identify sorption by mineral phases in soils at different moisture contents. Sorption on soil organic matter was greatly reduced because of the high solubility of organic pollutants in the nonpolar solvents. At 0.5 percent moisture, lindane uptake was decreased by a third over sorption on the dry soil. 2.5 percent moisture lead to a decrease in lindane uptake of approximately 95 percent. A dry soil high in mineral content (1.9 percent organic matter, 9 percent sand, 68 percent silt, and 21 percent clay) sorbed 5 times more lindane than a dry soil low in mineral content (51 percent organic matter, 9.8 percent sand, 36 percent silt, and 3.5 percent clay).

As noted above, moisture contents in soils vary considerably depending on soil type and environmental conditions. The few studies available, discussed above, indicate that the sorbent characteristics that may have a major influence on sorption of organic vapors are soil organic carbon content, mineral content or surface area, and moisture content. In the sections which follow, experimental data are presented which probe these dependencies. The experimental results provide a basis for quantitative prediction of the sorptive behavior of organic vapors in soils.
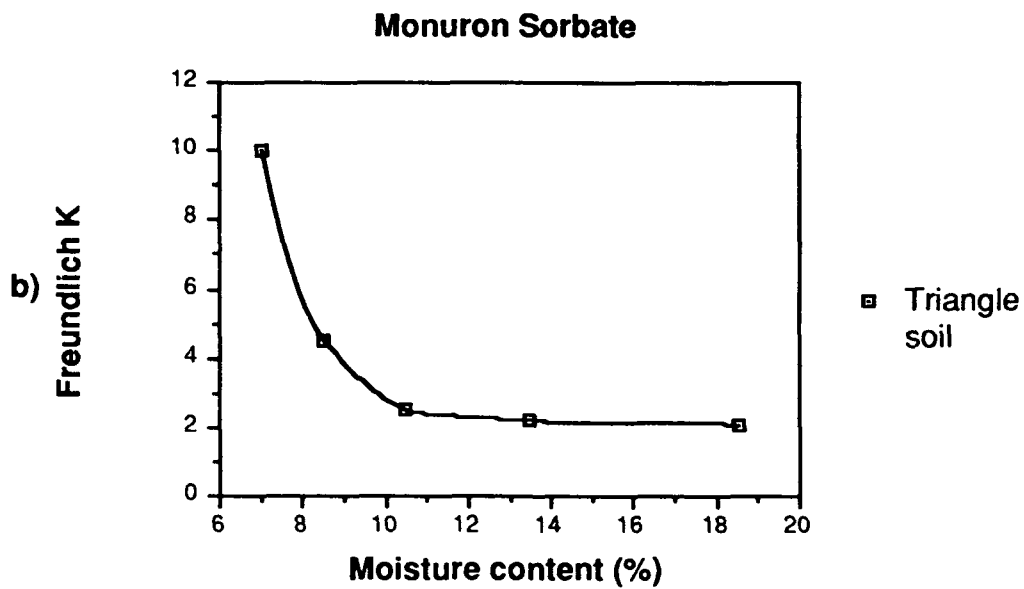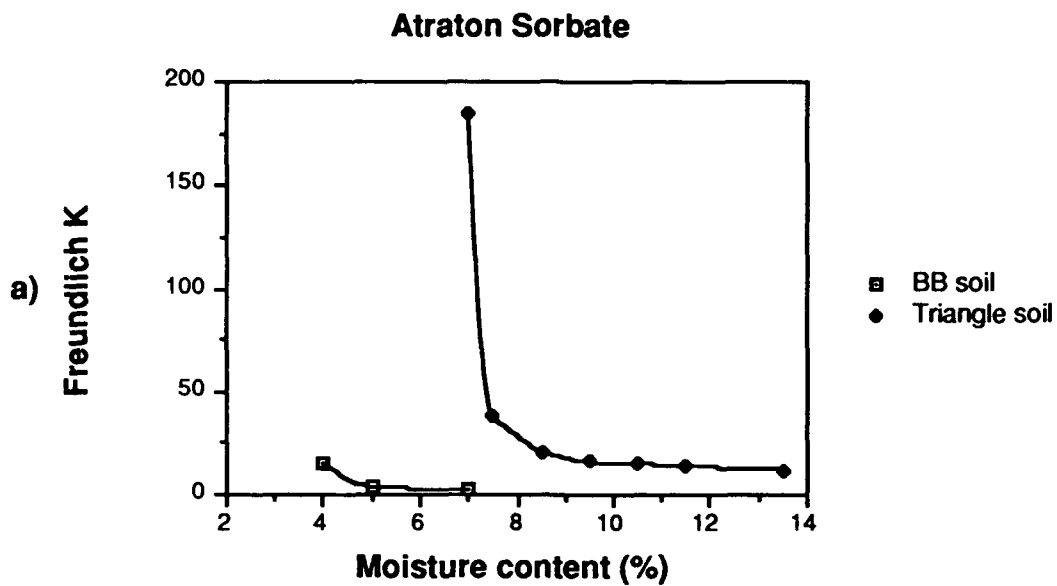
Figure A.7 Relationship of Freundlich K to Moisture Content for Sorption of Two Pesticides on Two Soils (after Hance, 1977)

REFERENCES

Abdul, A.S., T.L. Gibson, and D.N. Rai, 1987, "Statistical Correlations for Predicting the Partition Coefficient for Nonpolar Organic Contaminants Between Aquifer Organic Carbon and Water", Hazardous Waste & Hazardous Material, 4 (3), 211-222.

Abelson, P.R., 1985, "Chemicals from Waste Dumps", Science, 229, 335.

Abramowitz, M. and I.A. Stegun, (Eds.), 1972, Handbook of Mathematical Functions, with Formulas, Graphs, and Mathematical Tables, U.S. National Bureau of Standards, Applied Mathematics Series, 55, 17.

Abriola, L.M. and G.F. Pinder, 1985, "A Multiphase Approach to the Modeling of Porous Media Contamination by Organic Compounds 1. Equation Development", Wat. Resour. Res., 21(1), 11-18.

Adamson, A.W., 1967, Physical Chemistry of Surfaces, 2nd Ed., Interscience Publishers; J. Wiley & Sons; NY.

Amer. Soc. Test. Mater., 1958, Procedures for Testing Soils, 3rd Ed., American Society for Testing and Materials; Philadelphia, PA.

Allison, L.E., 1960, "Wet Combustion Apparatus and Procedure for Organic and Inorganic Carbon in Soil", Soil Sci. Soc. Am. Proc., 24, 36-40.

Allison, L.E., 1965, "Organic Carbon", in: Methods of Soil Analysis: Part 2. Chemical and Microbiological Properties; Black, C.A., (Ed.); Am. Soc. of Agronomy: Madison, Wisconsin, 1367-1378.

Atkins, P.W., 1986, Physical Chemistry, 3rd Edititon, W. H. Freeman and Co., New York.

Baehr, A.L., 1987, "Selective Transport of Hydrocarbons in the Unsaturated Zone due to Aqueous and Vapor Phase Partitioning", Water Resour. Res., 23 (10), 1926-1938.

Baehr, A.L. and M. Y. Corapcioglu, 1987, "A compositional multiphase model for groundwater contamination by petroleum products: 2. Numerical solution", Wat. Resour. Res., 23(1), 201-213.

Baehr, A.L., Hoag, G.E. and Marley, M.C. 1989, "Removing Volatile Contaminats from the Unsaturated Zone by Inducing Advective Air-phase Transport", J. Contaminant Hydrology, 4, 1-26

Bailey, G.W., and J.L. White, 1964, "Review of Adsorption and Desorption of Organic Pesticides by Soil Colloids with Implications Concerning Pesticide Bioactivity", J. of Agric. and Food Chem., 12 (4), 324-331.

Banerjee, P., M.D. Piwoni, and K. Ebeid, 1985, "Sorption of Organic Contaminants to a Low Carbon Subsurface Core", Chemosphere, 14 (8), 1057-1067.

Bohn, H., B.L. McNeal and G.A. O'Connor, 1979, Soil Chemistry, John Wiley and Sons, New York.

Bear, J., 1975, Dynamics of fluids in porous media, Amer. Elsevier Publ., New York.

Bolz, R.E. and G.L. Tuve, (Eds.), 1973, CRC Handbook of Tables for Applied Engineering Science, 2nd Edition, CRC Press: Cleveland, Ohio.

Boyd, S.A., M.M. Mortland, and C.T. Chiou, 1988, "Sorption Characteristics of Organic Compounds on Hexadecyltrimethylammonium-Smectite", Soil Sci. So. Am. J., 52, 652-657.

Briggs, G.G., 1981, "Theoretical and Experimental Relationships Between Soil Adsorption, Octanol-Water Partition Coefficients, Water Solubility, Bio-Concentration Factors, and the Parachlor", J. Agric. Food Chem., 29, 1050-1059.

Brunauer, S., P.H. Emmett, and E. Teller, 1938, "Adsorption of Gases in Multimolecular Layers", J. Amer. Chem. Soc., 60, 309-319.

Brunauer, S., L.S. Deming, W.E. Deming, and E. Teller, 1940, "On a Theory of the van der Waals Adsorption of Gases", J. Amer. Chem. Soc., 62, 1723-1732.

Brunauer, S., Copeland and Kantro, D.L., 1967, "The Langmuir and BET Theories", in: The Solid-Gas Interface, Vol. 1., E.A. Flood, (Ed.), Marcel Dekker, Inc.: New York, 77-103.

Cabaniss, S.E. and M.S. Shuman, 1988, "Copper Binding by Dissolved Organic Matter I. Suwanee River Fulvic Acid Equilibria", Geochim et Cosmochim Acta, 52 (1), 185-193.

Call, F., 1957a, "The Mechanisms of Sorption of Ethylene Dibromide on Moist Soils", J. Sci. Food Agri., 8, 630.

Call, F., 1957b, "Sorption of Ethylene Dibromide on Soils at Field Capacity", J. Sci. Food Agric., 8, 137-142.

Call, F., 1957c, "Diffusion of Ethylene Dibromide Through Soils", J. Sci. Food Agric., 8, 143-150.

Calvet, R., 1984, "Behavior of Pesticides in the Unsaturated Zone: Adsorption and Transport Phenomena", in: Pollutants in Porous Media: The Unsaturated Zone, Yaron, B. and Dagun, D, (Eds.), Springer-Verlag.

Carter, C.W. and I.H. Suffett, 1982, "Binding of DDT to Dissolved Humic Materials", Env. Sci. Tech., 16 (11), 735.

Carter, D.L., M.M. Mortland, and W.D. Kemper, 1986, "Specific Surface", in: Methods of Soil Analysis Part 1, Arnold Klue (Ed.), Soil Sc. Soc. Am.; Madison, Wisconsin, 413-423.

Cerny, S., 1970, "Theory of Adsorption on Active Carbon", in: Active Carbon: Manufacture, Properties, and Application; M. Smisek and S. Cerny, (Eds.), Elsevier Publishing Co: New York, 71-162.

Cherry, J.A., R.W. Gillham, and J.F. Barker, 1984, "Contaminants in Groundwater: Chemical Processes", in: Groundwater Contamination; National Academy Press: Wash., D.C., 46-66.

Chiou, C.T., and P.J. Ruecroft, 1977, "Adsorption of Phosgene and Chloroform by Activated and Impregnated Carbons", Carbon, 15, 49-53.

Chiou, C.T., L.J. Peters and J.H. Freed, 1979, "A Physical Concept of Soil-Water Equilibria for Nonionic Organic Compounds", Sci., 206, 831.

Chiou, C.T., 1981, "Partition Coefficient and Water Solubility in Environmental Chemistry", in: Hazard Assessment of Chemicals: Current Developments, 1, 117-153.

Chiou, C.T. and T.D. Shoup, 1985, "Soil Sorption of Organic Vapors and Effects of Humidity in Sorptive Mechanism and Capacity", Environ. Sci. Soc. Am. 19 (12), 1196-1200.

269

Chiou, C.T., T.D. Shoup, and P.E. Porter, 1985, "Mechanistic Roles of Soil Humus and Minerals in the Sorption of Nonionic Organic Compounds from Aqueous and Organic Solutions", Organic Geochem., 8, 9-15.

Chiou, C.T., D.E. Kile, and R.L. Malcolm, 1988, "Sorption of Vapors of Some Organic Liquids on Soil Humic Acid and its Relation to Partitioning of Organic Compounds in Soil Organic Matter", Env. Sci. & Tech., 22 (3), 298.

Cihacek, L.J. and J.M. Bremner, 1979, "A Simplified Ethylene Glycol Monoethyl Ether Procedure for Assessment of Soil Surface Area", Soil Sci. Soc. Am. J.., 43, 821-822.

Council on Environmental Quality, January 1981, Contamination of Groundwater by Toxic Organic Chemicals, Supt. of Documents, Washington, DC.

Culver, T.B., 1989, "Modeling the Transport of Volatile Organic Chemicals in Variably Saturated Subsurface Regions". M.S. Thesis. Cornell University, Ithaca, N.Y.

Culver, T.B., C.A. Shoemaker, and L.W. Lion, 1990, "Impact of Vapor Sorption on the Subsurface Transport of Volatile Organic Compounds: A Numerical Model And Analysis", Wat. Resour. Res., (submitted).

Degens, E.T., Mopper, K., 1976, "Factors Controlling the Distribution and Early Diagenesis of Organic Material in Marine Sediments" in: Chemical Oceanography, 6, J.P. Riley and R. Chester (Eds.), Academic Press, NY, 59-111.

deLevie, R., 1986, "When, Why and How to Use Weighted Least Squares", J. of Chem. Ed., 63, 10-15.

Donigan, A.S., Jr. and P.S.C. Rao, 1986, "Example Model Testing Studies in Vadose Zone Modeling of Organic Pollutants", in: Vadose Zone Modeling of Organic Pollutants; Hern, S. and S. Melancon (Eds)., Lewis Publishers, Inc., Chelsea, Michigan, 103-131.

Dowd, J.E. and D.S. Riggs, 1965, "A Comparison of Estimates of the Michaelis-Menten Kinetic Constants from Various Linear Transformations", J. Biol. Chem., 240, 863-869.

Draper, N.R. and H. Smith, 1981, Applied Regression Analysis, 2nd Ed. John Wiley and Sons, Inc.; NY.

Dzomback, D.A. and R.G. Luthy, 1984, "Estimating Sorption of Polycyclic Aromatic Hydrocarbons on Soils", Soil Science, 137, 292-308.

Ehlers, W., J.M. Letey, W.F. Spencer, W.J. Farmer, 1969a, "Lindane Diffusion in Soils: 1. Theoretical Consideration and Mechanisms of Movement", Soil Sci. Soc. Amer. Proc., 33, 501.

Ehlers, W., J.M. Letey, W.F. Spencer, W.J. Farmer, 1969b, "Lindane Diffusion in Soils: 2. Water Content, Bulk Density and Temperature Effects", Soil Sci. Soc. Amer. Proc., 33, 505.

Flick, E.W., 1985, Industrial Solvent Handbook, 3rd Edition, Noyes Data Corp., Park Ridge, NJ.

Foth, D. and L.M. Turk, 1972, Fundamentals of Soil Science, 5th Edition, John Wiley and Sons; New York.

Gammage, R.B. and S.J. Gregg, 1972, "The Sorption of Water Vapor by Ball-milled Calcite", J. Colloid Interface Sci., 38, 118.

Garbarini, D.R. and L.W. Lion, 1985, "Evaluation of Sorptive Partitioning of Nonionic Pollutants in Closed Systems by Headspace Analysis", Environ. Sci. Tech., 19, 1122.

Garbarini, D.R., 1985, "Sorption of Nonionic Volatile Organic Compounds: Headspace Analysis and Effect of the Nature of the Sorbent", M.S. Thesis, Cornell University.

Garbarini, D.R. and L.W. Lion, 1986, "Influence of the Nature of Soil Organics on the Sorption of Toluene and Trichloroethylene", Env. Sci. & Tech., 20, 1263-1269.

Gauthier, T.D., W.R. Seitz and C.L. Grant, 1987, "Effects of Structural and Compositional Variations of Dissolved Humic Materials on Pyrene K_{oc} Values", Env. Sci & Tech., 21 (3), 243.

Gavezzotti, A., 1985, "Molecular Free Surface: A Novel Method of Calculation and its Uses in Conformational Studies and in Organic Crystal Chemistry", Journal of the American Chemistry Society, 107, 962-967.

Ghiorse, W.C. and J.T. Wilson, 1988, "Microbial Ecology of the Terrestial Subsurface", Adv. in Appl. Microbiol., 33, 107-172.

Gossett, J.M., C.E. Cameron, B.P. Eckstrom, C. Goodman, and A.H. Lincoff, 1985, "Mass Transfer Coefficients and Henry's Constants for Packed Tower Air Stripping of Volatile Organics", U.S. Air Force, Engr. Serv. Center, Report ESL-TR-85-18.

Gregg, S.J., K.S.W. Sing, 1982, Adsorption, Surface Area and Porosity, 2nd Edition, Academic Press, New York.

Grim, R.E., 1953, Clay Mineralogy, McGraw Hill Book Co., Inc., New York, 174.

Gustafson, M.S., 1986, "Sorptive Binding and Transport of Trichloroethylene in Unsaturated Groundwater Environments", M.S. Thesis, Cornell University.

Hamaker, J.W., 1972, "Diffusion and Volatilization", In: Organic Chemicals in the Environment, C.A.I. Goring and J.W. Hamaker (eds), Marcel Dekkar, Inc., N.Y., pp. 341-397.

Hance, R.J., 1977, "The Adsorption of Atratron and Monuron by Soils at Different Water Contents", Weed Res., 17, 137-201.

Hanks, R.J. and G.L. Ashcroft, 1980, Applied Soil Physics, Springer-Verlag: New York.

Harter, R.D., 1984, "Curve-Fit Errors in Langmuir Adsorption Maxima", Soil Sci. Soc. of Am. J., 48, 749-752.

Harris, C.R., 1964, "Influence of Soil Type and Soil Moisture on the Toxicity of Insecticide in Soils to Insects", Nature, 202, 724.

Hayes, M.H.B., F.L. Himes, 1986, "Nature and Properties of Humus-Mineral Complexes", in: Interaction of Soil Minerals with Natural Organics and Microbes, P.M. Huang and M. Schnitzer (Eds.), Soil Sci. Soc. Amer., Pub. No. 17.

Heilman, M.D., D.L. Carter, and C.L. Gonzalez, 1965, "The Ethylene Glycol Monoethyl Ether (EGME) Technique for Determining Soil-Surface Area", Soil Sci., 100 (6), 409-413.

Herbel, C.H., and L.H. Gile, 1973, "Field Moisture Regimes and Morphology of Some Acid Land Soils in New Mexico", in: Field Soil Water Regime, R.R. Bruce, K.W. Flach and H.M. Taylor (Eds.) Soil Sci. Soc. Amer., Special Publ. No. 5., Madison, Wisconsin.

Hiemenz, P.C., 1986, Principles of Colloid and Surface Chemistry, 2nd Ed., Marcel Dekker, Inc., New York.

Hill, C., Jr., 1977, Introduction to Chemical Engineering Kinetics and Reactor Design, John Wiley and Sons, New York.

Hillel, D., 1982, Introduction to Soil Physics, Academic Press, Inc., New York.

Holmgren, G.G.S., R.L. Juve, R.C. Geschwender, 1977, "A Mechanically Controlled Variable Rate Leaching Device", Soil Sci. Soc. Am. J., 41 (6), 1207.

Horzempa, L.M. and D.M. DiToro, 1983, "The Extent of Reversibility of Polychlorinated Biphenyl Adsorption", Water Res., 17, 851-859.

Hutzler, N.J., J.S. Gierke, and L.C. Krause, 1989, "Movement of Volatile Organic Chemicals in Soils", in: Reactions And Movement Of Organic Chemicals In Soils, SSSA, Special Publ. no. 22, Madison, Wisconsin,pp 373-403.

Iwaki, T. and H.H.G. Jellinek, 1979, "Adsorption of Water Vapor on Block Copolymers", J. Colloid Interface Sci., 69, 17.

Jurinak, J.J., 1957, "Adsorption of 1,2-dibromo-3-chloropane Vapor by Soils", J. Agric. Food Chem., 5 (8), 598-601.

Jurinak, J.J., and D.H. Volman, 1957, "Application of the Brunauer, Emmet and Teller Equation to Ethylene Dibromide Adsorption by Soils", Soil Sci., 83, 487.

Jury, W.A., W.F. Spencer, W.J. Farmer, 1983, "Behaviour Assessment Model for Trace Organics in Soil: 1. Model Description", J. Environ. Quality, 12 (4), 558.

Jury, W.A., 1986, "Volatilization from Soil", in: Vadose Zone Modeling of Organic Pollutants; Hern, S. and S. Melancon (Eds.), Lewis Publishers, Inc., Chelsea, Michigan, 103-131.

Karickhoff, S.W., D.S. Brown, and T.A. Scott, 1979, "Sorption of Hydrophobic Pollutants on Natural Sediments", Water Research, 13, 241-248.

Karickhoff, S.W., 1980, "Sorption Kinetics of Hydrophobic Pollutants in Natural Sediments", in: <u>Contaminants and Sediments, Vol. 2, Analysis, Chemistry, Biology</u>, Baker, R.A., (Ed.); Ann Arbor Science: Ann Arbor, Michigan, 193-205.

Karickhoff, S.W., 1981, "Semi-Empirical Estimation of Sorption of Hydrophobic Pollutants on Natural Sediments and Soils", <u>Chemosphere</u>, <u>10</u>, 833-846.

Karickhoff, S.W., 1984, "Organic Pollutant Sorption in Aquatic Systems", <u>J. Hyd. Engrg.</u>, <u>110</u> (6), 707-735.

Kell, R.F., 1987, "Studies on Hazardous Vapour Transport in Soil", M.S. Thesis, Dept. of Civil Engr., Univ. of Waterloo; Waterloo, Ont., 156pp.

Kendall, M.G. and A. Stuart, 1977, <u>The Advance Theory of Statistics</u>, 3rd Ed. Hafner, New York.

Kenaga, E.E., 1980, "Predicted Bioconcentration Factor and Soil Sorption Coefficients of Pesticides and Other Chemicals", <u>Ecotoxicol Env. Saf.</u>, <u>4</u>, 26-38.

Khan, A., J.J. Hassett, W.L. Banwart, J.C. Means, and S.G. Wood, 1979, "Sorption of Acetophenone by Sediments and Soils", <u>Soil Sci.</u>, <u>128</u> (5), 297-302.

Kier, L.B. and L.H. Hall, 1976, "Molecular Connectivity in Chemistry and Drug Research", Academic Press, New York, 257.

Kier, L.B. and L.H. Hall, 1986, "Molecular Connectivity in Structure-Activity Analysis", Research Studies Press Letchworth, Hertfordshire, England, John Wiley and Sons, Inc., New York, 262.

Kinniburgh, D.G., 1986, "General Purpose Adsorption Isotherms", <u>Env. Sci. & Tech.</u>, <u>20</u> (9), 895.

Kreamer, D.K., E.P. Weeks, and G.M. Thompson, 1988, "A Field Technique to Measure the Tortuosity and Sorption-Affected Porosity for Gaseous Diffusion of Materials in the Unsaturated Zone with Experimental Results From Near Barnwell, South Carolina", <u>Wat. Resour. Res.</u>, <u>24</u>(3), 331-341.

Kuhlmeier, P.D., 1988, "Movement of Gasoline Components Through Unsaturated Heterogeneous Soils", in: Proceedings of the Twentieth Mid-Atlantic Industrial Waste Conference, Varma, M.M., and J.H. Johnson, Jr., (Eds.), Hazardous Materials Control Research Institute: Silver Srings, MD.

Lambe, T.W., 1951, Soil Testing for Engineers, John Wiley and Sons, Inc., New York.

Lambert, S.M., P.E. Porter, and R.H. Schieferstein, 1965, "Movement and Sorption of Chemicals Applied to the Soil", Weeds, 13, 185-190.

Lambert, S.M., 1968, "Omega (Ω), a Useful Index of Soil Sorption Equilibria", J. Agric. Food Chem., 16, 340-343.

Langmuir, I., 1918, "The Adsorption of Gases on Plane Surfaces of Glass, Mica, and Platinum", J. Am. Chem. Soc., 40, 1361-1403.

La Poe, R.G., 1985, "Sorption and Desorption of Volatile Chlorinated Aliphatic Compounds by Soils and Soil Components", Ph.D. Thesis, Cornell University.

Lincoff, A.H., and J.M. Gossett, 1984, "The Determination of Henry's Constant for Volatile Organics", in: Gas Transfer at Water Surfaces; Brutsaert, W. and G.H. Jirka, (Eds.); D. Reideal Publ. Co.: Holland, 17-25.

Lineweaver, M. and D. Burk, 1934, "The Determination of Enzyme Disassociation Constants", J. Am. Chem. Soc., 55, 658-666.

Livingston, H.F., 1949, "The Cross-Sectional Areas of Molecules Absorbed on Solid Surfaces", J. Colloid Sci., 4, 447.

Low, G.K. and G.E. Batley, 1988, "Comparative Studies of Adsorption of Polycyclic Hydrocarbons by Fly Ash from the Combustion of Some Australian Coals", Env. Sci & Tech., 22, 322-327.

Lowell, S. and J.E. Shields, 1984, Powder Surface Area and Porosity, 2nd Ed., Chapman and Hall Ltd.: New York.

Lyman, W.J., W.F. Reehl, and D.H. Rosenblatt, 1982, Handbook of Chemical Property Estimation Methods: Environmental Behavior of Organic Compounds, McGraw-Hill, New York.

Mackay, D., 1979, "Finding Fugacity Feasible", Env. Sci. & Tech., 13 (10), 1218-1223.

Mackay, D. and W.Y. Shiu, 1981, "A Critical Review of Henry's Law Constants for Chemicals of Environmental Interest", J. Phys. Chem. Ref. Data, 10 (4): 1175-1199.

Mackay, D.M. and S. Paterson, 1982, "Fugacity Revisited", Env. Sci. & Tech., 16 (2), 654a.

Mackay, D.M., W.P. Ball, and M.G. Durant, 1986, "Variability of Aquifer Properties in a Field Experiment on Groundwater Transport of Organic Solutes: Methods and Preliminary Results", J. Contam. Hyd., 1, 119-132.

Marrin, D.L. and Kerfoot, H.B., 1988, "Soil-gas Sampling Techniques", Environ. Sci. and Technol., 22(7):740-745.

Mayer, R., Farmer, W.J., and Letey, J., 1973, Models for Predicting Pesticide Volatilization Of Soil Applied Pesticides", Soil Sci. Soc. of America Proc. , 37(4):

McAuliffe, C., 1966, "Solubility in Water of Paraffin, Cycloparaffin, Olefin, Acetylene, Cycloolefin, and Aromatic Hydrocarbons", Journal of Physical Chemistry, 70, 1267-1275.

McConnell, G., D.M. Ferguson, and C.R. Pearson, 1975, "Chlorinated Hydrocarbons and the Environment", Endeavour, 34 (14), 13-18.

Means, J.C., S.G. Wood, J.J. Hassett, and W.L. Banwart, 1980, "Sorption of Polynuclear Aromatic Hydrocarbons by Sediments and Soils", Environ. Sci. & Tech., 14, 1524-1528.

Mehran, M., R.L. Olsen, and B.M. Rector, 1987, "Distribution Coefficient of Trichloroethylene in Soil-Water Systems", Groundwater, 25, 275-282.

Metcalfe, D.E. and G.J. Farquhar, 1987, "Modeling Gas Migration Through Unsaturated Soils from Waste Disposal Sites", Water, Air, and Soil Pollution, 32, 247-259.

Miller, C.T. and A.J. Weber, Jr., 1986, "Sorption of Hydrophobic Organic Pollutants in Saturated Soil Systems", J. Contam. Hyd., 1, 243-261.

Millington, R.J. and J.M. Quirk, 1961, 'Permeability of Porous Solids", Trans. Faraday Soc., 57, 1200-1207.

Mingelgrin, U. and Z. Gerstl, 1983, "Reevaluation of Partitioning as a Mechanism of Nonionic Chemical Adsorption in Soils", J. Environ. Qual., 12 (1), 1-11.

Mooney, R.W., Keenan A.C., Wood, L.A., 1952, "Adsorption of Water by Montmorillonite", J. Am. Chem. Soc., 74, 1367-1374.

Mohsen, M.F.N., G.J. Farquhar, and N. Kouwen, 1980, "Gas Migration and Vent Design at Landfill Sites", Water, Air, and Soil Pollution, 13, 79-97.

Nakayama, F.S. and A.D. Scott, 1962, "Gas Sorption by Soils and Clays Minerals: 1. Solubility of Oxygen in Moist Materials", Soil Sci., 94 (2), 106-110.

Newman, A.C.D., 1987, "The Interaction of Water with Clay Mineral Surfaces", in: Chemistry of Clays and Clay Minerals, A.C.D. Newman (Ed.), Mineralogical Society Monograph No. 6, Longman Sc. and Tech., England.

Nirmalakhandan, N.N., and R.E. Speece, 1988, "QSAR Model for Predicting Henry's Constant", Env. Sci. & Tech., 22 (11), 1349.

Nirmalakhandan, N.N., and R.E. Speece, 1989, "Prediction of Aqeous Solubility of Organic Chemicals Based on Molecular Structure 2. Application to PNAs, PCBs, PCDDs, etc.", Env. Sci. & Tech., 23, 708-713.

Noll, K.E., Aguwa, A.A., Fang, Y.P., Boulanger, P.T., 1985, "Adsorption of Organic Vapors on Carbon and Resin", ASCE J. Environ. Engrg., 111 (4), 487-500.

Parfitt, R.L., A.R. Frasen, C.V. Farmer, 1977, "Adsorption on Hydrous Oxides. III. Fulvic and Humic Acid on Geothite, Gibbsite and Imogolite", J. Soil Sci., 28, 289-296.

Peterson, M.S., L.W. Lion, C.A. Shoemaker, 1988, "Influence of Vapor Phase Sorption and Diffusion on the Fate of Trichloroethylene in an Unsaturated Aquifer System", Environ. Sci. & Tech., 22, 571-578.

Pinder, G.F. and L.M. Abriola, 1986 "On the Simulation of Nonaqueous Phase Organic Compounds in the Subsurface, Wat. Resour. Res., 22(9), 109s-119s.

Plumb, R.H. Jr., and A.M. Pitchford, 1985, "Volatile Organic Scans: Implications for Groundwater Monitoring", in: Proceedings: Petroleum Hydrocarbons and Organic Chemicals in Groundwater - Prevention, Detection and Restoration - Houston, TX, Nov. 13-15.

Press, W.H., B.P. Flannery, S.A. Tenkolsky and W.T. Vetterling, 1986, Numerical Recipes: The Art of Scientific Computing, Cambridge University Press, New York, 274-282.

Purtymun, W.D. and W.R. Kennedy, May 1971, "Geological and Hydrological of Mestra del Buey", Los Alamos Sc. Lab. Report, LA - 4660.

Pye, V.I. and R. Patrick, 1983, "Groundwater Contamination in the United States", Sciences, 213, 713-718.

Rao, P.S.C. and J.M. Davidson, 1980, "Estimation of Pesticide Retention and Transformation Parameters Required in Nonpoint Source Pollution Models", in: Environmental Impact of Nonpoint Source Pollution, M.R. Overcash and J.M. Davidson (Eds.), Ann Arbor Sci., Ann Arbor, MI, 23-67.

Rao, P.S.C., A.G. Hornsby, D.P. Kilcrease and P. Nkedi-Kizzi, 1985, "Sorption and Transport of Hydrophobic Organic Chemicals in Ageous and Mixed Solvent Systems: Model Development and Preliminary Evaluation", J. Env. Qual., 14 (3), 376.

Rao, P.S.C., R.D. Rhue, C.T. Johnson and R.A. Ogwada, 1988, "Sorption of Selected Volatile Organic Constituents of Jet Fuels and Solvents on Natural Sorbents from Gas and Solution Phases", U.S.A.F. Engineering Services Laboratory, Technical Report No. ESL-TR-88-02.

Rhue, R.D., P.S.C. Rao and R.E. Smith, 1988, "Vapor Phase Adsorption of Alkylbenzenes and Water on Soils and Clays", Chemosphere, 17 (4), 727-741.

Sabljic, A., 1984, "Predictions of the Nature and Strength of Sorption of Organic Pollutants by Molecular Topology", Journal of Agricultural Food and Chemistry, 32, 243-246.

Sabljic, A., 1987, "On the Prediction of Soil Sorption Coefficients of Organic Pollutants from Molecular Structure: Application of Molecular Topology Model", Env. Sci. & Tech., 21, 358-366.

Schwazenbach, R.P. and J. Westhall, 1981, "Transport of Nonpolar Organic Compounds from Surface Water to Groundwater. Laboratory Sorption Studies," Environ. Sci. & Tech., 15, 1360-1367.

Shearer, R.C., J.M. Letety, W.M. Farmers, and A. Klute, 1973, "Lindane Diffusion in Soil", Soil Sci. Soc. Amer. Proc., 37, 189.

Shoemaker, C.A., T.B. Culver, L.W. Lion, and M.G. Peterson, 1990, "Analytical Models of the Impact of Two Phase Sorption on Subsurface Transport of Volatile Chemicals", Water Resources Research. 26(4), 745-758.

Sittig, M., Handbook of Toxic and Hazardous Chemicals and Carcinogens, Noyes Publications: Park Ridge, New Jersey.

Sleep, B.E. and J.F. Sykes, 1989, "Modeling the Transport of Volatile Organics in Variably Saturated Media", Wat. Resour. Res., 25(1), 81-92.

Spencer, W.F. and M.M. Cliath, 1970, "Desorption of Lindane From Soil as Related to Vapor Density", Soil Sci. Soc. Amer. Proc., 34, 574.

Spencer, W. F., Farmer, W.J. and Cliath, M.M., 1973, "Pesticide Volatilization", in Residue Reviews, F.A. Gunther & J.D. Gunther (Eds.) 49:1-47, Springer Verlag, NY.

Spencer, W.F., W.V. Farmer and W.A. Jury, 1982, "Review: Behavior of Organic Chemicals in Soil, Air, Water Interfaces as Related to Predicting the Transport and Volatilization of Organic Pollutants", Env. Toxicology and Chemistry, 1, 17-26.

Springer, E.P., 1986, "Modelling of Organic Vapor Movement at Area L Disposal Site", Los Alamos, New Mexico, Technical Report, LA-UR-86-4359.

Sposito, G., R. Prost, 1982, "Structure of Water Adsorbed on Smectites", Chemical Reviews, 82 (6), 554-573.

Stauffer, T.B., W.G. MacIntyre, 1986, "Sorption of Low Polarity Organic Compounds on Oxide Minerals and Aquifer Material", Environ. Toxicology & Chem., 5, 949-955.

Stauffer, T.B., W.G. MacIntyre, and D.C. Wickman, 1989, "Sorption of Nonpolar Organic Chemicals on Low Carbon Content Aquifer Materials", Env. Tox. and Chem., 8 (10), 845-852.

Stephanatos, B.N., 1985, "Groundwater Pollution by Gas-Phase Transport of Contaminants Through the Vadose Zone", M.S. Thesis, University of Illinois, Urbana-Champaign, Ill..

Swanger, J.L., 1990, "Vapor Phase Sorption of Trichloroethylene and Toluene on Unsaturated Soils", M.S. Thesis, Cornell University.

Todd, D.K., 1980, Groundwater Hydrology, 2nd Ed., John Wiley and Sons, Inc., NY.

United States Department of the Interior, 1981, Ground Water Manual, Water Resources Technical Publication, 2nd ed., U.S. Govt. Printing Off., Denver, CO.

Valentine, R.L., 1986, "Nonbiological Transformation", in: Vadose Zone Modelling of Organic Pollutants; Hern, S.C. and S.M. Melacone, (Eds.); Lewis Publishers: Chelsea, Michigan, pp. 223-243.

van Olphen, H., and J.J. Fripiat, 1979, Data Handbook for Clay Materials and other Non-metallic Minerals, Pergamon Press, New York.

Verschueren, K., 1983, Handbook of Environmental Data on Organic Chemicals, 2nd Ed., Van Nostrand, New York.

Vilkner, V.L. and R.S. Parnas, 1986, "Analysis of Volatile Hydrocarbon Losses from Quiescent Water Solutions", Wat. Resour. Res., 22(5), 812-818.

Vogel, T.M. and P.L. McCarty, 1985, "Biotransformation of Tetrachloroethylene to Trichloroethylene, Dichloroethylene, Vinyl Chloride, and Carbon Dioxide Under Methanogenic Conditions", Applied and Environmental Microbiology, 49(10), 1080-1083.

Voice, T.C. and W.J. Weber Jr., 1983, "Sorption of Hydrophobic Compounds by Sediments, Soils and Suspended Solids - I. Theory and Background", Water Res., 17(10), 1433-1441.

Wade, P., 1955, "Soil Fumigation III - The Sorption of Ethylene Dibromide by Soils at Low Moisture Contents", J. Sci. Food Agric., 6, 1-3.

Wagner, H.M., 1969, Principles of Operations Research with Applications and Management Decisions, Prentice-Hall, Inc., Englewood Cliffs, NJ, 525-527.

Weber, W.J., Jr., 1972, "Adsorption", in: Physicochemical Process for Water Quality Control; Weber, W.J. Jr., (Ed); John Wiley and Sons: New York, 199-259.

Weber, W.J., T.C. Voice, M. Pirabazari, G.E. Hunt, and D.M. Ulanoff, 1983, "Sorption of Hydrophobic Compounds by Sediments, Soils, and Suspended Solids - II. Sorbent Evaluation Studies", Water Res., 17 (10), 1443-1452.

Weeks, E.P., D.E. Earp, and G.M. Thompson, 1982, "Use of Atmospheric Fluorocarbons F-11 and F-12 to Determine the Diffusion Parameters of the Unsaturated Zone in the Southern High Plains of Texas", Wat. Resour. Res., 18(5), 1365-1378.

Wilson, J.T., C.G. Enfield, W.J. Dunlap, R.L. Cosby, D.A. Foster. and L.B. Baskin, 1981, "Transport and Fate of Selected Organic Pollutants in a Sandy Soil", J. Environ. Qual., 10 (4), 501-506.

Wolfe, T.A., T. Demirel, E.R. Baumann, 1986, "Adsorption of Organic Pollutants on Montmorillonite Treated with Amines", J. Water Poll. Cont. Fed., 58 (1), 68-76.

Yaron, B., and S. Saltzman, 1972, "Influence of Water and Temperature on Adsorption of Parathion by Soils", Soil Sci. Am. Proc., 36, 583-586.

Yeh, G.T., 1987, "FEMWATER: A Finite Element Model of WATER Flow Through Saturated-Unsaturated Porous Media-First Revision", ORNL-5567/R1, Oak Ridge National Laboratory, Oak Ridge, Tennessee.

Yeh, G.T., 1988, "FEMWASTE: A Finite Element Model of WASTE Transport Through Saturated-Unsaturated Porous Media", ORNL-5601/R1, Oak Ridge National Laboratory, Oak Ridge, Tennessee.